OSE5312 – Light-Matter Interaction

David J. Hagan and Pieter G. Kik

This document represents the course notes for CREOL course OSE5312. The text is a work in progress, so if you have any comments, please let us know!

David Hagan: http://www.creol.ucf.edu/People/Details.aspx?PeopleID=300
Pieter Kik: http://www.creol.ucf.edu/People/Details.aspx?PeopleID=3407

CREOL, The College of Optics and Photonics
University of Central Florida
4000 Central Florida Blvd.
Orlando, FL 32816-2700

Date generated: January 10, 2019

Table of Contents

Chapter 1 - Introduction

➢ Corresponding handouts are available on http://kik.creol.ucf.edu/courses.html

The propagation of light traveling through materials is affected by the motion of electric charges, for example by the movement of bound electrons of the atoms in the material. We will derive physical models do describe the charge motion and the resulting optical properties in later Chapters. In this introductory Chapter we first develop an intuitive picture of the interaction of light with charge, and make a prediction of the wavelength dependent refractive index. A more detailed description of these arguments is given in Wooten, Chapter 2.

Phenomenological description of the refractive index
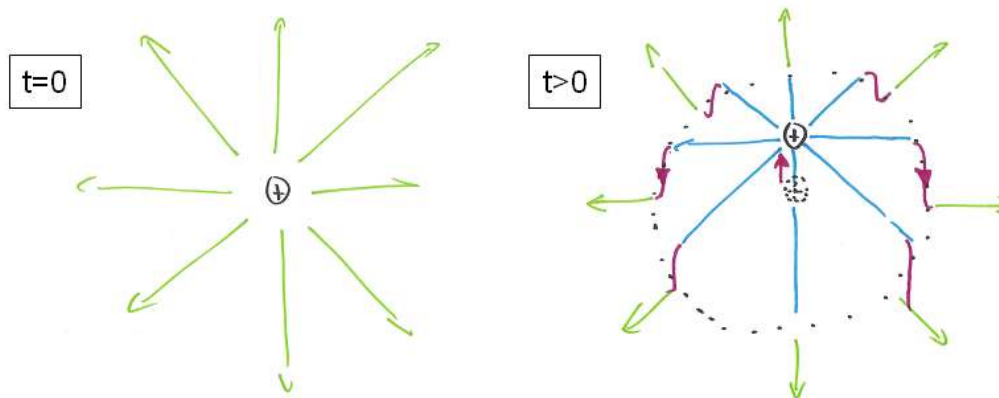
Figure 1.1

Light is usually encountered as a propagating transverse electromagnetic wave, meaning that the electric and magnetic fields oscillate in space and time, and that the direction of these fields is normal to the propagation direction. When a light wave encounters a charged particle (*electron, positive ion, negative ion, positron, ..*) the electric field exerts an electric force F_e=q·E where q is the charge of the particle, and E is the field strength.[i] The time dependent electric field accelerates the charge, and accelerating charge causes radiation. This is light-matter interaction in a nutshell: <u>optical radiation accelerates charges in a material, and accelerating charges emit light that adds to (or subtracts from) the incident light.</u>

To understand how accelerating charge gives rise to radiation, let's consider the electric field lines around a positive charge that is initially at rest, and that suddenly undergoes positive acceleration. The charge is initially surrounded by a purely radial electric field of strength $E = (\hat{r}/r^2)/4\pi\epsilon_0$ corresponding to straight field lines extending to infinity, as sketched above. Immediately after a brief acceleration field lines near the charge still point radially outward. However, at larger distances, the information about the new charge position is not yet known due to the finite speed of light. In order to connect these different field distributions, at an intermediate position the field lines need to have a transverse

---

[i] We will discuss units later. Note that we also ignore the Lorentz force $\vec{F}_l = q\,\vec{v} \times \vec{B}$.

component that is pointing downward. These transverse components move away from the charge at a velocity c, and represent the radiation pattern around accelerating charge. Note that no transverse components exist in the direction along the charge acceleration direction.[ii]

When light propagates inside gases, liquids or solids, electrons (negative charge) and atom cores (positive charge) are accelerated continuously. This results in an oscillating charge position, corresponding to an oscillatory dipole moment. The periodic charge acceleration produces radiation at a frequency that matches that of the incident light.[iii] This reradiated light adds to the incident light wave, which is now slightly modified. Thus, refractive index can be seen as the result of the re-radiation of light from a large collection of oscillating dipoles.
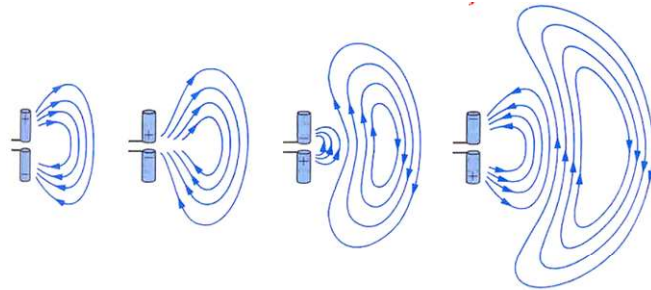
Figure 1.2 Development of dipole radiation, showing only electric field components

To understand the origin of the refractive index, and why it is usually larger than 1, we need to consider the *phase* of the charge oscillation. Let's first look at the response of a charge to an incident oscillating field. For a positive bound charge that is driven well below resonance, we find that the position of the charge is exactly in phase with the driving field, see graph below. The velocity can be seen to be 90° ahead in phase, and the acceleration is yet another 90° ahead. In the discussion above, we found that the field resulting from this acceleration is pointing in the direction opposite to the acceleration. Surprisingly, this analysis shows that the reradiated field at low frequencies is exactly in phase with the incident wave. This would correspond to a refractive index which is always exactly equal to 1, which we know is incorrect.
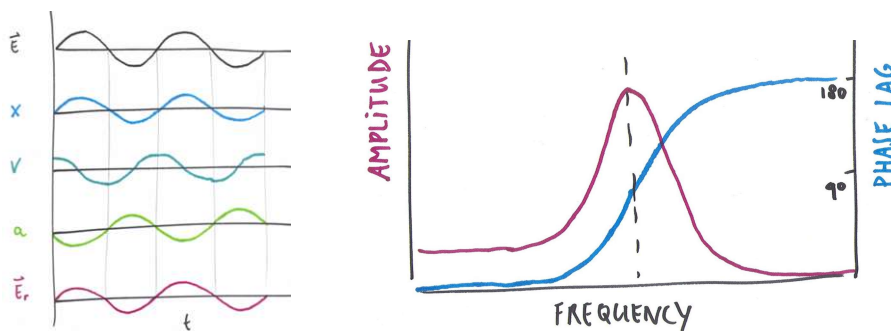
Figure 1.3 Charge motion under oscillatory driving field

[ii] From this analysis it also follows that static charges and charges with constant velocity do not radiate.
[iii] Except for very strong fields. In that case we would need to consider nonlinear optics, discussed in a later Chapter.

The error in the analysis lies in the fact that we considered only a single isolated charge. In reality, we need to consider the effect of many radiating dipoles, as shown below. The incident plane wave will drive a sheet of dipoles, all radiating in phase with the incident light. At a finite distance from these dipoles, the total field observed contains radiation contributions from many dipoles. On some optical axis of choice, radiation coming from off-axis dipoles will arrive a little later, causing a phase delay, or reduced apparent velocity of the light. By carefully integrating the effect of all dipoles, it follows that the total phase delay adds up to exactly 90° compared to the 'direct' wave. As a result, the low frequency refractive index is larger than 1, with the magnitude given by the number of dipoles contributing and their individual dipole moments.
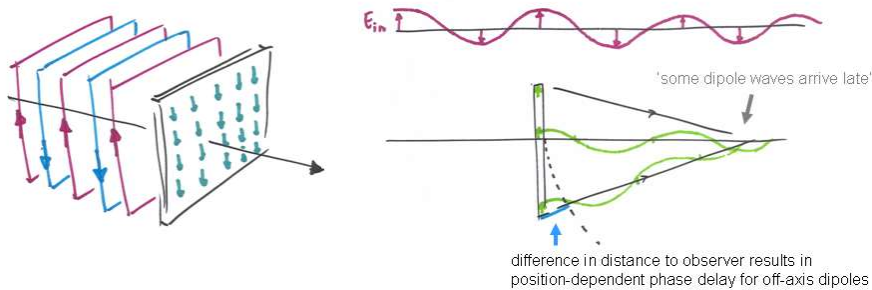
Figure 1.4 Excitation of a sheet of dipoles, and resultant field on optical axis

To understand the frequency dependence of the refractive index, we need to add the frequency dependent response of a Lorentz oscillator to this picture. We know that at low frequencies we obtain a finite dipole moment and zero phase delay, while near resonance the phase delay approaches 90° and the amplitude reaches a maximum. At high frequencies the phase difference approaches 180° and the amplitude approaches zero. The resulting changes of the refractive index are sketched below:
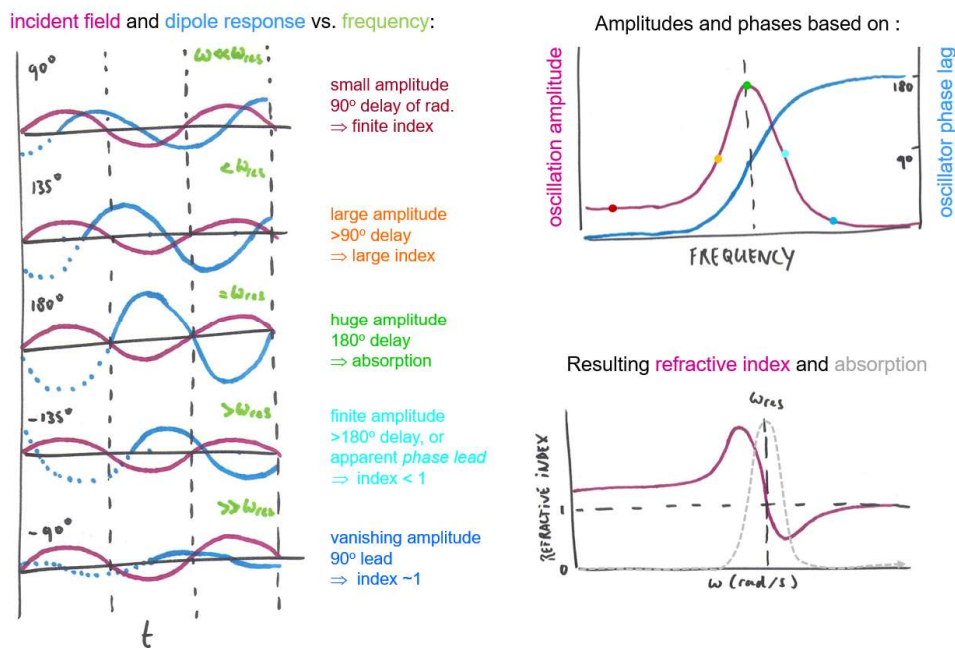
Figure 15.5 Field from sheet of dipoles excited at different frequencies

9

At low frequencies (top graph), the Lorentz oscillator responds in-phase with the incident light, but due to the collective 'dipole sheet' effect described above, the net phase delay is 0°(oscillator) + 90°(sheet effect) = 90°. By adding this finite phase-delayed response to the incident field, the light appears to propagate slightly slower, corresponding to a finite refractive index n>1. As the frequency increases, the oscillation amplitude goes up, as does the phase delay. Both effects together add up to a larger delay, and a higher refractive index. Exactly at the resonance frequency, the oscillation amplitude reaches a maximum. However, at this frequency the Lorentz oscillator responds with a phase delay of 90°, resulting in a total phase delay of 90°(oscillator)+90°(sheet effect)=180°. The dipoles can be seen to generate radiation that destructively interferes with the incident light, resulting in a change of the amplitude, but no change in the phase, corresponding to a real part of the refractive index close to 1, and finite absorption. At frequencies above the resonance, the phase delay exceeds 180°, which can be seen as a phase *lead*. The light appears to be *accelerated*, corresponding to a refractive index less than 1. The resulting refractive index curve is shown on the right side of the Figure. As we will see in later chapters, a more thorough model description of the polarization of atoms in a material leads to similar refractive index spectra.

Chapter 2 - Light propagation in lossless media

➢ Corresponding handouts are available on http://kik.creol.ucf.edu/courses.html

In Chapter 1 we saw that the refractive index of materials can be understood as the result of dipole radiation from charges accelerated by the electric field. In this chapter we will take a different viewpoint. Instead of considering separate contributions from individual atomic dipoles, we assume that materials can be described as having a smoothly distributed polarization. We will call this the '*continuum*' description. The effect of such a continuous medium on wave propagation is described by Maxwell's equations. In this Chapter we discuss light propagation through a material in which all charges respond instantly to applied fields, corresponding to a perfectly transparent (lossless) medium.

Wave propagation in vacuum

As mentioned in Chapter 1, light is an electromagnetic wave containing an oscillatory electric field and an oscillatory magnetic field. To fully describe a light wave we therefore need to know the magnitude and direction of E and B at every point in space. The corresponding field distributions are time dependent vector fields, written as $\vec{E}(\vec{r}, t)$ and $\vec{B}(\vec{r}, t)$.

Maxwell's equations describe the classical relations between charge (units Coulomb, C), current (C/s), electric field (V/m), and magnetic flux density B (Wb/m^2 or Tesla=10^4 Gauss). The complete Maxwell equations include terms related to free charge, see Appendix B, however here we focus on light propagating either in vacuum or in homogeneous media without localized free charge concentrations, which simplifies the equations.

Before we discuss light-matter interaction, let's first discuss light propagation in the absence of any matter. In <u>vacuum</u> (no material, no free charges), Maxwell's Equations are

$$\nabla \cdot \vec{E} = 0 \tag{2.1}$$

$$\nabla \cdot \vec{B} = 0 \tag{2.2}$$

$$\nabla \times \vec{E} = -\frac{\partial \vec{B}}{\partial t} \tag{2.3}$$

$$\nabla \times \vec{B} = \epsilon_0 \mu_0 \frac{\partial \vec{E}}{\partial t} \tag{2.4}$$

Here ϵ_0 is the *vacuum permittivity* and μ_0 is the *vacuum permeability*. These equations allow for electric and magnetic field solutions that oscillate in space and time, and that propagate together. Instead of trying to solve for B and E at once, we first use these equations to derive an expression that puts requirements on E and that does not explicitly depend on B. Taking the curl of Eq. 2.3 and the negative time derivative of Eq. 2.4, we find

$$\nabla \times \nabla \times \vec{E} = -\frac{\partial}{dt}(\nabla \times \vec{B}) \qquad (2.5)$$

$$-\frac{\partial}{\partial t}(\nabla \times \vec{B}) = -\epsilon_0 \mu_0 \frac{\partial^2 \vec{E}}{\partial t^2} \qquad (2.6)$$

Comparing these two relations we see that the following relation must be satisfied:

$$\nabla \times \nabla \times \vec{E} = -\epsilon_0 \mu_0 \frac{\partial^2 \vec{E}}{\partial t^2} \qquad (2.7)$$

Using the general vector relation $\nabla \times (\nabla \times \vec{F}) = -\nabla^2 \vec{F} + \nabla(\nabla \cdot \vec{F})$ we have

$$-\nabla^2 \vec{E} + \nabla(\nabla \cdot \vec{E}) = -\epsilon_0 \mu_0 \frac{\partial^2 \vec{E}}{\partial t^2} \qquad (2.8)$$

Since we are in vacuum, the field is divergence-free (no net charge present). We thus have found an equation linking a double spatial derivative (i.e. the *curvature*) of E to a double time derivative of E:

$$\nabla^2 \vec{E} = \epsilon_0 \mu_0 \frac{\partial^2}{\partial t^2} \vec{E} \qquad (2.9)$$

This is the wave equation in vacuum, which allows many different wave-like solutions, including spherical waves, cylindrical waves, and complicated phenomena like curved Airy beams and non-diffracting beams. It also allows a wide variety of time dependencies, including 'single-frequency' (narrowband) laser light, regular sequences of short pulses with evenly spaced frequency contributions (a 'frequency comb'), or a Gaussian distribution of frequency components producing a single short pulse. This text doesn't focus on such exotic cases. Instead, to understand light matter interaction we can focus on the simplest possible time-dependent solution to the wave equation: the plane wave, described by

$$\vec{E}(t, \vec{r}) = \vec{E}_r \cos(\vec{k} \cdot \vec{r} - \omega t + \phi). \qquad (2.10)$$

Here $\vec{E}_r = (E_{rx}, E_{ry}, E_{rz})$ is a fixed field amplitude vector of the wave in units V/m, ω is the angular frequency in rad/s, $\vec{k}$ is the wavevector, $\vec{r}$ is the position, and ϕ is a possible fixed phase offset. The angular frequency $\omega(rad/s)$ is simply given by $\omega = 2\pi f$ and is written as having units rad/s, to indicate a phase that varies by ω radians per second. The radian is not a physical unit so in principle it could be omitted, but the convention is to include it when dealing with angular frequency. The wavevector k describes spatial variation of the field, with a magnitude given by k=$2\pi/\lambda$ with λ the wavelength. The wavevector describes 'phase variation per distance' in radians per meter, but it is typically written as having units m^{-1}. The direction of the wavevector corresponds to the propagation direction of the wave.

Maxwell's equations put requirements on the allowed orientations of $\vec{B}$ and $\vec{E}$ relative to $\vec{k}$ and to each other, but in deriving the wave equation for $\vec{E}$ in vacuum we lost any requirements on the direction of the field vector (or its magnitude for that matter). Note that Eq. 2.9 represents three identical scalar wave equations for E_{rx}, E_{ry}, and E_{rz}. Apparently our field components each must satisfy the *scalar wave equation*:

$$\nabla^2 E = \epsilon_0 \mu_0 \frac{\partial^2}{\partial t^2} E \qquad (2.11)$$

Since vacuum is isotropic, light propagation occurs exactly the same way for any choice of propagation direction. To find requirements on the relation between angular frequency and wavevector, we can thus use a scalar trial function of the form

$$E(t,z) = E_r \cos(kz - \omega t) \qquad (2.12)$$

where we have chosen direction along the z axis, and set the phase offset to zero for simplicity of notation. Substituting this trial function into the scalar wave equation, and taking the temporal and spatial derivatives we find

$$-\omega^2 E_r \cos(kz - \omega t) = -k^2 \epsilon_0 \mu_0 E_r \cos(kz - \omega t) \Rightarrow \frac{\omega}{k} = \sqrt{\frac{1}{\epsilon_0 \mu_0}} \equiv c \qquad (2.13)$$

It can easily be shown that the quantity ω/k is the speed at which phase fronts move through space, known as the *phase velocity* v_p. Apparently Maxwell's Equations demand that light moves through vacuum at a fixed velocity, independent of the frequency. This speed is known as 'light speed', denoted by c.

The wavelength of light in vacuum λ_0 follows simply from

$$\frac{\omega}{k} = \frac{\omega}{2\pi/\lambda_0} = c \quad \Rightarrow \quad \lambda_0 = \frac{2\pi c}{\omega} \qquad (2.14)$$

Note that we haven't proven that our trial wave is a solution to Maxwell's Equations. We have only proven that our trial wave with phase velocity c satisfies our scalar wave equation for the electric field. To satisfy Maxwell's equations, we still need to find a combination of $\vec{E}$, $\vec{B}$ and $\vec{k}$ that satisfies relations 2.3 and 2.4. Substituting a vectorial trial wave for E and B with the same phase velocity and a shared wavevector $\vec{k}$ it can be shown that E and B are normal to each other with a relative magnitude c, and that both are normal to the direction of the wavevector. This is known as a transverse electromagnetic wave.

Field-induced polarization in materials

In vacuum, light of any frequency propagates along $\vec{k}$ at a constant speed c. Inside materials however, light propagation is modified by the interaction between the electromagnetic fields and charges. Materials are composed of atoms that contain positive and negative charge in the form of protons in the atom core and electrons surrounding the core. In metals the outermost electrons, known as valence electrons, are free to move, while in non-metals ('dielectrics'), the valence electrons are bound to the atoms. These charged particles experience forces when electromagnetic fields are present, causing them to move in response to the fields. Consequently light propagation inside materials becomes a combined phenomenon of charge motion and field oscillation, changing – among other things – the speed at which light moves through the material.

A large part of light-matter interaction can be understood in terms of a property known as polarization $\vec{P}$(C/m^2), representing the dipole moment per unit volume. Polarization inside a material develops due to forces on the electrons and the atom cores in the presence of an

electromagnetic wave. An electric field E tends to move the positive atom core in one direction and the electrons in the opposite direction. The atom core is several orders of magnitude heavier than the electron and therefore moves much less than the electrons, so the movement of the core is usually ignored. The small displacement r of the electrons *relative to the atom core* corresponds to a dipole moment

$$\vec{\mu}(t) = q_e\vec{r} = -e\vec{r} \tag{2.15}$$

with q_e=-e the charge of the electron. If the material contains N(m^{-3}) of such electrons per unit volume that all respond in the same way, the dipole moment per unit volume simply becomes

$$\vec{P} = -eN\vec{r} \tag{2.16}$$

The electron displacement is typically less than a millionth of the atomic diameter, depending on the field strength, but as we will see in Chapters 5 and 6, the combined effect of the many electrons in typical solids still has a significant effect on light propagation.

In principle the polarization response of materials to an applied field can be complicated. For example, while the electrons move in response to the field, the polarization can have a different time dependence than the electric field, or even a different direction than the applied electric field. This makes it challenging to find solutions to Maxwell's Equations inside materials. However many materials are isotropic, in which case the electrons move along the field direction, and thus polarization points along the same axis as the electric field. Moreover, electrons are very light and consequently they can accelerate rapidly (recall F=m·a), i.e. they respond very quickly to the field. In the simplest possible model we might expect that the dipole moment related to the movement of bound electrons is linearly dependent on the applied field strength, according the following relation:

$$\vec{P}(t) = \epsilon_0\chi_\delta\vec{E}(t) \tag{2.17}$$

where χ is a unitless scaling factor. This is <u>not</u> a general relation. It is an approximate relation that assumes that the electron response is *instantaneous*, meaning that the dipole moment appears immediately when a field is applied, and *linear,* meaning that doubling the electric field doubles the magnitude of the dipole moment. Nevertheless, these assumptions are helpful in beginning to understand the effect of polarization on light propagation.[iv]

The unitless quantity χ is known as the electric susceptibility, where the subscript δ indicates that its use in this time dependent relation is appropriate for instantaneous response only. We will derive a more general expression for χ in the next chapter. The vectorial notation with a scalar (non-tensorial) χ is only allowed in isotropic media. Despite all these assumptions and approximations, this relation actually represents quite a reasonable description of the response of transparent media excited at frequencies well below any absorption band. Next, we will discuss the effect of instantaneous polarization on wave propagation.

[iv] We will discuss what happens when we go beyond these approximations in Chapters 3 and 8.

Wave propagation in a lossless medium

Previously we found that Maxwell's equations in vacuum allow for transverse electromagnetic waves propagating with a phase velocity c. In the presence of matter (free electrons, atoms containing protons and electrons), two things change about Maxwell's equations. First, the divergence of the field may become nonzero:

$$\nabla \cdot \vec{E} = \frac{\rho}{\epsilon_0} \tag{2.18}$$

Here $\rho(C/m^3)$ is the total charge density. Inside homogeneous isotropic neutral (uncharged) materials the charge density remains zero, even when excited with light, so we will continue to use $\nabla \cdot \vec{E} = 0$. Nevertheless, it's important to realize that this is not generally true. Second, the relation describing the curl of the magnetic field changes as follows:

$$\nabla \times \vec{B} = \epsilon_0 \mu_0 \frac{\partial \vec{E}}{\partial t} + \mu_0 \left[J_f + \nabla \times \vec{M} + \frac{\partial \vec{P}}{\partial t} \right] \tag{2.19}$$

The newly introduced terms between the square brackets are 'matter' related terms: free electric current density J_f, magnetization current density $\nabla \times \vec{M}$, and polarization current density $\partial \vec{P}/\partial t$. This equation directly shows how electromagnetic waves inside materials are different from those in vacuum. The added terms thus represent '*light matter interaction*'. In this text, we discuss the polarization current density caused by light-induced charge motion[v], which we will model in Chapters 5 and 6.

To understand the effect of polarization on light propagation, we reconsider the wave equation. In the absence of magnetization and free current density, we have

$$\nabla \times \vec{E} = -\frac{\partial \vec{B}}{dt} \tag{2.20}$$

$$\nabla \times \vec{B} = \epsilon_0 \mu_0 \frac{\partial \vec{E}}{\partial t} + \mu_0 \frac{\partial \vec{P}}{\partial t} \tag{2.21}$$

Taking the curl of the top equation and the negative time derivative of the bottom equation as we did before, we find

$$\nabla \times \nabla \times \vec{E} = -\frac{\partial}{dt} \left(\nabla \times \vec{B} \right) \tag{2.22}$$

$$-\frac{\partial}{\partial t} \left(\nabla \times \vec{B} \right) = -\epsilon_0 \mu_0 \frac{\partial^2 \vec{E}}{\partial t^2} - \mu_0 \frac{\partial^2 \vec{P}}{\partial t^2} \tag{2.23}$$

Comparing these two relations we see that the following is also true:

$$\nabla \times \nabla \times \vec{E} = -\epsilon_0 \mu_0 \frac{\partial^2 \vec{E}}{\partial t^2} - \mu_0 \frac{\partial^2 \vec{P}}{\partial t^2} \tag{2.24}$$

---

[v] Note that the equation doesn't limit us to only light induced polarization. For example, shooting an electron through a thin piece of material will also cause charge motion, producing polarization and a field response that can in large part be described by Maxwell's equations.

Again using the general vector relation $\nabla \times (\nabla \times \vec{F}) = -\nabla^2 \vec{F} + \nabla(\nabla \cdot \vec{F})$ we have

$$-\nabla^2 \vec{E} + \nabla(\nabla \cdot \vec{E}) = -\epsilon_0 \mu_0 \frac{\partial^2 \vec{E}}{\partial t^2} - \mu_0 \frac{\partial^2 \vec{P}}{\partial t^2} \qquad (2.25)$$

Recall that $\nabla \cdot \vec{E} = \rho/\epsilon_0$. Now that there are charges present (electrons, protons) we cannot generally state that $\nabla \cdot \vec{E} = 0$ inside materials. However, when dealing with homogeneous isotropic neutral materials excited with light, the resulting fields remain divergence-free. Under these assumptions we have obtained a similar wave equation as for the case of vacuum, but with an additional term related to polarization:

$$\nabla^2 \vec{E} = \epsilon_0 \mu_0 \frac{\partial^2}{\partial t^2}\left(\vec{E} + \frac{\vec{P}}{\epsilon_0}\right). \qquad (2.26)$$

This relation still properly describes materials with a realistic non-instantaneous and even possibly a nonlinear and anisotropic response. In materials with a *linear*, *isotropic*, and *instantaneous* polarization response we can further simplify by using the relation $\vec{P}(t) = \epsilon_0 \chi_\delta \vec{E}(t)$, giving

$$\nabla^2 \vec{E} = \epsilon_0 \mu_0 (1 + \chi_\delta) \frac{\partial^2 \vec{E}}{\partial t^2}. \qquad (2.27)$$

This relation states that electric fields that oscillate quickly (large double temporal derivative) must have large curvature in space (large double spatial derivative), i.e. must have short wavelength. In addition, it shows that a higher susceptibility also results in a shorter wavelength. Like the case of vacuum, this relation allows for plane-wave solutions, however with a modified phase velocity. We again substitute a scalar plane wave of the form

$$E(t, z) = E_r \cos(kz - \omega t) \qquad (2.1)$$

into the scalar wave equation, giving

$$\nabla^2 (E_r \cos(kz - \omega t)) = \epsilon_0 \mu_0 (1 + \chi_\delta) \frac{\partial^2}{\partial t^2} (E_r \cos(kz - \omega t)) \qquad (2.28)$$

The double spatial derivative on the left adds a factor $-k^2$ while the double temporal derivative on the right adds a factor $-\omega^2$. Dividing out common terms on the left and right results in the following *dispersion relation* linking ω and k:

$$\frac{\omega}{k} \equiv v_p = \frac{c}{\sqrt{1 + \chi_\delta}} \qquad (2.29)$$

Note that the solution with the negative sign is again omitted, since it simply represents a wave propagating in the opposite direction. If there is no polarizable material (meaning $\chi=0$) we reproduce the result of light propagation in vacuum at a phase velocity c. If on the other hand light is propagating inside a material with nonzero χ, we find that the speed of the wave is reduced by a factor $\sqrt{1 + \chi_\delta}$. The wavelength is also reduced:

$$\frac{\omega}{k} = \frac{\omega}{2\pi/\lambda} = \frac{c}{\sqrt{1 + \chi_\delta}} \quad \Rightarrow \quad \lambda = \frac{2\pi c}{\omega} \frac{1}{\sqrt{1 + \chi_\delta}} = \frac{\lambda_0}{\sqrt{1 + \chi_\delta}} \qquad (2.30)$$

We see that inside a polarizable material, both the speed of light and the wavelength are reduced by the same factor $\sqrt{1 + \chi_\delta}$. This quantity is known as the *refractive index* n. For this somewhat unrealistic case of instantaneous response, we have

$$v_p = \frac{c}{\sqrt{1 + \chi_\delta}} \equiv \frac{c}{n}, \quad \lambda = \frac{\lambda_0}{\sqrt{1 + \chi_\delta}} = \frac{\lambda_0}{n} \tag{2.31}$$

We see that our trial plane wave with perfectly constant amplitude is an allowed solution to the wave equation. This corresponds to a wave that propagates 'forever' without losing amplitude. Apparently a material with instantaneous polarization response is entirely lossless. In the next Chapter we will consider a more realistic case, allowing for a finite response time for the electrons.

Chapter 3 - Light propagation in dispersive media

> Corresponding handouts are available on http://kik.creol.ucf.edu/courses.html

In the preceding Chapter we described light propagation in a material with instantaneous response, and we found an expression for the refractive index that did not depend on the frequency of the light. This is a reasonable approximation in transparent materials in a limited spectral range, but it is not generally applicable to realistic materials. In the following we consider materials in which polarization takes some finite time to build up in response to a field, which will result in a frequency-dependent complex refractive index and non-zero absorption.

Time-dependent susceptibility – the impulse response

As discussed in Chapters 1 and 2, applying an electric field to atoms in a material results in the appearance of dipole moment as a result of the electric force on the electron. In Chapter 2 we assumed for simplicity that bound electrons respond instantaneously to the field, meaning that the dipole moment would be perfectly in-phase with the electric field. In reality, an electron once pushed will keep moving for a while, meaning that charge motion (and dipole moment) can be changing *after* the force was applied. As an example in the sketch below, after briefly pushing an object, we might see some oscillatory motion after the push. In this case the position is clearly not linearly proportional to the force.
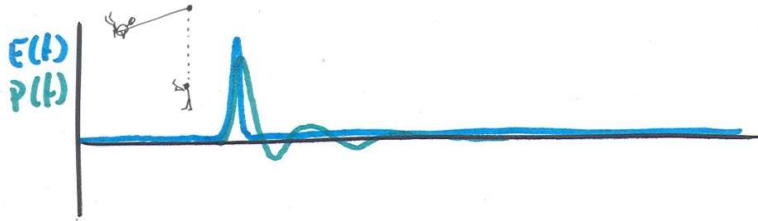
Figure 3.1

To describe a time-dependent response to a time-varying field, we consider a time-dependent susceptibility[vi] $\chi(t)$. This function represents the response to a single short (read: "delta function") electric field pulse, and is called the 'impulse response'.

We can understand the concept of a $\chi(t)$ function as follows: after a short electric pulse $E(t')$, electrons in the material will have acquired some velocity that follows from the integration of their acceleration. For electrons initially at rest, the velocity after the short pulse is thus

$$v(t) = \int_{-\infty}^{t} a(t')dt' = \int_{-\infty}^{t} \frac{F_e(t')}{m_e} dt' = -\frac{e}{m_e} \int_{-\infty}^{t} E(t')dt'$$

We see that the electron velocity after a short pulse scales with the time integral of the electric field. After the short pulse the electrons will keep moving until the material slows

---

[vi] After Chapter 4 we will exclusively work with the *frequency* dependent susceptibility $\chi(\omega)$, but it is helpful to understand how $\chi(t)$ and $\chi(\omega)$ are related.

them down. The resulting time-dependent charge movement and associated dipole moment will thus depend on the material response (damping that slows down the electrons, binding forces that pull back the electrons), which can be represented by a time-dependent susceptibility $\chi(t)$ (s^{-1}).[vii] In general, to determine the polarization at some arbitrary time t, we would need to know all forces that the electrons experienced at *all* earlier times. Mathematically this can be written as:

$$P(t) = \epsilon_0 \int_{-\infty}^{\infty} E(t')\,\chi(t-t')dt' \tag{3.2}$$

Here t' means "*when was the field applied*", (t-t') means "*how long ago was that*", and $\chi(t-t')$ tells us "*should we still expect a response this much later*". Note that the integral seems to consider electric fields in the future (t'>t), but those signals do not contribute in since $\chi(t)$ is zero for t<0. This makes sense: there should be no response before the force is applied, which is also known as the material having a 'causal response'.

In short, we have seen that in a realistic case of electrons with a non-instantaneous response to fields, we clearly cannot write a simple proportional relation between P(t) and E(t). Instead we need to carry out a somewhat complicated integral. However, if the material response is *linear*, i.e. if doubling the field strength produces double the polarization, it turns out that we can still find a simple relation between P and E, provided we consider excitation *at a single frequency*. The reason for this is that in linear media, exciting the electrons with a perfectly harmonic (sinusoidal) electric field results in an electron position (and thus polarization) that is *also* sinusoidal in time, but possibly with a phase delay. To describe such a phase-delayed polarization response to a harmonic field, we thus need two parameters: the *magnitude* of the response, and the *phase delay* of the response. This can be achieved with the use of a complex susceptibility, as discussed below.

Real electric fields as a sum of complex exponents

Before discussing the effect of complex susceptibility, we first introduce the notion of complex field amplitude. Measureable properties such as the electric field, the polarization, current, etc. are *real* quantities (as in "not complex"). A propagating oscillatory electric field is described by a real harmonic function such as a sine or cosine, for example

$$E(t,z) = E_r \cos(k_z z - \omega t + \phi). \tag{3.3}$$

Here φ is a possible phase offset and E$_r$ is a real field amplitude. Although the field must be real, we can choose to describe this real field with complex numbers, using the general relation $e^{i\theta} = \cos(\theta) + i\sin(\theta) \Rightarrow \cos(\theta) = \frac{1}{2}(e^{i\theta} + e^{-i\theta})$. With this relation we can write our real electric field as

$$E(t,z) = \frac{1}{2} E_r\, e^{i(k_z z - \omega t + \phi)} + \frac{1}{2} E_r e^{-i(k_z z - \omega t + \phi)} \tag{3.4}$$

We can rewrite this as follows:

$$E(t,z) = \frac{1}{2} E_r\, e^{i\phi} e^{i(k_z z - \omega t)} + \frac{1}{2} E_r e^{-i\phi} e^{-i(k_z z - \omega t)}. \tag{3.5}$$

[vii] Since the charge response depends on field strength *and* on the duration of the pulse, if follows that $\chi(t)$ must have units s^{-1}.

If we define a complex field amplitude $E_0 = E_r e^{i\phi}$ we can write our *real* field as a sum of complex oscillatory contributions:

$$E(t,z) = \frac{1}{2} E_0 \, e^{i(k_z z - \omega t)} + c.c. \tag{3.6}$$

where c.c. stands for *complex conjugate*, meaning 'with the opposite complex phase' (achieved by changing all *i* terms to -*i*). Note that the *complex amplitude* E_0 now contains information about both the *magnitude* of the field oscillation (given by $|E_0|$) and the *phase offset* φ, described by the argument of the complex exponent. As stated earlier, this is exactly what we need to describe the polarization response of a material with a non-instantaneous response.

The analysis above helps understand the meaning of complex Fourier transforms. A time-dependent real electric field E(t) cannot in general be described with a single harmonic wave, but according to Fourier theory it *can* be described as a superposition of harmonic functions with different frequencies and phases. The complex amplitude for all these frequencies is described by the Fourier amplitude E(ω). A real field at some fixed location z can thus be written as

$$E(t) = \int_{-\infty}^{\infty} E(\omega) \, e^{-i\omega t} d\omega \tag{3.7}$$

Note that we don't explicitly have a complex conjugate term anymore. Instead this term is captured by including 'negative frequencies' in the Fourier integral. To clarify this, note that the integral above is exactly equal to the following integral over positive frequencies only:

$$E(t) = \int_{0}^{\infty} E(\omega) \, e^{-i\omega t} + E(-\omega) \, e^{+i\omega t} \, d\omega. \tag{3.8}$$

We see that the negative frequency contribution represents the complex conjugate term which ensures that we end up with a real field. Note that it follows that the Fourier transform of a real field time dependent field must satisfy the following relation:

$$E(\omega) = E^*(-\omega) \tag{3.9}$$

where the asterisk indicates taking the complex conjugate. This is known as the *reality condition*, which can also be written as

$$E'(\omega) = E'(-\omega) \quad E''(\omega) = -E''(-\omega) \tag{3.10}$$

where the single prime indicates the real part, and the double prime indicates the imaginary part. This is a general rule for the Fourier transform of real time-dependent quantities.

Frequency dependent susceptibility

Now that we understand complex amplitudes and Fourier transforms, we can derive a simplified relation between P and E in a realistic non-instantaneous material. First we write all time dependent quantities in their Fourier form, i.e. we use our Fourier description of E(t), as well as polarization P(t) and susceptibility χ(t), i.e. we will use

$$P(t) = \int_{-\infty}^{\infty} P(\omega)\, e^{-i\omega t}\, d\omega \qquad (3.11)$$

and

$$\chi(t) = \int_{-\infty}^{\infty} \chi(\omega)\, e^{-i\omega t}\, d\omega \qquad (3.12)$$

Substituting these descriptions of P(t), χ(t), and E(t) into Eq. 3.2, repeated here with the integration limits omitted for simplicity of notation:

$$P(t) = \epsilon_0 \int E(t')\, \chi(t - t')\, dt' \qquad (3.2)$$

we obtain

$$\int P(\omega)\, e^{-i\omega t}\, d\omega = \epsilon_0 \int\int E(\omega)\, e^{-i\omega t'}\, d\omega \int \chi(\omega')\, e^{-i\omega'(t-t')}\, d\omega'\, dt' \qquad (3.13)$$

where we have replaced the frequency argument in the Fourier integral of χ(t) with ω' to distinguish it from the frequency argument of $E(t)$. Switching the order of integration and grouping terms that depend on t' we get the following:

$$\int P(\omega)\, e^{-i\omega t}\, d\omega = \epsilon_0 \int\int E(\omega)\, d\omega\, \chi(\omega')\, e^{-i\omega' t} \int e^{i(\omega'-\omega)t'}\, dt'\, d\omega'. \qquad (3.14)$$

The integral $\int e^{i(\omega'-\omega)t'}\, dt' = 2\pi\delta(\omega' - \omega)$, giving

$$\int P(\omega)\, e^{-i\omega t}\, d\omega = \epsilon_0 \int\int E(\omega)\, d\omega\, \chi(\omega')\, e^{-i\omega' t}\, 2\pi\delta(\omega' - \omega)\, d\omega'. \qquad (3.15)$$

Integrating over ω' we are left with

$$\int P(\omega)\, e^{-i\omega t}\, d\omega = 2\pi\epsilon_0 \int \chi(\omega) E(\omega) e^{-i\omega t}\, d\omega. \qquad (3.16)$$

In this expression and the preceding ones, $\chi(\omega)$ always represented the Fourier transform of $\chi(t)$, also written as $\mathcal{F}[\chi(t)]$. The relation above needs to satisfied for arbitrary distributions E(ω), which in turn implies that it must be true for each separate frequency component.[viii] We have arrived at the relation

$$P(\omega) = \epsilon_0\, (\, 2\pi\mathcal{F}[\chi(t)]\,)\, E(\omega). \qquad (3.17)$$

The *entire* quantity $2\pi\mathcal{F}[\chi(t)]$ is commonly written as $\chi(\omega)$ even though it's not strictly speaking the Fourier transform of $\chi(t)$. In practice this rarely leads to confusion, since frequency dependent response is usually measured or modeled, rather than being determined from a measured time-dependent susceptibility. With that convention in mind, we have found

---

[viii] This can by shown formally by Fourier transforming both sides of the equation, e.g. replacing frequency arguments left and right with ω' and ω'', and doing a Fourier Transform to ω on both sides. This introduces exponents of the form $e^{i(\omega-\omega')t}$ which act as a delta function, removing the integrals.

$$P(\omega) = \epsilon_0\, \chi(\omega) E(\omega). \tag{3.18}$$

We have derived a linear relation between the field and the polarization, but now in the frequency domain. Crucially, we have found that $\chi(\omega)$ in a realistic causal system is an intrinsically <u>complex</u> quantity that describes the *magnitude* of the polarization response, as well as the *phase delay* of the polarization response relative to a harmonic excitation field. The sketch below shows an example: a harmonic driving field induces a harmonic oscillating polarization. The polarization appears with a phase delay with respect to the driving field. This means that the phase argument of $P(\omega)$ needs to be different than that of $E(\omega)$. This is captured by the phase argument of $\chi(\omega)$.
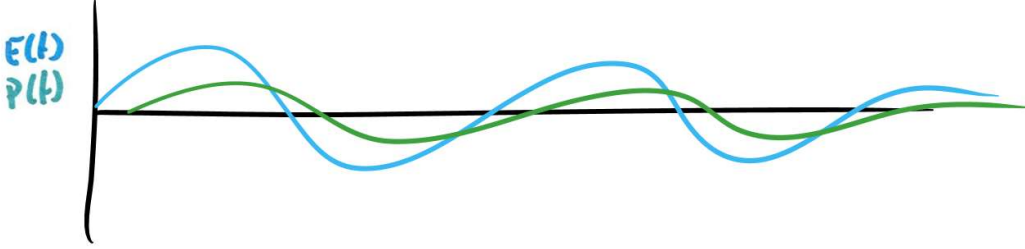
Figure 3.2

In short, we see that in a realistic material, the susceptibility automatically becomes complex. This behavior is unavoidably accompanied by absorption, as discussed below.

Wave propagation in a material with complex susceptibility

We previously found the scalar wave equation which describes wave propagation inside homogeneous, isotropic materials:

$$\nabla^2 E = \epsilon_0\mu_0 \frac{\partial^2}{\partial t^2}\left(E + \frac{P}{\epsilon_0}\right) \tag{3.19}$$

We try solutions of the form

$$E(x,t) = \int E(\omega)e^{i(k_\omega x-\omega t)}d\omega, \quad P(x,t) = \int P(\omega)e^{i(k_\omega x-\omega t)}d\omega. \tag{3.20}$$

Here k_ω is the as yet unknown wavevector required to satisfy the wave equation at for the field contribution oscillating at ω. We showed that in linear systems at a given ω, P and E have a fixed phase relation. To achieve this, at a minimum P and E must move at the same velocity, i.e. they must have the same wavevector. If the scalar wave equation must hold for electric fields and polarizations, it can easily be shown that the scalar wave equation must also hold for individual frequency contributions in the Fourier integrals. For real waves described by complex amplitudes, apparently we must have

$$\nabla^2\left(E(\omega)e^{i(k_\omega x-\omega t)}\right) = \epsilon_0\mu_0 \frac{\partial^2}{\partial t^2}\left(E(\omega)e^{i(k_\omega x-\omega t)} + \frac{P(\omega)e^{i(k_\omega x-\omega t)}}{\epsilon_0}\right) \tag{3.21}$$

Taking the spatial and temporal derivatives and dividing out all shared factors $e^{i(k_\omega x-\omega\ )}$, we arrive at the relation

$$-k_\omega^2 E(\omega) = \epsilon_0\mu_0(-\omega^2 E(\omega) - \omega^2 P(\omega)/\varepsilon_0) \tag{3.22}$$

Now substituting the complex relation between P and E, and simplifying we find[ix]

$$k(\omega) = \frac{\omega}{c}\sqrt{1 + \chi(\omega)} \tag{3.23}$$

where we have written k_ω as $k(\omega)$, and where ω/c is simply the vacuum wavevector $k_0 = 2\pi/\lambda_0$. We can also define a complex relative permittivity ε_r as

$$\varepsilon_r \equiv 1 + \chi(\omega) \tag{3.24}$$

which leads to the relation

$$k(\omega) = \frac{\omega}{c}\sqrt{\varepsilon_r(\omega)} \tag{3.25}$$

Comparing with our previous relation $k = n\omega/c$, we can also write this in terms of a complex refractive index, which we will write as $\eta(\omega)$.

$$k(\omega) = \frac{\omega}{c}\eta(\omega) \tag{3.26}$$

We have found a dispersion relation describing the link between wavevector and angular frequency. Critically, the susceptibility, dielectric function, and refractive index are all complex. This means that if we excite a real material at a constant frequency ω, Maxwell's equations dictate that our plane wave must have a complex wavevector! As we will see below, this implies nonzero absorption of the wave. First, let's establish the relations between χ, η, and ε_r.

We have the relation

$$\eta(\omega) = \sqrt{\varepsilon_r(\omega)} = \sqrt{1 + \chi(\omega)} \tag{3.27}$$

The real and imaginary parts of η will be written as n and κ, i.e.

$$\eta(\omega) \equiv n(\omega) + i\kappa(\omega) \tag{3.28}$$

The real and imaginary parts of the susceptibility will be written as χ' and χ'', i.e.

$$\chi(\omega) \equiv \chi'(\omega) + i\chi''(\omega) \tag{3.29}$$

Explicitly writing the real and imaginary parts of η and χ we thus have[x]

$$n(\omega) + i\kappa(\omega) = \sqrt{1 + \chi'(\omega) + i\chi''(\omega)} \tag{3.30}$$

Taking the square of both sides, grouping real and imaginary parts, and omitting the frequency arguments, we find

$$n^2 - \kappa^2 = 1 + \chi' = \varepsilon_r' \qquad 2n\kappa = \varepsilon_r'' = \chi'' \tag{3.31}$$

These relations provide a straightforward way to find the susceptibility from a complex refractive index. Finding the refractive index from a complex dielectric function is more involved. The simplest way is taking a complex root of ε_r on a calculator. If that's not an option, the following relations can be used:

[ix] We ignore the negative root here, which simply represents a wave propagating in the opposite direction.
[x] This still ignores magnetic effects, and assumes that the material is isotropic, homogeneous, and linear.

$$n = \sqrt{(|\varepsilon_r| + \varepsilon_r')/2} \qquad \kappa = \sqrt{(|\varepsilon_r| - \varepsilon_r')/2} \tag{3.32}$$

where the magnitude of ε_r is simply $|\varepsilon_r| = \sqrt{\varepsilon_r'^2 + \varepsilon_r''^2}$. While these relations are exact, they may give inaccurate results for κ on a calculator in the common case of small imaginary index (and small absorption). In such cases it is better to use the low-absorption approximation described in Appendix H.

As stated above, a complex refractive index implies that the wavevector, given by $k = \eta\omega/c$, also becomes complex:

$$k(\omega) \equiv k'(\omega) + ik''(\omega) = \eta(\omega)\left(\frac{\omega}{c}\right) = nk_0 + i\kappa k_0 \tag{3.33}$$

where we have again used the free-space wavevector $k_0 = \omega/c = 2\pi/\lambda_0$. A plane wave of the form

$$E(t,z) = \frac{1}{2}E_0\, e^{i(k_z z - \omega t)} + c.c. \tag{3.34}$$

with a complex wavevector $k = \eta k_0 = (n + i\kappa)k_0$ becomes

$$E(t,z) = \frac{1}{2}E_0\, e^{i((n+i\kappa)k_0 z - \omega t)} + c.c. = e^{-\kappa k_0 z}\left(\frac{1}{2}E_0 e^{i(nk_0 z - \omega t)} + c.c.\right) \tag{3.35}$$

We see that the complex nature of the refractive index results in a position dependent field amplitude of magnitude $|E(z)| = |E_0 e^{-\kappa k_0 z}|$.

Absorption coefficient

The position dependent field amplitude derived in the preceding section implies light absorption. Propagating EM waves carry optical power, which is described by the quantity *irradiance*, representing incident power per unit area (W/m²). Using the expressions for the energy density in electric and magnetic fields, as well as the expression for the speed[xi] of light and the ratio between E and B from Maxwell's equations, it can be shown that a plane wave with amplitude E carries an irradiance:

$$I\left(\frac{W}{m^2}\right) = \frac{1}{2}nc\epsilon_0|E|^2 \tag{3.36}$$

In our non-instantaneous material, we thus find a position dependent irradiance given by

$$I(z) = \frac{1}{2}nc\epsilon_0|E(z)|^2 = \frac{1}{2}nc\epsilon_0|E_0|^2\, e^{-2\kappa k_0 z} \equiv I_0 e^{-\alpha z} \tag{3.37}$$

where I_0 is the initial irradiance at position z=0. The term α is known as the *absorption coefficient*, given by

$$\alpha = 2\kappa k_0 = 2\kappa\frac{\omega}{c} = \frac{4\pi}{\lambda_0}\kappa \tag{3.38}$$

[xi] Technically we need the group velocity in this analysis rather than phase velocity, but in most cases the phase velocity and group velocity are almost identical.

Associated with the absorption coefficient is the quantity *1/e depth $d_{1/e}$* or '*skin depth*' δ, a term that is most commonly used when describing highly absorbing materials such as metals. The skin depth is the depth d at which the irradiance[xii] has dropped by a factor e, reaching ~36.8% of its initial value. This occurs when the term $\alpha z = 1$, resulting in

$$\delta = \frac{1}{\alpha} = \frac{1}{2\kappa k_0} = \frac{c}{2\kappa\omega} = \frac{1}{4\pi\kappa}\,\lambda_0 \tag{3.39}$$

The last version of the expression of the 1/e depth provides a convenient way of estimating the absorption depth based on a given κ. If we make the extremely crude approximation that $4\pi \approx 10$, we easily see that an imaginary index of 0.1 gives a 1/e depth of ~λ_0. Apparently, an imaginary index of $\kappa = 0.1$ causes most of the incident light to be absorbed within one optical wavelength. This is a *huge* absorption coefficient. If you memorize this single data point, all other values of κ are easily estimated: for every reduction of κ by a factor 10 the 1/e depth becomes a factor 10 larger. We found $\kappa = 0.1 \rightarrow d_{1/e} \approx 1\lambda_0$ so it follows that $\kappa = 0.01 \rightarrow d_{1/e} \approx 10\lambda_0$, and $\kappa = 0.001 \rightarrow d_{1/e} \approx 100\lambda_0$ etc. This approximate relation is worth memorizing, because it will help make a quick estimate of light transmission through thick samples.

Example: if green light ($\lambda_0 = 0.5\ \mu m$) enters a 1 mm thick piece of glass with a seemingly small $\kappa(\omega) = 0.0001$, we now know that the 1/e depth is about a thousand wavelengths, or ~0.5 mm. Ignoring reflection losses, a 1mm piece of this glass will thus transmit about $(1/e)^2$ of the incident light (a factor 1/e for every 0.5 mm), resulting in a transmission of about 14%. Apparently even a 'small' value of $\kappa = 10^{-4}$ is enough to produce a very significant amount of absorption in samples that are of the order of 1 mm thick.

[xii] Note, in electrical engineering the term "skin depth" usually refers to the 1/e depth of the *electric field* magnitude, resulting in double the skin depth compared to the values used in this text.

Chapter 4 – Kramers-Kronig relations

➢ Corresponding handouts are available on http://kik.creol.ucf.edu/courses.html

In the preceding Chapter we learned that a material with a realistic non-instantaneous electron response had a complex refractive index, with frequency dependent real refractive index ('dispersion') and frequency dependent absorption coefficient. This implies that absorption and refractive index are related quantities. It turns out that there is an elegant relation that links measured absorption spectra to the corresponding index spectrum. This relation is one of the Kramers-Kronig relations. In this Chapter we will derive the Kramers-Kronig relations, and show some examples of how they can be used to make predictions about dispersion.

Kramers-Kronig relations for susceptibility

"Kramers-Kronig" relations link $\chi'(\omega)$ and $\chi''(\omega)$, $n(\omega)$ and $\alpha(\omega)$, and $R(\omega)$ and $\theta(\omega)$. We start by deriving the KK relation linking $\chi'(\omega)$ and $\chi''(\omega)$. The starting point is the time-dependent polarization:

$$P(t) = \varepsilon_0 \int_{-\infty}^{\infty} E(t') \chi(t - t') dt' \tag{4.1}$$

$\uparrow$ response function (linear)

The polarization response function must obey causality, i.e. the effect cannot precede the cause. This can be explained mathematically as follows:

Mathematical statement of causality:

$$E = 0, \quad t < 0 \tag{4.2}$$

i.e. no response before E applied

$$\Rightarrow \chi(t) = 0 \text{ for } t < 0$$

$$\text{or } \chi(t - t') = 0 \text{ for } t < t'.$$

This can be expressed quite compactly using the "step function"

$$\Rightarrow \chi(t) = \theta(t)\chi(t) \tag{4.3}$$

where, $\theta(t) = \begin{cases} 0 & t < 0 \\ 1 & t > 0 \end{cases}$ is the Heaviside function or unit step function

Actually, any function that equals unity for t>0 and equals anything but unity for t<0, will do. For example, the Signum function, defined as

$$Sgn(t) = \begin{cases} -1 & t < 0 \\ 1 & t > 0 \end{cases}, \tag{4.4}$$

will work just as well. (As it must.)

So we now have a time-domain statement of causality that can be Fourier transformed for give a frequency domain statement of causality:

$$\chi(\omega) = F\{\theta(t)\chi(t)\} = \int_{-\infty}^{\infty}\theta(t)\chi(t)e^{i\omega t}\,dt \tag{4.5}$$

but,

$$\chi(t) = \int_{-\infty}^{\infty}\chi(\omega')e^{i\omega' t}\,d\omega' \tag{4.6}$$

$$\Rightarrow \chi(\omega) = \int_{-\infty}^{\infty}dt\int_{-\infty}^{\infty}d\omega'\theta(t)\chi(\omega')e^{i(\omega-\omega')t}$$

$$= \int_{-\infty}^{\infty}d\omega'\chi(\omega')\int_{-\infty}^{\infty}dt\,\theta(t)e^{i(\omega-\omega')t}\,. \tag{4.7}$$

Hence,

$$\chi(\omega) = \int_{-\infty}^{\infty}d\omega'\chi(\omega')\int_{-\infty}^{\infty}dt\,\theta(t)e^{i(\omega-\omega')t}$$

$$= \int_{-\infty}^{\infty}d\omega'\chi(\omega')\theta(\omega-\omega'). \tag{4.8}$$

Now the Fourier Transform of the step function is well known:

$$\theta(\omega) = F\{\theta(t)\} = \frac{1}{2}\delta(\omega) + \frac{i}{2\pi\omega} \tag{4.9}$$

$$\Rightarrow \chi(\omega) = \int_{-\infty}^{\infty}d\omega'\chi(\omega')\frac{1}{2}\delta(\omega-\omega') + i\int_{-\infty}^{\infty}d\omega'\frac{\chi(\omega')}{2\pi(\omega-\omega')} \tag{4.10}$$

$$\Rightarrow \quad \frac{1}{2}\chi(\omega) = \frac{i}{2\pi}\int_{-\infty}^{\infty}d\omega'\frac{\chi(\omega')}{2\pi(\omega-\omega')}\,. \tag{4.11}$$

Which gives the statement of causality in the frequency domain:

$$\Rightarrow \chi(\omega) = \frac{i}{\pi}\int_{-\infty}^{\infty}\frac{\chi(\omega')}{\omega-\omega'}\,d\omega'\,. \tag{4.12}$$

We can make use of the "i" in the relationship to find cross relations for the real and imaginary parts of χ. Splitting $\chi(\omega)$ into its real and imaginary parts:

$$\chi(\omega) = \chi'(\omega) + i\chi''(\omega)$$

$$= \frac{i}{\pi}\int_{-\infty}^{\infty}\frac{\chi'(\omega')}{\omega-\omega'}\,d\omega' - \frac{1}{\pi}\int_{-\infty}^{\infty}\frac{\chi''(\omega')}{\omega-\omega'}\,d\omega' \tag{4.13}$$

Which yields two equations:

$$\chi'(\omega) = -\frac{1}{\pi}\int_{-\infty}^{\infty}\frac{\chi''(\omega')}{\omega-\omega'}\,d\omega' \tag{4.14}$$

$$\chi''(\omega) = \frac{1}{\pi}\int_{-\infty}^{\infty}\frac{\chi'(\omega')}{\omega-\omega'}\,d\omega' \tag{4.15}$$

These are the "Kramers-Kronig" relations for $\chi(\omega)$.

We can use the results of the reality condition, ($\chi'(\omega)$ is even, $\chi''(\omega)$ is odd) to re-write these integrals in terms of positive frequencies only:

$$\chi'(\omega) = -\frac{2}{\pi}\int_0^\infty \frac{\omega'\chi''(\omega')}{\omega'^2-\omega^2}d\omega' \tag{4.16}$$

and

$$\chi''(\omega) = -\frac{2\omega}{\pi}\int_0^\infty \frac{\chi'(\omega')}{\omega'^2-\omega^2}d\omega' . \tag{4.17}$$

Relation between (κ and X'') and (n and X') for weak susceptibility

For a weak susceptibility (rarified media, gases), we have $|\chi'|$, $|\chi''| \ll 1$. In this case,

$$n(\omega) + i\kappa(\omega) = \sqrt{1 + \chi'(\omega) + i\chi''(\omega)} \approx 1 + \frac{\chi'(\omega)}{2} + i\frac{\chi''(\omega)}{2} , \tag{4.18}$$

so that,

$$n(\omega) \approx 1 + \frac{\chi'(\omega)}{2} \quad , \quad \text{and} \tag{4.19}$$

$$\kappa(\omega) \approx \frac{\chi''(\omega)}{2} \quad \rightarrow \quad \alpha(\omega) \approx \frac{\omega}{c}\chi''(\omega) \tag{4.20}$$

We can now use these approximate relations to find the *Kramers-Kronig relation for index and absorption*:

$$\chi'(\omega)\!\big/_{\!2} = n(\omega) - 1 = \frac{1}{\pi}\int_0^\infty \frac{\omega'\alpha(\omega')c/\omega'}{\omega'^2-\omega^2}d\omega'$$
$$\Rightarrow \quad n(\omega) = 1 + \frac{c}{\pi}\int_0^\infty \frac{\alpha(\omega')}{\omega'^2-\omega^2}d\omega' \tag{4.21}$$

Although this has been derived for a weak susceptibility, it is actually true in general. This is a very useful relation, as it is relatively easy to measure $\alpha(\omega)$ over a broad wavelength band.

The dispersion of refractive index around a resonance

It is worth looking at the form of the Kramers-Kronig integrals, to see what the lead us to expect about the relationship between $n(\omega)$ and $\alpha(\omega)$, etc. Let us consider a material with a single, moderately narrow absorption line. In Figure 4.1 we sketch such a line, where ω_{res} is the resonance frequency, or frequency. (This could be 1 rad/s, 1 Hz, or one hundred terahertz, or whatever units we desire.) The refractive index at any frequency ω depends on the integral of $\alpha(\omega')$, multiplied by $1/(\omega'^2 - \omega^2)$, so we also plot the function $1/(\omega'^2 - \omega^2)$ below for two cases: one where the frequency, ω, is just above the peak absorption and one where ω is just below the peak absorption.

Clearly for $\omega > \omega_{res}$, the integral of the product is negative which is to say that the $n(\omega)$ due to a particular resonance is < 1 for frequencies above that resonance. Similarly, frequencies below a resonance, the refractive index arising from that resonance is positive. If the resonance is symmetric, then for $\omega = \omega_{res}$, the refractive index due to the absorption line will be unity – i.e. the absorption line will not affect the refractive index exactly at the resonance frequency.
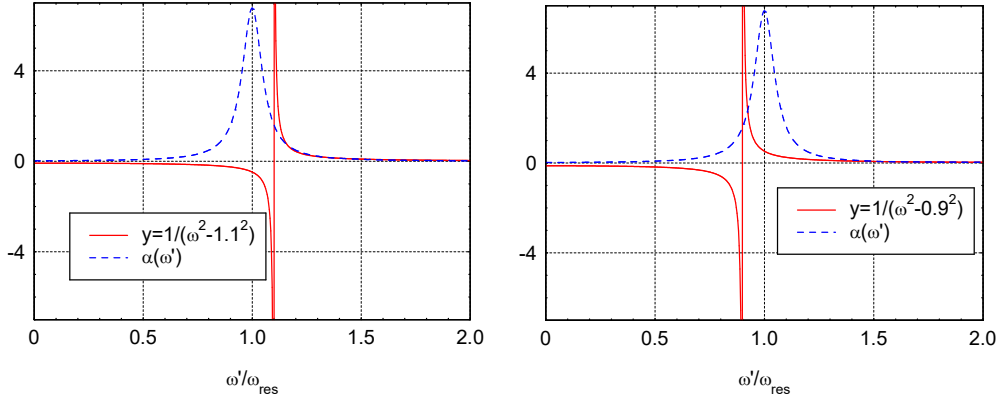
Figure 4.1

The above observations are generally true, regardless of the precise shape of the absorption resonance. Certainly, the exact shape of $\alpha(\omega)$ will affect the precise shape of $n(\omega)$, but here we are only talking in generalities. It is also important to note that we make no assumptions about the physical process giving rise to the absorption line, as it is irrelevant to these general observations. – There can be no exception to the Kramers – Kronig relations. – If there is an absorption line in a material, then it will cause the refractive index to be increased below resonance and decreased above. Usually, a material will have several absorption resonances, which may occur in the infrared, in the visible and in the ultraviolet. At very low frequencies, say in the far infrared, which lie below all resonances, the index may therefore be quite high, as all absorption resonances contribute positively at these low frequencies. We can also conclude that at very high frequencies, say in the ultraviolet, for which all resonances are at lower frequencies, the refractive index must be below unity. This last fact is not widely known, but as we see from our analysis, it is inescapable and must be true for all materials. As we examine different types of materials and physical processes that give rise to light-matter interactions, we will see again and again that these general predictions that come from the Kramers-Kronig relations are always fulfilled.
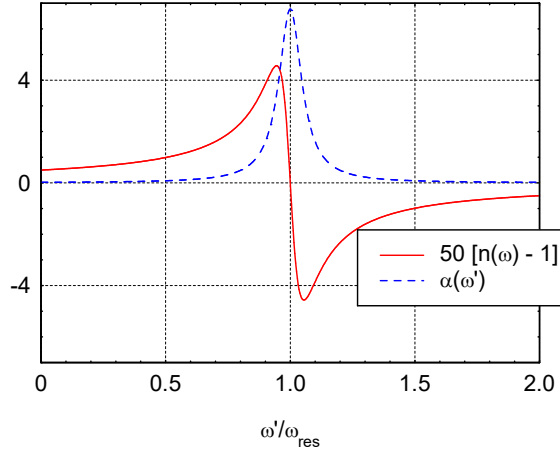
Figure 4.2

To get a general spectrum of n(ω), (usually referred to as the *dispersion* of n) we just calculate the result of the Kramers-Kronig integral repeatedly for many values of ω. The result for n(ω) for the absorption line shown in Figure 4.2, where we have arbitrarily expanded the scale for (n-1) to show it on the same scale as $\alpha(\omega)$.

Derivation of Kramers-Kronig relations by Cauchy's integral theorem

Given that,

$$P(t) = \varepsilon_0 \int_{-\infty}^{\infty} E(t')\chi(t-t')dt' \ , \tag{4.22}$$

and that

$$P(\omega) = \varepsilon_0 \chi(\omega)E(\omega) \ , \tag{4.23}$$

where,

$$\chi(\omega) = \int_{-\infty}^{\infty} \chi(t)e^{i\omega t}dt \ . \tag{4.24}$$

Now by causality, the above integral need only run over positive times:

$$\therefore \chi(\omega) = \int_{0}^{\infty} \chi(t)e^{i\omega t}dt \ , \tag{4.25}$$

i.e. t is always positive in the integral. Now, we can let ω be complex, so that, $\omega = \omega' + i\omega''$ giving

$$\chi(\omega) = \int_{0}^{\infty} \chi(t)e^{i\omega't}e^{-\omega''t}dt \ . \tag{4.26}$$

and since t is always positive, the factor $e^{-\omega''t}$ tells us that for positive ω'', the function $\chi(\omega)$ has a regular analytic continuation in the positive imaginary half of the complex plane of ω.

31

By Cauchy's integral theorem, the closed path integral of a function that is analytic in a simple domain yields a zero result. Now we consider the integral

$$\oint_c \frac{\chi(\omega)d\omega}{\omega-\Omega} = 0 , \tag{4.27}$$

where C is a closed path in the upper half plane of ω that avoids all poles (singularities), as shown on the next page.
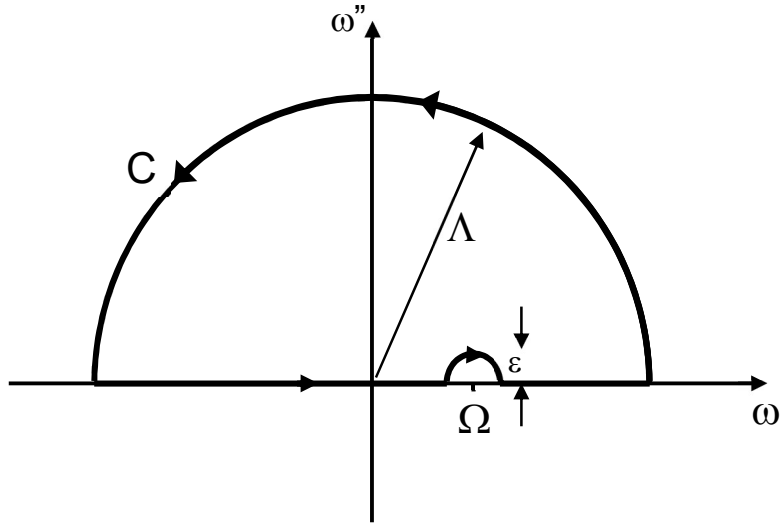
Figure 4.3

We can look at the four main parts of the integral. First, the large semicircle, defined by $\omega = \Lambda e^{i\theta}$, where θ runs from 0 to π. In the limit as $\Lambda \to \infty$, this part of the integral becomes zero, provided that $\chi(\omega)$ is reasonably well behaved, or more specifically, provided that

$$\lim_{\omega\to\infty}\left[\frac{\chi(\omega)}{\omega}\right]=0 .$$

The small semicircle is centered on a pole caused by the $1/(\omega-\Omega)$ term. By the Residue Theorem, in the limit of vanishingly small radius, ε, we have,

$$\int_\varepsilon \frac{\chi(\omega)d\omega}{\omega-\Omega} = -i\pi\chi(\Omega) , \tag{4.28}$$

(i.e. a "half-residue" of the integrand at Ω.) The straight sections of the integral, in the limit of $\varepsilon \to 0$, become;

$$\lim_{\varepsilon\to 0}\left\{\int_{-\infty}^{\Omega-\varepsilon}\frac{\chi(\omega)d\omega}{\omega-\Omega}+\int_{\Omega+\varepsilon}^{\infty}\frac{\chi(\omega)d\omega}{\omega-\Omega}\right\}=\wp\int_{-\infty}^{\infty}\frac{\chi(\omega)d\omega}{\omega-\Omega} \tag{4.29}$$

where $\wp$ denotes the Cauchy Principal Value. Hence the sum of the four parts of the path integral becomes

$$0 - i\pi\chi(\Omega) + \wp \int_{-\infty}^{\infty} \frac{\chi(\omega)d\omega}{\omega - \Omega} = 0, \qquad (4.30)$$

i.e.

$$\chi(\Omega) = \frac{1}{i\pi} \wp \int_{-\infty}^{\infty} \frac{\chi(\omega)d\omega}{\omega - \Omega} = 0, \qquad (4.31)$$

which is the Kramers-Kronig relation as previously derived. This is basically just Cauchy's Integral Theorem. (The principal value ($\wp$) label really just means that we should avoid the pole, but in practice, this turns out to be trivial, so we will not continue to use $\wp$.)

The above analysis is less physically insightful than the one given before, but this is the treatment usually given for Kramers Kronig relations in most texts. It is also convenient to use, since any causal function that is analytic in the upper-half plane can be treated in the same way, and this can save some time in deriving Kramers-Kronig relations. This is the case for the relations for the relations between the amplitude and phase of a reflected wave, which we treat next.

Kramers-Kronig relations for Reflected Amplitude and Phase

There exists a very useful type of Kramers-Kronig relation that relates the phase and amplitude of reflection from an interface. Now the reflectance,

$$R(\omega) = r(\omega)r^*(\omega) \qquad (4.32)$$

Where $r(\omega)$ is the electric field amplitude reflection coefficient, which for an air-material interface, is given by

$$r(\omega) = \frac{1 - n(\omega) - i\kappa(\omega)}{1 + n(\omega) + i\kappa(\omega)} . \qquad (4.33)$$

Now we can also write $r(\omega)$ in terms of a phase and an amplitude:

$$r(\omega) = \rho(\omega)e^{i\theta(\omega)}, \qquad (4.34)$$

where $\theta(\omega)$ is the phase shift upon reflection. *(Note – this is NOT the unit step function, $\theta(t)$, used earlier.)* Clearly, if we can completely determine both $r(\omega)$ and $\theta(\omega)$, we can completely determine both $n(\omega)$ and $\kappa(\omega)$. Now, it is relatively straight forward to determine $R(\omega)$, but it is hard to imagine how we could easily measure $\theta(\omega)$ over a large spectral range. We would like to find a Kramers-Kronig relation that relates $\theta(\omega)$ to $\rho(\omega)$, but we note that while we can do this for complex analytic functions of the form $\chi(\omega) = \chi'(\omega) + i \chi''(\omega)$, or $\eta(\omega) = n(\omega) + i \kappa(\omega)$, we cannot do so for a function of the form $r(\omega) = \rho(\omega)\exp(i\theta(\omega))$. – We could always find a Kramers-Kronig relation between $r'(\omega)$ and $r''(\omega)$, but this is of no particular use, as we cannot easily individually measure either the real or the imaginary part of $r(\omega)$. However, if we take the *log* of $r(\omega)$, we get

$$\ln\{r(\omega)\} = \ln\{\rho(\omega)\} + i\theta(\omega), \qquad (4.35)$$

for which, via the Cauchy integral theorem, we can write down a pair of Kramers-Kronig relations:

$$\ln\{\rho(\omega)\} = -\frac{1}{\pi}\int_{-\infty}^{\infty}\frac{\theta(\omega')\,d\omega'}{\omega'-\omega}$$

$$\theta(\omega) = \frac{1}{\pi}\int_{-\infty}^{\infty}\frac{\ln\{\rho(\omega')\}\,d\omega'}{\omega'-\omega}$$

(4.36)

where, as usual, the "principal value" of the integral is to be taken. Clearly the second of the two relations is the more useful, in the same sense that the relation that gives n(ω) in terms of $\alpha(\omega)$ is more useful than one that gives α in terms of n. – It is much easier to measure amplitudes than phase. We can re-write this integral in terms of positive frequencies only:

$$\theta(\omega) = \frac{2\omega}{\pi}\int_{0}^{\infty}\frac{\ln\{\rho(\omega')\}\,d\omega'}{\omega'^2-\omega^2}$$

(4.37)

Note that our previous approach of applying causality in the form of a step function in the time domain is not valid in the same way as for χ, as for t < 0, $\rho = 0$ gives $\ln\rho = -\infty$, which is not so easy to handle. For the same reason, one might look at this integral and conclude that it probably will not work, as for regions where R(ω) $\to$ 0, $\ln\rho \to -\infty$. Nevertheless, it still seems to work, as we shall see from the homework assignment. Those who are interested may read the details in Wooten, but the scope of this course is limited to the results.

There is a useful trick to remove the singularity at $\omega' = \omega$. We may simply subtract the quantity

$$\frac{2\omega}{\pi}\int_{0}^{\infty}\frac{\ln\{\rho(\omega)\}\,d\omega'}{\omega'^2-\omega^2} = \frac{2\omega}{\pi}\ln\{\rho(\omega)\}\int_{0}^{\infty}\frac{d\omega'}{\omega'^2-\omega^2} \equiv 0$$

(4.38)

from the integral in the KK relation. Hence

$$\theta(\omega) = \frac{2\omega}{\pi}\int_{0}^{\infty}\frac{\left[\ln\{\rho(\omega')\}-\ln\{\rho(\omega)\}\right]d\omega'}{\omega'^2-\omega^2}$$

$$= \frac{\omega}{\pi}\int_{0}^{\infty}\frac{\ln\{R(\omega')/R(\omega)\}\,d\omega'}{\omega'^2-\omega^2}.$$

(4.39)

Hence as $\omega \to \omega'$, R(ω')/R(ω) $\to$ 1 and hence $\ln\{$ R(ω')/R(ω) $\} \to 0$. We can apply the L'Hopital rule to see that the divergence is removed.

Chapter 5 – Lorentz model of the optical properties of dielectrics

➢ Corresponding handouts are available on http://kik.creol.ucf.edu/courses.html

In Chapter 3 we learned that optical effects such as reflection, transmission, and absorption are related to the refractive index, which followed from the complex susceptibility. This means that we can make a prediction of the optical properties of materials if we can develop a model for $\chi(\omega)$. In this chapter we will discuss the optical response of materials that have a strong absorption at one or more well-defined frequencies. We will first derive the response of a simplified atom using what is known as the Lorentz model, which describes the electrons that surround atoms as being bound to the atom core with a phenomenological spring constant. It gives a fairly realistic prediction of dispersion of the refractive index in regions of low absorption, and an approximate understanding of n and κ trends near strong absorptions.

Classical Lorentz oscillator model for absorption & dispersion

Atoms consist of a positive atom core containing protons (charge per proton $+1e$) and neutrons. The total electric charge of the atom core is $+eZ$ where Z is the atomic number Z. The atomic number of most commonly used materials ranges from 1-100. A neutral atom is surrounded by a total of Z electrons. These electrons are bound to the atom core by Coulomb interaction forces, orbiting the core with a spatial distribution described by quantum mechanics (see Chapter 9). For atoms with large Z, some of the electrons are bound very tightly to the core, called *core electrons*, orbiting the cores at small distance. Other electrons occupy larger orbits, circling the positive core and its tightly bound core electrons. Consequently, these outer electrons experience a smaller net positive charge from the core, and therefore smaller Coulomb binding forces. The outermost electrons that finally make the atom neutral are called the valence electrons. These electrons 'see' the least attractive force, and are therefore easiest to move. As a result, the valence electrons often account for most of the polarization response of atoms.
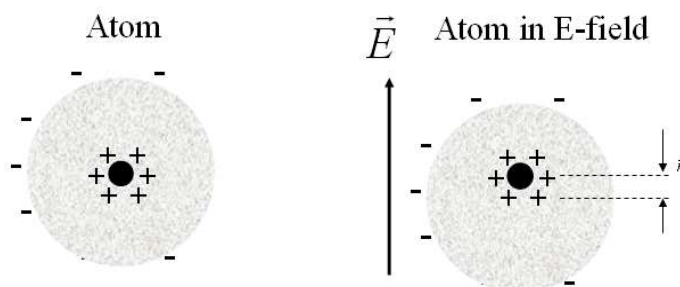
Figure 5.1

The Lorentz model takes all these elements to build the simplest possible mechanical model of an atom. This model makes several key assumptions. **First** of all, it assumes that movement of the atom core can be neglected, which is reasonable given that the core mass is well over three orders of magnitude larger than the electron mass. **Second**, the Lorentz model considers only the valence electrons, assuming that the core electrons are so tightly bound that the electromagnetic wave is practically unable to move them ('no core electron response'). **Third**, it assumes that valence electrons are bound to the core in an effectively

harmonic (quadratic) binding potential. This somewhat reasonable: without an applied electric field the electrons are in a steady state around the core, and therefore in a minimum-energy configuration. Moving the electrons out of equilibrium will result in a restoring force that tries to bring the electrons back into equilibrium. The Lorentz model assumes that this restoring force is linearly dependent on the displacement from equilibrium r, a relation known as Hooke's Law:

$$\vec{F}_r = -K\,\vec{r} \tag{5.1}$$

Here K is the 'spring constant' (units N/m) in analogy with the classical mass-on-a-spring model. This linear force response implies that the potential energy increases quadratically with increasing position, which is called a 'harmonic' binding potential. **Fourth**, it assumes that the atom responds isotropically and along the applied driving force, which allows us describe the electron position with a scalar $r(t)$, the distance from the core.

Before investigating the various forces that determine the electron motion, we first rewrite the spring constant by considering the response of the electron without an external electric field. Newton's second law of motion states that $F = m\,a = m\,\ddot{r}$. In the absence of any external driving forces this predicts that the position r of a valence electron will behave as

$$\ddot{r}(t) = -\frac{K}{m_e}r \tag{5.2}$$

with m_e the electron rest mass. This type of relation can be satisfied by oscillatory functions of the form r(t) $\propto$ sin(ωt) or r(t) $\propto$ cos(ωt), or[xiii] r(t) $\propto$ exp(-iωt). Substituting a trial solution of the form r(t)=r$_0$ exp(-iωt) with r$_0$ related to the motion amplitude we find

$$\ddot{r}(t) = -\omega^2 r_0\,e^{-i\omega t} = -\frac{K}{m_e}r_0\,e^{-i\omega t} \;\Rightarrow\; \omega = \sqrt{\frac{K}{m_e}} \tag{5.3}$$

The see that the valence electron in this simple model has a natural oscillation frequency which we will refer to as 'the resonance frequency', labeled as ω_0. We have thus found a relation between the spring constant K and the resonance frequency:

$$K = m\omega_0^2 \tag{5.4}$$

In many of the upcoming equations we will write the spring constant K as $m\omega_0^2$.

As in any realistic physical system electron motion will not continue forever. The electron motion is said to be 'damped', with the electron gradually losing energy as it oscillates, leading to a reduced amplitude over time. In the Lorentz model this is phenomenologically described by a 'friction force' F_f corresponding to momentum loss at a rate Γ (units s^{-1}) :

$$F_f(t) = \frac{d(mv(t))}{dt} = -\Gamma\,(mv(t)) \;\Rightarrow\; F_f = -m\,\Gamma\,\dot{r}(t) \tag{5.5}$$

In reality this 'friction' represents many possible causes of loss of motion, for example random collisions with other atoms, coupling to vibrations in a crystal ('electron-phonon coupling'), emission of light ('radiative relaxation'), energy transfer to other electrons ('electron-electron interactions' including effects such as Auger relaxation), to name a few.

[xiii] The exponential expression leads to a complex amplitude, which can be turned into a real amplitude by also considering an oscillatory term with the opposite angular frequency, as shown in Chapter 3

To predict the optical response of valence electrons in the presence of an oscillatory electromagnetic field the Lorentz model only considers electric forces given by

$$F_e(t) = -eE(t) \tag{5.6}$$

where e is again the electric unit charge. The electron response follows from the equation of motion F=ma taking into account the electric driving force, the friction force (damping rate), and the restoring force. The total *equation of motion* thus becomes

$$m\,\ddot{r}(t) = -eE(t) - m\Gamma\dot{r}(t) - m\omega_0^2\,r(t) \tag{5.7}$$

In a linear system we expect that driving at single frequency ω results only in responses that occur at that same frequency. We can assume a real electric field E(t) of the form

$$E(t) = \frac{1}{2}E(\omega)e^{-i\omega t} + c.c. \tag{5.8}$$

and assume that the electron position occurs at the same frequency, described by:

$$r(t) = \frac{1}{2}r(\omega)e^{-i\omega t} + c.c. \tag{5.9}$$

We substitute a trial solution containing only the positive ω contribution.[xiv] After dividing out common terms on both sides, this results in:

$$-m\omega^2\,r(\omega)\; -m\Gamma i\omega\,r(\omega) + m\omega_0^2\,r(\omega) = -e\,E(\omega) \tag{5.10}$$

This leads to an expression for the (complex) harmonic motion amplitude r(ω) in response to a harmonic driving field with amplitude E(ω):

$$r(\omega) = -\frac{e}{m_e}\frac{1}{\omega_0^2 - \omega^2 - i\Gamma\omega}E(\omega) \tag{5.11}$$

We can now find an expression for the dipole moment μ, which is defined as charge times separation distance. Since the atom core is assumed to be stationary at position zero, the dipole moment becomes simply $q_e\,r = -er$. The Lorentz model thus predicts an oscillatory dipole moment with amplitude

$$\mu(\omega) = \frac{e^2}{m_e}\frac{1}{\omega_0^2 - \omega^2 - i\Gamma\omega}E(\omega) \tag{5.12}$$

Before we convert this expression to polarization, it's helpful to look at some limiting behavior. The Lorentz description of the dipole moment of a valence electron on a single atom reproduces several properties that were already predicted in Chapter 1. For example: at very low frequencies (ω → 0) we see an amplitude

$$\mu(0) = \frac{e^2}{m_e}\frac{1}{\omega_0^2}E(\omega)\,. \tag{5.13}$$

Note that μ(0) that is real and positive, which means that the dipole moment is *in-phase* with the driving field. This is expected: Hooke's law in constant field leads to equilibrium when $F_e + F_r = 0$, leading to a fixed dipole moment linearly proportional to E. Also note

---

[xiv] The corresponding negative frequency component follows simply by exchanging –ω for each ω term.

that this static dipole moment depends inversely on ω_0^2. This also makes sense: we saw that $K \propto \omega_0^2$. If the spring is twice as stiff, the same force will yield half as much electron displacement, and thus half as much dipole moment.

As the excitation frequency increases the term $\omega_0^2 - \omega^2$ initially reduces, the magnitude of the denominator drops rapidly, corresponding to a larger magnitude of μ. This is something we predicted in Chapter 1: for excitation near resonance we expect larger motion amplitude. As we approach ω_0 the imaginary contribution $-i\Gamma\omega$ in the denominator becomes more significant. Since the numerator in the expression for the dipole moment is real, the complex nature of the denominator includes all phase information about the dipole response relative to the driving field. When we excite on resonance, i.e. when we use $\omega = \omega_0$ we find

$$\mu(\omega_0) = \frac{e^2}{m_e} \frac{1}{-i\Gamma\omega} E(\omega) = \frac{e^2}{m_e} \frac{i}{\Gamma\omega} E(\omega).$$

(5.14)

Note that our time dependent field for positive ω was described by a field contribution of the $E(\omega)e^{-i\omega t}$ corresponding to a clockwise rotating complex vector. We see that when this field contribution is positive and real, the dipole moment is entirely imaginary, corresponding to a 90° phase delay relative to the driving field. Also note that small damping (small Γ) results in large dipole moment on resonance, as expected.

When we excite at high frequency with $\omega \gg \Gamma$, we see that

$$\mu(\omega \to \infty) = -\frac{e^2}{m_e} \frac{1}{\omega^2} E(\omega) \approx 0$$

(5.15)

We see that the dipole moment is in anti-phase with the driving field, and the dipole moment vanishes as the frequency increases. We have found that bound electrons do not produce much polarization at high frequency. This is the reason why materials become transparent at sufficiently high frequency: when illuminated at sufficiently high frequency, none of the electrons (neither the valence electrons or the core electrons) can respond significantly, and therefore there is little absorption or refraction. Indeed, sufficiently high energy X-Rays can propagate freely through most materials.

We sometimes describe the ability to generate dipole moment with a quantity known as the polarizability α. This links dipole moment and driving field according to $\mu = \alpha E$, resulting in an expression for the Lorentz polarizability α:

$$\alpha(\omega) = \frac{e^2}{m_e} \frac{1}{\omega_0^2 - \omega^2 - i\Gamma\omega}$$

(5.16)

Note that here we assumed an isotropic response, which is reasonable for isolated atoms. If we describe the electronic polarization of molecules we often find that the polarization is not exactly aligned with the driving field, necessitating the use of a polarizability tensor, however in most of this book we will deal with isotropic responses that are described by a scalar polarizability. Be careful not to confuse the polarizability α with the absorption coefficient α.

With our expression for dipole moment we can now easily derive an expression for polarization, or dipole moment per unit volume. With N atoms per unit volume, the net dipole moment per unit volume is

$$\vec{P}(\omega) = N\vec{\mu}(\omega) = N\alpha(\omega)E(\omega) \tag{5.17}$$

This assumes that the atoms respond isotropically. For isotropic mixes of anisotropic molecules one has to do orientational averaging, see for example Chapter 12 on the optical response of molecular liquids.

With the Lorentz expression for polarization $N\alpha(\omega)E(\omega)$ with the relation $P(\omega) = \epsilon_0\chi(\omega)E(\omega)$ we have obtained an expression for the frequency dependent susceptibility:

$$\chi(\omega) = \frac{Ne^2}{m_e\epsilon_0} \frac{1}{\omega_0^2 - \omega^2 - i\Gamma\omega} \tag{5.18}$$

Note that N in fact represents the 'number of oscillators', and in this case the *number of electrons that contribute to the resonance of interest.* For example, a single atom may have multiple valence electrons that contribute to a resonance. In this case, N becomes the number of atoms per unit volume, multiplied by the number of valence electrons per atom. Remember that atoms may have many more electrons, but that the dielectric response is often dominated by the outermost (valence) electrons since those are relatively weakly bound *i.e.* most easily polarizable. A possible exception is high-frequency illumination: when irradiating atoms at far-UV and x-ray frequencies, optical resonances related to excitation of strongly bound core electrons can be observed, however such transitions are not discussed in detail here.

We have assumed local and macroscopic fields are equal, and have ignored spatial averaging - assumed all dipoles are free to point in direction of field.

Note that χ is dimensionless, so that the term $\frac{Ne^2}{\epsilon_0 m}$ has dimensions of ω^2. We set

$$\omega_p^2 = \frac{Ne^2}{\epsilon_0 \, m} \tag{5.19}$$

For reasons that will become apparent later, ω_p is known as the "plasma frequency". We can split the Lorentz susceptibility into its real and imaginary parts:

$$
\begin{aligned}
\Rightarrow \quad \chi(\omega) &= \frac{\omega_p^2}{\omega_0^2 - \omega^2 - i\Gamma\omega} \\
&= \frac{\omega_p^2}{\omega_0^2 - \omega^2 - i\Gamma\omega} \cdot \frac{\omega_0^2 - \omega^2 + i\Gamma\omega}{\omega_0^2 - \omega^2 + i\Gamma\omega} \\
\Rightarrow \quad \chi'(\omega) &= \omega_p^2 \frac{\omega_0^2 - \omega^2}{\left(\omega_0^2 - \omega^2\right)^2 + \Gamma^2\omega^2} \\
\& \quad \chi''(\omega) &= \omega_p^2 \frac{\Gamma\omega}{\left(\omega_0^2 - \omega^2\right)^2 + \Gamma^2\omega^2}
\end{aligned}
\tag{5.20}
$$

See fig 3.1 in Wooten for plots of these quantities.

Resonance Approximation

We can simplify these expressions near resonance, under the approximation $|\omega_0 - \omega| \ll \omega_0$. In this case, $\omega_0 + \omega \cong 2\omega_0$, therefore

$$\left(\omega_0^2 - \omega^2\right)^2 = \left[\left(\omega_0 - \omega\right)\left(\omega_0 + \omega\right)\right]^2 \approx \left(2\omega_0\right)^2 \left(\omega_0 - \omega\right)^2 \qquad (5.21)$$

Hence, we see that in this "resonance approximation" we have

$$\chi'(\omega) \approx \frac{\omega_p^2}{2\omega_0} \frac{\omega_0 - \omega}{\left(\omega_0 - \omega\right)^2 + \left(\Gamma/2\right)^2}$$

$$\& \quad \chi''(\omega) = \frac{\omega_p^2}{2\omega_0} \frac{\Gamma/2}{\left(\omega_0 - \omega\right)^2 + \left(\Gamma/2\right)^2} \qquad (5.22)$$

Γ is the Full width at half maximum (FWHM) of the imaginary part of χ, which has a "Lorentzian" functional form.

Note the symmetry of the real & imaginary parts. The imaginary part of the susceptibility, χ'' is symmetric about ω_0, while χ' is antisymmetric about ω_0. Notice that in the resonance approximation that χ' appears antisymmetric (i.e. about $\omega = 0$) while χ'' appears symmetric. The converse is actually true, as seen before from the reality condition. This highlights that the resonance approximation is strongly invalid far from resonance.

Real Atoms & TRK Sum Rule

In general, atoms & molecules have several resonances, not just a single one as in our model. - Quantum mechanically, there are several resonances electronic resonances, and molecules may exhibit vibrational and rotational resonances also. It turns out that perturbation methods in quantum mechanics yield a result very similar to the classical one. We find

$$\Rightarrow \quad \chi(\omega) = \frac{Ne^2}{\epsilon_0 m} \sum_j \frac{f_j}{\omega_j^2 - \omega^2 - i\Gamma_j\omega} \qquad (5.23)$$

ω_j is the frequency for a transition between two electronic states with energy difference $\hbar\omega_j$. Γ_j is the decay rate for the final state and f_j is known as the "oscillator strength", which obeys the Thomas-Reich-Kuhn sum rule:

$$\sum_j f_j = Z \qquad (5.24)$$

for an atom with Z electrons. This tells us that the total absorption, integrated over all frequencies is dependent only on Z. Usually one resonance dominates all others.
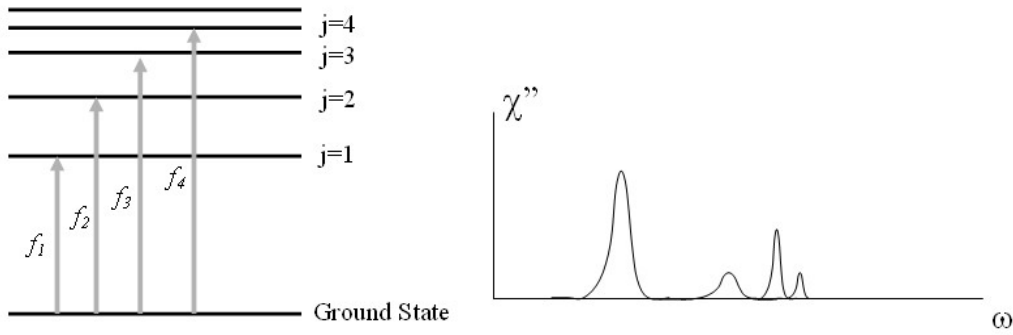
Figure 5.2

The "natural" linewidth is dictated by Γ. Recall Γ is a damping or decay rate, which corresponds to (1/lifetime) of a state. This could range from kHz to GHz. Often the electronic states are split into many sub states. In molecules, each electronic state can exist for many possible vibrational or rotational states of the molecule. Which strongly broadens the electronic "states" into "bands". In solids, the electronic levels are broadened into very broad electronic energy bands. All of these broaden out the optical resonances far in excess of Γ.

In addition to several electronic resonances, other degrees of freedom, such as atomic motions, including molecular vibrations, lattice vibrations, molecular rotations, can interact with the electromagnetic field, producing many resonances over the electromagnetic spectrum. This is illustrated in Wooten, Fig. 3.2.

Our classical, or quantum, model gives the real and imaginary parts of the susceptibility, from which it is easy to obtain the dielectric function, $\varepsilon_r(\omega) = 1 + \chi(\omega)$. Here $\varepsilon_r = \varepsilon / \varepsilon_0$ is the relative permittivity. It is less straightforward, but still not difficult to find expressions for $n(\omega)$ and $\kappa(\omega)$. We start from:

$$n^2(\omega) - \kappa^2(\omega) = \varepsilon_r{}'(\omega)$$
$$2n(\omega)\kappa(\omega) = \varepsilon_r{}''(\omega)$$

(5.25)

From which we obtain

$$n(\omega) = \sqrt{\tfrac{1}{2}\left(\sqrt{\varepsilon_r{}'^2 + \varepsilon_r{}''^2} + \varepsilon_r{}'\right)}$$
$$\kappa(\omega) = \sqrt{\tfrac{1}{2}\left(\sqrt{\varepsilon_r{}'^2 + \varepsilon_r{}''^2} - \varepsilon_r{}'\right)}$$

(5.26)

Armed with n and κ, we can find the absorption and reflectance of the material. Wooten illustrates this in Figs. 3.3 and 3.4. It is often illustrative to plot n, κ, absorption α and R for different values of ω_0, ω_p and Γ. On the next page is an example, using values of 4, 8 and 1, for each of these parameters, respectively. - These seem like strange, unrealistic numbers to use, but our expression for χ contains only frequencies, so the scale is relative. However, it is realistic to think of these numbers as photon energies, $\hbar\omega$, in electron volts (eV).

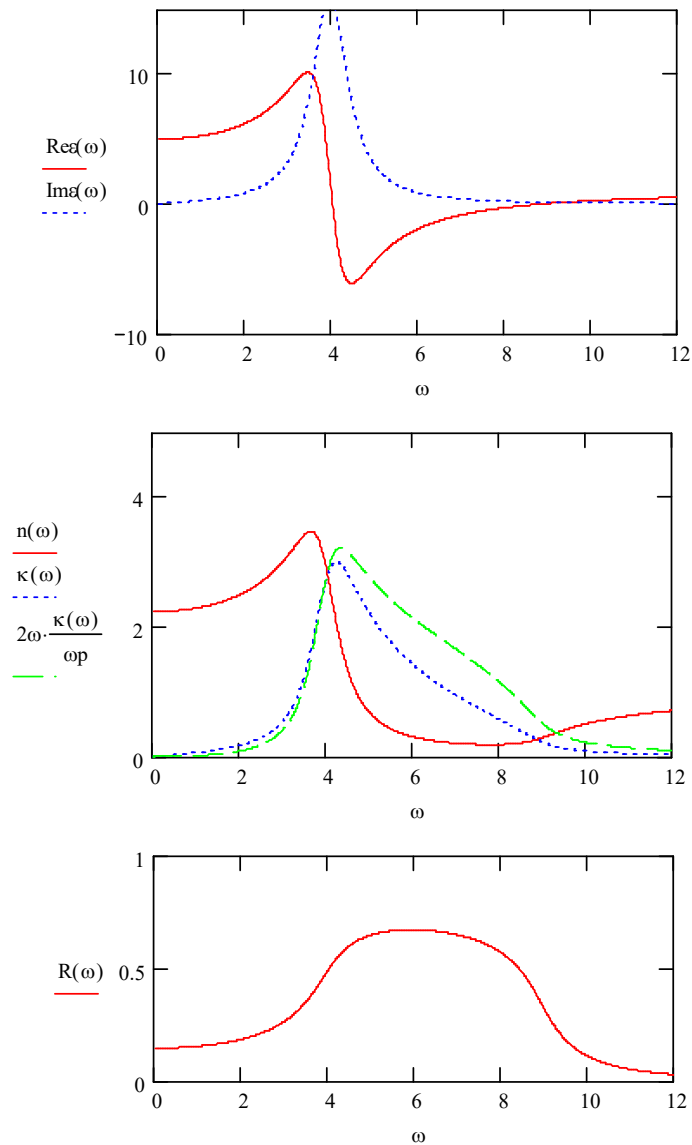Lorentz model for $\omega_0 = 4$, $\omega_p = 8$, $\Gamma = 1$.

Figure 5.3

Note the shapes of the curves are as we would expect from Kramers-Kronig relations. Also note that ε drops below zero between ω_0 and ω_p. We can calculate n and κ from the above relations. n is small over the region where ε is negative. Above ω_p, n gradually rises to 1. Noting that $\alpha = 2\omega \kappa/c$, we have also plotted a scaled version of α, by plotting $2\omega\kappa$, scaled to ω_p. Note how α is skewed to higher frequencies. R is large in the region where n is small, which makes sense, as in the limit of n→0, R →1.

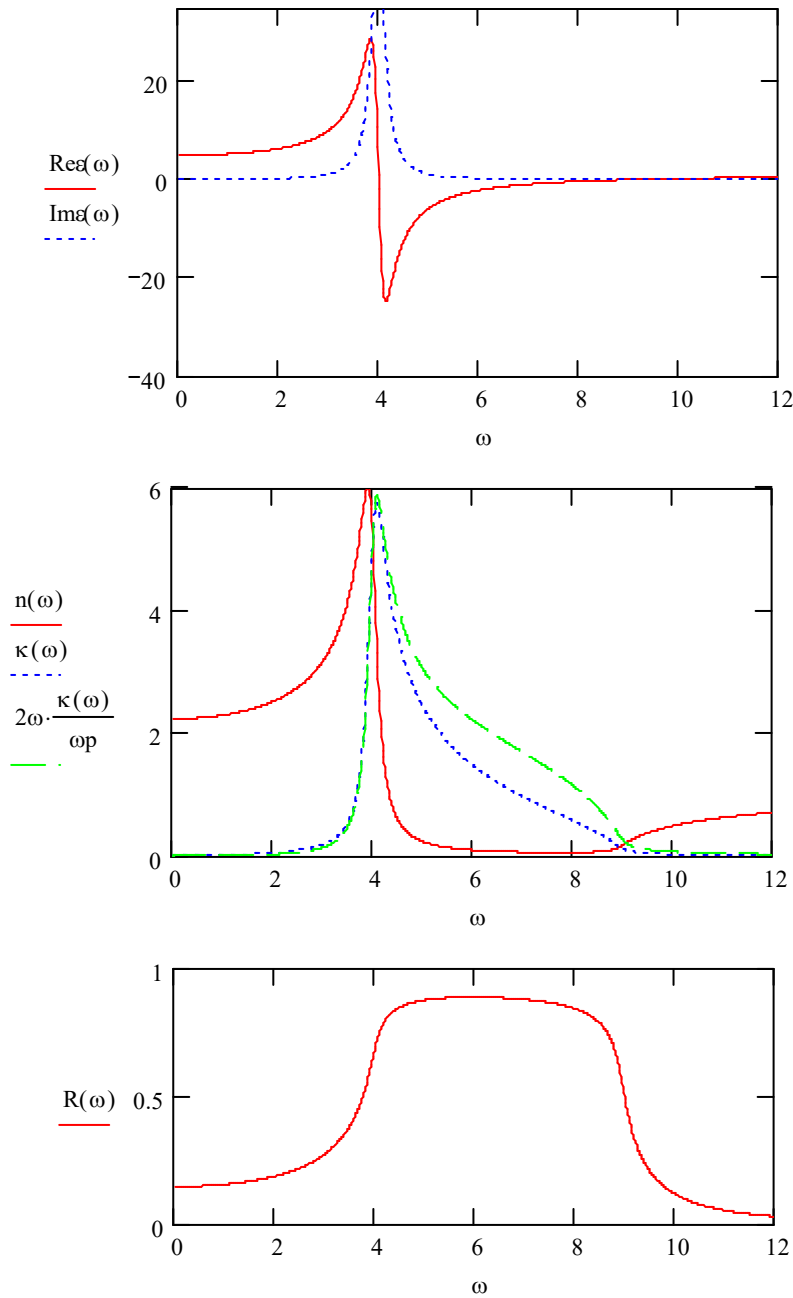Lorentz model for $\omega_0 = 4$, $\omega_p = 8$, $\Gamma = 0.3$.

42

Figure 5.4

As expected, for a smaller damping, $\Gamma = 0.3$, the curves are narrower and have larger maximum values. Above ω_0, n is well below unity. Above ω_p, n rises, but only in the high-frequency limit does n approach unity. This is a good predictor of actual materials. - Above the highest frequency resonance, usually in the deep UV/soft x-ray region, n is indeed less than unity. Causality is not violated, though. Note that near ω_p, $\varepsilon \sim 0$ and hence $n \sim \kappa$. The reflectance is much higher and has sharper edges. Note the high R starts around ω_0 and falls near ω_p. This is because $\kappa \gg n$ in the reflecting band. Note κ is large above ω_0 even where χ'' has dropped to a small value.

T-A-R-T

As described in Wooten, the material has four distinct regions of optical properties,

Transmissive,	$\omega < \omega_0 - \Gamma/2$,
Absorptive,	$\omega_0 - \Gamma/2 < \omega < \omega_0$
Reflective,	$\omega_0 + \Gamma/2 < \omega < \omega_p$
Transmissive	$\omega > \omega_p$

These frequency ranges are approximate. The regions are more distinct for smaller Γ and larger ω_p.

Applicability of the Lorentz model to real materials

(i) Insulators

The Lorentz model works surprisingly well, provided we remember that real materials correspond to a collection of Lorentz oscillators with different frequencies. The outer, or valence, electrons predominantly determine the characteristics of the optical properties a solid. In an ionically – bonded material, e.g. alkali-halides such as KCl, the valence electrons are quite strongly localized at the negative ion (for KCl, this would be the Cl atom), and hence the optical spectrum contains some atomic-like features, with many resonances. As the valence electrons are tightly bound, the resonance frequency is high so that these materials may have a transparency range that extends far into the UV. This can be seen in the reflectance spectrum for KCl shown below (taken from Wooten, Ch. 3.) For these types of materials, the external field and the local field can be quite different and it is not trivial to calculate the local field. For this reason, the Lorentz model does not give quantitatively accurate results for ionic materials.
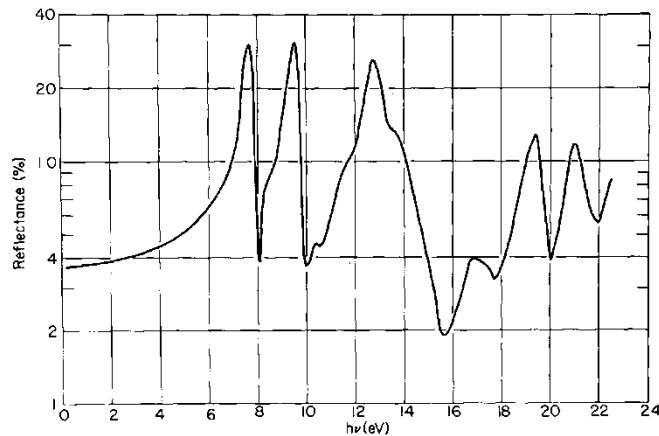
Fig. 3.6 The spectral dependence of the reflectance of KCl. The region of transparency extends to about 7 eV. Above 7 eV, there are a number of sharp peaks related to narrow energy bands and excitons. [From H. R. Philipp and H. Ehrenreich, *Phys. Rev.* 131, 2016 (1963).]

Figure 5.5

(ii) Doped Insulators

Doped insulators, for example ions in glass, behave somewhat like the ions would in a gas, except that the locally strong electric fields of the host materials may distort the spectrum slightly. Figure 5.6 shows the absorption of Nd^{3+} ions in a glass host material.
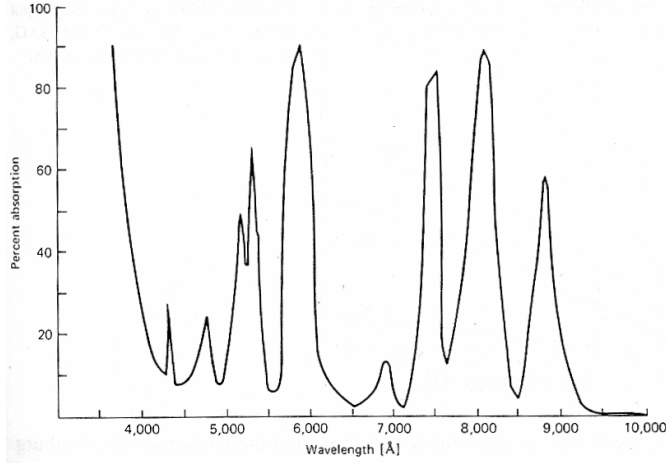

Fig. 2.9. Absorption versus wavelength of Nd : glass. (Material: ED-2; thickness: 6.3 mm)

Figure 5.6

Usually, the absorption of the dopant material is in a region of transparency of the host so that we can approximate the polarization as a superposition of polarizations due to the host and dopant material. For the case of a single resonant absorption line, we may write

$$P_{tot} = P_{host} + P_{dopant} = \varepsilon_0 \left\{ \chi_{host} + \frac{\omega_p^2}{\omega_0^2 - \omega^2 - i\Gamma\omega} \right\} E \qquad (5.27)$$

where χ_{host} is assumed to be real and constant. Hence;

$$\varepsilon_r(\omega) = 1 + \chi_{host} + \frac{\omega_p^2}{\omega_0^2 - \omega^2 - i\Gamma\omega} \qquad (5.28)$$

Often, we label $1 + \chi_{host}$ as the "high frequency dielectric constant", ε_∞, so that

$$\varepsilon_r(\omega) = \varepsilon_\infty + \frac{\omega_p^2}{\omega_0^2 - \omega^2 - i\Gamma\omega} . \qquad (5.29)$$

The static dielectric constant, defined as $\varepsilon_{st} = \varepsilon_r(0)$ is therefore given by setting $\omega = 0$ in the above expression, so that

$$\varepsilon_{st} = \varepsilon_\infty + \frac{\omega_p^2}{\omega_0^2} . \qquad (5.30)$$

Hence, the static dielectric function of a material is affected by dopants, even though the resonant frequency for the dopant is far away from $\omega = 0$.

45

The absorption cross-section

When a material contains a small amount of distinct atoms or charges such as a small concentration of optically absorbing atoms or free charges, the absorption per atom (or charge) is often expressed in terms of an absorption cross-section. The absorption cross-section σ_{abs} is the physical cross-section of a perfectly absorbing disk that would produce the same absorption as the atom. The absorbed power by a single atom can thus be described by

$$P_{abs} = \sigma_{abs}I \tag{5.31}$$

with I the incident irradiance. When a transparent material is doped with a small concentration of N absorbing atoms per unit volume, there is a simple relation between the absorption coefficient and the absorption cross-section, given by

$$\alpha = \sigma_{abs}N. \tag{5.32}$$

This relation can be easily understood under certain simplifying assumptions. A thin slab of the doped material with thickness Δz contains $N{\times}\Delta z$ absorbing atoms per square meter. Each of these atoms contributes an absorbing area of size σ_{abs}. The total absorbing area in the thin slab is thus σ_{abs} N Δz. The fraction of irradiance lost per distance Δz is thus σ_{abs} N. Considering infinitesimally thin slice with thickness dz we can write this as a differential equation:

$$\frac{dI}{I(z)} = -\sigma_{abs}Ndz \quad \Rightarrow \quad \frac{dI}{dz} = -\sigma_{abs}N\,I(z). \tag{5.33}$$

The solution to this type of differential equation is

$$I(z) = I_0\,e^{-\sigma_{abs}Nz}. \tag{5.34}$$

We see that a concentration of N absorbers each with a physical size of σ_{abs} leads to an exponential decay of the irradiance, described by an absorption coefficient $\alpha = \sigma_{abs}N$.
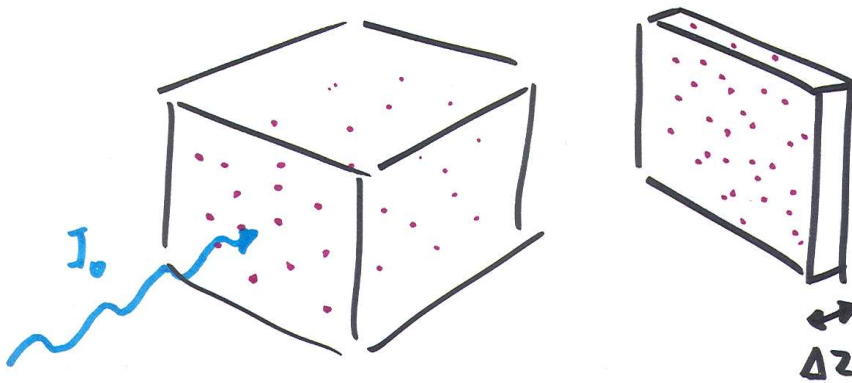
Chapter 6 - Drude model of the optical properties of metals

➢ Corresponding handouts are available on http://kik.creol.ucf.edu/courses.html

The dielectric function of the ideal free electron gas

We can extend the Lorentz model to metals, in which case, since the electrons are unbound or "free", they experience zero restoring force and hence the resonance frequency, $\omega_0^2 =$ K/m is also zero. This is known as the "Drude" model. The equation of motion a free charge is

$$m\frac{\partial^2 \vec{r}(t)}{\partial t^2} + m\Gamma \frac{\partial \vec{r}(t)}{\partial t} = -e\vec{E}(t) \tag{6.1}$$

which has solution

$$\vec{r}(\omega) = \frac{e}{m}\frac{\vec{E}(\omega)}{\left(\omega^2 + i\Gamma\omega\right)}. \tag{6.2}$$

We can again convert position to dipole moment by using $\mu(\omega) = -er(\omega)$, convert this to $P(\omega) = N\mu(\omega)$, and compare it with $P(\omega) = \epsilon_0\chi(\omega)E(\omega)$ resulting in the following expression for $\chi(\omega)$:

$$\chi(\omega) = -\frac{\omega_p^2}{\omega^2 + i\Gamma\omega} \tag{6.3}$$

where once again the plasma frequency is defined by $\omega_p^2 = Ne^2/\varepsilon_0 m$. Note that the answer is (as it should be) equal to the Lorentz susceptibility with $\omega_0=0$. Splitting this into real and imaginary parts we find

$$\chi'(\omega) = -\omega_p^2 \frac{1}{\omega^2 + \Gamma^2}, \qquad \chi''(\omega) = \omega_p^2 \frac{\Gamma/\omega}{\omega^2 + \Gamma^2} \tag{6.4}$$

If we only consider a hypothetical collection of free charges (known as an ideal 'free electron gas') we obtain the following relative permittivity expressions:

$$\varepsilon_r'(\omega) = 1 - \omega_p^2 \frac{1}{\omega^2 + \Gamma^2}, \qquad \varepsilon_r''(\omega) = \omega_p^2 \frac{\Gamma/\omega}{\omega^2 + \Gamma^2}. \tag{6.5}$$

Now, in a metal, the damping term Γ is just the electron collision rate, which is the inverse of the mean electron collision time, τ, i.e. $\Gamma = \tau^{-1}$. Hence,

$$\varepsilon_r'(\omega) = 1 - \frac{\omega_p^2 \tau^2}{1 + \omega^2\tau^2}, \qquad \varepsilon_r''(\omega) = \frac{\omega_p^2 \tau}{\omega\left(1 + \omega^2\tau^2\right)} \tag{6.6}$$

The collision rate can be quite rapid - tens of femtoseconds, corresponding to damping rate of the order of 10^{14} s^{-1}. But for optical frequencies, (e.g. for $\lambda = 500$ nm, $\omega = 2\pi c/\lambda = 3.8\times10^{15}$ rad/s) $(\omega\tau)^2 >> 1$. Under this approximation, we find

$$\varepsilon_r{}'(\omega) \approx 1 - \frac{\omega_p^2}{\omega^2}, \qquad \varepsilon_r{}''(\omega) \approx \frac{\omega_p^2}{\omega^3 \tau} = \frac{\omega_p^2 \Gamma}{\omega^3}. \tag{6.7}$$

It is useful to look at some plots of $\varepsilon_r(\omega)$, $n(\omega)$, $\alpha(\omega)$ and $R(\omega)$. These are plotted below for $\omega_p = 10$ and for $\Gamma \approx 0$ or $\Gamma = 0.5$. In the limit of no damping, the $n = 0$ and $R = 1$ for $0 < \omega < \omega_p$. Above ω_p, κ is zero and the reflectance drops as n rises from zero to unity. Note that even for $\varepsilon_r'' = 0$, κ and hence α is not zero. Introducing some damping causes R to be < 1 and the reflectance drop at ω_p is less severe. The behavior of ε_r, n and κ is consistent with what we now expect for a Lorentz oscillator with $\omega_0 = 0$.

Clearly, the sharp edge in the reflectance seen at the plasma frequency can be expected to be the predominant spectral feature in the optical properties of metals.
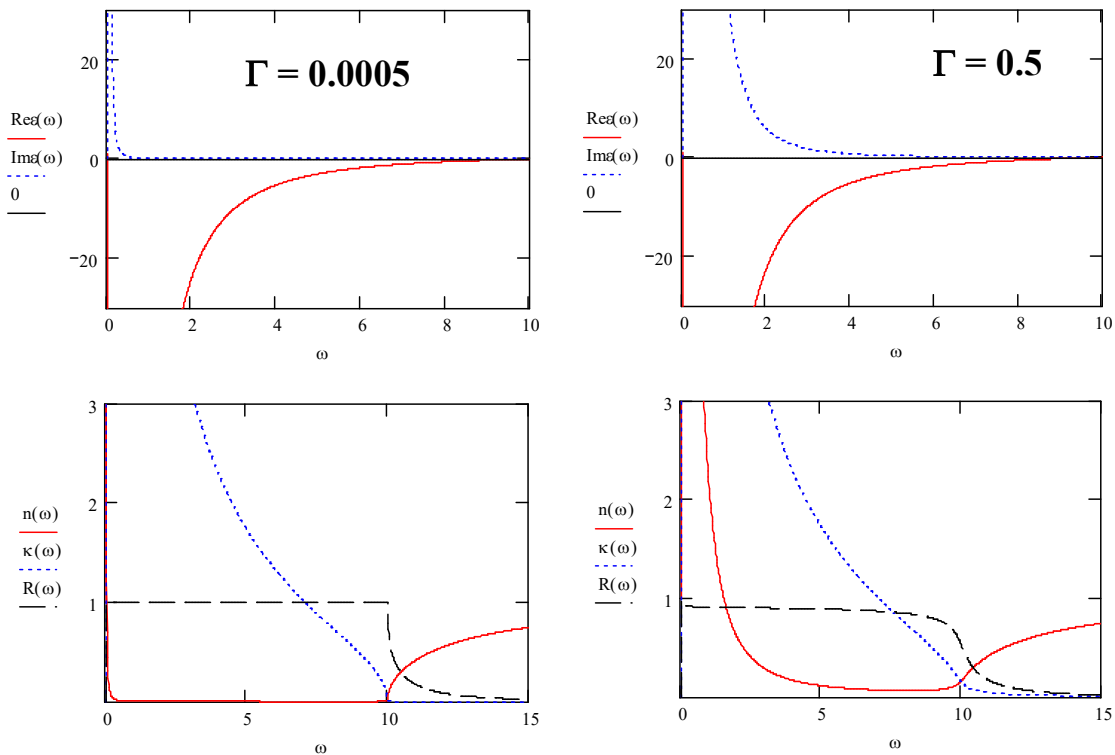

Figure 6.1

Note that in real materials we have not only the free charges, but also the core electrons of the metal atoms. We thus expect the dielectric function of real metals to be a mix of the response of the bound (core) electrons and the free electrons. However for frequencies well below the plasma frequency, the free charge response typically dominates the dielectric function.

Optical absorption in low electron density materials – Semiconductors

Optoelectronic devices are typically made out of semiconductors with small concentrations of free charges. These free charges can introduce a small amount of absorption, known as

free carrier absorption. In the following we will derive the typical frequency dependence of free carrier absorption.

The total dielectric function of such doped semiconductors is given by the dielectric function of the undoped semiconductor host ε_{host}, plus a small Drude susceptibility contribution from the free charges. Assuming a fixed host dielectric constant this gives a total dielectric function of

$$\varepsilon_r(\omega) = \varepsilon_{host} + \chi_{Drude} = n_{host}^2 - \frac{\omega_p^2}{\omega^2 + i\Gamma\omega} \tag{5.35}$$

The free charges change both the real part and the imaginary part of the dielectric function. Typically the free charge (or 'free carrier') concentration is quite low, resulting in a very low plasma frequency that lies in the infrared region. This means for many optical frequencies we satisfy $\omega \gg \omega_p$. In this case the real part of the dielectric function of the semiconductor is not strongly affected by the free charges. In this case we find the approximate response

$$\varepsilon_r(\omega \gg \omega_p) \approx n_{host}^2 + \left(\frac{\Gamma}{\omega}\right)\frac{\omega_p^2}{\omega^2 + \Gamma^2}i \tag{5.36}$$

The added imaginary part can introduce significant absorption. The absorption coefficient is given by $\alpha(\omega) = 2\kappa\omega/c$. We also know $2n\kappa = \varepsilon_r''$. To use this relation we would need to calculate the real index of the doped semiconductor, but as argued above the real index is not changed significantly by the free charges. We can thus use $\kappa \approx \varepsilon_r''/2n_{host}$. This allows us to write

$$\alpha(\omega \gg \omega_p) = 2\kappa\frac{\omega}{c} \approx 2\frac{\varepsilon_r''}{2n_{host}}\frac{\omega}{c} = \frac{1}{n_{host}}\frac{\Gamma}{c}\frac{\omega_p^2}{\omega^2 + \Gamma^2} \approx \frac{1}{n_{host}}\frac{\Gamma}{c}\frac{\lambda_0^2}{\lambda_p^2} \tag{5.37}$$

where in the last step we have assumed that $\omega \gg \Gamma$, and with λ_p the wavelength corresponding to the plasma frequency. The derived λ^2 dependence of α is commonly seen in semiconductors, where dopant densities are typically in the range of 10^{16} to 10^{19} cm^{-3} as compared to $\sim 10^{22}$ cm^{-3} in metals. We can thus recognize *free-carrier absorption* in absorption spectra by noticing a quadratic rise in absorption as a function of wavelength below the semiconductor absorption edge (band gap).

Significance of the plasma frequency

The expressions have been written for ε_r rather than for χ as they more clearly reveal something significant about the plasma frequency in this form. Notice that at $\omega = \omega_p$, the real part of the dielectric constant becomes zero. Hence $n(\omega_p) = 0$, which means the phase velocity - ∞. A more rational way to describe this is that the wavelength, $\lambda = 2\pi c/n\omega \to \infty$ as $\omega \to \omega_p$. This means that all the electrons are oscillating in phase throughout the propagation length of the material.
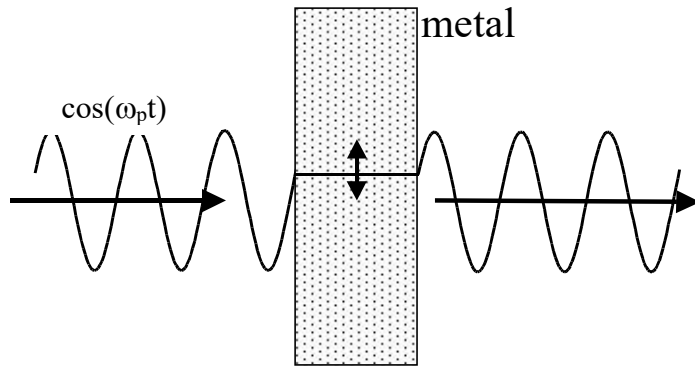
Figure 6.2

Note that as all the electrons are moving together, there is no charge separation (polarization) and hence no restoring force or sustained oscillation after the field is removed.

Plasma oscillations

The above figure shows an entirely transverse field (compared to the surfaces of the material). Should there be a component of the field perpendicular to the surface, there can be a net surface charge as a result of the applied field.
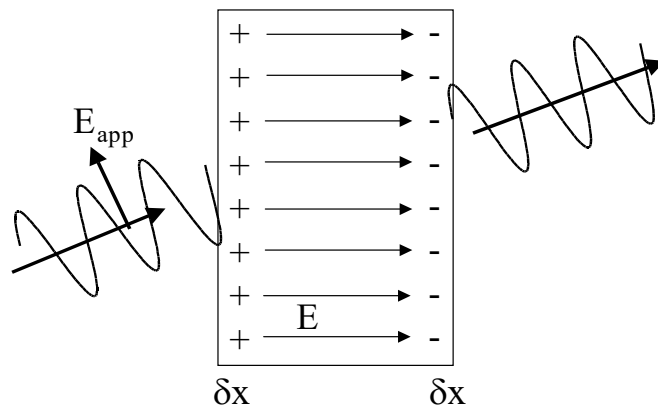

Figure 6.3

The attractive (restoring) force between the surface charges can result in a free oscillation.

For no net charge, (q_f = 0) then D = 0 = $\varepsilon_0 \varepsilon_r E$. But E $\neq$ 0, so then $\varepsilon_r = \varepsilon_r' + i\varepsilon_r'' = 0$. Hence, $\varepsilon_r' = 0$. Now, P = charge x displacement /volume. Thus

$$P = -\frac{NeA\,\delta x \cdot L}{AL} = -Ne\,\delta x$$

$$\&\quad E = -\frac{P}{\epsilon_0} = \frac{Ne\,\delta x}{\epsilon_0}.$$

(6.8)

The restoring force is given by: -eE:

$$\therefore \quad -eE = \frac{Ne^2 \delta x}{\epsilon_0}, \tag{6.9}$$

which is equal and opposite to the acceleration:

$$m \frac{\partial^2 \delta x}{\partial t^2} = \frac{Ne^2 \delta x}{\epsilon_0}, \tag{6.10}$$

which is the equation of motion:

$$\frac{\partial^2 \delta x}{\partial t^2} + \frac{Ne^2}{m \epsilon_0} \delta x = 0. \tag{6.11}$$

Hence the resonance frequency for the plasma oscillation is given by

$$\omega_p^2 = \frac{Ne^2}{m \epsilon_0}. \tag{6.12}$$

We have found that the plasma frequency has a physical meaning: it corresponds to the natural collective electron oscillation in a thin metal plate.

Modifications of Drude theory in real metals

The Drude model implies that the only the plasma frequency should dictate the appearance of metals. This works for many metals – see the example of Zinc (Fig. 3.12 in Wooten.) – But is does not explain why copper is red, gold is yellow and silver is colorless. In fact the appearance of these metals is characterized by an edge in the reflectance spectrum, similar to that predicted by the Drude model, but the problem is that all three metals have the same number of valence electrons. Also, the calculated plasma frequency for all three should lie at about 9 eV, - well outside the visible region, so the plasma frequency cannot in itself account for the colors of Cu and Au.

All three have filled d-shells. Copper has the electronic configuration $[\mathbf{Ar}].\mathbf{3d}^{10}.\mathbf{4s}^1$, Silver $[\mathbf{Kr}].\mathbf{4d}^{10}.\mathbf{5s}^1$ and Gold $[\mathbf{Xe}].\mathbf{4f}^{14}.\mathbf{5d}^{10}.\mathbf{6s}^1$. (These metals are known as the "Noble Metals".) The d-electron bands lie below the Fermi energy of the conduction band: Transitions from the d-band to the empty states above the Fermi level can be occur over a fairly narrow band of energies, around $\hbar \omega_0 = E_F - E_d$ which can be modeled as additional Lorentz oscillator. The combined effects of the free-electrons (Drude model) and the interband transitions due to bound d-electrons (Lorentz model) influence the reflectance properties of the metal.
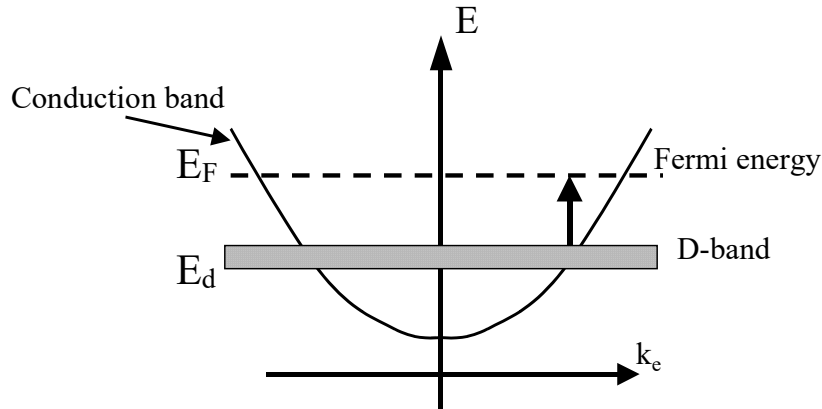
Figure 6.4

Hence, $\varepsilon_r = 1 + \chi_{\text{free}} + \chi_{\text{bound}}$. Where ε_f is described by the Drude model ($\omega_0 = 0$), and ε_b is described by the Lorentz model. ($\omega_0 = [E_F - E_d]/\hbar$.)

Examples: silver, copper, and indium-tin-oxide (ITO)

Silver

The reflectance spectrum of silver shows a strong drop at about 4 eV, well below the expected plasma frequency. The reflectance also rises again for frequencies just above 4 eV. (See Wooten, Fig. 3.15, shown below.)

It turns out that this behavior is because Silver has a d-band resonance at $\hbar\omega \approx 4$ eV. This can be determined from experimental data by fitting the Drude model to the low frequency data, as shown in Wooten, Fig. 3.18.(Shown below.) The difference between dielectric functions from Drude model and from experiment gives the dielectric function due to the d-band resonance, $\varepsilon_{\text{bound}}$ (written as $\delta\varepsilon^{(b)}$ in Wooten.) The effect is to "pull" the $\varepsilon_r' = 0$ frequency in from 9 eV to about 3.9 eV
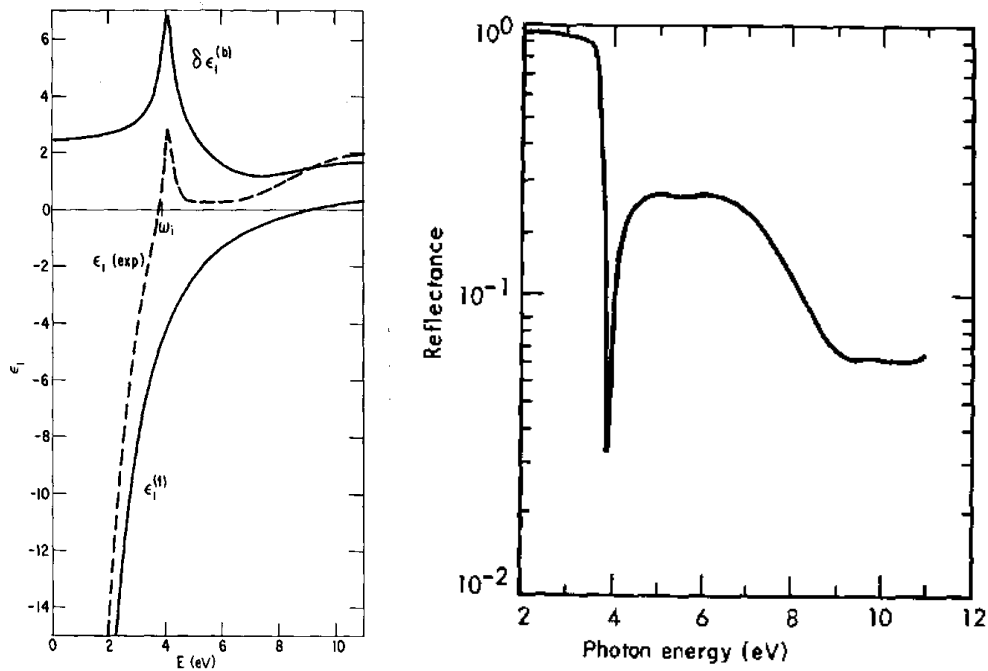
Figure 6.5 Real part of dielectric constant for Silver (from Wooten, Fig 3.18)

This shift in ω_p means that there is a shift in the free plasma oscillation in silver due to the d-electrons. This can be explained by noting that the highly polarizable d-electrons will reduce the electric field that provides the restoring force involved in these oscillations, illustrated on page 6. A reduced restoring force gives a reduced oscillation frequency. See Wooten fig. 3.20 for an illustration of how the d-electrons do this.

Copper

The case of copper is almost identical to that of silver, except that the d-band resonance is at about 2 eV. Now since ε'_{free} becomes very large and negative at low frequencies, it turns out that ε'_{bound} due to the d-electrons is not sufficient to pull the net ε through zero. Hence ε' becomes small at about 2 eV, but there is no true plasma frequency there. However, the effect of this is sufficient to cause R to start to drop at 2 eV, but the reduction is gradual throughout the visible. This gives copper its characteristic red-orange appearance.

53

Figure 6.6 (a) Dielectric function of Cu (Wooten, Fig 3.22) (b) Reflectance of Cu (Wooten 3.21)
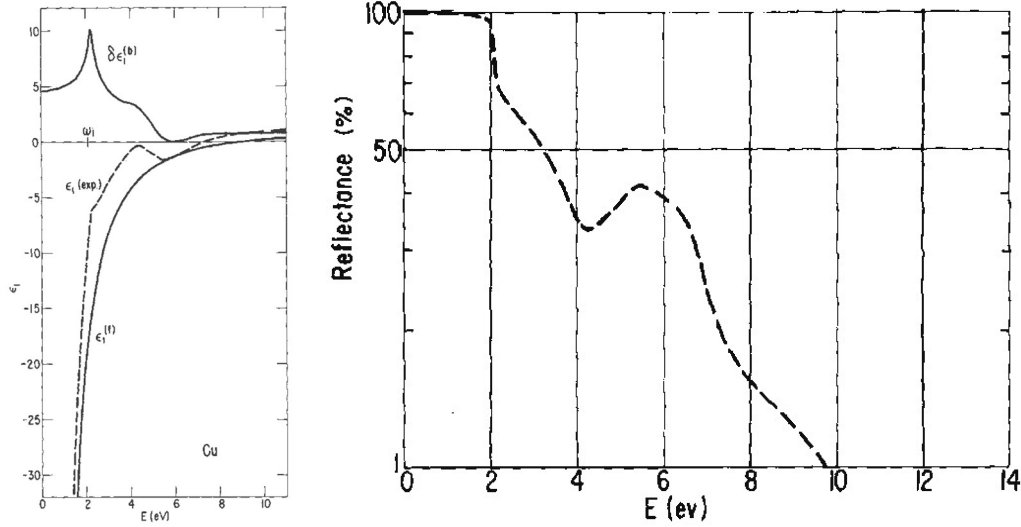
Tin-doped Indium Oxide (ITO) - a transparent conductor

ITO is a semiconducting material that gives quite high electrical conductivity, yet is transparent in the visible. It is particularly useful in low-current applications, such as liquid crystal displays. This is achieved by having a material with low electron density, but those electrons should be highly mobile, which means they travel through the material with relatively few collisions. By choosing the right density of tin doping, ITO can be highly effective. Below, we show the real and imaginary part of ε for ITO from a paper by Hamberg and Granqvist, Journal of Applied Physics, Volume 60, Issue 11, 1986, Pages R123-R159. The plasma frequency, dependent of the Sn density, is typically around 0.7 eV, which corresponds to $\lambda \sim 1.7\mu m$. Due to this, and the free carrier absorption described above, ITO is not as useful in the near infrared ($\lambda > 1 \ \mu m$) as it is in the visible.

Figure 6.7 from Hamberg and Granqvist, Model (right) from David Tanner, University of Florida

54
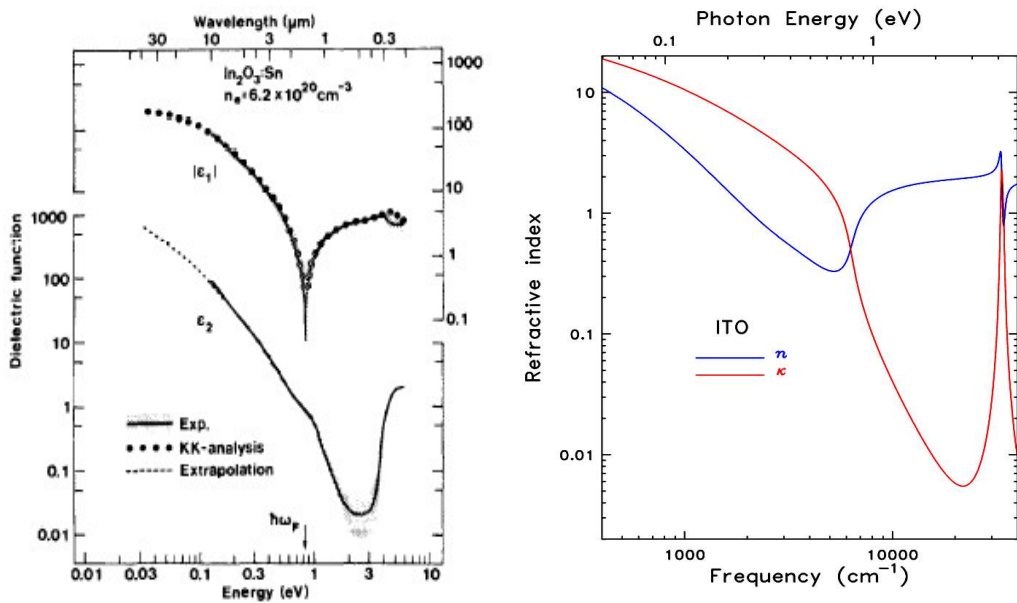
A more recent study by D. Tanner et. al. at the University of Florida, shows that the properties of ITO can be well modeled by the combination of Drude and Lorentz models. Using a model for ε_r that sums contributions from the Drude model to describe the free-carriers, and from the Lorentz model to describe bound carriers, which have a resonant absorption at $\bar{v} = 40{,}000$ cm^{-1} ($\bar{v} = 1/\lambda = v/c$) or $\lambda = 250$ nm. i.e.

$$\varepsilon_r = \varepsilon_\infty + \frac{\omega_{pb}^2}{\omega_0^2 - \omega^2 - i\Gamma_b\omega} - \frac{\omega_{pf}^2}{\omega^2 + i\Gamma_f\omega} \tag{6.13}$$

where ε_∞ is a background high-frequency dielectric constant, and subscripts, b and f, correspond to bound and free electrons (i.e. Drude and Lorentz contributions, respectively. The plasma frequencies and damping times for the bound and free electrons are of course different. The results of their model is shown below. (Courtesy, David Tanner, University of Florida.)

Drude conductivity and skin depth

We already took a look at how the conductivity affects the optical properties in a homework exercise. There we looked mainly at the effect when the free-carrier contribution to the susceptibility is weak. Since we are mainly considering metals, we will not look at the effect of charges in the case of good conductors, where the free carrier effects are large.

Recall that the Drude model gave us

$$\varepsilon_r'(\omega) = 1 - \omega_p^2 \frac{1}{\omega^2 + \Gamma^2},$$
$$\varepsilon_r''(\omega) = \omega_p^2 \frac{\Gamma/\omega}{\omega^2 + \Gamma^2} \tag{6.14}$$

from which we can find the optical constants, n and κ from

$$n(\omega) = \sqrt{\frac{1}{2}\left(\sqrt{\varepsilon_r'^2 + \varepsilon_r''^2}\right) + \varepsilon_r'^2}$$
$$\kappa(\omega) = \sqrt{\frac{1}{2}\left(\sqrt{\varepsilon_r'^2 + \varepsilon_r''^2}\right) - \varepsilon_r'^2} \tag{6.15}$$

We can also describe the optical properties of a free-electron conductor in terms of the conductivity, which can also be determined by the Drude model.

First, we note that the current density is related to the velocity of motion by

$$\vec{j} = -Ne\vec{v} \tag{6.16}$$

and the current is also related to the electric field by, $\vec{j}(\omega) = \sigma\vec{E}(\omega)$.

Now we already wrote down to equation of motion for electrons in an electric field as

$$m\frac{d^2\vec{r}(t)}{dt^2} + m\Gamma\frac{d\vec{r}(t)}{dt} = -e\vec{E}(t), \tag{6.17}$$

and noting that $\vec{v} = \dfrac{d\vec{r}}{dt}$, we can rewrite the equation of motion for the velocity:

$$m\frac{d\vec{v}}{dt} + m\Gamma\vec{v}(t) = -e\vec{E}(t)\,.$$

(6.18)

Now, $\Gamma = 1/\tau$, so that the solution for v is

$$\vec{v}(\omega) = \frac{-e\tau}{m}\frac{1}{1-i\omega\tau}\vec{E}(\omega)\,,$$

(6.19)

or,

$$\vec{j}(\omega) = -Ne\vec{v}(\omega) = \frac{Ne^2\tau}{m}\frac{1}{1-i\omega\tau}\vec{E}(\omega)$$
$$= \sigma(\omega)\vec{E}(\omega)$$

(6.20)

Hence,

$$\sigma(\omega) = \frac{Ne^2\tau}{m}\frac{1}{1-i\omega\tau}$$

(6.21)

is the Drude conductivity. Setting, $\sigma_0 = Ne^2\tau/m$, we have,

$$\sigma(\omega) = \frac{\sigma_0}{1-i\omega\tau}\,,$$

(6.22)

Where σ_0 is the DC conductivity.

Inserting the conductivity into Maxwell's equations for a medium with free charge carriers we find that we can write

$$\varepsilon_r(\omega) = 1 + \chi(\omega) + i\frac{\sigma(\omega)}{\varepsilon_0\omega}\,.$$

(6.23)

If we assume that only free carriers contribute to the optical properties, then this becomes,

$$\varepsilon_r(\omega) = 1 + i\frac{\sigma(\omega)}{\varepsilon_0\omega} = 1 + i\frac{\sigma_0}{\varepsilon_0\omega(1-i\omega\tau)}$$

(6.24)

we can separate ε_r into its real and imaginary parts to get

$$\varepsilon_r(\omega) = 1 - \frac{\sigma_0\tau}{\varepsilon_0(1+\omega^2\tau^2)} + i\frac{\sigma_0}{\omega\varepsilon_0(1+\omega^2\tau^2)}$$

(6.25)

Now, $\sigma_0 = Ne^2\tau/m \implies \sigma_0/\varepsilon_0 = \omega_p^2\tau$, so that,

$$\varepsilon_r(\omega) = 1 - \frac{\omega_p^2\tau^2}{1+\omega^2\tau^2} + i\frac{\omega_p^2\tau}{\omega(1+\omega^2\tau^2)}\,,$$

(6.26)

which is exactly as we obtained before. So now we can estimate the optical properties of a metal based on the DC conductivity, as an alternative to requiring knowledge of the electron density.

We will now look at the low-frequency limit of a good conductor. A said before, typically, $\tau \sim 10$'s of femtoseconds, so that if we are looking at low frequencies (far infrared or microwaves or longer wavelengths) then $\omega \ll \tau^{-1}$ or $\omega\tau \ll 1$. In this case,

$$\varepsilon_r{}'(\omega) \approx 1 - \omega_p^2 \tau^2,$$

$$\varepsilon_r{}''(\omega) \approx \frac{\omega_p^2 \tau}{\omega} = \frac{\omega_p^2 \tau^2}{\omega\tau} \tag{6.27}$$

Hence, $\varepsilon_r{}'' \gg \varepsilon_r{}'$, so that ,

$$n \approx \kappa \approx \sqrt{\frac{\varepsilon_r{}''}{2}} = \sqrt{\frac{\omega_p^2 \tau}{\omega}} = \sqrt{\frac{\sigma_0}{2\omega\varepsilon_0}} . \tag{6.28}$$

Hence, the complex refractive index under these conditions may be written as

$$\eta(\omega) = \sqrt{\frac{\sigma_0}{2\omega\varepsilon_0}}(1+i). \tag{6.29}$$

The absorption coefficient is then given by,

$$\begin{aligned} \alpha(\omega) &= \frac{2\omega\kappa}{c} = \frac{2\omega}{c}\sqrt{\frac{\sigma_0}{2\omega\varepsilon_0}} \\ &= 2\omega\sqrt{\frac{\sigma_0}{2\omega\varepsilon_0 c^2}} . \\ &= \sqrt{2\sigma_0\omega\mu_0} \end{aligned} \tag{6.30}$$

Now, the irradiance depends on propagation depth, z, as

$$I(z) = I(0)e^{-\alpha(\omega)z}, \tag{6.31}$$

which could be written as

$$I(z) = I(0)e^{-z/\delta(\omega)}, \tag{6.32}$$

where $\delta(\omega) = 1/\alpha(\omega)$ is a penetration depth, at which point the irradiance drops to 1/e or 0.36 of its incident value. Since this depth is usually very small in metals, it is referred to as the "skin depth", which is then given by

$$\delta(\omega) = \sqrt{\frac{1}{2\sigma_0\omega\mu_0}} . \tag{6.33}$$

Bear in mind the approximation ($\omega\tau \ll 1$) under which this result was obtained. For higher (mid – infrared, visible, UV) frequencies, this is no longer valid, and we just have to include

the whole expression for ε_r. Additionally, it was assumed that there are no other contributions to ε_r, which is not exactly true because of bound electron resonances (i.e. transitions) at higher frequencies. Should it be necessary, these can also be included in our models.

Chapter 7 – Optical Activity and Magneto-Optics

➢ Corresponding handouts are available on http://kik.creol.ucf.edu/courses.html

In Chapter 3 we derived a scalar wave equation to describe light propagation. We assumed isotropic electric response, and ignored any magnetization effects. In the first part of the present Chapter we will see that an oscillating electric field can induce an oscillating magnetic moment in some molecules. This will require us to consider a vectorial wave equation. This effect will lead to the phenomenon of *optical activity*, the ability of molecules to gradually rotate linear polarization. In the second part of the Chapter we will see that the application of an external magnetic field along the wave propagation will introduce an additional transverse force on the oscillating bound electrons. This leads to a phenomenon known as *Faraday rotation*, the magnetically controlled gradual rotation of linear polarization, enabling nonreciprocal optical systems.

Optical Activity

In some *isotropic* media, (e.g. sugar solution in water) it is found that the polarization of linearly polarized light is rotated in proportion to the propagation distance.
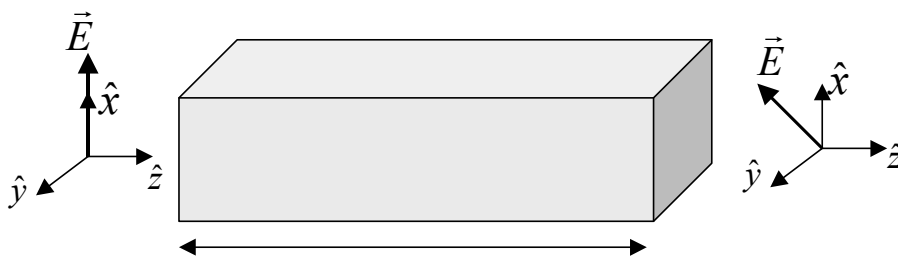

Figure 7.1

i.e.
$$\vec{E} = E_{in}\{\hat{x}\cos\Delta z + \hat{y}\sin\Delta z\},$$

where Δ is the rotatory coefficient (°/m or rad/m). The effect typically occurs in liquids solutions of chiral molecules, a special class of molecules that is not mirror-symmetric. W.T. Kelvin defined chirality as "*any geometrical figure, or group of points, if its image in a plane mirror cannot be brought to coincide with itself.*"

A simple example of a chiral molecule is shown below:[xv]

"Left handed"   *"Right handed"*
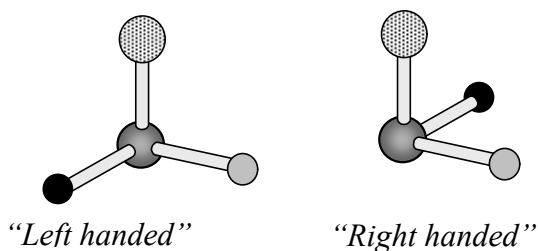
[xv] In this example the choice on calling either of the two configurations is arbitrary. For real molecules the choice of right vs. left-handed is linked to the sign of the rotatory coefficient.

Note that the left molecule contains four different atom types. It is not possible to rotate the left molecule to make it overlap with the right molecule.

For each chiral molecule there exists a left-handed and a right-handed isomer. These special isomers are called *enantiomers*. While they have the same composition (same atom types, same number of bonds), they may interact differently with left and right handed enantiomers of other molecules. This is particularly important in biology. For example, orange peel and lemon peel contain opposite enantiomers of the molecule limonene. These are responsible for the smell of the fruit. d-limonene smells of orange, l-limonene smells of lemon. The letter 'd' comes from the Latin word *dexter* for 'right', and the letter 'l' comes from the Latin word *laevus* meaning 'left'.

d-limonene (orange)   l-limonene (lemon)
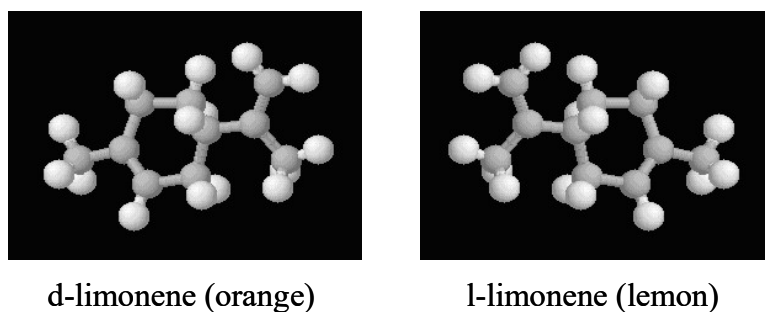
Figure 7.2

Common table sugar is sucrose, which is a combination of glucose (dextrose - right-handed sugar) and fructose (levulose - left-handed sugar). The dextrose molecule is shown below:
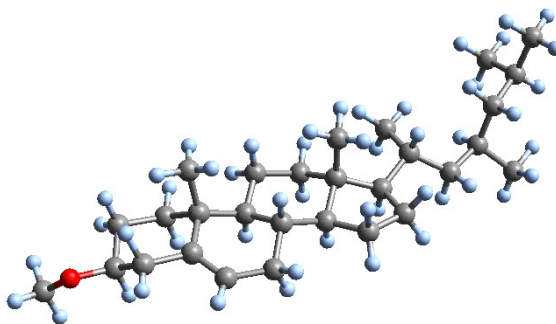

Figure 7.3

Link between chirality and optical rotation

An extreme case of a chiral molecule would be a molecule shaped like a helix ('coil'). For simplicity, let's imagine that valence electrons can move freely along the molecule. In the figure below, we see that an electric field would drive charge motion along the helical molecule. The resulting curved charge motion is accompanied by a magnetic response, in the same way that an electromagnet uses current to generate a magnetic field. A helical molecule (and a chiral molecule in general) can thus produce a magnetic field *along* the

direction of the electric field. Such an effect was not considered in the derivation of the scalar wave equation. In the following we will reconsider the wave equation, but this time taking into account the possible influence of chiral molecules.
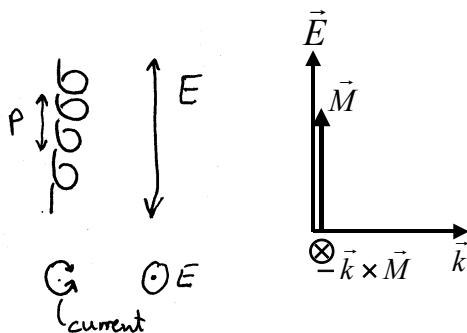

Figure 7.4

Note that if the molecule were flipped by 180°, the effect would be the same. The is a crucial observation, as it explains why the effect does not average to zero inside isotropic media. A solution of chiral molecules will be isotropic, since it contains randomly oriented molecules. The optical activity is caused by the subset of molecules that are either aligned 'along or against' the electric field, while some molecules may contribute less because they are not ideally aligned.

When optical activity (the ability to rotate linear polarization) is observed in solutions of molecules, we expect that the amount of polarization rotation is dependent on the concentration of molecules. To describe concentration dependent optical activity, we use the *specific rotatory power* or *specific rotation* Δ_s. It is defined as the amount of polarization rotation per unit length, per concentration. For a specific rotation given in units degrees cm^2/g the polarization rotation angle θ after a distance z is thus given by:

$$\theta(z) \ [°] = z[cm] \ \cdot \Delta_s \left[°\frac{cm^2}{g}\right] \cdot C \left[\frac{g}{cm^3}\right]$$

Other common units used for specific rotation are degrees (or radians) per 10 cm / (g/liter), i.e. with all length units described in units of 10 cm.

Describing optical activity with the vectorial wave equation

As mentioned above, optical activity is caused by electrically induced *magnetic* moment on molecules, with an magnetic average contribution oriented along the electric field. To find this effect from Maxwell's equations, we need to consider the $\nabla \times \vec{M}$ contribution to the current.

Recall, $\vec{B} = \mu_0 \left[\vec{H} + \vec{M}\right]$, and

$$\vec{\nabla} \times \vec{B} = \mu_0 \vec{J} + \mu_0 \vec{\nabla} \times \vec{M} + \varepsilon_0 \mu_0 \frac{\partial \vec{E}}{dt} + \mu_0 \frac{\partial \vec{P}}{dt} \tag{7.1}$$

and

$$\bar{\nabla} \times \bar{E} = -\frac{\partial \bar{B}}{\partial t} ,$$
(7.2)

so that

$$\bar{\nabla} \times \bar{\nabla} \times \bar{E} = -\frac{\partial}{\partial t} \{ \bar{\nabla} \times \bar{B} \}$$

$$\Rightarrow \quad -\nabla^2 \bar{E} = -\frac{\partial}{\partial t} \left\{ \mu_0 \vec{\nabla} \times \vec{M} + \varepsilon_0 \mu_0 \frac{\partial \bar{E}}{dt} + \mu_0 \frac{\partial \bar{P}}{dt} \right\}$$
(7.3)

for isotropic media and $J_f = 0$. Hence.

$$\nabla^2 \bar{E} - \frac{1}{c^2} \frac{\partial^2 \bar{E}}{dt^2} = \mu_0 \frac{\partial^2 \bar{P}}{dt^2} + \mu_0 \frac{\partial}{\partial t} \vec{\nabla} \times \vec{M}$$
(7.4)

So there is a term due to the curl of the magnetization that looks like a contribution to the polarization. Taking the Fourier transform, we get

$$\left(-k^2 + \frac{\omega^2}{c^2} \right) \vec{E}(\vec{k}, \omega) = -\omega^2 \mu_0 \vec{P}(\vec{k}, \omega) + \mu_0 (-i\omega)(i\vec{k} \times \vec{M})$$
(7.5)

$$\therefore \left(k^2 - \frac{\omega^2}{c^2} \right) \vec{E}(\vec{k}, \omega) = \omega^2 \mu_0 \left[\vec{P}(\vec{k}, \omega) - \frac{\vec{k} \times \vec{M}}{\omega} \right]$$
(7.6)

now we can compare magnitudes on the right hand side:

$$\frac{\left| \vec{k} \times \vec{M} \right|}{\left| \vec{P} \right| \omega} \approx \frac{kM}{\omega P} = \frac{M}{cP}$$
(7.7)

In most cases, this ratio $\ll 1$ (see homework), so that if $\vec{k} \times \vec{M}$ is parallel or antiparallel to P, we can ignore it. This corresponds to M being parallel to B, as shown below. This case is not interesting, as $\left| \vec{k} \times \vec{M} / \omega \right|$ is very small compared to P. (Note that we have assumed isotropic media, so that E and P are always parallel.)
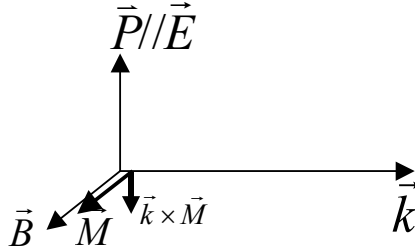

$$\vec{P} // \vec{E}$$

Figure 7.5

However, if M is parallel to P, then $\vec{k} \times \vec{M}$ is perpendicular to P, as shown below:
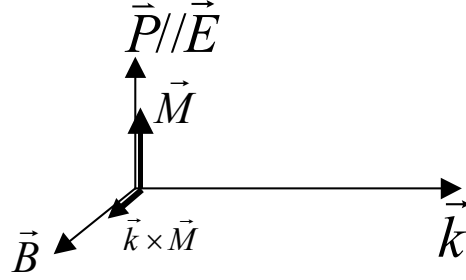
Figure 7.6

Hence the effective polarization, $\vec{P}_{eff} = \vec{P} - \dfrac{1}{\omega}\vec{k} \times \vec{M}$, has a small component perpendicular to the applied field. This is what leads to the rotation of the electric field.

Propagation equations for optically active media

Now $\vec{M} = \widetilde{\widetilde{\chi}}_M \cdot \vec{H}$, where $\widetilde{\widetilde{\chi}}_M$ is the magnetic susceptibility tensor.

$$\nabla \times \vec{H} = \frac{\partial \vec{D}}{\partial t} \quad \Rightarrow \quad i\vec{k} \times \vec{H} = -i\omega \vec{D} \; , \tag{7.8}$$

and since the medium is isotropic,

$$\vec{k} \times \vec{H} = -\omega \in_0 n^2 \vec{E}$$

$$\therefore \quad \left|\vec{H}\right| = \frac{\omega}{k} \in_0 n^2 \left|\vec{E}\right| . \tag{7.9}$$

Since $\vec{M}$ is parallel to $\vec{E}$, we may treat it as a scalar when relating M and E. Hence we may write χ_M as a scalar:

$$\vec{M} = \chi_M \left|\vec{H}\right|\hat{E} = \frac{\omega}{k} \in_0 n^2 \chi_M \vec{E} \tag{7.10}$$

Hence

$$\frac{-1}{\omega}\vec{k} \times \vec{M} = - \in_0 n^2 \chi_M \hat{k} \times \vec{E} \tag{7.11}$$

- we will take the direction of k as z. Hence we will write $\hat{k} = \hat{z}$.

The wave equation therefore becomes

$$\left(k^2 - \frac{\omega^2}{c^2}\right)\vec{E} - \mu_0\omega^2 \in_0 \chi_E \vec{E} = -\mu_0\omega^2 \in_0 n^2 \chi_M \hat{z} \times \vec{E}$$

$$\therefore \quad \left(k^2 - \left(\frac{n\omega}{c}\right)^2\right)\vec{E} + \left(\frac{n\omega}{c}\right)^2 \chi_M \hat{z} \times \vec{E} = 0 \tag{7.12}$$

63

Now, $\vec{E} = E_x\hat{x} + E_y\hat{y}$, so that

$$\hat{z} \times \vec{E} = \begin{vmatrix} \hat{x} & \hat{y} & \hat{z} \\ 0 & 0 & 1 \\ E_x & E_y & 0 \end{vmatrix} = \left(-E_y, E_x, 0\right) \tag{7.13}$$

Equating x and y components of the wave equation gives

$$\left(k^2 - \left(\frac{n\omega}{c}\right)^2\right)E_x - \left(\frac{n\omega}{c}\right)^2 \chi_M E_y = 0$$

$$\left(\frac{n\omega}{c}\right)^2 \chi_M E_x + \left(k^2 - \left(\frac{n\omega}{c}\right)^2\right)E_y = 0 \tag{7.14}$$

So for a nontrivial solution, the determinant must be zero:

$$\begin{vmatrix} k^2 - \left(\frac{n\omega}{c}\right)^2 & -\left(\frac{n\omega}{c}\right)^2 \chi_M \\ \left(\frac{n\omega}{c}\right)^2 \chi_M & k^2 - \left(\frac{n\omega}{c}\right)^2 \end{vmatrix} = 0 \tag{7.15}$$

Hence for an eigenmode of the wave equation we have

$$\left(k^2 - \left(\frac{n\omega}{c}\right)^2\right)^2 + \left(\frac{n\omega}{c}\right)^4 \chi_M^2 = 0$$

$$\Rightarrow \quad k_\pm^2 - \left(\frac{n\omega}{c}\right)^2 = \pm i\left(\frac{n\omega}{c}\right)^2 \chi_M \tag{7.16}$$

But recall that

$$\left(k^2 - \left(\frac{n\omega}{c}\right)^2\right)E_x - \left(\frac{n\omega}{c}\right)^2 \chi_M E_y = 0, \tag{7.17}$$

so that plane wave modes $k_\pm$ satisfy

$$E_x = \mp i E_y \tag{7.18}$$

Hence an eigenmode of an isotropic chiral medium is one where e_x and E_y are equal and $\pi/2$ out of phase. – i.e. circular polarization. So we can write the eigenmode as

$$\therefore \quad E_\pm = \frac{1}{\sqrt{2}}(\hat{x} \pm i\hat{y})E_0, \tag{7.19}$$

where E_0 is the field amplitude and the + and – case correspond to left-circularly polarized light (LCP) and right-circularly polarized light (RCP) respectively. These modes have wavevectors:

$$k_\pm^2 = \left(\frac{n\omega}{c}\right)^2 \pm i\left(\frac{n\omega}{c}\right)^2 \chi_M$$

$$\text{or, } k_\pm = \left(\frac{n\omega}{c}\right)\sqrt{1+i\chi_M}$$

(7.20)

but $\chi_M \ll 1$, so,

$$k_\pm = \left(\frac{\omega}{c}\right)n(1\pm i\chi_M/2).$$

(7.21)

Hence the RCP and LCP waves experience different refractive indices:

$$n_\pm = n(1\pm i\chi_M/2).$$

(7.22)

Now, at this point, it appears that the χ_M component of the index is going to give rise to loss, as it appears to give an imaginary component to n. However, we should recall that while the electric polarization is proportional to the displacement, r, of charge, i.e. $p \propto e \cdot r$, the magnetic polarization is proportional to the current, i.e. $m \propto e\dot{r} = i\omega er$. Hence for p real ($\therefore r$ real), the induced magnetic dipole is purely imaginary. Therefore

$$\chi_M = \text{Re}\{\chi_M\} + i\,\text{Im}\{\chi_M\} = 0 + i\,\text{Im}\{\chi_M\} \implies i\chi_M = -\,\text{Im}\,\chi_M.$$

(7.23)

This gives purely real refractive indices:

$$n_\pm = n(1 \mp \text{Im}(\chi_M/2))$$

(7.24)

So we now clearly see that the RCP and LCP eigenmodes propagate at different speeds. To deal with linear polarizations, we use the fact that a linearly polarized wave can be written as a sum of equal amplitude RCP and LCP components:

$$\vec{E}_T = \frac{1}{2\sqrt{2}}\{\vec{E}_+ \exp[i(k_+z - \omega t)] + \vec{E}_- \exp[i(k_-z - \omega t)]\} + c.c.$$

$$= \frac{E_0}{4}\{(\hat{x} + i\hat{y})\exp[i(k_+z - \omega t)] + (\hat{x} - i\hat{y})\exp[i(k_-z - \omega t)]\} + c.c.$$

(7.25)

We can simplify by setting $\dfrac{k_+ + k_-}{2} \cong \dfrac{n\omega}{c} = \bar{k}$, and $\dfrac{k_- - k_+}{2} = \Delta$. This yields:

$$\vec{E}_T(z,t) = \frac{1}{2}(\hat{x}\cos\Delta z + \hat{y}\sin\Delta z)\{E_0 \exp[i(\bar{k}z - \omega t)] + c.c\}$$

(7.26)

From this, we can see that Δ gives the rotation of the linear polarization per unit length. Hence Δ is termed the "*rotatory power*", given by

$$\Delta = \frac{n\omega}{2c}\text{Im}\{\chi_M\} \quad \text{(in °/m or rad/m)}.$$

(7.27)

Zeeman Splitting

Here we are interested in the effect of an external magnetic field, B, on the optical properties of a medium. (This is somewhat similar to the case of chiral media, except here the "chirality" is imposed by an external magnetic field.) The general term for the use of magnetic fields to modify optical properties is *"Magneto-Optics"*

In general for a medium exposed to an external magnetic field, B:

$$P_i = \epsilon_0 \sum_j \chi_{ij} E_j + \epsilon_0 \sum_j \chi_{ijk}^{Z,F} E_j B_k \ , \tag{7.28}$$

where $\chi_{ijk}^{Z,F}$ describes the linear magneto-optic effects known as the Zeeman and Faraday effects. Here, we will consider an isotropic material, so that χ_{ij} is scalar. We also let B be oriented along the direction of propagation, i.e. $\vec{B} = B\hat{z}$. Hence the force on an electron in the medium is given by the Lorentz force law:

$$\vec{F} = e\vec{E} + e\vec{v} \times \vec{B} = e\vec{E} + e\vec{v} \times \hat{z}B \ . \tag{7.29}$$

Now for a general velocity, $\vec{v} = (\dot{x}, \dot{y}, \dot{z})$ hence,

$$\vec{v} \times \hat{z}B = \begin{vmatrix} \hat{x} & \hat{y} & \hat{z} \\ \dot{x} & \dot{y} & \dot{z} \\ 0 & 0 & B \end{vmatrix} = (\dot{y}B, -\dot{x}B, 0). \tag{7.30}$$

For a plane wave propagating along z, $\vec{E} = (E_x, E_y, 0)$, so we have 2 equations of motion for a bound electron in the field:

$$m(\ddot{x} + \gamma\dot{x} + \omega_x^2 x) = eE_x + eB\dot{y}$$
$$m(\ddot{y} + \gamma\dot{y} + \omega_y^2 y) = eE_y - eB\dot{x} \tag{7.31}$$

Since the medium is isotropic, then $\omega_x = \omega_y = \omega_0$.

Now, a free electron with velocity v perpendicular to a magnetic field will make circular orbits around the z-axis, as shown in the figure below. Hence free electrons in a magnetic field would have a resonant absorption at the cyclotron resonance frequency of $\omega_c = eB/m$, (also known as the "Larmor Precession frequency"). In our case, we have bound electrons, so we might expect that the bound electron resonance is modified by the cyclotron resonance.
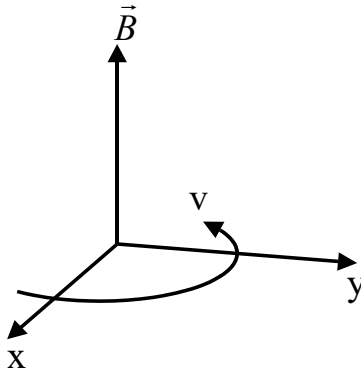
$$evB = m\omega^2 r$$

$$\Rightarrow e\frac{v}{r}B = m\omega^2$$

$$\Rightarrow eB = m\omega$$

$$\Rightarrow \omega_c = \frac{eB}{m}$$

Figure 7.7

Now, for electric field components defined by

$$E_x = \tfrac{1}{2}E_{x0}e^{-i\omega t} + c.c.$$
$$E_y = \tfrac{1}{2}E_{yx0}e^{-i\omega t} + c.c.,$$

we anticipate the x and y components of the electron motion to be

$$x = \tfrac{1}{2}x_0 e^{-i\omega t} + c.c.$$
$$y = \tfrac{1}{2}y_0 e^{-i\omega t} + c.c.$$

Therefore the equations of motion become

$$\left(-\omega^2 - i\gamma\omega + \omega_0^2\right)x_0 = \frac{e}{m}E_{x0} + \frac{e}{m}B\left(-i\omega y_0\right)$$

$$\left(-\omega^2 - i\gamma\omega + \omega_0^2\right)y_0 = \frac{e}{m}E_{y0} - \frac{e}{m}B\left(-i\omega x_0\right)$$

For convenience, we write $D(\omega) = (\omega_o^2 - \omega^2 - i\gamma\omega)$, so that

$$x_0 = \frac{e}{mD(\omega)}\left(E_{x0} - i\omega B y_0\right)$$

$$y_0 = \frac{e}{mD(\omega)}\left(E_{y0} + i\omega B x_0\right)$$

Anticipating circular motion in our solutions, we define an amplitude, Q, corresponding to such motions:

$$Q_\pm = \frac{x_0 \pm iy_0}{\sqrt{2}}$$

(7.32)

(7.33)

(7.34)

(7.35)

(7.36)

$$\therefore \quad Q_\pm = \frac{1}{\sqrt{2}} \frac{e}{mD(\omega)} \left\{ \left(E_{x0} \pm iE_{y0} \right) - i\omega By_0 \pm i(i\omega Bx_0) \right\}$$

$$= \frac{e}{mD(\omega)} E_\pm \mp \frac{1}{\sqrt{2}} \frac{e\omega B}{mD(\omega)} \left(x_0 \pm iy_0 \right) \tag{7.37}$$

$$= \frac{e}{mD(\omega)} E_\pm \mp \frac{e\omega B}{mD(\omega)} Q_\pm$$

$$\Rightarrow \quad Q_\pm \left(1 \pm \frac{e\omega B}{mD(\omega)} \right) = \frac{e}{mD(\omega)} E_\pm$$

$$\therefore \quad Q_\pm = \frac{\dfrac{e}{mD(\omega)} E_\pm}{\left(1 \pm \dfrac{e\omega B}{mD(\omega)} \right)} = \frac{e}{m} \frac{E_\pm}{D(\omega) \pm \frac{e}{m}\omega B}$$

i.e. $\quad Q_\pm = \dfrac{e}{m} \dfrac{E_\pm}{\omega_0^2 - \omega^2 - i\gamma\omega \pm \frac{e}{m}\omega B}$ $\tag{7.38}$

Hence $Q_\pm$ corresponds to the amplitude of electron motion for illumination with right (+) and left (-) circularly polarized light. Note that B = 0 yields the regular result from the Lorentz model.

The resonance frequencies occur for $\omega_0^2 - \omega^2 \pm \omega eB/m = 0$, which, under the resonance approximation, becomes $2\omega(\omega_0 - \omega) \pm \omega eB/m \cong 0$, giving resonance frequencies for the two states of circularly polarized light as

$$\omega_\pm \cong \omega_0 \pm \frac{eB}{2m} \tag{7.39}$$
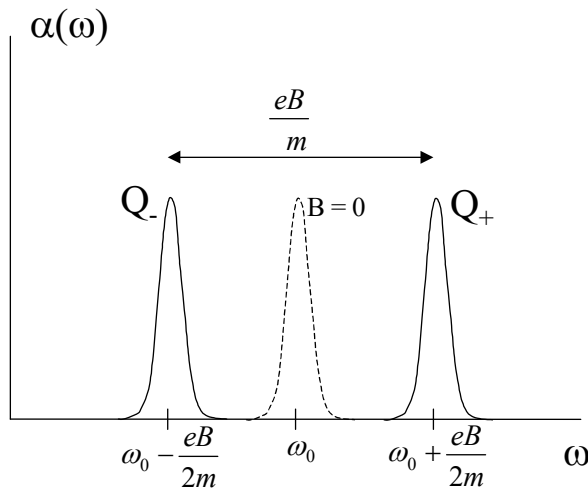
This is known as "Zeeman splitting"

Figure 7.8

Faraday Rotation

While the Zeeman effect gives the splitting of the absorption lines for left and right circular polarizations due to the magnetic field, the Faraday effect is the rotation of polarization far from resonance due to the consequent slight difference in refractive indices for the two polarization states.
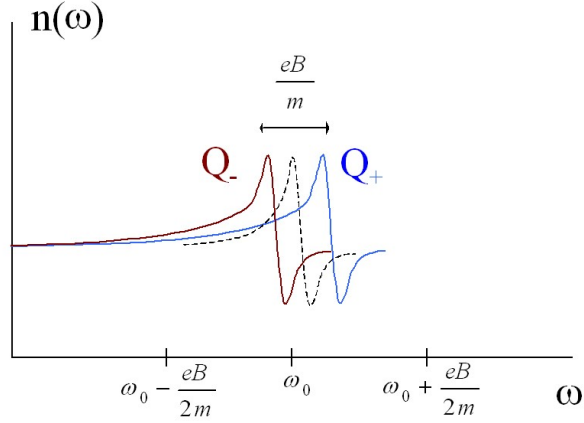

Figure 7.9

To analyze this, we take the far from resonance approximation:

$$\omega_0^2 - \omega^2 >> \omega\gamma$$

$$\therefore \quad Q_\pm = \frac{e/m \, E_\pm}{\omega_0^2 - \omega^2 \pm e\omega B/m} \tag{7.40}$$

For $\omega_0^2 - \omega^2 >> e\omega B/m$, we can expand to first order:

$$Q_\pm = \frac{e \, E_\pm}{m(\omega_0^2 - \omega^2)}\left(1 \mp \frac{e\omega B}{m(\omega_0^2 - \omega^2)}\right) \tag{7.41}$$

Now,

$$P_\pm = NeQ_\pm = \epsilon_0 \, \chi_\pm E_\pm$$

$$\therefore \quad P_\pm = \frac{Ne^2}{m(\omega_0^2 - \omega^2)}\left(1 \mp \frac{e\omega B}{m(\omega_0^2 - \omega^2)}\right)E_\pm \tag{7.42}$$

Hence the susceptibility becomes

$$\chi_\pm(\omega, B) = \frac{Ne^2/\epsilon_0 \, m}{(\omega_0^2 - \omega^2)} \mp \frac{Ne^3/\epsilon_0 \, m^2}{(\omega_0^2 - \omega^2)^2}\omega B$$

$$= \chi_0(\omega) \mp \frac{2nVc}{\omega}B \tag{7.43}$$

where

$$V = \frac{Ne^3\omega^2}{2n\,\epsilon_0\,m^2 c\left(\omega_0^2 - \omega^2\right)^2} \qquad (7.44)$$

is the Verdet coefficient.

The refractive index for left and right circularly polarized light may hence be written as

$$n_\pm^2 = 1 + \chi_0(\omega) \mp \frac{2nVc}{\omega}B$$

$$= n^2 \mp 2n\frac{Vc}{\omega}B \qquad (7.45)$$

$$\therefore \quad n_\pm \cong n \mp \frac{Vc}{\omega}B$$

Hence left and right circularly polarized waves see different refractive indices, which again leads to rotation of linear polarization, i.e.,

$$\vec{E}_T(z,t) = \frac{1}{2}\left(\hat{x}\cos VBz + \hat{y}\sin VBz\right)\left\{E_0 \exp\left[i\left(\bar{k}z - \omega t\right)\right] + c.c\right\} \qquad (7.46)$$

Highly dispersive materials will have large Verdet coefficients. In practice, the magnetic susceptibility will also determine how large a Verdet coefficient of a material will be. – Paramagnetic and diamagnetic materials would actually have Verdet coefficients of different sign. Full understanding of the Zeeman effect requires a quantum mechanical analysis. Note that the sign of B gives the sign of rotation of polarization. Compare this to the case of optical activity where there is no applied field and since the material is isotropic, the sign of rotation is intrinsic to the material, depending only on the sign of χ_M.
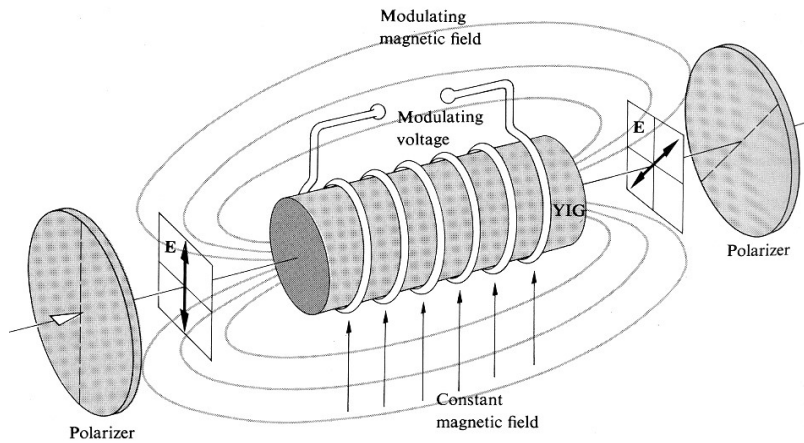

Figure 7.10 Faraday Cell

70

Chapter 8 – Nonlinear Optical materials

➢ Corresponding handouts are available on http://kik.creol.ucf.edu/courses.html

For very high irradiance beams, the electric field is large enough that the polarization response, usually written as

$$P(\omega) = \varepsilon_0 \chi(\omega)\varepsilon(\omega) \tag{8.1}$$

is no longer linearly dependent on the field strength. This is because the electron displacements from equilibrium are so large that Hooke's law, F = -Kx, is no longer exactly true. To examine the effect of a nonlinear restoring force, we expand the polarization into a power series in E:

$$P(E) = P^{(1)} + P^{(2)} + P^{(3)} + \ldots = \varepsilon_0 \left[\chi^{(1)}E + \chi^{(2)}E^2 + \chi^{(3)}E^3 + \cdots \right] \tag{8.2}$$

Note that we have omitted frequency arguments for simplicity here. In general, new frequencies are generated, so we will deal with the appropriate frequencies on a case-by-case basis.

Anharmonic oscillator model

While there is no simple general answer to the polarization response of an anharmonic oscillator, we can find an approximate response starting from Hooke's law, and adding the nonlinear response as a small perturbation. Hooke's law (F = -Kx) corresponds to a purely parabolic or 'harmonic' binding potential:

$$V(x) = -\int F dx = \frac{1}{2}Kx^2 = \frac{1}{2}m\omega_0^2 x^2 \tag{8.3}$$

Note that V(x) here represents the position dependent potential energy of the electron in joules, not the electric potential in volts. The parabolic description is a good approximation for small deviations from equilibrium, but the binding potential cannot remain parabolic for all values of x. A more realistic potential may be obtained from a power series representation:
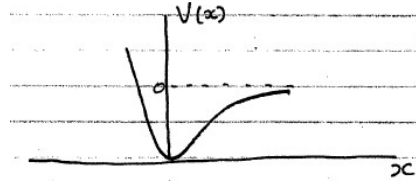
$$V(x) = \frac{1}{2}m\omega_0^2 x^2 + \frac{1}{3}max^3 + \frac{1}{4}mbx^4 + \ldots \tag{8.4}$$

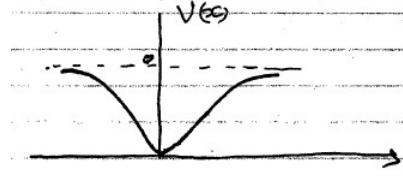where a and b are anharmonicity coefficients. The "modified Hooke's law" now becomes

$$F(x) = -\frac{dV}{dx} = -m\omega_0^2 x - max^2 - mbx^3 - \ldots \tag{8.5}$$

The magnitude of the anharmonicity coefficients depends – among other things – on the symmetry of the material. For a centrosymmetric medium, V(x)=V(-x), we have only even-order terms:

$$V(x) = \frac{1}{2}m\omega_0^2 x^2 + \frac{1}{4}m\,bx^4 + \cdots$$

$$F(x) = -m\omega_0^2 x - mbx^3 - \cdots \tag{8.6}$$

Non-centrosymmetric potential   *Centrosymmetric potential*

For each type of material, we will consider only the lowest anharmonic terms, since those tend to dominate over the higher order terms.

Non-centrosymmetric materials – SHG and optical rectification

We will solve the equation of motion for x(t) and hence for P(t) using a simple perturbation method. First, we will consider non-centrosymmetric media, with only the lowest order anharmonic term:

$$\frac{d^2x}{dt^2} + \gamma\frac{dx}{dt} + \omega_0^2 x + ax^2 = -\frac{e}{m}E(t) \tag{8.7}$$

To solve this equation, we treat the ax^2 term as a small perturbation. If ax^2 is small, under excitation with a harmonic driving field E(t) the electron oscillation x(t) will also be predominantly harmonic ('sinusoidal'). This sinusoidal component of the electron motion will be called $x^{(1)}(t)$ where the superscript (1) indicates that this represents the first order (linear) response. In the following we'll first have a qualitative look at the effect of the term ax^2 on the response.

From the equation above we see that there will be a small extra force $a \cdot x(t)^2$ on the electron. In the presence of a sinusoidal driving field E(t) the motion is also approximately sinusoidal, i.e. $x(t) \approx x^{(1)}(t)$. This means that our extra force will scale approximately with $[x^{(1)}(t)]^2$ and thus approximately with $E(t)^2$. For harmonic excitation we thus observe extra forces of the form $\sin^2(\omega t) = \frac{1}{2}(1-\cos(2\omega t))$. This immediately suggests that for materials with a finite anharmonicity coefficient *a*, a large linear response (large-amplitude sinusoidal motion) will introduce a small contribution to the electron motion at *zero frequency* due to the term '1' in the argument above, and a small contribution at *twice the frequency* of the driving field due to the term $\cos(2\omega t)$ from above. The generation of these two terms are called *optical rectification* and *second harmonic generation* respectively.

The fact that the $[x^{(1)}(t)]^2$ term is proportional to $1-\cos(2\omega t)$ tells us that the strength of the extra restoring force at both these new frequencies will be equal. The actual induced additional electron response resulting from these extra force contributions will depend on the response of the atom to these new driving forces, i.e. on the linear equation of motion.

We have found that the coefficient *a* can lead to new force (compared to Hooke's Law) and therefore a contribution to the electron oscillation that scales with $[x^{(1)}(t)]^2$ and thus with $E(t)^2$. The resulting displacement x with the same functional form as $E(t)^2$ will be called the second order displacement $x^{(2)}$ with a corresponding second order polarization $P^{(2)}$. Both $x^{(2)}$ and $P^{(2)}$ can contain terms with different frequencies (in this example zero frequency and the second harmonic). In order to describe the resulting polarization $P^{(2)}$ in terms of E^2 we will need an expression for the second order susceptibility $\chi^{(2)}$ that specifies

the magnitude and phase of the polarization response at each of the new frequencies, denoted $\chi^{(2)}(0)$ and $\chi^{(2)}(2\omega)$.

The arguments above state that the anharmonic oscillator model will yield a polarization response that looks almost exactly like the linear response $P^{(1)}$, but that will contain a small (multi-frequency) contribution denoted $P^{(2)}$ that scales with $E(t)^2$ as a result of the anharmonicity parameter a. A similar analysis involving anharmonicity parameter b shows that the polarization will also contain a third order polarization contribution $P^{(3)}$ that is proportional to $x(t)^3$ and thus approximately to $[x^{(1)}]^3$ and to $E(t)^3$. The total polarization can thus be described by an equation of the form

$$P(E) = P^{(1)} + P^{(2)} + P^{(3)} + \dots$$

$$= \varepsilon_0 [\chi^{(1)}E + \chi^{(2)}E^2 + \chi^{(3)}E^3 + \dots] \tag{8.8}$$

Note that the analysis above can also be used when $E(t)$ contains multiple frequencies (e.g. two laser beams) but first we will investigate the case of a single driving frequency.

To find the second order motion amplitudes $x^{(2)}(0)$ and $x^{(2)}(2\omega)$ and the corresponding expressions for $\chi^{(2)}(0)$ and $\chi^{(2)}(2\omega)$, we need to solve the nonlinear equations of motion. To derive the nonlinear equations of motion, we will set the driving field to be $\lambda E(t)$ with $\lambda \ll 1$. Note λ is a scaling parameter, <u>not the wavelength</u>. We look for motion amplitudes $x^{(i)}$ that scale with λ according to

$$x(t) = \lambda x^{(1)}(t) + \lambda^2 x^{(2)}(t) + \lambda^3 x^{(3)}(t) + \dots \tag{8.9}$$

Substituting this into the nonlinear equation of motion (Eq. 8.7) results in terms proportional to $\lambda, \lambda^2, \lambda^3$, etc. Solving separately for only those terms that scale linearly with λ gives an equation of motion proportional to λ describing a linear response to the driving field:

$$\lambda^1 \quad : \quad \ddot{x}^{(1)} + \gamma \dot{x}^{(1)} + \omega_0^2 x^{(1)} = -\frac{e}{m}E(t) . \tag{8.10}$$

Solving Separately for only those terms that scale with λ^2 yields a second order equation of motion:

$$\lambda^2 \quad : \quad \ddot{x}^{(2)} + \gamma \dot{x}^{(2)} + \omega_0^2 x^{(2)} = -a\left(x^{(1)}(t)\right)^2 \tag{8.11}$$

Note that if $a=0$, this second order equation has no driving term, resulting in only one solution: $x=0$, indicating that no nonlinear contribution to the electron motion occurs.

To solve for the response for finite values of a, we first solve the first order equation of motion, which will give us the linear response. If we take a harmonic driving field:

$$E(t) = \frac{1}{2}E_1(\omega_1)e^{-i\omega_1 t} + c.c. \tag{8.12}$$

the first order equation yields

$$x^{(1)}(\omega) = -\frac{e}{m}\frac{E_1(\omega_1)}{\omega_0^2 - \omega^2 - i\omega\gamma} \tag{8.13}$$

which gives the first order macroscopic polarization:

$$P^{(1)}(\omega) = -Nex^{(1)}(\omega_1) = \frac{Ne^2}{m} \frac{E_1(\omega_1)}{\omega_0^2 - \omega_1^2 - i\omega_1\gamma} \tag{8.14}$$

Realizing that

$$P^{(1)}(\omega) = \varepsilon_0 \chi^{(1)}(\omega)E(\omega) \tag{8.15}$$

we have found that

$$\chi^{(1)}(\omega) = \frac{Ne^2}{\varepsilon_0 m} \frac{1}{\omega_0^2 - \omega^2 - i\omega\gamma} \tag{8.16}$$

This is simply the Lorentz susceptibility, as expected for a system with a linear restoring force. We will simplify the notation in the following substantially by defining a function that represents the resonance term in the denominator:

$$D(\omega) = \omega_0^2 - \omega^2 - i\omega\gamma \tag{8.17}$$

which allows us to write the linear susceptibility of our nonlinear material as

$$\chi^{(1)}(\omega) = \frac{\omega_p^2}{D(\omega)} \tag{8.18}$$

as we found before using the (linear) Lorentz model.

With the obtained linear response we now have an approximate description of the driving term in the second order equation of motion:

$$\ddot{x}^{(2)} + \gamma \dot{x}^{(2)} + \omega_0^2 x^{(2)} = -a \left(x^{(1)}(t) \right)^2 . \tag{8.19}$$

This assumes that x(t) looks approximately like the first order response only, which is only reasonable when the nonlinear contribution is small. Based on the expression for $x^{(1)}(t)$

$$x^{(1)}(t) = \frac{1}{2} x^{(1)}(\omega_1)e^{-i\omega_1 t} + \frac{1}{2} x^{(1)}(-\omega_1)e^{i\omega_1 t} \tag{8.20}$$

we find that

$$\left(x^{(1)}(t) \right)^2 = \frac{1}{4} \left(x^{(1)}(\omega_1) \right)^2 e^{-2i\omega_1 t} + c.c. + \frac{1}{2} \left| x^{(1)}(\omega_1) \right|^2 \tag{8.21}$$

We see that this term introduces a force that contains a frequency component $\pm 2\omega_1$ and a zero frequency component. Consequently the second order displacement $x^{(2)}$ will also contain amplitude at these new frequencies. We can describe our second order motion *at this double frequency* as

$$x^{(2)}(t) = \frac{1}{2} x^{(2)}(2\omega_1)e^{-i2\omega_1 t} + c.c. \tag{8.22}$$

Substituting the first term into the second order equation of motion gives

$$-(2\omega_1)^2 \frac{1}{2} x^{(2)}(2\omega_1)e^{-i2\omega_1 t} - i2\omega_1\gamma \frac{1}{2} x^{(2)}(2\omega_1)e^{-i2\omega_1 t} +$$
$$\omega_0^2 \frac{1}{2} x^{(2)}(2\omega_1)e^{-i2\omega_1 t} = -\frac{a}{4} \left(x^{(1)}(\omega_1) \right)^2 e^{-2i\omega_1 t} \tag{8.23}$$

which together with

$$x^{(1)}(\omega) = -\left(\frac{e}{m} \right) \frac{E_1(\omega_1)}{D(\omega_1)} \tag{8.24}$$

leads to:

$$[-(2\omega_1)^2 - i\gamma(2\omega_1) + \omega_0^2]\, x^{(2)}(2\omega_1) = -\frac{a}{4}\left(\frac{e}{m}\right)^2 \frac{(E_1(\omega_1))^2}{[D(\omega_1)]^2} \tag{8.25}$$

The left term between the square brackets is in fact $D(2\omega_1)$. Dividing left and right side by $D(2\omega_1)$ produces an expression for the second order contribution to the electron amplitude at the second harmonic frequency 2ω:

$$x^{(2)}(2\omega_1) = -\frac{a}{4}\left(\frac{e}{m}\right)^2 \frac{(E_1(\omega_1))^2}{D(2\omega_1)[D(\omega_1)]^2} \tag{8.26}$$

Note that the amplitude of the oscillation at $2\omega_1$ is large for excitation at $\omega_1=\omega_0$ and for excitation at $2\omega_1=\omega_0$.

Now we can derive the second order polarization from our expansion

$$P = P^{(1)} + P^{(2)} + \cdots \tag{8.27}$$

using our obtained second order contribution to the electron position:

$$P^{(2)}(2\omega_1) = \varepsilon_0\chi^{(2)}(2\omega_1; \omega_1, \omega_1)E^2(\omega_1) = -Nex^{(2)}(2\omega_1) \tag{8.28}$$

Substituting the expression for $x^{(2)}(2\omega_1)$ gives

$$\varepsilon_0\chi^{(2)}(2\omega_1; \omega_1, \omega_1)E^2(\omega) = \frac{aNe}{4}\left(\frac{e}{m}\right)^2 \frac{E_1^2}{D(2\omega_1)[D(\omega_1)]^2}$$

$$\Rightarrow \chi^{(2)}(2\omega_1; \omega_1, \omega_1) = \frac{a}{4}\left(\frac{e}{m}\right)\frac{\omega_p^2}{D(2\omega_1)D(\omega_1)D(\omega_1)} \tag{8.29}$$

This is the component of the second order susceptibility that describes the second order polarization and therefore the second harmonic generation in a non-centrosymmetric medium ($a\neq0$) under illumination with a single-frequency wave at ω. We will discuss later how this leads to the generation of a second harmonic wave that can grow to be quite large.

In addition to second harmonic generation, we see that there is also a zero frequency component to $P^{(2)}$. Solving for the zero frequency part of $(x^{(2)}(t))^2$ i.e. $x^{(2)}(0)$ we have

$$(0 + 0 + \omega_0^2)x^{(2)}(0) = -\frac{a}{2}\left|x^{(1)}(\omega_1)\right|^2$$

$$x^{(2)}(0) = -\frac{a}{2\omega_0^2}\left(\frac{e}{m}\right)^2 \frac{E_1 E_1^*}{D(\omega_1)D^*(\omega_1)}$$

$$= -\frac{ae^2}{2m^2}\frac{|E_1|^2}{D(0)D(\omega_1)D^*(\omega_1)}$$

$$\tag{8.30}$$

Where we have used

$$D(0) = (\omega_0^2 - 0^2 - i\gamma0) = \omega_0^2 \quad \text{and} \quad D^*(\omega_1) = D(-\omega_1) \tag{8.31}$$

Defining

$$P^{(2)}(0) = \varepsilon_0\chi^{(2)}(0; \omega_1, -\omega_1)\cdot 2E_1 E_1^* \tag{8.32}$$

we find

$$\chi^{(2)}(0; \omega_1, -\omega_1) = \frac{a}{4}\left(\frac{e}{m}\right)\frac{\omega_p^2}{D(0)D(\omega_1)D(-\omega_1)} \tag{8.33}$$

Non-centrosymmetric materials – SFG and DFG

In the above we have seen that a single input frequency can give rise to second harmonic generation and to optical rectification. When using multiple driving frequencies (e.g. illuminating a material with two different laser beams) we find a more general solution. If we take such a driving field

$$E(t) = \frac{1}{2}E_1 e^{-i\omega_1 t} + \frac{1}{2}E_2 e^{-i\omega_2 t} + c.c. \tag{8.34}$$

then $(x^{(1)}(t))^2$ becomes

$$\begin{aligned}
\left(x^{(1)}(t)\right)^2 &= \frac{1}{4}\left(x^{(1)}(\omega_1)\right)^2 e^{-2i\omega_1 t} + \frac{1}{4}\left(x^{(1)}(\omega_2)\right)^2 e^{-2i\omega_2 t} + c.c \\
&+ \frac{1}{2}x^{(1)}(\omega_1)x^{(1)}(\omega_2)e^{-i(\omega_1+\omega_2)t} + c.c. \\
&+ \frac{1}{2}x^{(1)}(\omega_1)\left(x^{(1)}(\omega_2)\right)^* e^{-i(\omega_1-\omega_2)t} + c.c. \\
&+ \frac{1}{2}\left|x^{(1)}(\omega_1)\right|^2 + \frac{1}{2}\left|x^{(1)}(\omega_2)\right|^2
\end{aligned} \tag{8.35}$$

showing that we also obtain terms with a frequency that is the sum of the original driving frequencies, and terms with a frequency that is given by the difference between the driving frequencies. The corresponding processes are called sum frequency generation and difference frequency generation.

The nonlinear susceptibilities describing sum and difference frequency mixing are defined by

$$P^{(2)}(\omega_1 + \omega_2) = \varepsilon_0 \chi^{(2)}(\omega_1 + \omega_2; \omega_1, \omega_2)2E_1 E_2 \tag{8.36}$$

$$\chi^{(2)}(\omega_1 + \omega_2; \omega_1, \omega_2) = \frac{Ne^3 a}{4\varepsilon_0 m^2}\frac{1}{D(\omega_1+\omega_2)D(\omega_1)D(\omega_2)} \tag{8.37}$$

and hence

$$P^{(2)}(\omega_1 - \omega_2) = \varepsilon_0 \chi^{(2)}(\omega_1 - \omega_2; \omega_1, -\omega_2)2E_1 E_2^* \tag{8.38}$$

$$\chi^{(2)}(\omega_1 - \omega_2; \omega_1, -\omega_2) = \frac{a}{4}\left(\frac{e}{m}\right)\frac{\omega_p^2}{D(\omega_1-\omega_2)D(\omega_1)D(-\omega_2)} \tag{8.39}$$

The shows that we have resonances at each of the three frequencies involved in the process.

While the anharmonic oscillator model is somewhat limited in accuracy, we should take away some important messages from it:

$\chi^{(2)}$ processes require a medium that lacks inversion symmetry
$\chi^{(2)}$ processes result in sum and difference frequency generation. In the case of degenerate ($\omega 1 = \omega 2$) mixing, these correspond to second harmonic generation and optical rectification.

Resonance enhancement of $\chi^{(2)}$ can result if any of the frequencies involved lies close to a material resonance. In quantum mechanical systems where there are several resonances more than one frequency can be resonantly enhanced.
The nonlinear susceptibilities are related to the linear susceptibilities.

The last comment relates to *Miller's rule*, which can be argued as follows:

We found: (note: factor 1/4 missing – check)

$$\chi^{(2)}(\omega_1 + \omega_2; \omega_1, -\omega_2) = \frac{Ne^3a}{\varepsilon_0 m^2} \frac{1}{D(\omega_1 + \omega_2)D(\omega_1)D^*(-\omega_2)}$$

(8.40)

but we also found that

$$\chi^{(1)}(\omega) = \frac{Ne^2/\varepsilon_0 m}{D(\omega)}$$

(8.41)

or

$$\frac{1}{D(\omega)} = \chi^{(1)}(\omega)\frac{\varepsilon_0 m}{Ne^2}$$

(8.42)

This allows us to write

$$\chi^{(2)}(\omega_1 + \omega_2; \omega_1, \omega_2) = \frac{\varepsilon_0^3 m^3}{N^3 e^6}\chi^{(1)}(\omega_1 + \omega_2)\chi^{(1)}(\omega_1)\chi^{(1)}(\omega_2) \times \frac{Ne^3}{\varepsilon_0 m^2}a$$

$$= \frac{\varepsilon_0^2 ma}{N^2 e^3}\chi^{(1)}(\omega_1 + \omega_2)\chi^{(1)}(\omega_1)\chi^{(1)}(\omega_2)$$

(8.43)

If we know a/N^2 and $\chi^{(1)}$ at each frequency in the process, we will have an estimate of $\chi^{(2)}$.

Miller (Appl. Phys. Lett. 5, 17 (1964)) noted that for all non-centrosymmetric materials a/N^2 appears to be roughly constant, i.e. he found that for several different materials

$$\frac{\chi^{(2)}(\omega_1 + \omega_2; \omega_1, \omega_2)}{\chi^{(1)}(\omega_1 + \omega_2)\chi^{(1)}(\omega_1)\chi^{(1)}(\omega_2)} \sim constant = \delta$$

(8.44)

where

$$\delta = \frac{\varepsilon_0^2 ma}{N^2 e^3}$$

This constant is known as Miller's delta. Variations in Miller's δ are limited to a factor ~2. Miller's rule allows us to estimate the value of $\chi^{(2)}$ for a material without having to measure it. Typically, δ ~2.5×10⁻¹³ m/V.

In a medium with n≈1.5, we have $X \approx n^2-1$ ~1.25. In this case we have

$$\chi^{(1)}(\omega_1 + \omega_2)\chi^{(1)}(\omega_1)\chi^{(1)}(\omega_2) \approx 2$$

(8.45)

Typical values of $\chi^{(2)}$ are 5E-13 m/V or 0.5 pm/V.

Centrosymmetric materials – THG and nonlinear refraction

Centrosymmetric materials are materials that are invariant under the transformation $r \rightarrow -r$. For such materials, a=0, and hence $\chi^{(2)}$ is zero. Hence the lowest order anharmonic term is mbx^3. The equations of motion in this case become

$$\lambda^1 \; : \quad \ddot{x}^{(1)} + \gamma \dot{x}^{(1)} + \omega_0^2 x^{(1)} = -\frac{e}{m} E(t)$$

$$\lambda^3 \; : \quad \ddot{x}^{(3)} + \gamma \dot{x}^{(3)} + \omega_0^2 x^{(3)} = -b\left(x^{(1)}(t)\right)^3 \qquad (8.46)$$

Note that all materials (including the non-centrosymmetric ones) have a finite third order anharmonicity coefficient b. This means that the effects described below can be observed in all materials at sufficient incident irradiance.

For a monochromatic driving field

$$E(t) = \frac{1}{2} E_1 e^{-i\omega t} + c.c. \qquad (8.47)$$

we have

$$x^{(1)}(\omega t) = \frac{1}{2} x^{(1)}(\omega) e^{-i\omega t} + c.c. \qquad (8.48)$$

In the third order equation of motion this leads to a driving term proportional to

$$\left(x^{(1)}(t)\right)^3 = \frac{1}{2}\left(x^{(1)}(\omega)\right)^3 e^{-3i\omega_1 t} + cc$$

$$+ \frac{1}{2} \cdot 3 x^{(1)}(\omega)\left|x^{(1)}(\omega)\right|^2 e^{-i\omega t} + c.c.$$

$$(8.49)$$

resulting in a polarization component oscillating at 3ω, the third harmonic, and a component oscillating at a frequency ω. This intensity dependent contribution to the susceptibility at the fundamental frequency results in an intensity dependent refractive index and intensity dependent absorption.

Now, for the component at ω we have

$$x^{(3)}(\omega) = -\frac{-3be^3/(2m)^3}{D(\omega)D(\omega)D(\omega)D(-\omega)}|E_1|^2 E_1$$

$$P^{(3)}(\omega) = -Nex^{(3)}(\omega) = \frac{-3Nb\,e^4/(2m)^3}{D^3(\omega)D(-\omega)}|E_1|^2 E_1$$

$$(8.50)$$

But

$$P^{(3)}(\omega) = \varepsilon_0 \chi^{(3)}(\omega; \omega, \omega, -\omega)|E_1|^2 E_1$$

$$\chi^{(3)}(\omega; \omega, \omega, -\omega) = \frac{b}{8} \left(\frac{e}{m}\right)^2 \frac{\omega_p^2}{D(\omega)D(\omega)D(\omega)D(-\omega)}$$

$$(8.51)$$

and

$$\chi^{(3)}(3\omega; \omega, \omega, \omega) = \frac{b}{8} \left(\frac{e}{m}\right)^2 \frac{\omega_p^2}{D(3\omega)D(\omega)D(\omega)D(\omega)}$$

$$(8.52)$$

corresponding to the third order susceptibility contribution giving rise to a third harmonic signal.

Chapter 9 – Quantum mechanics

➢ Corresponding handouts are available on http://kik.creol.ucf.edu/courses.html

The preceding Chapters described light-matter interaction in classical terms. To fully understand many modern optical effects it is necessary to realize that under certain conditions matter must be described as having wave-like properties. For bound electrons this leads to distinct possible states with energies that can only take on specific values. This in turn means that optical transitions that change the energy of a system must involve discrete amounts of electromagnetic energy, leading to the surprising realization that our continuous EM waves must be seen as containing 'packets' of energy, known as photons. Most of this course deals with the semiclassical view of light-matter interaction, which means that EM waves are treated as classical waves, while electrons are described with quantum mechanical states.

More in-depth CREOL courses dealing with quantum mechanics:

OSE6349 Applied Quantum Mechanics for Optics and Engineering: Elements of quantum mechanics that are essential for understanding many areas in modern optics and photonics.

OSE6347 Quantum Optics: Semi-classical treatment of light/matter interaction (quantized atomic states and Maxwell's equations), density matrix theory, coherent optical transition, pulse propagation.

For the CREOL course OSE5312 the quantum mechanical description of light matter interaction is taught from select chapters in David A. Miller's book 'Quantum Mechanics for Scientists and Engineers'. The topics that are covered in OSE5312 are listed in Appendix K. Below follows an abbreviated (but ever expanding) description.

The early days

In the late 19th century, it was found that measurements on optical transitions in the hydrogen atom could not be explained using the classical mechanical model of a negatively charged electron orbiting a positively charged core, held together by the Coulomb force ($F = q_1 q_2 / 4\pi\varepsilon_0 r^2$). The classical model would predict that the electron could orbit at any arbitrary distance, and have a continuous spectrum of allowed energies. When taking into account that the orbiting electron should radiate energy (recall: accelerating charge radiates, Ch1), the classical model incorrectly predicts that the electron would lose energy as it orbits, and would therefore spiral toward the core causing all matter to collapse. Thankfully this doesn't happen.

By carefully studying the hydrogen absorption and emission spectra, Rydberg found that hydrogen absorbs light at very specific frequencies, corresponding to free space wavelengths λ_0 that follow a surprisingly simple relation:

$$\frac{1}{\lambda_0} = R_H \left(\frac{1}{n_1} - \frac{1}{n_2} \right)$$

with R_H the Rydberg constant 1.097 um^{-1}, and $n_1 < n_2$ both integers. Based on this work and analysis by Bohr, Louis the Broglie hypothesized that any moving object has an associated wave character with a wavelength given by $\lambda = h/p$ where h is the Planck constant (6.626 10^{-34} Js). Here p represents the momentum of the moving particle, here the electron orbiting the ion core. This led to the following important relation between quantum mechanical momentum, and the matter wavelength $\lambda = \frac{h}{p}$ known as the de Broglie wavelength. This hypothesis was later found to accurately describe electron diffraction by a Ni crystal http://prola.aps.org/abstract/PR/v30/i6/p705_1 (1927). The wave-like behavior of particles has many profound consequences in physics. Here we will focus mostly on the effect of the wave-like nature of electrons on their possible energies and movement.

The wavefunction

As discussed above, electrons show behavior that is wave-like. This means that we can no longer fully describe an electron simply with a position and a velocity. Instead we need a function that describes the 'matter wave amplitude' as a function of position. This kind of particle amplitude is called a *wavefunction*, typically written as $\psi(x, y, z)$.[xvi] While 'matter amplitude' doesn't have a classical analog, it can be used to calculate a wide range of observable physical properties.

If ψ is the electron wavefunction, then the probability of finding the electron in infinitesimal volume dxdydz is proportional to

$$P_{dV} \propto |\psi(x, y, z)|^2 dxdydz \qquad (9.1)$$

We can change the 'proportional' sign in this equation to an 'equals' sign if we normalize the wavefunction as follows:

$$\psi_N = \frac{\psi}{\sqrt{\int |\psi|^2 dxdydz}} \qquad (9.2)$$

In the following we will assume that we are dealing with normalized wavefunctions, meaning that $|\psi|^2$ represents the *probability density*, i.e. the probability of finding the electron per unit volume.

Note that the wave description of electrons has some similarities to the wave description of light.[xvii] We know that light intensity ('photon probability') scales with $|E|^2$, just like the electron probability scales with $|\psi|^2$.

Electron momentum and kinetic energy

As mentioned above, the wavelength of the electron was experimentally found to be related to its momentum:

[xvi] In OSE5312 we exclusively look at single-particle wavefunctions, but the concept can also be extended to states involving multiple particles, with e.g. a wavefunction $\psi(\vec{r}_1, \vec{r}_2)$ describing '*what is the probability (amplitude) that particle 1 is at position r_1, and particle 2 is at position r_2?*'
[xvii] There are also some very important differences: the electron amplitude is scalar, not vectorial. Electrons cannot be absorbed or dissipated in the way that light can. Electrons are fermions, photons are bosons, which has – among other things – important consequences for thermal distributions.

$$\lambda_e = \frac{h}{p} \tag{9.3}$$

This is called the *de Broglie* wavelength of the electron.[xviii]

If ψ describes an electron wave with a well-defined momentum p everywhere, then apparently it should have the same wavelength everywhere. This means that a freely moving electron with constant momentum can be described by a wave with a fixed wavevector k. The (unnormalized) wavefunction of a free undisturbed electron is then

$$\psi_e(z) = e^{ikz}. \tag{9.4}$$

In this expression the electron wavevector is linked to the wavelength in the usual way: $k = \frac{2\pi}{\lambda_e}$. Comparing this with the de Broglie wavelength, we find the following expression for the electron momentum:

$$p = \hbar k. \tag{9.5}$$

Note that this expression for the momentum is only valid for a particle with a perfectly defined momentum everywhere.[xix] At any point in space we can extract the momentum by investigating the wavelength of this plane wave, which we can do by taking a single spatial derivative. For an electron moving along the z direction we have

$$\frac{d}{dz}\psi_e(z) = \frac{d}{dz}e^{ik_z z} = ik_z\, e^{ik_z z} = i\frac{p_z}{\hbar}e^{ik_z z} \tag{9.6}$$

where the last step uses $\lambda = h/p$. We have found the relation

$$-ih\frac{d}{dz}\psi_e(z) = p_z\; e^{ik_z z} \tag{9.7}$$

where p_z is the momentum of the electron along the z-direction. We see that taking the spatial derivative of our wavefunction places a multiplier in front of our original wavefunction that tells us about momentum. The operation that we carry out on the left is called an 'operator', here specifically the *momentum operator*. Operators are written with a 'hat', so we have

$$\hat{p}_z = -i\hbar\frac{d}{dz} \tag{9.8}$$

When the electron wavefunction has a well-defined ('single valued') property everywhere, the electron is said to be in an *Eigenstate*, and in this case ψ is said to be an *Eigenfunction*. Our free electron apparently satisfies the relation

$$\hat{p}_z\,\psi_e(z) = p_z\,\psi_e(z) \tag{9.9}$$

This says: wherever you look, the electron wave has the same periodicity, and therefore the same momentum. In this case ψ is apparently a *momentum Eigenfunction*: the operation $\hat{p}_z$ acting on wavefunction ψ produces a result with the same shape as ψ, just multiplied

---

[xviii] This is a general property of matter. For example, a moving neutron also has a de Broglie wavelength related to its momentum. Since the neutron is much heavier than the electron, at the same velocity it will have a much higher momentum and a much smaller wavelength.

[xix] In fact this is also the appropriate expression for the momentum of a photon, a massless quantum particle of light.

by its momentum value. This also explains the name Eigenfunction: the word 'Eigen' comes from German meaning 'self', and an 'Eigenfunction' of the momentum operator is a function that turns into itself (maintains its original shape) when you carry out the momentum operation.

We saw that we can learn about the momentum of a particle by investigating the single spatial derivative of the wavefunction. It turns out that we can also investigate related properties that depend on momentum, for example the kinetic energy $\frac{1}{2}mv^2 = \frac{p^2}{2m}$. We can use the momentum operator to construct an operator that represents the kinetic energy. For an electron in a momentum Eigenstate we had relation 9.9. Since the right-hand side is a constant times the momentum Eigenfunction, it's easy to see that our free electron also satisfies

$$\hat{p}_z[\hat{p}_z \psi_e(z)] = -i\hbar\frac{d}{dz}[p_z \psi_e(z)] = -i\hbar p_z\frac{d}{dz}\psi_e(z) = p_z^2\psi_e(z) \tag{9.10}$$

We write the act of applying operator $\hat{p}_z$ twice in a row as $\hat{p}_z^2$, so we have:

$$\hat{p}_z^2\psi(z) \equiv \hat{p}_z[\hat{p}_z \psi_e(z)] \tag{9.11}$$

For general statements about operators we often omit the wavefunction, so the previous relation is often written as

$$\hat{p}_z^2 \equiv \hat{p}_z\hat{p}_z \tag{9.12}$$

We have seen that in a constant potential an Eigenfunction of $\hat{p}_z$ is also an Eigenfunction of $\hat{p}_z^2$. We can now construct an operator that represents kinetic energy:

$$\frac{\hat{p}_z^2}{2m_e}\psi(z) = -i\hbar\frac{d}{dz}\left[-i\hbar\frac{d}{dz}\right]\frac{1}{2m_e}\psi(z) = -\frac{\hbar^2}{2m_e}\frac{d^2}{dz^2}\psi(z) \tag{9.13}$$

We have constructed the *kinetic energy operator*:

$$\hat{E}_{kin}\psi(z) = -\frac{\hbar^2}{2m_e}\frac{d^2}{dz^2}\psi(z) \quad \Rightarrow \quad \hat{E}_{kin} \equiv -\frac{\hbar^2}{2m_e}\frac{d^2}{dz^2} \tag{9.14}$$

A system that has perfectly defined kinetic energy[xx] must be in a kinetic energy Eigenstate, and must therefore satisfy

$$\hat{E}_{kin}\psi(z) = -\frac{\hbar^2}{2m_e}\frac{d^2}{dz^2}\psi(z) = E_{kin}\,\psi(z) \tag{9.15}$$

with E_{kin} on the right hand side a number. Substituting our momentum Eigenfunction in vacuum $\psi_e(z) = e^{ikz}$ into this relation we find

$$\hat{E}_{kin}\psi(z) = -\frac{\hbar^2}{2m_e}\frac{d^2}{dz^2}e^{ikz} = \frac{\hbar^2 k^2}{2m_e}\,\psi(z) \tag{9.16}$$

We have found the 'dispersion relation of free electrons', showing the free electron energy as a function of wavevector. Note that this follows simply from the de Broglie wavelength: previously we found (for a plane wave) $p = \hbar k$, and we already knew that classically

---

[xx] Note that having a single kinetic energy value means that the potential energy is not allowed to change. This relation thus only holds for electrons in a flat potential, e.g. in vacuum without applied fields.

$E_{kin} = p^2/2m$, so the quadratic dependence of energy on wavevector is an expected result for a free electron.

The Time-independent Schrödinger Equation

If an electron is placed near a positive charge or even just in a constant applied field, it will have a position-dependent potential energy, which here we call $V(\vec{r})$. This is not the electric potential: in most quantum mechanical formulas the function $V(\vec{r})$ represents potential energy, which for an electron in an electric potential $V_e(\vec{r})$ is simply given by $V(\vec{r}) = -eV_e(\vec{r})$. Energy conservation states that if an electron moves to a region with lower potential energy, it must gain a corresponding amount of kinetic energy. With this in mind, we can also construct an operator that describes the total electron energy E that is the sum of kinetic and potential energy. We will call this simply 'the energy'. If an electron has a well-defined energy then apparently the sum of the kinetic and potential energy is the same at every position. Such an *energy Eigenfunction* must satisfy:

$$\hat{E}_{tot}\psi(z) = \left[\hat{E}_{kin} + V(z)\right]\psi(z) = E\psi(z) \tag{9.17}$$

The term between the square brackets is the 'total energy operator' known as the *Hamiltonian $\hat{H}$*:

$$\hat{H}\psi(z) = \left[-\frac{\hbar^2}{2m_e}\frac{d^2}{dz^2} + V(z)\right]\psi(z) \tag{9.18}$$

An electron in a static potential distribution can have a well-defined energy only if the wavefunction is an *energy Eigenfunction* that satisfies

$$\left[-\frac{\hbar^2}{2m_e}\frac{d^2}{dz^2} + V(z)\right]\psi(z) = E\psi(z). \tag{9.19}$$

This is known as the *Time-independent Schrödinger equation*. For a three-dimensional system the Time-independent Schrödinger equation is:

$$\left(-\frac{\hbar^2}{2m_0}\nabla^2 + V(\vec{r})\right)\psi(\vec{r}) = E\,\psi(\vec{r}) \tag{9.20}$$

Solutions to the time-independent Schrödinger equation are Energy Eigenfunctions, which represent possible stationary electron distributions, for example bound electron states of an atom.

We noted previously that a momentum Eigenfunction in constant potential is also a kinetic energy Eigenfunction. Substituting a trial function $\psi_e(z) = e^{ikz}$ into the TISE with constant potential we find

$$\left[-\frac{\hbar^2}{2m_e}\frac{d^2}{dz^2} + V\right]e^{ikz} = Ee^{ikz} \Rightarrow E = \left[\frac{\hbar^2 k^2}{2m} + V\right] \tag{9.21}$$

The graph below shows the relation between total energy for a free electron in a constant potential of 0 eV (green curve) and a constant potential of 2 eV (blue curve). The frequency axis will be discussed later. Note that unlike photons (massless particles) in vacuum, electrons in vacuum have a quadratic dispersion relation, which is typical for particles with mass.
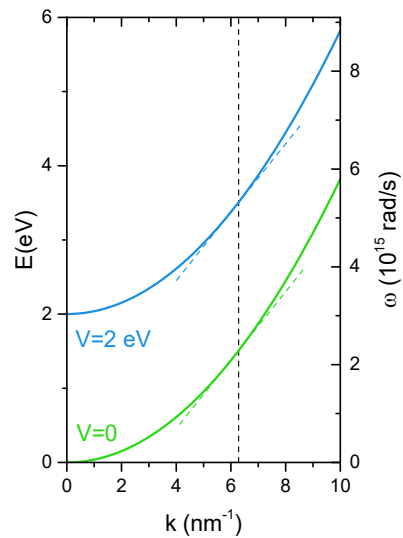
Figure 9.1 Free electron dispersion

Energy Eigenfunctions in important binding potentials

The time-independent Schrödinger equation only allows for wavefunctions that represent *stationary electron distributions* with a *well-defined energy* in the presence of a *static potential distribution*. Such allowed electron waves are known as 'electron states'. Our bound electrons from the Lorentz model (see Chapter 5) are electrons in such bound states around an atom core. To understand light-matter interaction from a quantum mechanical perspective, we first need to consider possible electron states, i.e. look at solutions to the time-independent Schrödinger equation in a static binding potential. Once we have found such allowed bound states, we will analyze how an applied electric field modifies the states ('push the electron around').

Important examples for optical materials are (quasi) free electrons, already discussed above), the Coulomb potential which describes bound electrons around an atom core, quantum wells in semiconductors that support trapped electron states with energies that depend on the well width, and the harmonic binding potential which describes molecular vibrations (and in fact the electromagnetic field, but this is outside the scope of these notes). The allowed states in these potentials will be discussed below.

Electron wavefunctions in a one-dimensional infinitely deep square well

One of the easiest to analyze 'electron binding potentials' is the one-dimensional infinite square well, which is represented by a region where the potential energy is constant, surrounded by regions where the potential energy is infinitely high. This seems like an entirely unphysical test system, but surprisingly it turns out that this system is very relevant to modern optics: it resembles to a great degree the situation in semiconductor quantum wells, which will be discussed later.

The figure below shows the position dependent potential of a square well extending from z=0 to z=L_z (the 'length along the z direction'). Inside the well we set the V=0, and outside we set the potential to a constant value V_0. For an infinite square we take $V_0 \to \infty$. Under

this condition, the electron cannot leave the well, meaning that the probability density outside the well will be zero, and therefore also ψ=0 outside the well.
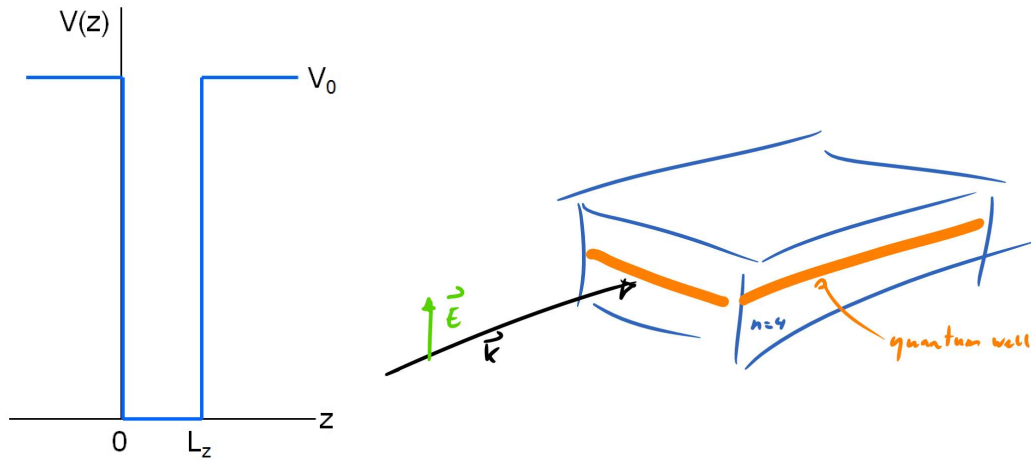
Figure 9.2 Schematic of square quantum well and example physical system

To find all possible wavefunctions inside the infinite square well, we are looking for solutions to the time independent Schrödinger equation

$$\left(-\frac{\hbar^2}{2m_0}\nabla^2 + V(\boldsymbol{r})\right)\psi = E\psi$$

which in this one-dimensional situation simplifies to

$$-\frac{\hbar^2}{2m_0}\frac{\mathrm{d}^2\psi(z)}{dz^2} + V(z)\psi(z) = E\psi(z)$$

Since we have set V=0 inside the well, wavefunctions in the well should satisfy

$$-\frac{\hbar^2}{2m_0}\frac{\mathrm{d}^2\psi(z)}{dz^2} = E\psi(z)$$

It is easy to recognize that this will lead to solutions of the form $\psi \propto e^{ikz}$ where the wavevector will be energy dependent (larger E ⟹ larger double derivative needed = larger k ⟹ shorter wavelength). Substituting this in Eq. x we find the relation

$$\frac{\hbar^2 k^2}{2m_0}\psi(z) = E\psi(z)$$

We have obtained a simple relation between energy and wavevector:

$$E = \frac{\hbar^2 k^2}{2m_0}$$

Note that this relation assumes that V=0. The more general result including a position independent potential energy would yield

$$E_{kin} = E - V = \frac{\hbar^2 k^2}{2m_0}$$

Solutions to the TISE must satisfy certain boundary conditions. In general, in any realistic potential distributions the wavefunction must be (1) finite, (2) continuous, and (3) continuously differentiable. For the limiting case of infinitely high potential walls, the third requirement is not considered.

Since ψ=0 for z ≤ 0 and z ≥ L$_z$, our solutions must reach zero amplitude for z=0 and z=L$_z$. This requirement cannot be satisfied by solutions containing only a single wavevector k, since functions of the form $\psi \propto e^{ikz}$ have a nonzero amplitude everywhere. To solve this problem we consider superpositions of the form

$$\psi = A\, e^{ikz} + B\, e^{-ikz}$$

To satisfy the requirement of zero amplitude at z=0, we require

$$A + B = 0$$

or A= -B. To satisfy the requirement of zero amplitude at z=L$_z$, we thus require

$$A\, e^{ikL_z} - A\, e^{-ikL_z} = 0$$

This is equivalent to requiring

$$e^{ikL_z} - e^{-ikL_z} = 2i \sin kL_z = 0$$

The condition $\sin kL_z = 0$ is satisfied whenever the argument of the sine term is nπ with n an integer, i.e. $kL_z = n\pi$, or $k = n\left(\frac{\pi}{L_z}\right)$. We thus have an infinite number of allowed solutions of the form

$$\psi = A_n \sin\left(\frac{n\pi}{L_z} z\right)$$

where A$_n$ the magnitude of A$_n$ is determined by requiring that the wavefunction is normalized, and with an arbitrary complex phase.

The energy of the allowed wavefunctions or 'energy Eigenstates' is given by[xxi]

$$E_n = \frac{\hbar^2 k^2}{2m} = \frac{\hbar^2}{2m}\left(\frac{n\pi}{L_z}\right)^2$$

Note: the energy of the wavefunction increases quadratically with *n*, and decreases as the well width is increased.

One important conclusion is that for any well size, the lowest energy solution has a non-zero energy given by

$$E_1^\infty = \frac{\hbar^2}{2m}\left(\frac{\pi}{L_z}\right)^2$$

[xxi] Note: strictly speaking this is the kinetic energy term only, but since we have set V=0 inside the well, the total energy E is equal to the kinetic energy $\hbar^2 k^2/2m$ in this case.

where the superscript ∞ will be used to represent the fact that this is the solution of the infinite square well. This type of minimum energy is called the 'zero point energy' of the system. It is easy to understand that such minimum energy exists: the requirement of zero wavefunction amplitude at the well edges and nonzero amplitude inside the well implies finite curvature (double spatial derivative) of the wavefunction, which is associated with finite kinetic energy through the TISE.

This same zero-point energy also explains the concept of 'quantum confinement': the (lowest) energy of an electron can be increased by confining the electron in ever smaller volumes. This forms the basis of the tuning of light emission in semiconductor quantum dots.
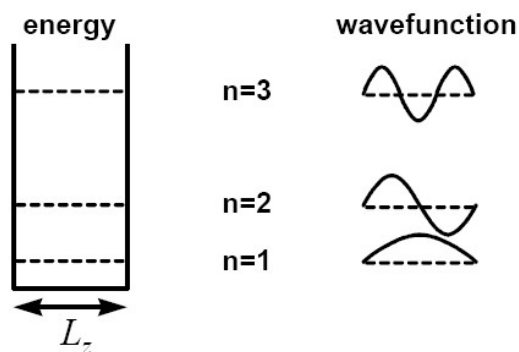
Figure 9.3 The first three Eigenstates of the infinite square well

Parity of quantum mechanical states

In the case of the infinite square well we saw that the allowed quantum states or Energy Eigenfunctions had well-defined symmetry properties. Our binding potential is inversion symmetric, and so is the probability distribution of all corresponding states. The wavefunction itself though can be either symmetric (n=1,3,5,…) or anti-symmetric (n=2,4,6, …). The symmetry of wavefunctions is described by the term *parity*. Symmetric states are said to have even parity, while anti-symmetric wavefunctions are said to have odd parity.[xxii] In our square well example wavefunctions are either perfectly odd or perfectly even. We will find later that light can induce transitions between states with opposite parity, while it cannot induce transitions between states with equal parity. This kind of relation that selectively allows specific transitions is called a *selection rule*. We will discuss this in more detail when we cover optical excitation and time-dependent perturbation theory.

States of the finite square well

In the previous section we discussed the somewhat unrealistic but very instructive case of the infinite square well. In that case the wavefunction probability became mathematically zero at the boundary because the electron has zero chance to enter this infinitely high potential region. In this case our continuous solutions went from having finite amplitude and slope to having zero amplitude and slope at the boundary. In the present section we

---

[xxii] Note that in our choice of n=1 for the ground state, even states are unfortunately described by an odd number. Even parity means that the wavefunction is left-right symmetric, not that the number n is even.

discuss the more realistic case of a *finite* potential barrier, and we will see that the results for the infinite well is simply a limiting case of the finite well.

For a wavefunction encountering a sharp finite potential barrier, the kinetic energy will suddenly drop, corresponding to a sudden change in the double spatial derivative. This means in this case the *slope* of the wavefunction is continuous. In the following we will consider bound states, meaning the electron will not have sufficient energy to overcome the barrier, in other words the total electron energy inside the well is less than the potential energy in the barrier. If we set the potential energy in the well to be V=0 and the barrier height is V_0, this means $E<V_0$. Inside the well the potential energy is flat, meaning the kinetic energy is constant, which is described by oscillatory solutions with a wavevector $k = \sqrt{2mE/\hbar^2}$. Outside the well, the kinetic energy expression E-V_0 becomes negative, corresponding to an imaginary wavevector $k = \pm i\sqrt{2m(V_0 - E)/\hbar^2}$. The allowed solutions are thus oscillatory in the well, with finite and continuous slope at the boundaries, and exponential decay outside the well. Example solutions are shown below (from Miller). The corresponding solutions look similar to those of the infinite well with well-defined parity (even, odd, even), however there are several key differences. First, there is a limited number of bound states, due to the requirement $E<V_0$. Second, we see some finite probability just outside the well region, and higher-energy solutions extend the furthest outside the well. And last, the energy levels are a bit lower than the corresponding levels in the infinite square well. This can be understood by realizing that by allowing the amplitude to be finite a the well boundary, the wavefunction is allowed to be a bit more 'spread out', corresponding to reduced curvature and thus reduced E.
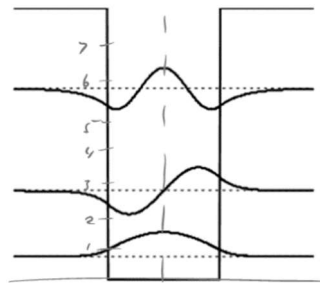
Figure 9.4 The <u>only</u> three Eigenstates of a particular finite square well

States of the harmonic oscillator

Another important quantum mechanical binding potential is the harmonic potential well. This describes for example mass held in place by a binding force that is linear in displacement, which is observed for example in molecular bonds, see Chapter 11. It also describes the electromagnetic field, with an energy that depends quadratically on field amplitude. The latter example is encountered in quantum optics, and is linked to properties such as spontaneous emission.

Before looking at the solutions of the quantum harmonic oscillator, let's first consider the classical harmonic oscillator. A 'harmonic binding potential' occurs in a system that follows Hooke's law, with a restoring force $F = -Kx$. This kind of restoring force produces a parabolic potential energy distribution $V = \frac{1}{2}Kx^2$, and for a bound mass m allows for a single resonance frequency $\omega_0 = \sqrt{K/m}$. The classical harmonic oscillator has a continuous range of allowed amplitudes and allowed total energies. At the center of

the potential well the potential energy is the lowers, and thus the oscillator moves the fastest.

The time independent Schrödinger equation for the harmonic binding potential is

$$-\frac{\hbar^2}{2m}\frac{d^2}{dz^2}\psi(z) + \frac{1}{2}m\omega_0^2 z^2\psi(z) = E\psi(z)$$

Solving the time-independent Schrödinger equation for allowed electron states in a harmonic binding potential, we thus expect solutions that have high kinetic energy and thus short wavelength in the center, and evanescent ('disappearing') amplitude where the energy is less than the potential energy, see the discussion of the finite well. It turns out that these requirements do not allow a continuous range of allowed energies. Instead, we find discrete and evenly spaced allowed energy levels, with energies given by

$$E_n = \left(n + \frac{1}{2}\right)\hbar\omega_0$$

where ω_0 is the classical resonance frequency based on the shape of the potential energy and the electron mass. Here n is an integer, with the minimum value of n=0 corresponding to the zero point energy $E_0 = \frac{1}{2}\hbar\omega_0$ of an electron in a harmonic potential (assuming V(0)=0). The corresponding normalized wavefunctions mathematically turn out to be products of a Hermite polynomial and a Gaussian.

$$\psi_n(z) = \sqrt{\frac{1}{2^n n!}\sqrt{\frac{m\omega}{\pi\hbar}}}\exp\left(-\frac{m\omega}{2\hbar}z^2\right)H_n\left(\sqrt{\frac{m\omega}{\hbar}}z\right)$$

These wavefunctions make up a complete orthonormal set. The lowest energy state is again even, just like in all our symmetric binding potentials, and every next level has the opposite parity.

slow   fast   slow   slow fast slow
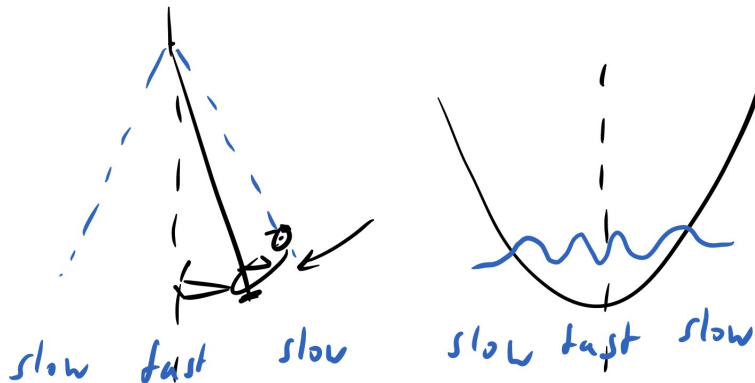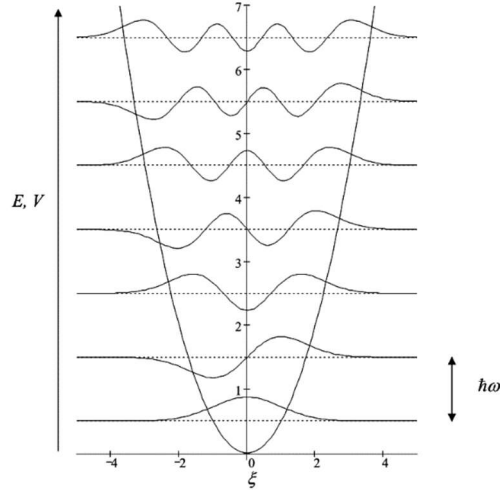
Figure 9.5 The lowest seven energy Eigenfunctions of a harmonic binding potential (from Miller)

For realistic finite binding potentials the shape does not remain parabolic forever. It is typically observed that energy level spacings drop for high motion amplitude (large quantum number).

States of the Coulomb potential

The preceding examples all describe one-dimensional systems. To understand real-world systems we need to consider three-dimensional binding potentials. One important example involves the Coulomb potential of the hydrogen atom. The atom core of a hydrogen atom has a charge $+1e$, and a corresponding potential energy

$$V(\vec{r}) = -\frac{1}{4\pi\epsilon_0}\frac{e^2}{|\vec{r}|}$$

This is a centrosymmetric potential, with vanishing attractive force and constant potential V=0 at large distance, and infinitely negative potential energy at r=0. Based on the preceding sections we might thus expect that the solutions will look oscillatory, and 'infinitely curved' in the center. One key difference with the prior 1D cases is that the wavefunction may be curved in multiple directions, and consequently finding the kinetic energy involves taking a double spatial derivative along x, y, and z. The time independent Schrödinger equation for an electron around a hydrogen core is thus

$$\hat{H}\psi(\vec{r}) = \left[-\frac{\hbar^2}{2m}\nabla^2 - \frac{1}{4\pi\epsilon_0}\frac{e^2}{|\vec{r}|}\right]\psi(\vec{r})$$

with r the electron position and the core assumed to be stationary at r=0. This is a reasonable approximation given that the atom core is more than thousand times heavier than the electron. Here we will not derive the solutions, but we will briefly discuss their properties. First of all, since the binding potential is spherically symmetric, at a fixed distance the potential energy is constant. This means that an energy Eigenfunction will have a constant kinetic energy at a fixed distance from the core. We thus expect to see something resembling a well-defined wavelength as we move around the atom. The allowed energies are again discrete, with the possible energies described by principal quantum number *n* and are given by

$$E_n = -\frac{Ry}{n^2}$$

with Ry ≈ 13.6 eV the Rydberg unit of energy. Note that this energy dependence explains the observation made at the beginning of this chapter: possible transitions in the hydrogen atom occurred for wavelengths that satisfied the relation

$$\frac{1}{\lambda_0} = E_f - E_i = \left(\frac{1}{n_i^2} - \frac{1}{n_f^2}\right) Ry.$$

The lowest-energy state with n=1 is strongly concentrated around the atom core. The next possible state with n=2 has higher total energy and higher kinetic energy, meaning 'more waves' or 'more curvature'. Since this is a three dimensional system, this extra curvature may be observed either tangentially or radially. In other words, there may be additional angular momentum and/or additional radial variation. The angular motion is described by angular momentum quantum number l, an integer with possible values l=0 ('only radial waves') up to maximum value $n=l$ ('only tangential waves'). One last degree of freedom is the orientation of tangential motion. For a state with finite angular momentum, e.g. l=1, the electron may rotate 'along the equator' (along φ in polar coordinates), but there may also be amplitude variation 'from pole-to-pole' (along θ in polar coordinates). The amount of variation along the equator is described by magnetic quantum number m, also an integer. Since rotation can be clockwise or counterclockwise, the magnetic quantum number can be positive or negative, with a maximum magnitude of $|m|=l$ (all angular moment along the equator). Together, the quantum numbers n, l, m fully describe motion of a single electron in a spherical binding potential.[xxiii]

The spherical symmetry of the binding potential allows only very specific angular distributions, known as spherical harmonics. These wave solutions appear for example in spherical quantum dots and in the optical modes of spherical optical resonators. The functional form of the spherical harmonics looks fairly complicated, but is determined entirely by quantum numbers l and m, with a ϕ dependent phase given by $e^{im\phi}$ and a θ dependent real amplitude, see Appendix J.

For some principal quantum number n, there are solutions with relatively small angular momentum quantum number, i.e. l<n. In that case there must then be some 'residual curvature' that implies radial (along r) variation of the wavefunction. For example, if a state has zero angular momentum (l=0), but a principal quantum number n=3, then there must be a lot of radial variation in the wavefunction. Once the shape of V(r) is known, the radial behavior is entirely determined by the quantum numbers n and l, see Appendix J.
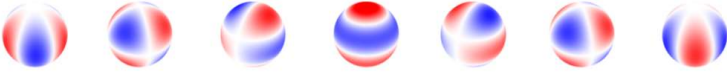
[xxiii] This excludes electron spin, spin-orbit interactions, reduced mass effects.
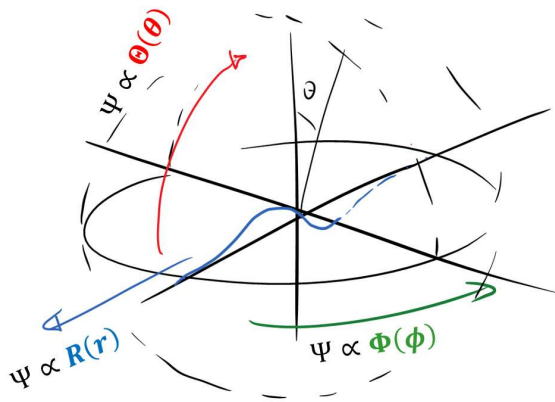
The total wavefunction is written as

$$\psi_{n,l,m}(r, \theta, \phi) = R_{n,l}(r)\, Y_l^m(\theta, \phi)$$

Where $Y_l^m(\theta, \phi)$ are the spherical harmonics, and $R_{n,l}(r)$ is the radial wavefunction. Examples of the spherical harmonics are shown below, the coloring indicating the real amplitude of the wavefunction. Also shown separately are the first few radial wavefunctions.

Orbital name   Surface plots of Re(Y$_{lm}$) with red=positive, blue=negative   Max electrons:

s $l=0$
requires n≥1
2

p $l=1$
requires n≥2
6

d $l=2$
requires n≥3
10

f $l=3$
requires n≥4
14

(2 spins per [l,m])

HYDROGEN ATOM

Radial wave functions

n	l			
		R_{10}	$=$	$2\left(\dfrac{Z}{a_0}\right)^{\frac{3}{2}} e^{-Zr/a_0}$
		R_{20}	$=$	$2\left(\dfrac{Z}{2a_0}\right)^{\frac{3}{2}}\left(1-\dfrac{Zr}{2a_0}\right) e^{-Zr/2a_0}$
		R_{21}	$=$	$\dfrac{1}{\sqrt{3}}\left(\dfrac{Z}{2a_0}\right)^{\frac{3}{2}}\left(\dfrac{Zr}{a_0}\right) e^{-Zr/2a_0}$
		R_{30}	$=$	$2\left(\dfrac{Z}{3a_0}\right)^{\frac{3}{2}}\left(1-\dfrac{2Zr}{3a_0}+\dfrac{2\,(Zr)^2}{27a_0^2}\right) e^{-Zr/3a_0}$
		R_{31}	$=$	$\dfrac{4\sqrt{2}}{3}\left(\dfrac{Z}{3a_0}\right)^{\frac{3}{2}}\left(\dfrac{Zr}{a_0}\right)\left(1-\dfrac{Zr}{6a_0}\right) e^{-Zr/3a_0}$
		R_{32}	$=$	$\dfrac{2\sqrt{2}}{27\sqrt{5}}\left(\dfrac{Z}{3a_0}\right)^{\frac{3}{2}}\left(\dfrac{Zr}{a_0}\right)^{2} e^{-Zr/3a_0}$

Two low-energy electron states of the hydrogen are show below, the ground state ($n=0$, $l=0$, $m=0$, and the first excited state with finite angular momentum ($n=1$, $l=1$, $m=1$). Note that the ground state is symmetric, while this first excited state is odd. We will find later that this makes it possible to excited a hydrogen atom from the ground state to the first excited state using light.
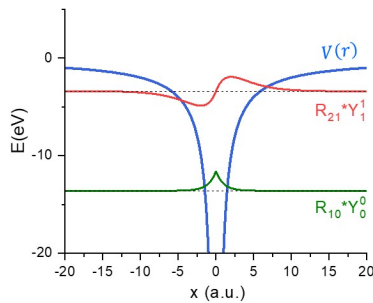
Orthonormal complete sets

To be added. Discuss based on infinite square well.

Inner product of functions f and g defined as

$$\int f(x)^* g(x)\, dx$$

Solutions to the infinite square well were of the form

$$\psi_n(z) = \sqrt{\frac{2}{L}}\sin\left(\frac{n\pi}{L}z\right)$$

It is easy to prove that the inner product of two *different* energy Eigensolutions of the infinite square well results in zero:

$$\int \psi_n^* \psi_m\, dx = 0 \ \ for\ m \neq n$$

95

This is easy to see for states 1 and 2:

$$\int \psi_1^* \psi_2 \, dz \propto \int_0^L \sin(\pi z/L) \sin(2\pi z/L) \, dz = 0$$

The latter step can be seen intuitively since the first sine wave is even about the center of the well, and the second one is odd. The product will be odd, so the integral will be zero.

Our Eigenstates are called 'orthogonal' since the inner product of different states gives zero. Similar to inner product of unit vectors (1,0,0) and (0,1,0): inner product zero means orthogonal.

Other special property: normalized. It's easy to prove that the inner product of one of our energy Eigenfunctions with itself produces 1:

$$\int \psi_n^* \psi_n \, dx = 1$$

Our Eigenfunctions are said to be normalized. Similar to 'unit vectors': inner product of (1,0,0) with itself has 'unit length'.

Final special property: completeness. Note: our Eigensolutions look like the terms in a Fourier series. Recall: Fourier series can be used to approximate any single-valued functional form on some finite domain (or any periodic functional form on an infinite domain), for example inside the infinite square well. In principle we'd need cosine terms as well, but our solutions must be zero at boundaries. Because we can build any $\psi(x)$ that satisfies the boundary conditions out of ψ_n we call the set of ψ_n a complete set.

Recall: ψ_n were normalized, orthogonal, and complete. ψ_n is a complete orthonormal set.

Expansion coefficients

To be added. Once normalized, expansion coefficient squared represents probability.

Dirac notation

To be added. Discuss overlap integral, projection onto basis.

Expectation value

To be added. Being in superposition of states implies average energy, give formula in Dirac notation. Energy expectation, position expectation, dipole moment expectation value.

Oscillatory dipole moment

To be added. Eigenstate has time dependent amplitude, but constant probability distribution. Show that superposition of odd and even states has time dependent dipole moment. If light can induce oscillatory dipole moment, apparently light can 'put some amplitude in state with opposite parity'. Can lead to dipole moment or disappearance of photons (=absorption). Discussed in time dependent perturbation theory.

Time dependent perturbation theory – excitation rate

To be added. Effect of perturbation Hamiltonian, describe potential distribution of plane wave. Introduce line shape, joint density of states, cross section

Time dependent perturbation theory – susceptibility

To be added. Derive formula for dipole moment.

The Time-Dependent Schrödinger Equation

The previously discussed time-*independent* Schrödinger equation tells us possible *stationary* charge distributions (electron probability distributions) with well-defined energy in a static potential. However to describe light-matter interaction we will need to consider situations where we excite our quantum system (e.g. a bound electron) with an electromagnetic wave. The oscillatory electric field adds an oscillatory contribution to the potential energy, so the total potential energy distribution $V(\vec{r}, t)$ contains both a static binding potential $V_0(\vec{r})$ and a contribution due to the presence of the EM wave $V_{EM}(\vec{r}, t)$. The response of the electron wavefunction to such time-dependent potential distributions is described by the time-dependent Schrödinger equation, given by

$$\left(-\frac{\hbar^2}{2m_0} \nabla^2 + V(\vec{r}, t) \right) \psi(\vec{r}, t) = i\hbar \frac{\partial}{\partial t} \psi(\vec{r}, t) \tag{9.22}$$

This relation can describe both the time dependent behavior of the electron in a dynamic potential, as well as the time dependent behavior of an electron in a static potential.

Note that the time-dependent Schrödinger equation is much less restrictive than the time-Independent Schrödinger equation. While the TISE only allows for wavefunctions with a perfectly defined energy in a static potential, the TDSE describes generally what happens to the electron in the presence of a binding potential and any applied electric fields. The TDSE states "*if the electron has energy at a given position, the wavefunction at that position must change over time*". This means that this equation allows for an infinite range of complicated temporal and spatial behavior.

The TDSE equation produces some important results when we consider a free electron in vacuum without any applied electric fields (V constant). In this case, and considering a one-dimensional situation (all movement along the z-axis), the time-dependent Schrödinger equation (TDSE) tells us

$$\left[-\frac{\hbar^2}{2m_0} \frac{\partial^2}{\partial z^2} + V \right] \psi(z, t) = i\hbar \frac{\partial}{\partial t} \psi(z, t) \tag{9.23}$$

We already know that in vacuum we can have momentum Eigenstates which had the form of a plane wave, and we saw that those plane waves in vacuum also happened to be energy Eigenstates. If we multiply our entire plane electron wave by a constant, the result is still an energy Eigenstate. This is even true if the constant is time-dependent. Substituting such a time dependent energy Eigenfunction

$$\psi(z, t) = f(t)e^{ik_z z} \tag{9.24}$$

into the TDSE we find a requirement on the time dependence:

$$\left[-\frac{\hbar^2}{2m_0}\frac{\partial^2}{\partial z^2} + V\right] f(t)e^{ik_z z} = i\hbar\frac{\partial}{\partial t}f(t)e^{ik_z z}$$

$$\Rightarrow f(t)\left[-\frac{\hbar^2}{2m_0}\frac{\partial^2}{\partial z^2} + V\right] e^{ik_z z} = i\hbar e^{ik_z z}\frac{\partial}{\partial t}f(t)$$

$$\Rightarrow f(t)E e^{ik_z z} = i\hbar e^{ik_z z}\frac{\partial}{\partial t}f(t) \tag{9.25}$$

$$\Rightarrow \frac{\partial}{\partial t}f(t) = -\frac{i}{\hbar}E\,f(t)$$

$$\Rightarrow f(t) = e^{-iEt/\hbar}$$

We see that a free electron in an energy Eigenstate must oscillate with an angular frequency of $\omega = E/\hbar$, in other words the total energy is linked to frequency according to $E = \hbar\omega$. This looks exactly the same as the formula for photon energy, but note that E here represents the total energy. This means that the frequency of the electron wavefunction can be changed with a static potential, while the photon frequency is not affected by a static potential.

We can apparently have a time dependent energy Eigenfunction in vacuum of the form

$$\psi(z,t) = e^{i(k_z z - \frac{E}{\hbar}t)} \tag{9.26}$$

We have found that a free electron in an energy Eigenstate is described by a *propagating* wave representing probability amplitude. This seems surprising: previously we stated that energy Eigenfunctions represented static probability distributions, but here we find an energy Eigenfunction that is a running wave. These statements are in fact not in conflict: calculating the probability density of our electron wave, we find for this energy Eigenstate

$$|\psi(z,t)|^2 = \psi^*(z,t)\psi(z,t) = e^{-i\left(k_z z - \frac{E}{\hbar}t\right)}e^{+i\left(k_z z - \frac{E}{\hbar}t\right)} = 1 \tag{9.27}$$

We see that our electron wave has a constant probability density everywhere, so the observable quantity 'probability' is actually not moving.

Superposition of time dependent energy Eigenfunctions

If we want to describe a moving free electron, we can construct an 'electron wavepacket' by superposing multiple plane momentum Eigenfunctions. This is in fact allowed by the TDSE: if we find different solutions to the TDSE then the superposition of these solutions is also a solution to the TDSE. This is easy to verify – try it. If we add electron plane waves with similar wavevector around an average wavevector $\bar{k}$ we can produce a localized probability distribution. This 'particle pulse' moves at a velocity known as the group velocity, which is given by

$$v_g(\bar{k}) = \left(\frac{d\omega}{dk}\right)_{k=\bar{k}} \tag{9.28}$$

Looking at Eq. 9.21 and using $E = \hbar\omega$ we see that for free electrons we have

$$E = \hbar\omega = \frac{\hbar^2 k^2}{2m} + V \implies v_g = \frac{\hbar\bar{k}}{m} = \frac{\bar{p}}{m} \qquad (9.29)$$

where $\bar{p}$ is the average momentum of the electron waves. We see that an electron pulse with an average quantum mechanical momentum $p = \hbar k$ moves at a velocity given by $v = p/m$, which is what we expect classically.

Uncertainty principle

Note that our electron wavepacket no longer has a perfectly defined momentum. If the momentum was perfectly defined, then the electron wavefunction must continue oscillating in exactly the same way everywhere, meaning that the electron probability is infinitely spread out. By making a superposition of waves with different momentum (different wavevector), we can make a wavepacket that is localized in space. A more strongly localized wavepacket (small Δx)   requires the use of a wider range of wavevectors (Δk). This kind of relation is called an *uncertainty relation*. The uncertainty relation for momentum and position is

$$\Delta x \Delta k \geq \frac{1}{2} \qquad (9.30)$$

or equivalently after multiplying by $\hbar$

$$\Delta x \Delta p \geq \frac{\hbar}{2} \qquad (9.31)$$

Here the Δ represents the standard deviation. The 'larger or equal' part of the uncertainty relations implies that the superposition of many wavevectors doesn't necessarily make a confined wavepacket; a maximally localized wavepacket requires the choice of very specific phases and amplitudes.

For processes that have a time dependence related to the addition of wavefunctions with different energy (and thus different time dependence ω) there is an energy-time uncertainty relation given by

$$\Delta\omega \Delta t \geq \frac{1}{2} \qquad (9.32)$$

or equivalently

$$\Delta E \Delta t \geq \frac{\hbar}{2} \qquad (9.33)$$

Chapter 10 – Homogeneous and inhomogeneous broadening

➢ Corresponding handouts are available on http://kik.creol.ucf.edu/courses.html

In the preceding chapters we have seen optical transitions that occur at specific frequencies, with a linewidth determined by some damping process described by a damping constant Γ (s^{-1}). We might expect that a system containing many such oscillators will result in an absorption line with the same linewidth Γ. If the linewidth of a collection of oscillators is practically the same as that of each individual oscillator, we call that line *homogeneously broadened*.

In real world situations however it is often found that the oscillators in a system all behave slightly differently. This can happen for example with molecules in a gas laser, quantum dots in a quantum dot detector, or rare earth dopant ions in a fiber amplifier. In these cases an absorption line may be broad not because Γ is large, but instead because ω_0 is a little different for the different elements in the system. If the linewidth of a collection of oscillators is larger than that of each individual oscillator, we call the line *inhomogeneously broadened*.

Inhomogeneous broadening due to variations in local environment

In many solid state systems, the atoms do not experience the same environment. In some cases, they may be in some random host matrix (e.g. a glass) where the surrounding electric field is slightly different and somewhat random for each atom, causing the resonance frequency of each atom to be slightly different. If the shift in the resonance frequency of each atom is random, the probability of having a given frequency shift with relative to the mean frequency is usually described by a Gaussian distribution. In this case each atom has a different resonant frequency, which is known as *inhomogeneous broadening*.
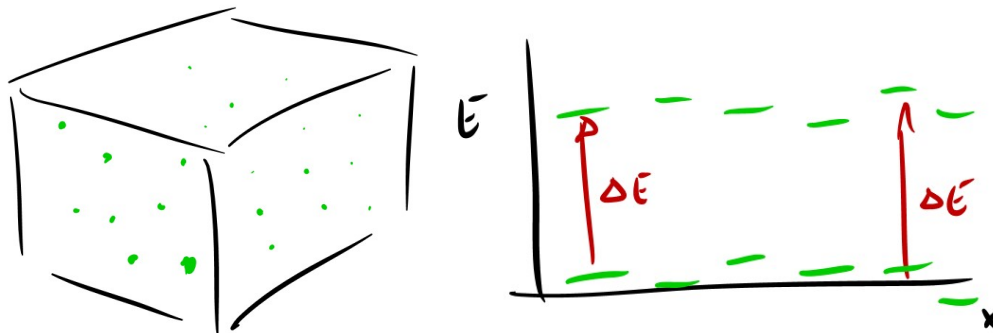
Figure 10.1: (left) Sketch of a block of glass containing dopants with an absorption line, and (right) sketch of the ground state and excited state energy levels. Variation in the local environment leads to variation in energy levels and transition energies, causing inhomogeneous broadening.

Doppler broadening

According to statistical mechanics of ideal gases, atoms (or molecules) in the gas phase have an isotropic temperature-dependent velocity distribution, described by the Maxwell-Boltzmann distribution, given by

$$f_{MB}(v) = \left(\frac{m}{2\pi kT}\right)^{3/2} 4\pi v^2 e^{-mv^2/2kT}$$

Here $f_{MB}(v)dv$ represents the fraction of atoms with a thermal velocity magnitude between v and v+dv, with m the mass of the atom (or ion, or molecule), and k the Boltzmann constant. When such a gas is illuminated using laser light propagating along the x-direction, some of the atoms travel away from the laser at velocity v_x. These atoms will experience an electromagnetic wave with a reduced frequency, which affects the absorption spectrum. The modified frequency ω' experienced by the atoms is

$$\omega' = 2\pi \frac{c - v_x}{\lambda_0} = 2\pi c \frac{1 - v_x/c}{\lambda_0} = \omega \left(1 - \frac{v_x}{c}\right)$$

This frequency shift is called a Doppler shift. If the stationary atom had resonance frequency ω_0, we need a laser with a slightly higher frequency in order to excite this atom to compensate for this Doppler shift.[xxiv] The atom thus appears to have a modified resonance frequency ω_0' that is given by

$$\omega_0' = \frac{\omega_0}{1 - \frac{v_x}{c}} \approx \omega_0 \left(1 + \frac{v_x}{c}\right)$$

The total absorption spectrum of a gas is thus composed of an ensemble of absorption lines from all atoms or molecules, slightly shifted depending on the velocity component toward or away from the excitation source. For fast atoms (high temperature or low atomic mass) the Doppler shift can be larger than the original atom linewidth. In this case we observe line broadening, a reduction of the peak absorption, and a change in the nature of the line shape, as discussed below.

The inhomogeneously broadened absorption spectrum of atoms or molecules in a gas is related to the thermal velocity distribution. The Maxwell-Boltzmann distribution describes the probability distribution for the *magnitude* of the velocity $|v| = \left(v_x^2 + v_y^2 + v_z^2\right)^{1/2}$. However since the Doppler shift depends on the atom velocity *along the laser propagation direction*, we need a probability distribution along a specific direction, e.g. v_x. It can easily be shown that this projected velocity distribution, called the Maxwellian velocity distribution, is given by

$$f_M(v_x) = \left(\frac{m}{2\pi kT}\right)^{1/2} e^{-mv_x^2/2kT}.$$

The graphs below show the Maxwell-Boltzmann distribution (left) and Maxwellian distribution (right) at room temperature (T=293 K) for a gas containing hydrogen molecules, oxygen molecules, and Xe atoms (or ions).

Note that at the same temperature molecules with low weight (e.g. H_2) move much faster, and that the typical room temperature velocities are hundreds of meters per second. Also note that it is relatively likely to have zero velocity along the x direction (right graph, maximum probability for v_x=0). This tells us that most atoms contributing to the total absorption have $v_x \approx 0$, and we therefore expect that the absorption of a hot gas will still be

---

[xxiv] Note that this effect seems opposite to the redshift observed in astronomy. Hydrogen related lines appear red-shifted because distant stars are moving away from us, while here we are required to use a blue-shifted laser to excite molecules that are moving away from us. Are these observations in conflict with each other?

maximum at the original ω_0. However there are also many atoms with $v_x \neq 0$ which means that we will observe some blue-shifted and red-shifted absorption, corresponding to *Doppler broadening*.
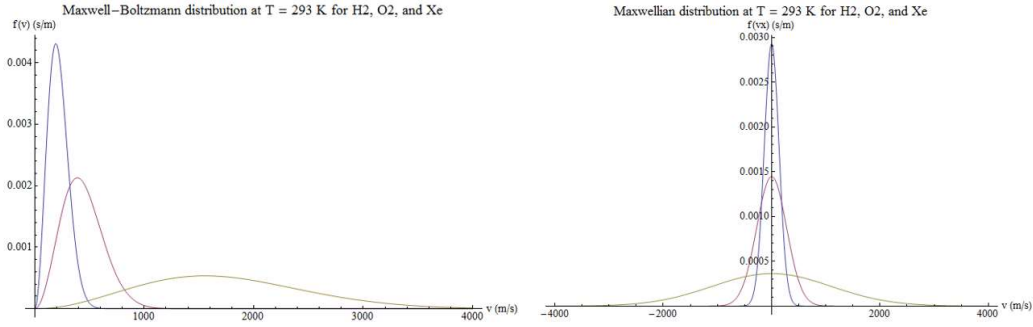
Figure 10.2: Maxwell-Boltzmann (left) and Maxwellian (right) velocity distribution for a room-temperature gas of H_2, O_2, and Xe.

We can learn about the resulting lineshape by considering each atom as a Lorentz oscillator with a susceptibility given by

$$\chi(\omega) = \frac{\omega_p^2}{\omega_0^2 - \omega^2 - i\Gamma\omega}$$

but realizing that each atom will have its own modified resonance frequency

$$\omega_0'(v_x) = \omega_0 \left(1 + \frac{v_x}{c}\right)$$

with probability $f_M(v_x)$. The total susceptibility spectrum then follows from the addition (integration) of all susceptibility contributions for all possible v_x:

$$\chi(\omega) = \int_{-\infty}^{\infty} \frac{\omega_p^2}{\omega_0'(v_x)^2 - \omega^2 - i\Gamma\omega} f_M(v_x) \, dv_x$$

Substituting f_M this gives

$$\chi(\omega) = \left(\frac{m}{2\pi kT}\right)^{1/2} \int_{-\infty}^{\infty} \frac{\omega_p^2}{\omega_0'(v_x)^2 - \omega^2 - i\Gamma\omega} e^{-mv_x^2/2kT} dv_x$$

With a known concentration $N(m^{-3})$ this describes the entire complex dielectric function, and we can therefore calculate the Doppler-broadened absorption spectrum. We can find an approximate expression for the absorption coefficient by considering the resonance approximation $\omega \approx \omega_0$, which we may do if the (Doppler-broadened) linewidth is much smaller than ω_0. In the resonance condition we have

$$\chi''(\omega) \approx \frac{\omega_p^2}{2\omega_0} \left(\frac{m}{2\pi kT}\right)^{1/2} \int_{-\infty}^{\infty} \frac{\Gamma/2}{(\omega_0'(v_x) - \omega)^2 + (\Gamma/2)^2} e^{-mv_x^2/2kT} dv_x$$

For small susceptibility (n≈1) which is reasonable in the gas phase, we can approximate the absorption coefficient as $\alpha = 2\kappa\frac{\omega}{c} \approx \frac{\chi''\omega}{c}$ resulting in the Doppler broadened absorption spectrum:

$$\alpha(\omega) \approx \frac{\omega_p^2}{2c}\left(\frac{m}{2\pi kT}\right)^{1/2} \int_{-\infty}^{\infty} \frac{\Gamma/2}{(\omega_0'(v_x) - \omega)^2 + (\Gamma/2)^2} e^{-mv_x^2/2kT} dv_x$$

The spectral shape of this inhomogeneously broadened absorption line is known as the *Voigt lineshape*. We can look at the extreme cases of mostly homogeneous broadening and strong inhomogeneous broadening. Note that the integrand is just a product of a Gaussian function and a Lorentzian. Thermal line broadening dominates when $\frac{\sqrt{kT/m}}{c} \gg \frac{\Gamma}{\omega_0}$. In this case the Lorentzian function becomes approximately a delta function that peaks when $\omega = \omega_0'(v_x)$, i.e when $v_x = \frac{(\omega-\omega_0)c}{\omega_0}$, resulting in a Gaussian lineshape:

$$\alpha(\omega) \approx \frac{\omega_p^2}{2c}\left(\frac{m}{2\pi kT}\right)^{1/2} e^{-\frac{m(\omega_0-\omega)^2}{2kT}\left(\frac{c}{\omega_0}\right)^2}$$

If the homogeneous width dominates, i.e. when $\frac{\sqrt{kT/m}}{c} \ll \frac{\Gamma}{\omega_0}$, then the Gaussian acts like a delta function and the absorption line reverts back to the original Lorentzian lineshape:

$$\alpha(\omega) \approx \frac{\omega_p^2}{2c} \frac{\Gamma/2}{(\omega_0 - \omega)^2 + (\Gamma/2)^2}$$

This transition from Lorentzian to Gaussian is highlighted in the graph below, which shows the lineshape in an argon gas with resonance at 514 nm, with an assumed linewidth of 10^9 rad/s, shown at '0 K', 10 K, and 293 K. Note that already at 10 K the thermally induced broadening becomes comparable to the 10^9 rad/s linewidth. Also note that the broadening results in a reduced peak absorption, and therefore also in a predicted reduction in the peak emission cross-section, and a reduced maximum gain if this transition is used for lasing or optical amplification.
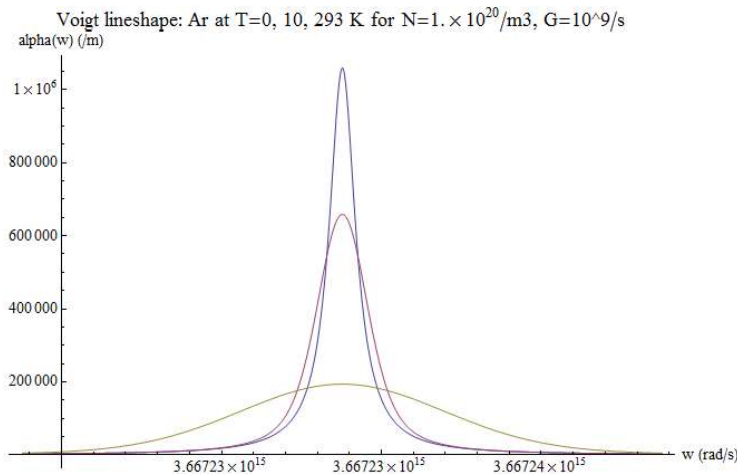
Figure 10.3: Examples of the Voigt lineshape for different temperatures

Chapter 11 – Interaction of light with molecular vibration and rotation

➢ Corresponding handouts are available on http://kik.creol.ucf.edu/courses.html

In Chapter 5 we studied the Lorentz oscillator model to describe electronic motion in response to a high frequency electromagnetic wave. There we ignored any motion of the nucleus, which was a reasonable approximation because atomic nuclei are at least three orders of magnitude heavier than electrons. However, atoms with a net charge (ions) can be moved by low-frequency light, resulting in NIR and IR absorption features associated with nuclear motion. In addition, we will see that a slight variation of electronic polarizability during vibration leads to Raman scattering.

Molecular bonds

To understand vibrational transitions in molecules, we first need to understand what holds molecules together. Let's consider a hydrogen molecule, consisting of two hydrogen atoms. Each atom core with a charge of +1e is surrounded by an electron with charge -1e, making each atom neutral. Classically we might thus expect that separate hydrogen atoms don't attract or repel each other, and therefore it's not entirely obvious that a molecular bond would form. The reason for chemical bonds lies in quantum mechanics.

From quantum mechanics (Chapter 9) we know that bound electron states are described by the Schrödinger Equation, where the electron position and energy are described by a wavefunction. Electron wavefunctions in a system of two attractive potentials (here the hydrogen cores) can occupy states where the electron probability between the atoms is zero, as well as states where the probability between the atoms is finite. The former state has a higher energy than the system of the separate hydrogen atoms, and is called an 'anti-bonding' state, and the latter has a lower energy than the separate hydrogen atoms, and is called a '*bonding state*'. The energy of the bonding state depends on the distance between the atoms. The system energy as a function of separation between the atoms (bond length) is often described phenomenologically by the Morse Potential, which describes the potential energy of the molecule as a function of bond length r:

$$U(r) = E_b \left(1 - e^{-a\,(r - r_0)}\right)^2 \tag{11.34}$$

where E_b is the binding energy, r_0 is the equilibrium bond length, and a is a constant that describes how rapidly the energy varies with bond length. The graph below shows an example with E_b=250 meV, r_0 = 1.15 Å, and a=1.5 Å^{-1}.
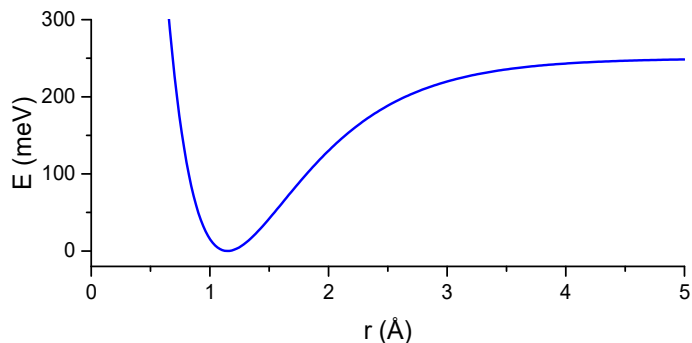
Figure 11.1: Example of the Morse potential vs. inter-atomic separation r.

Note that when the atoms are far apart (large bond length) the potential is almost flat, corresponding to free atoms. As the atoms approach each other the energy is reduced, resulting in binding. Trying to push the positive cores closer together to within sub-angstrom distances rapidly raises the energy, in part due to Coulomb repulsion. The system has a minimum energy at $r=r_0$, and decreasing or increasing the bond length takes energy. The molecular bond thus acts as a 'spring' that tries hold the system at its equilibrium bond length. For small motion amplitude, the resulting restoring force is approximately described by Hooke's law. Using the Morse potential from above we find a spring constant K given by

$$K\left(\frac{N}{m}\right) = \left(\frac{d^2U(r)}{dr^2}\right)_{r=r_0} = 2\,E_b(J)\,a(m^{-1})^2\,.$$

(11. 35)

We thus expect that a diatomic molecule can undergo harmonic oscillation of the bond length at a frequency determined by the atomic masses and the bond strength. Before investigating how light can induce such molecular vibration, we first will introduce the concepts of normal coordinates and normal modes.

Normal modes

In order to model the movement of ion or atom positions we need to track each individual atom in three dimensions. Modeling the atom positions of a molecule containing N atoms would therefore require 3N coordinates, or 3N *degrees of freedom*. As systems become more complicated (large molecules or even solids), it becomes impractical to describe the motion of each atom separately. Instead we will describe vibration and rotation in terms of *normal coordinates* that represent motion patterns of several of the atoms at once. We will choose 3N such normal coordinates such that we can still describe an arbitrary arrangement of the atoms. The simplest possible system for which we can do such a mode decomposition is the diatomic molecule.
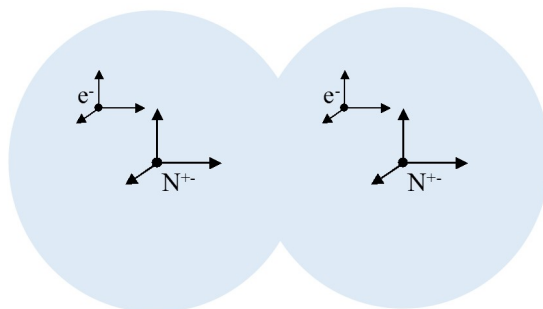
Figure 11.2: Nitrogen molecule configuration described by the two atom positions and the position of two valence electrons

An example of a diatomic molecule is the nitrogen molecule, N_2. In order to describe all possible configurations of this molecule we need $3N = 6$ coordinates. Instead of describing the atom positions (x_1, y_1, z_1) and (x_2, y_2, z_2) separately, it is more convenient to describe their joint motion or position in terms of normal coordinates. One such normal coordinate is the location of the *center of mass*, which requires three coordinates (x, y, z). The corresponding motion is 'change of center of mass position', or *translation*. A second

coordinate is the bond length, which requires one coordinate (r). The corresponding motion is 'change of the bond length', or *vibration*. Thus far we have used a total of 4 coordinates. The remaining two are needed for orientation. For this linear molecule, the orientation can be described by angles φ and θ. The corresponding motion is 'change in orientation' or *rotation*. Note that we can now describe any arbitrary position of the diatomic molecule atoms, and we have again used a total of 3N=6 normal coordinates: three for the center of mass, one for bond length, and two for orientation. For molecules that are not linear (e.g. that have two-dimensional or three-dimensional structure) φ and θ together don't cover all possible orientations; we would need a third angular coordinate: rotation about a chosen molecular axis.

We can now predict the number of vibrational normal modes (motion patterns) that can exist on particular molecules. Molecules with N atoms can be described with 3N coordinates. Out of these, 3 are needed for translation. In the case of linear molecules, we need 2 angular coordinates for orientation. That leaves 3N-5 normal coordinates for vibrational modes. For 2D and 3D molecules we need 3 angular coordinates, leaving 3N-6 vibrational coordinates. This means that most molecules will support many different vibrations, each with its own frequency. For example, a water molecule (H_2O, three-dimensional because the two H-O bonds are not collinear) will have three vibrational modes, and an ammonia molecule NH_3 (also a 3D molecule) will support six vibrational modes. As a consequence, vibrational spectra rapidly become complicated. This also has a benefit: we can identify molecules by measuring their vibration spectra, since these spectra provide a lot of information about bond strength and atomic masses present in the molecule.

Note that the chosen coordinates are independent[xxv]: we can have a molecule vibrate while its center of mass is stationary, but it can vibrate in exactly the same way while the molecule is moving (time dependent center of mass). This makes them "*normal coordinates*", and their corresponding time dependent motion "*normal modes*".

The center of mass motion is rarely of interest in optics, except for the realization that center-of-mass motion can lead to Doppler shifts in absorption lines (Chapter 10). The more interesting coordinates for light-matter interaction are the vibrational and rotational normal coordinates of the molecule. Depending on the charge distribution on the molecule, these motions can introduce NIR and IR absorption features related to vibrational, rotational, and *rovibrational* transitions (combined rotation plus vibration) as discussed below. In addition, since the vibrating atoms in the molecule are surrounded by bound electrons, we will find that combined electronic plus vibrational transitions can also occur, the so called *vibronic transitions*.

[xxv] This is a first order approximation. For example, we will see later that fast rotation will stretch the molecule due to centrifugal forces, so the coordinates are not exactly independent.
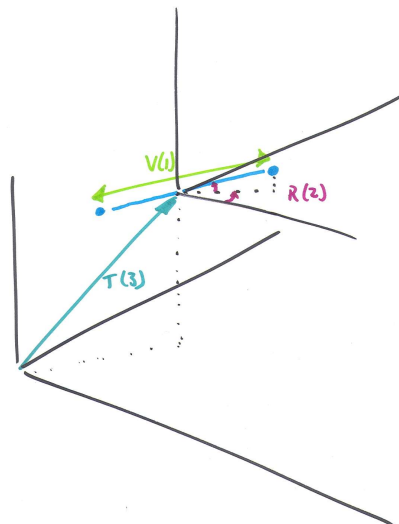
Figure 11.3: Sketch of the normal coordinates of a diatomic molecule (blue) showing translation (three coordinates), vibration (one coordinate), and rotation (two coordinates)

Atoms: N	
Total nuclear coordinates: 3N	
3 translational coordinates (center of mass of molecule)	
Linear molecules	*Other molecules (2D, 3D)*
2 rotational modes 3N-5 vibrational modes	3 rotational modes 3N-6 vibrational modes

Number of normal coordinates needed to describe N-atom molecules

Born-Oppenheimer Approximation

To describe the rotation and vibration related optical response we would in principle have to model how the valence electrons follow the moving atom cores. Thankfully, the low mass of electrons means that they can respond quickly to forces (F=m·a, so small mass implies a fast response). For many practical situations the electrons respond so quickly compared to the nuclear motions that we can consider the electrons as following the atom core positions "instantaneously" as the molecules vibrate or rotate. This assumption is called the *Born-Oppenheimer approximation*.

Typical spectral ranges for vibrational and rotational transitions

Most atoms contain many protons and neutrons, each of which weighs approximately 1 $amu \approx 1.66 \times 10^{-27}$ kg. Even the lightest atom (hydrogen) with a core mass of 1 amu is already 1800 times heavier than an electron which has a mass of $m_0 = 9.1 \times 10^{-31} kg$. When subjected to similar forces, atoms thus accelerate much less than electrons, and consequently molecular vibrations occur at relatively low frequencies that are 10-100× slower than typical electronic transition energies. Rotational energies are much lower than vibrational energies. The corresponding wavelength ranges are summarized below.

Vibrational: near infrared to long wave infrared, about 1-50 µm

Rovibrational: Combination of rotation and vibration changes, also at 1-50 μm

Purely rotational: Far infrared, about 100 - 500 μm

Dipole active modes

As we saw, most molecules support several vibrational modes. It turns out that light can usually only directly excite a limited subset of all these modes, the so-called dipole active modes. This can be understood by first considering the effect of a static electric field on a molecule. If the molecule contains atoms with different total charge (core charge + electron charge), the field will push the positively charged atoms in one direction, and pull the negatively charged atoms in the opposite direction. The field can therefore stretch the molecular bond and increase the dipole moment on such molecule. If the field oscillates, it can induce an oscillatory motion and oscillatory dipole moment, corresponding to periodic vibration and/or rotation. Modes that can be excited by an oscillating electric field are called *dipole active modes*. From another perspective, a mode is dipole active when its total dipole moment changes during its vibration or rotation.

The simplest dipole *inactive* mode is the stretch vibration of symmetric diatomic molecules. Diatomic (and thus linear) molecules have 3N-5=1 vibrational mode. If the molecule contains only one type of atom, e.g. O_2, N_2, etc., it does not have a net dipole moment because of symmetry: both atoms are the same, and there is no reason for one of them to attract electrons more than the other. Each identical atom has the same net charge of zero, and therefore light does not accelerate either of the atoms. The molecules *can* vibrate, but their dipole moment (zero) does not change while they do this.[xxvi] Consequently, the vibration is called *dipole inactive*. Light cannot cause move motion of the atoms, so there is no absorption related to vibration or rotation.

The simplest possible example of a *dipole active mode* is the stretch vibration of a heterogeneous diatomic molecule. A diatomic molecule containing different atom types will still support only a single stretch vibration. However, the different atoms will have slightly different affinity for electrons, i.e. a different electronegativity, and as a result one of the atoms will end up being slightly negatively charged, while the other atom will be slightly positive. For example, in a HCl molecule, the chlorine atom has a net charge of approximately -0.2e, and the hydrogen atom has a net charge of approximately +0.2e. In this case the molecule has a net dipole moment, and stretching the molecule increases the dipole moment. The stretch vibration therefore has a time-dependent dipole moment, making this mode dipole active. In addition, since the HCl molecule has a permanent dipole moment electric fields can also exert a torque on the molecule, meaning its rotational modes are also dipole active. Or vice versa, as the molecule rotates, the (vectorial) dipole moment changes over time, and thus rotation of the HCl molecule is called dipole active.

A slightly more complicated example is the carbon dioxide molecule, CO_2. This molecule contains two collinear double bonds, schematically shown as follows: O=C=O. This is also considered a one-dimensional (linear) molecule. The oxygen atoms are more electronegative than the carbon atom, and therefore the molecule contains two polar bonds. However, since the negative oxygen atoms are symmetrically placed around the carbon

---

[xxvi] As it turns out, their electronic polarizability does change during vibration, resulting in a modulation of scattered light, resulting in an effect known as Raman scattering, discussed later in this Chapter.

atom, the net dipole moment is still zero. Another way of saying this is that the dipole moments of the two bonds are pointed in opposite direction (outward with equal magnitude), and their sum is zero. During the rotation of a CO_2 molecule the net dipole moment remains zero, and therefore purely rotational motion of CO_2 is not a dipole active mode, and light cannot excite a purely rotational motion in CO_2. We will see later that light *can* excite a vibration while simultaneously changing the rotation of CO_2, called a rovibrational transition.

The CO_2 molecule does not have a net dipole moment, but we noted that it does have charge separation (different net charge on different atoms). As a result some of its vibrational modes turn out to be dipole active. Let's consider all of its normal modes. Recall, to describe nuclear motion on the linear CO_2 molecule we need two rotational coordinates and 3N-5 = 4 vibrational modes. The image below shows these modes. The top mode is called the *symmetric stretch mode*, with the oxygen atoms moving in opposite direction while the carbon atom is stationary. During this vibration the two bonds both have a time-dependent dipole moment, but the sum of these dipole moments remains zero. Or alternatively, at each time during the vibration the average position of the negative charge is identical to the average position of the positive charge. This vibration is therefore dipole inactive. The middle image shows a mode known as the *asymmetric stretch vibration*. In this mode the oxygen atoms move in the same direction, while the carbon atom moves in the opposite direction. In this mode whenever the left bond stretches (and therefore has an increasing dipole moment) the right bond compresses (and therefore has a reducing dipole moment). The result is that a net dipole moment develops during this vibration, making this mode dipole active. An alternative viewpoint is that the negative atoms move in one direction, and the positive atom in the other. The average negative and positive charge positions move in different directions, meaning that dipole moment is changing. Finally, the bottom image shows a vibration known as a *bending mode*. Again the oxygen atoms move together in one direction, and the carbon atom in the opposite direction. This too corresponds to a time dependent dipole moment, and the bending mode of CO_2 is therefore also a dipole active vibration. This bending mode can occur in-plane and out-of-plane, so we need two of these normal modes to describe bending in an arbitrary direction. This mode therefore counts for two normal modes, with identical energy. Such modes with the same energy are called *degenerate*.

One important note: changing the length of a bond typically takes more energy than bending a bond. That means that stretch vibrations typically occur at higher energy than bending vibrations.
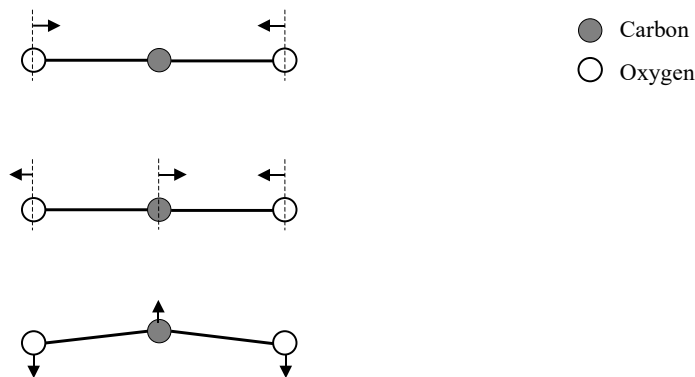
Figure 11.4: the vibrational modes of the CO₂ molecule. The top symmetric stretch is dipole active, while the asymmetric stretch (middle) and bending mode (bottom) are dipole active.

Classical description of vibrations in molecules and solids

In the following sections we will describe vibrations on molecules and in solids using an entirely classical oscillator model.

Vibration Modes in a Diatomic Molecule

As discussed above in the section 'molecular bonds', the energy of a molecule depends on the bond length. Any changes in the bond length result in a restoring force. We can thus attempt to describe vibrating molecules by a system of masses held together by springs. To find allowed vibration frequencies and their associated motion patterns (normal modes) we solve the equation of motion for all atoms at the same time, and look for oscillatory solutions with a single oscillation frequency. In three dimensional large molecules, a normal mode can be some complicated vectorial motion pattern where atoms oscillate along different directions with different amplitudes. Here we will discuss the simple case of a heterogeneous diatomic molecule, and assume that all motion will be along a single dimension (for example the x-axis), meaning we can make use of scalar rather than vectorial position coordinates.

We consider a diatomic molecule with masses m_1 and m_2, positions x_1 and x_2 relative to the equilibrium position of the left and right atom respectively, and held together by a chemical bond with a spring constant K. When $x_2 > x_1$, the spring has lengthened, resulting in a positive force on atom 1, and a negative force on atom 2. The equation of motion for the two atoms thus becomes

$$m_1 \ddot{x}_1 = K(x_2 - x_1)$$

$$m_2 \ddot{x}_2 = -K(x_2 - x_1)$$

We are looking for a normal mode with a single frequency, so we will substitute $x_1(t) = x_1(\omega)e^{i\omega t}$ and similar for x_2. Importantly, we thus demand that both atoms oscillate at the same frequency. For simplicity of notation here we omit the complex conjugate which would be needed to obtain real amplitudes. Substituting this harmonic motion into the EOM, taking the time derivative, and dividing out all common exponential terms, we end up with

$$-m_1 \omega^2 \, x_1(\omega) = K\big(x_2(\omega) - x_1(\omega)\big)$$

$$-m_2\omega^2 \, x_2(\omega) = -K\big(x_2(\omega) - x_1(\omega)\big)$$

Grouping all x_1 and x_2 terms and moving them to the left results in

$$[-m_1\omega^2 + K]x_1(\omega) - Kx_2(\omega) = 0$$

$$-Kx_1(\omega) + [-m_2\omega^2 + K]x_2(\omega) = 0$$

This can be written as a matrix relation

$$\begin{pmatrix} K - m_1\omega^2 & -K \\ -K & K - m_2\omega^2 \end{pmatrix} \begin{bmatrix} x_1(\omega) \\ x_2(\omega) \end{bmatrix} = 0$$

This equation has solutions if the determinant of the matrix is zero, corresponding to

$$(K - m_1\omega^2)(K - m_2\omega^2) - K^2 = 0$$

$$\Rightarrow -Km_2\omega^2 - Km_1\omega^2 + m_1 m_2 \omega^4 = 0$$

$$\Rightarrow \omega^2(-K(m_1 + m_2) + m_1 m_2 \omega^2) = 0$$

This has one trivial solution, $\omega = 0$, corresponding to an absence of relative motion, which does not correspond to a vibrational mode. If $\omega \neq 0$, we can divide out the term ω^2 and find a solution if the remaining term between brackets is zero, resulting in

$$\omega^2 = K \, \frac{m_1 + m_2}{m_1 m_2} = K\left(\frac{1}{m_1} + \frac{1}{m_2}\right)$$

This is often written in terms of a quantity known as the *reduced mass* μ, defined by

$$\frac{1}{\mu} = \frac{1}{m_1} + \frac{1}{m_2}$$

We have thus found an allowed normal mode with a frequency

$$\omega_{vib} = \sqrt{\frac{K}{\mu}}$$

To find the corresponding motion pattern associated with this normal mode, we substitute the obtained frequency in our trial solutions for $x_1(t)$ and $x_2(t)$ and substitute these into one of the EOM gives

$$\frac{x_1(\omega)}{x_2(\omega)} = -\frac{m_2}{m_1}$$

We see that the mode with this frequency has a motion pattern in which atom 1 and atom 2 move in opposite directions, which stretches the bond. We have found a *stretch vibration.* If $m_1 < m_2$ then atom 1 has a larger motion amplitude than atom 2. Note that we don't know anything about the *total* amplitude: all we know is that at the stretch vibration frequency the atoms will be moving in anti-phase, with a *relative* amplitude given by the mass ratio.

Together with E_b and a from the Morse potential for the H-Cl bond we can now predict the vibration resonance frequency of the HCl molecule. The chemical bond determines the spring constant K, and we can look up the atomic masses to find m_1 and m_2, giving us μ, which together with K gives us ω_{vib}.

Some interesting limiting cases: if $m_2 \gg m_1$ we find $x_1 \gg x_2$, i.e. atom 2 moves very little. In this case the reduced mass approaches $\mu \approx m_1$, and the vibration frequency becomes $\omega_{vib} \approx \sqrt{K/m_1}$ corresponding to a single mass on a spring with spring constant K, attached to an immobile object. This is reasonable for large m_2.

Another useful limiting case is the situation where both masses are identical with $m_1=m_2=m$. Note that this would correspond to a molecule with no charge separation, and therefore the mode would be dipole inactive. For such molecule we find that $\mu = m/2$ resulting in $\omega_{vib} \approx \sqrt{K/(m/2)} = \sqrt{2K/m}$. This looks like the vibration frequency of an atom with half the mass on a spring with spring constant K, hence the term 'reduced mass' for μ. This result can be understood by realizing that the masses undergo correlated motion. For every Δx of motion of atom 1, the spring lengthens by $2\Delta x$, since the other atom is moving in the opposite direction. The restoring force is thus twice as large as expected based on Δx_1, resulting in a spring that appears twice as strong.

With the analysis developed above we can make some predictions about the vibration frequencies of the CO_2 molecule. For the symmetric stretch we see that both O atoms oscillate on a fixed central C atom, so we anticipate a symmetric stretch frequency of

$$\omega_{SS} = \sqrt{\frac{K_L}{m_O}}$$

where the subscript L indicates that this is for longitudinal motion. As argued earlier, this mode is dipole inactive. For the dipole active asymmetric stretch vibration we see that there is a total mass $2m_O$ moving to the right and a mass m_C moving to the left. If we define a corresponding reduced mass for this particular motion pattern

$$\frac{1}{\mu_{CO_2}} = \frac{1}{m_C} + \frac{1}{2m_O}$$

and noting that the forces on the C atom are twice as large as expected for a single bond, we anticipate an asymmetric stretch vibration frequency of

$$\omega_{AS} = \sqrt{\frac{2K_L}{\mu_{CO_2}}}$$

Note that this $\mu_{CO_2} < 2m_O$ and therefore $\omega_{AS} > \omega_{SS}$.

Finally, the dipole active bending mode is expected at lower frequency because of the fact that the 'transverse spring constant' K_T associated with bond angle deformation ('bending') is generally lower than K_L.

Quantum description of light interaction with rotation and vibration

Unlike vibrational modes, rotational modes have no resonance in the classical picture. We might thus expect that molecules con rotate at arbitrarily low speeds, and we classically we don't expect absorption resonances from rotations. And yet, such rotational absorption

resonances exist. To look understand absorption resonances due to rotational modes, we must consider quantum mechanics.

Classically the rotational energy of a rotating object can be varied continuously by changing the angular frequency of motion, as given by

$$E_{rot} = \tfrac{1}{2} I\omega^2 = \frac{(I\omega)^2}{2I} = \frac{L^2}{2I},$$ (13.1)

where L is the angular momentum, and I is the moment of inertia. However, since moving mass has a wave-like behavior (See Chapter 9), allowed sustained rotational motion requires that one roundtrip of the molecule fits an integer number of waves. The result is a *quantized* rotational energy spectrum, with discrete energy Eigenvalues E_{rot}^J given by

$$E_{rot}^J = \frac{J(J+1)\hbar^2}{2I}, \qquad J = 0,1,2,...$$

$$= J(J+1)\hbar\omega_{rot}$$ (13.2)

Since J is an integer, the rotational energy levels will end up separated by multiples of the quantity $\hbar\omega_{rot}$ so this quantity is not "the rotational energy". Note that ω_{rot} follows from the moment of inertia according to $\omega_{rot} = \hbar/(2I)$. In the literature instead of using the quantity ω_{rot} people often use $\bar{v}_{rot}(cm^{-1}) = 1/\lambda(cm)$. Both ω and v are linear in energy. To convert from ω_{rot} to v_{rot}, simply convert the energy $\hbar\omega_{rot}$ to the corresponding wavelength in cm, and take the inverse. In this case,

$$E_{rot}^J = J(J+1)hc\,\bar{v}_{rot}.$$ (13.3)

Sometimes $\bar{v}_{rot}$ is labeled as "B".[xxvii] Note that J(J+1) is a quadratic in J, so that the spacing between energy levels increases with J. For a molecule with an angular momentum quantum number J, the distance to the next higher energy level is:

$$\begin{aligned} E^{J+1} - E^J &= \left[(J+1)(J+2) - J(J+1)\right]hc\,\bar{v}_{rot} \\ &= \left[J^2 + 3J + 2 - J^2 - J\right)\right]hc\,\bar{v}_{rot} \\ &= 2(J+1)hc\,\bar{v}_{rot} \end{aligned}$$ (13.4)

We see that the energy level *spacing* increases linearly with J. This observation, together with a selection rule for rotational transitions, determines the kind of rotational and rovibrational absorption spectra that are commonly observed. We already saw an example of a quantum mechanical selection rule in Chapter 9, where light could only cause transitions between states with opposite parity. For rotational transitions, we have a different selection rule. Optically induced changes of J must follow the rule

$$\Delta J = 0, \pm 1.$$ (13.5)

[xxvii] For higher rotational energy states, centrifugal force stretches the molecule and this lowers the energy, which may be written as $E_{rot}^J = J(J+1)hcB - J^2(J+1)hcD$, but we will not consider this correction in this course.

Light incident on a polar molecule (i.e. with a net dipole moment) can increase the rotation of the molecule ('speed up its rotation') by increasing J by one. In an extremely cold gas with most molecules in the J=0 state we might expect that light can only cause a transition from J=0 with energy $E_{rot}^{J} = J(J+1)\hbar\omega_{rot} = 0$ to a state with J=1 with energy $E_{rot}^{J} = J(J+1)\hbar\omega_{rot} = 2\hbar\omega_{rot}$. We thus would expect exactly one absorption peak at energy $2\hbar\omega_{rot}$. But, if some molecules are already rotating, e.g. with J=1, light could cause a transition from J=1 with energy $E_{rot}^{J} = 2\hbar\omega_{rot}$ to J=2 with energy $E_{rot}^{J} = J(J+1)\hbar\omega_{rot} = 6\hbar\omega_{rot}$. These molecules would add an absorption line at energy $4\hbar\omega_{rot}$. We see: molecules that rotate faster absorb at higher energy. For a hot gas with molecules in various rotational states we thus expect to see an absorption spectrum with peaks that are evenly spaced, located at multiples of $2\hbar\omega_{rot}$ and therefore spaced by $2\hbar\omega_{rot}$. In the sketch below we see an example of such a purely rotational absorption spectrum and one of the responsible transitions indicated by the red arrow. Each absorption peak corresponds to molecules with a distinct initial value of J.
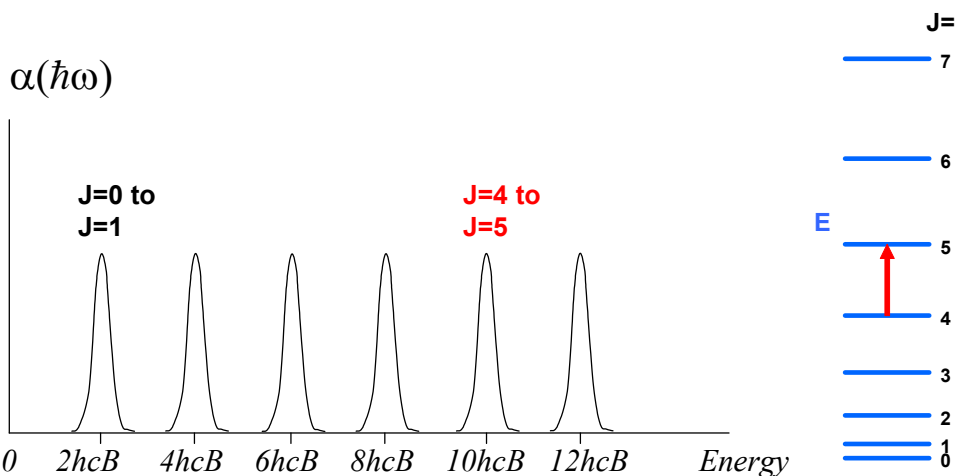
Figure 11.5

Typical rotational transition energies

For molecular Hydrogen, H_2, hcB = 5.8 x 10^{-22} J, so the lowest energy transition it can make is from E_{rot}^{0}=0 to E_{rot}^{1} = 2(J+1) hcB = 1.16 X 10^{-21} Joule or 7.25 meV. The corresponding free-space wavelength is 171 μm, which lies in the far infrared (FIR) region. Although H_2 does not exhibit dipole-allowed rotational transitions, the calculated transition energy represents an estimate for the energy of rotational absorption lines of other molecules. In general, these energies will be lower, since H_2 is the lightest possible molecule and hence has the smallest moment of inertia.

Thermal population of rotational states

When comparing the calculated energy of the lowest H_2 rotational transition to the thermal energy, kT, at room temperature (~25 meV) it is clear that several rotational levels in H_2 will be populated at room temperature. But the population of levels reduces exponentially with energy, resulting in an exponential drop-off in the strength of the absorption lines with frequency.

$$\alpha(\hbar\omega)$$

0   2hcB   4hcB   6hcB   8hcB   10hcB   12hcB   Energy
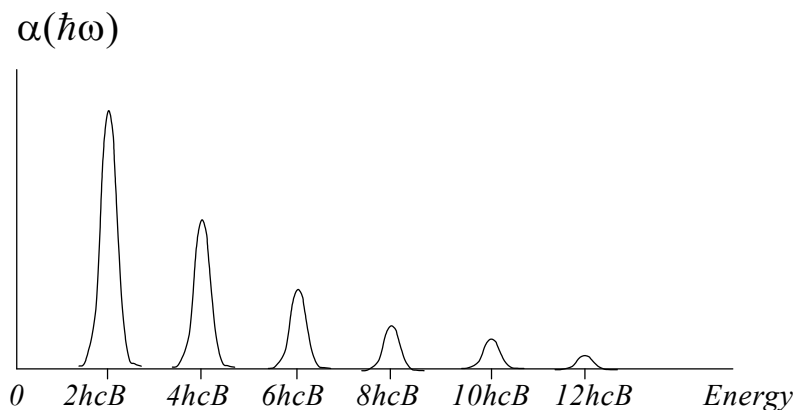
Figure 11.6

Vibrational transitions

The approximation that atoms in a molecule experience a linear restoring force turns out to be a reasonably good one. This means that the potential that the atoms sit in is close to parabolic, for small displacements. The behavior of the bond length can be modeled by a quantum harmonic oscillator, for which the solutions are well known:

$$E_{vib} = (v + \tfrac{1}{2})\hbar\omega_0 , \quad v = 0, 1, 2, \dots \qquad (13.6)$$

with v the vibrational quantum number, and with $\omega_0 = \sqrt{K/\mu}$ the classical resonance frequency. For a perfectly parabolic potential, the energy levels are equally spaced. The absorption spectrum is again affected by a selection rule: $\Delta v = \pm 1$. Since the energy level spacing is fixed, there is only a single absorption frequency, regardless of the initial state of the system. However, anharmonicity of the potential (i.e. the potential is not exactly parabolic, see the Morse potential earlier in this Chapter) results in a slight relaxation of this rule, which can result in weakly-allowed excitation of multiple vibration quanta ($\Delta v=\pm 2, \pm 3$), etc. Anharmonicity also results in slightly unevenly spaced energy levels, as shown below:

Figure 13.7

116
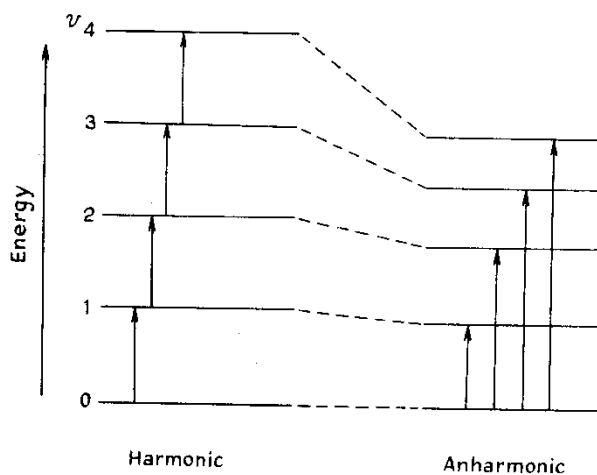
For a polyatomic molecule, we have multiple resonances corresponding to the different vibration modes of the molecule:

$$E_{vib} = (v_1 + \frac{1}{2})\hbar\omega_1 + (v_2 + \frac{1}{2})\hbar\omega_2 + \ldots \tag{13.7}$$

where there are 3N-5 or 3N-6 vibrational modes, and there is one absorption/emission resonance frequency for each mode.

Vibrational rotational transitions

Whenever there is a dipole active vibrational mode, light can also exert a torque on the molecule during the vibration. As a result, excitation of vibration almost always also changes the amount of rotation of the molecule. Since vibration energies are much larger than rotation energies, the change of rotation has relatively little effect on the transition energy. In other words: the energies of combined vibrational and rotational transitions (rovibrational transitions) will be close to those of a typical vibration energy $\hbar\omega_{vib}$. Since the rotation may increase or decrease, the total energy needed for the transition may be a bit more or a bit less than $\hbar\omega_{vib}$, and we thus expect to see absorption lines slightly below and above the vibrational energy. The selection rules for these transitions are the same as discussed above: rovibrational transitions require $\Delta v = \pm 1$ (and sometimes ± 2).

For $\Delta J = -1$, this is called the   "P-branch"
For $\Delta J = 0$ "Q-branch" (often forbidden)
For $\Delta J = +1$ "R-branch"
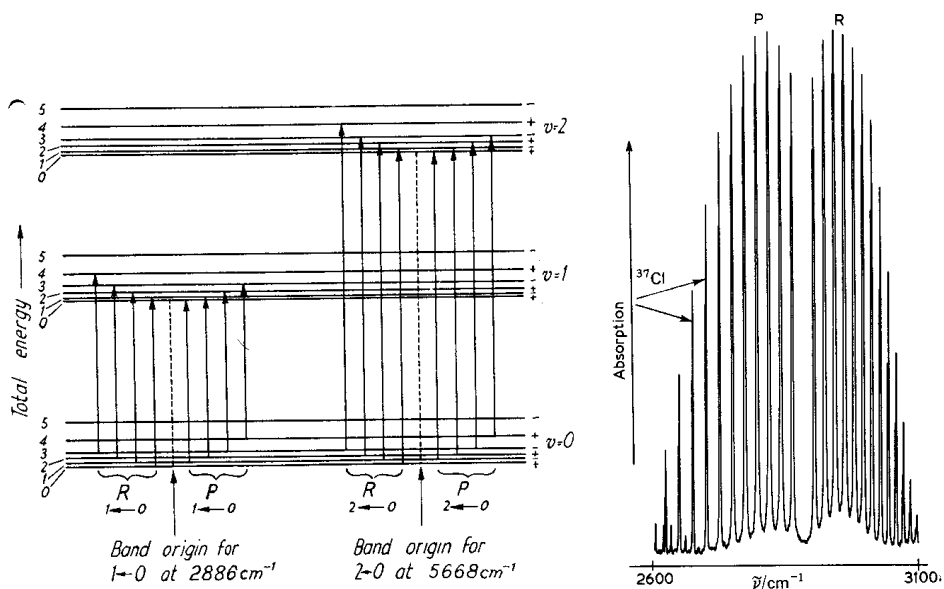
Figure 13.8

Above are the vibration-rotation transitions for HCl, showing the strongly allowed $\Delta v = 1$ (fundamental band), along with the weakly allowed $\Delta v = 2$ (overtone band). The associated absorption spectrum for HCl is shown below.

117

Coupled electron/vibration transitions in molecules
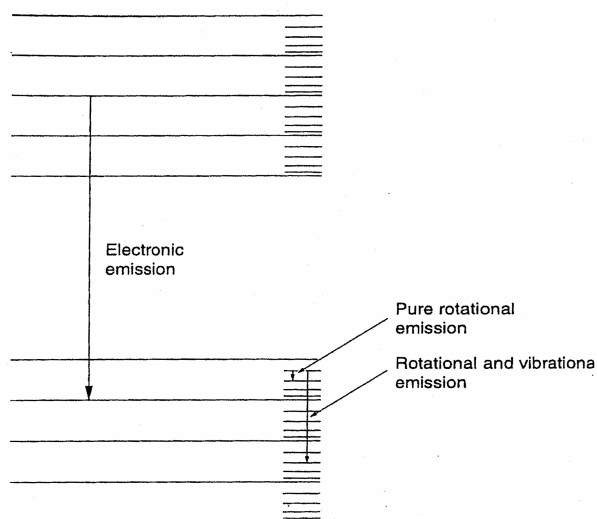
Figure 11.9

Similarly, electronic transitions can terminate in different vibrational and rotational states, resulting in broad electronic absorption/emission bands. There are no simple selection rules here, but the *Franck-Condon principle* states that the vibrational coordinate should not change during a transition, (see below). Since the electrons have highest probability of being at the extreme positions of their excursions, this controls which transitions are most possible, which strongly affects the shape of the absorption band.
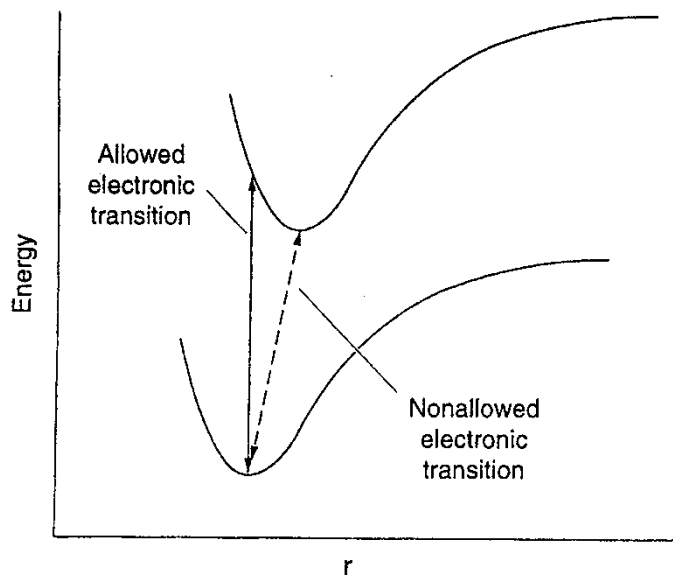
Figure 13.10

Due to the Franck-Condon principle and the tendency for molecules to relax to the bottom of the vibration bands, the emission spectrum is shifted to longer wavelengths than the absorption spectrum, and the emission band usually looks like a mirror image of the absorption band
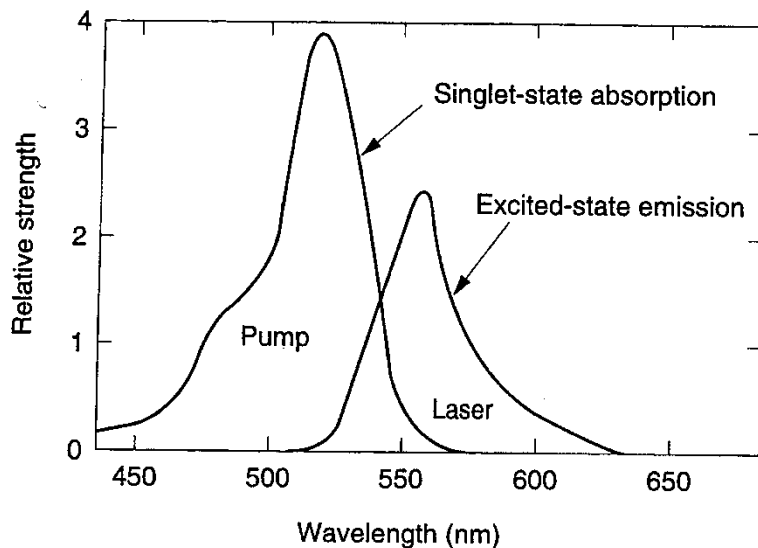
Figure 11.11

Raman active modes

Modes that are not dipole-active can also interact with electromagnetic radiation indirectly. For example, vibrational and rotational modes in H_2 are not dipole active, but if an electric field is applied, the electrons move in response to the field, thus polarizing the entire molecule. If the electronic polarizability depends on the molecule length (or orientation), the induced dipole moment with frequency ω_i will be modulated by the vibrational (or rotational) mode: a dipole active mode has effectively been induced through the electronic polarization. This leads to "Raman Scattering", and this type of dipole inactive mode is sometimes termed "Raman Active". The effect of the configuration dependent electronic polarizability is that a high-frequency electromagnetic wave can interact with the rotational or vibrational modes. This can result in the rotational or vibrational state of the molecule being changed by the incident radiation. This is analyzed classically in *Hopf & Stegeman*, chapter 3, but we will not discuss the analysis in this class in detail. Usually, Raman scattering is described quantum mechanically as shown in the following diagram:

119
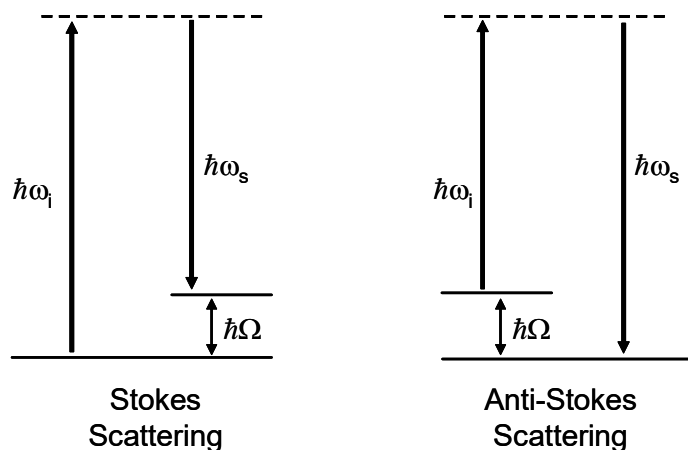
Figure 11.12

An incident wave with frequency ω_i, is incident on the molecule, polarizing the molecule through a dipole-active mode (e.g. electronic polarization). There is no absorption, as ω_i is usually far from the resonance of the dipole-active mode. The dashed line is not a real state, but referred to as a "virtual state" (dashed line), which is just to say that the molecule is being driven at the incident frequency, ω_i without absorption. When in the virtual state, the molecule can interact with the electric field, and may gain (or lose) a quantum of vibrational or rotational energy from (or to) the EM field. Hence, the scattered light with frequency ω_s will be emitted with either a smaller photon energy , $\hbar\omega_s = \hbar\omega_i - \hbar\Omega$, which

is referred to as *Stokes scattering* or with a larger photon energy, $\hbar\omega_s = \hbar\omega_i + \hbar\Omega$, which is

referred to as *Anti-Stokes scattering*. We will discuss later what a "quantum of vibrational or rotational energy" is, when we look at quantum mechanical variations from classical models.

As a simplified example of how these new frequencies are generated, we will consider a di-atomic molecule that has a bond length that oscillates in time according to

$$L(t) = L_0 + \Delta L \times \cos(\omega_{vib} t)$$

Here ω_{vib} is the frequency of the stretch vibration, which we assume lies in the near-infrared. Now let's assume that the polarizability of this molecule to first order depends on the bond length according to

$$\alpha(t) = \alpha_0 + (L(t) - L_0)\frac{d\alpha}{dL}$$

This equation shows that the polarizability is approximately α_0, but varies as L(t) deviates from L_0. The leads to a time dependent polarizability given by

$$\alpha(t) = \alpha_0 + \Delta L \times \cos(\omega_{vib} t)\frac{d\alpha}{dL}$$
$$\approx \alpha_0 + \Delta\alpha \times \cos(\omega_{vib} t)$$

with $\Delta\alpha$ the amplitude of the polarizability variations. Let's look at the dipole moment $\mu(t)$ that develops under monochromatic illumination of this molecule:

120

$$E(t) = E_0 \cos(\omega_{exc} t)$$

with ω_{exc} the angular frequency of the incident laser irradiation. This gives rise to a time dependent dipole moment given by:

$$\mu(t) = \alpha(t) \times E(t)$$
$$= (\alpha_0 + \Delta\alpha \times \cos(\omega_{vib} t)) \times E_0 \cos(\omega_{exc} t)$$
$$= \alpha_0 E_0 \cos(\omega_{exc} t) + E_0 \Delta\alpha \cos(\omega_{vib} t) \cos(\omega_{exc} t)$$

The first term is simply the induced dipole moment at the laser frequency, which gives rise to normal dipole radiation (Rayleigh scattering). More importantly, the last term contains *both the vibration and the excitation frequency*, and can be written as:

$$\Delta\mu(t) = E_0 \Delta\alpha \times \cos(\omega_{vib} t) \cos(\omega_{exc} t)$$
$$= \frac{1}{4} E_0 \Delta\alpha \left(e^{-i\omega_{vib} t} + e^{+i\omega_{vib} t}\right)\left(e^{-i\omega_{exc} t} + e^{+i\omega_{exc} t}\right)$$
$$= \frac{1}{4} E_0 \Delta\alpha \left[e^{-i(\omega_{vib}+\omega_{exc})t} + e^{-i(\omega_{vib}-\omega_{exc})t} + e^{+i(\omega_{vib}-\omega_{exc})t} + e^{+i(\omega_{vib}+\omega_{exc})t}\right]$$
$$= \frac{1}{2} E_0 \Delta\alpha \left[\cos((\omega_{exc} - \omega_{vib})t) + \cos((\omega_{exc} + \omega_{vib})t)\right]$$

We thus have found:

$$\mu(t) = \alpha_0 E_0 \cos(\omega_{exc} t) + \frac{1}{2} E_0 \Delta\alpha \left[\cos((\omega_{exc} - \omega_{vib})t) + \cos((\omega_{exc} + \omega_{vib})t)\right]$$

This represents a dipole moment that oscillates predominantly at the frequency of the incident radiation, but with *two small contributions that oscillate at slightly lower and slightly higher frequency than the incident laser light*. These frequencies $\omega_{exc}-\omega_{vib}$ and $\omega_{exc}+\omega_{vib}$ correspond respectively to the Stokes shifted and the anti-Stokes shifted lines.

Chapter 12 – Debye model of the optical properties of polar liquids

➢ Corresponding handouts are available on http://kik.creol.ucf.edu/courses.html

In the preceding Chapters we modeled the optical response of atoms in dilute gases with the Lorentz model, and described the response of solids using the Lorentz model (bound electrons, linear and nonlinear response) and the Drude model (free electrons). A state of matter that we have not discussed yet is the liquid. This Chapter introduces the Debye model, which can be used to describe the low-frequency ('microwave', far infrared, GHz) response of polar liquids.

Liquids are composed of molecules or atoms that are densely packed (similar densities as solids), but the molecules still have the freedom to move around and reorient. Since the molecules in the liquid contain bound electrons, we expect that light can excite the electrons, just like in insulators. This results in optical absorption at visible and UV frequencies, which we can attempt to describe with the Lorentz model. In addition, liquids containing molecules that have a net dipole moment, for example water, show another type of polarization response at low frequency, related to the slow field-induced alignment of the molecules in the liquid. To model this kind of electromagnetic response we will make use of results from statistical mechanics.
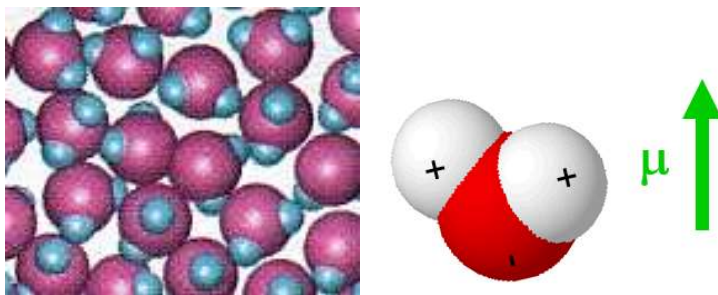
Figure 12.4: Schematic view of densely packed water molecules, and (right) illustration of the net dipole moment of a water molecule. The oxygen atom is negatively charged, which together with the bond angle results in a net dipole.

Hindered rotational modes

In Chapter 11 we saw that polar molecules (molecules with a net dipole moment) in a gas could be made to rotate by infrared light. This gives rise to a series of discrete and narrow absorption lines, related to the various quantum mechanical rotational states. These absorption lines could be sharp because the molecular rotation could continue freely for a long time, corresponding to well-defined energies. In a liquid, the situation is quite different.

Liquids are dense, with densities similar to those of solids. In molecular liquids, for example water, the molecules have the freedom to reorient since they are not chemically bound to their neighbors. However because of the high density, collisions with neighbors occur very frequently. As a result, in liquids we do not see sharp lines related to continued rotation such as we saw in gases. The orientation of molecules in liquids is continually being changed by collisions with neighbors. The number of collisions will depend on

temperature, with high temperature causing more collisions and faster randomization of the molecular orientation. If the collision frequency is similar to or higher than the rotation frequency, we call the rotation *hindered*.

Despite the thermal randomization of the molecular orientation, we can still see light-induced dipole moment related to the in liquids containing polar molecules. As we will see, electric fields can partly *align* polar molecules resulting in a net polarization, while collisions are counteracting this alignment. The result is a low-frequency polarization that increases with field strength, and that decreases with temperature. In the following we derive the corresponding susceptibility with a model known as the *Debye model*.

Molecular alignment in polar liquids

To evaluate light-induced polarization in polar liquids, we will make use of thermodynamics to describe the probability of particular molecular orientations. First we will evaluate the potential energy of a polar molecule as a function of orientation relative to an applied electric field. Consider a molecule with a permanent dipole moment of magnitude p_0 and oriented at an angle θ away from the applied electric field. It can easily be shown that the potential energy U of this molecule will depend on the angle as

$$U(\theta) = -p_0 \mathrm{E} \cos(\theta) \tag{12.1}$$

We will call this potential energy contribution the *interaction potential*. For now, we assume that E is a constant field, but note that our interaction potential U does not depend on this assumption. We see that a molecule that is aligned with the field ($\theta=0$) has the lowest energy. Rotating the molecule and moving the plus charge against the electric force takes work, raising the potential energy.
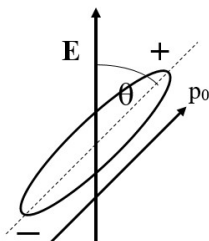
Figure 12.13: Polar molecule in applied electric field.

In classical (non-quantum mechanical) thermodynamics the probability $f(E_{tot})$ for observing a particular state with total energy E_{tot} is described by Boltzmann statistics:

$$f(E_{tot}) \propto e^{-E_{tot}/k_B T} \tag{12.2}$$

with k_B the Boltzmann constant. High energy states are less likely to occur than low energy states. We can use Boltzmann statistics to determine the probability of finding aligned molecules, which will in turn allow us to find the total polarization vs. temperature.

The Boltzmann factor $e^{-E_{tot}/k_B T}$ informs us about the (relative) probability for finding a given orientation, but note that this orientation will be described by both the 'misalignment angle' θ as well as the angle φ. To find a description of the total dipole moment, we will

consider all possible orientations ϕ, θ, and add up (integrate) their contribution to the total polarization.
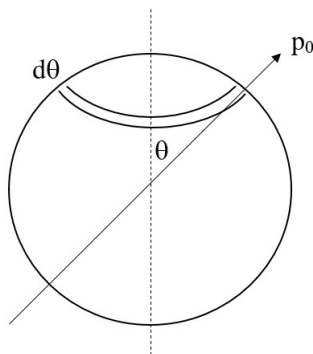
Figure 12.5: possible dipole orientations within a range dθ

A molecule with orientation ϕ, θ contributes a projected dipole moment along the field of $\vec{p} \cdot \hat{E} = p_0\ cos(\theta)$ with $\hat{E}$ the field unit vector. The average dipole moment along the field contributed by a molecule is thus given by

$$\langle \vec{p} \rangle \propto \iint_{\phi,\theta} p_0\ cos(\theta)\ f\big(U(\theta, \phi)\big) \sin\theta\ d\phi d\theta \qquad (12.3)$$

where the term $\sin(\phi)$ is required in polar coordinates to properly add up all possible solid angles. Now note that the interaction potential U does not depend on ϕ, meaning that the integrand doesn't depend on ϕ. The integral over ϕ thus simply adds a factor 2π, reducing our double integral to the following single integral:

$$\langle \vec{p} \rangle \propto \int_{\theta} p_0\ cos(\theta)\ f\big(U(\theta, \phi)\big)\ 2\pi \sin\theta\ d\theta \qquad (12.4)$$

The term $f\big(U(\theta, \phi)\big)\ 2\pi \sin\theta$ is the relative probability of finding a molecule at angle θ, which we can write as P(θ). The term $2\pi \sin\theta$ effectively acts as a 'orientational density of states', saying that there are not many orientations ('states') with perfect alignment, but many different orientations that are misaligned by e.g. 90°. Substituting Boltzmann statistics gives us

$$P(\theta) = e^{-U/k_B T}\ 2\pi \sin\theta = e^{p_0 E\ cos(\theta)/k_B T}\ 2\pi \sin\theta \qquad (12.5)$$

Our projected dipole moment as written above is only a relative measure, because our expression for the angular probability distribution was not normalized to a total probability of 1. To get an absolute result, we divide our result by the integrated 'relative probability', giving[xxviii]

[xxviii] Note that this normalization resolves a question that you might have had: we don't know the 'absolute energy' of our molecule, only changes in its energy related to its orientation, so how can we evaluate the Boltzmann factor. It turns out that adding an offset to our energy U(θ) is equivalent to multiplying by a constant factor. This constant factor will always be divided out in the normalization process, whatever its actual numerical value. The result is thus independent of absolute energy, and only depends on angle-dependent *changes* to the energy.

$$\langle \vec{p} \rangle \propto \frac{\int_\theta p_0 \, cos(\theta) \, P(\theta) \, d\theta}{\int_\theta P(\theta) \, d\theta}. \tag{12.6}$$

The total integral for finding the average dipole moment per molecule is now

$$\langle \vec{p} \rangle = \frac{\int_\theta p_0 \, cos(\theta) \, e^{p_0 E \, cos(\theta)/k_B T} \, 2\pi \sin\theta \, d\theta}{\int_\theta e^{p_0 E \, cos(\theta)/k_B T} \, 2\pi \sin\theta \, d\theta}. \tag{12.7}$$

Realizing $sin(\theta) \, d\theta = -d(cos(\theta))$ and renaming $cos(\theta)$ as q we find

$$\langle \vec{p} \rangle = -p_0 \frac{\int_{q=1}^{-1} q \, e^{x \, q} \, dq}{\int_{q=1}^{-1} e^{x \, q} \, dq} = p_0 \frac{\int_{q=-1}^{1} q \, e^{-x \, q} \, dq}{\int_{q=-1}^{1} e^{-x \, q} \, dq}. \tag{12.8}$$

Where we have substituted $x = p_0 E/k_B T$. The ratio of integrals has a solution known as the Langevin function:

$$L(x) = \coth(x) - \frac{1}{x} \tag{12.9}$$

Substituting $x = p_0 E/k_B T$ we have found an average dipole moment per molecule of

$$\langle \vec{p} \rangle = p_0 \left[\coth\left(\frac{1}{x}\right) - x \right] = p_0 \left[\coth\left(\frac{p_0 E}{k_B T}\right) - \frac{k_B T}{p_0 E} \right]. \tag{12.10}$$

The Langevin function is shown below. Note that we observe several physically reasonable results. For small applied fields (small x) we have small average dipole moment. Increasing the field results in more alignment. Increasing the temperature *reduces* x, lowering the average dipole moment. This makes sense: at higher temperature, the molecules undergo more collisions, randomizing their alignment. Finally, for very strong fields the polarization saturates. This also makes sense: when all molecules are completely aligned, there is no further angle change that can increase the average dipole moment per molecule.
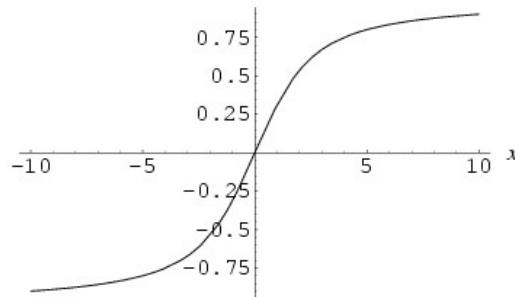
Figure 12.6: The Langevin function. Note the linear section for small argument, and the saturation for large argument.

For small x (low field and/or high temperature) we see that the Langevin function is approximately linear in field strength. A Taylor expansion shows that the slope in x is equal to 1/3. For small fields we can thus write

$$\langle \vec{p} \rangle = \frac{1}{3}p_0 \frac{p_0 E}{k_B T} = \frac{p_0^2}{3k_B T}E. \tag{12.11}$$

The total dipole moment per unit volume is now simply

$$P = N\frac{p_0^2}{3k_B T}E. \tag{12.12}$$

with N the number of molecules per unit volume, assuming these are all the same polar molecules with permanent dipole moment p_0. Comparing with $P = \epsilon_0 \chi E$ we find a low-frequency susceptibility contribution of

$$\chi(0) = \frac{N}{\epsilon_0}\frac{p_0^2}{3k_B T}. \tag{12.13}$$

due to field-induced (partial) alignment of the polar molecules.

Note that our susceptibility depends quadratically on the dipole moment. This makes sense: each molecule contributes dipole moment proportional to p_0, but in addition, our *ability to align* the molecule (the 'torque' we can apply on each molecule) also depends linearly on p_0. Together these two effects give the observed quadratic dependence on dipole moment.

So far, we have considered a static electric field. In this case it is easy to understand that thermal equilibrium following the Boltzmann distribution can develop. To understand the response to time-varying fields we need to consider the dynamics of the orientation process. Note that our expression for polarization represents a dynamic equilibrium: the electric field tries to align the molecules, while collisions are randomizing their orientation. If we were to suddenly turn off the field, the molecules will gradually return to an isotropic (randomized) orientational distribution with zero average dipole moment. This behavior is addressed phenomenologically in the *Debye model*. This model assumes that the randomization of the molecular alignment takes place on a time scale described by the *rotational correlation time* τ. Upon suddenly turning off the applied field, the polarization is expected to change according to

$$\frac{d\vec{P}}{dt} = -\frac{\vec{P}}{\tau} \quad \Rightarrow \quad \vec{P}(t) = \vec{P}(0)e^{-t/\tau} \tag{12.14}$$

Note that this relation simply *assumes* that the relaxation process leads to an exponential decay. This is thus only a phenomenological description of the relaxation process, ignoring the details of the relaxation process. The rotational correlation time τ is linked to the viscosity η of the liquid according to $\tau = \eta V/k_B T$ with V the volume per molecule. For water (H_2O) the rotational correlation time is approximately 40 ps. This already tells us that water molecules will not be able to react strongly to fields that change faster than once per 40 ps, so we expect orientational polarization effects to occur at frequencies below tens of GHz (wavelength at least several centimeters).

Optical response in Debye description

Previously we derived the susceptibility for zero frequency, and we have a relation describing the polarization relaxation in zero externally applied field. We can now

construct a relation that provides the correct static response *and* the correct exponential response to sudden changes of the field:

$$\tau \frac{d\vec{P}}{dt} + \vec{P} = \frac{Np_0^2}{3k_BT} \vec{E}(t)$$ (12.15)

This equation is known as the Debye relaxation equation. Note that for static fields the time derivative will become zero, producing exactly the static polarization from Eq. 12.12 which we found using statistical mechanics. Also note that if the field is turned off, our relation becomes exactly of the form of Eq. 12.14, describing the assumed exponential decay of P(t).

We can now derive the frequency-dependent susceptibility by substituting a harmonically oscillating field in Eq. 12.15, i.e. we substitute $E(t) = E(\omega)e^{-i\omega t} + c.c.$ and we assume that the response is linear, meaning the polarization will oscillate at the same frequency: $P(t) = P(\omega)e^{-i\omega t}$. Carrying out the time derivative, and dividing out common frequency terms this gives

$$-i\omega\tau P(\omega) + P(\omega) = \frac{Np_0^2}{3k_BT} E(\omega) \Rightarrow P(\omega) = \frac{Np_0^2}{3k_BT} \frac{1}{1 - i\omega t} E(\omega)$$ (12.16)

Comparing to the definition of susceptibility we have found

$$\chi(\omega) = \frac{Np_0^2}{3kT\varepsilon_0} \frac{1}{(1 - i\omega\tau)}$$ (12.17)

This is the Debye susceptibility, representing the susceptibility contribution due to molecular alignment in a polar liquid. The corresponding complex refractive index curves including *only* the susceptibility from molecular reorientation are shown below for a rotational correlation time of 100 ps. Note that there is maximum absorption when $\omega = 1/\tau$. In reality we would at least need to add the low-frequency electronic susceptibility of the liquid to get more realistic results.
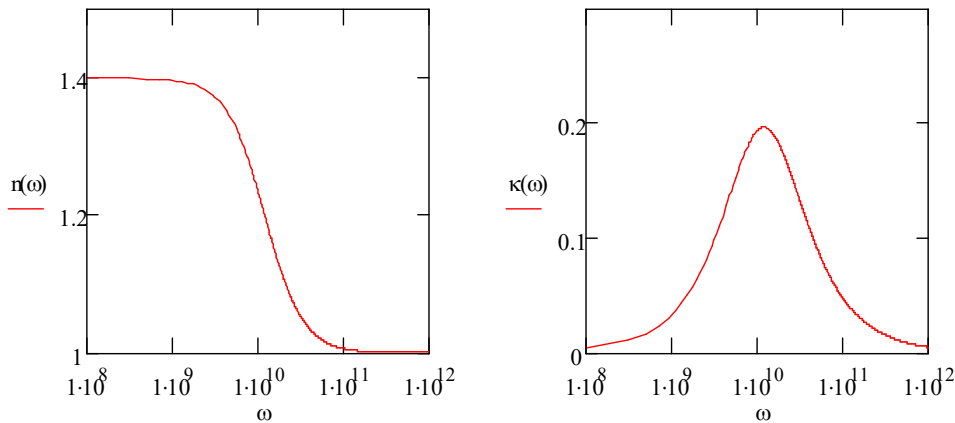
Figure 12.7. Typical optical response predicted by the Debye relaxation model

The calculated curves show that we can absorb GHz radiation in a polar liquid, causing the liquid to heat up. This is the operating principle of microwave ovens: food or drinks containing water molecules are irradiated with strong EM radiation at a frequency that falls

within the absorption band related to the rotational correlation time of water, causing heat generation. Our microwaves are thus specifically optimized for heating water, and would not necessarily work well for heating up other polar liquids. An interesting related fact is that molecules in ice cannot easily reorient, so it is initially difficult to heat up frozen foods using microwave radiation, until some of the H_2O becomes liquid.

Below is the *measured* complex refractive index of water on a log scale. Note that the low-frequency (long wavelength) response matches the behavior predicted by the Debye model. There is a large index contribution at wavelengths longer than 1mm due to alignment, and a related absorption peak for a wavelength of ~10mm, or a frequency of 30 GHz. At wavelengths below 10 μm (E >~124 meV) we see additional peaks in κ largely due to the excitation of vibrations. At a wavelength around 500nm we see minimum absorption, followed by the onset of strong electronic absorption. We see that the transparency range of water occurs between vibrational transitions and electronic transitions, which conveniently happens to coincide with the visible range.
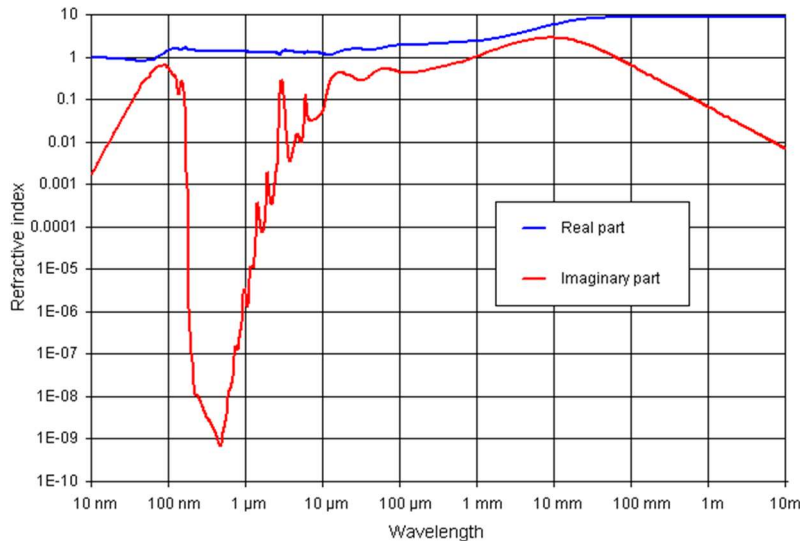
Figure 12.8: The refractive index of water, from http://www.philiplaven.com/p20.html . Note the Debye like response at wavelengths above 100 μm (frequencies below 3 THz), as well as some vibrational lines between 1 μm and 10 μm.

129

Chapter 13 – Interaction of light with vibrations in solids

➢ Corresponding handouts are available on http://kik.creol.ucf.edu/courses.html

In Chapter 11 we studied how molecules supports vibrational normal modes, with frequencies that depend on the chemical bond strength and on the masses of the atoms in the molecule. In solids similar effects occur, with the major different that the atoms are bound in a three-dimensional crystal lattice. In this chapter we will see that non-metallic compound solids support dipole active vibrations that extend throughout the entire crystal, resulting in resonances and strong Lorentz-like contributions to the dielectric function at IR frequencies.

Vibrational modes in a monatomic 1D lattice

In a crystal atoms are bound in an extended lattice, and the resulting vibrational normal modes extend throughout the entire crystal. These extended vibrational modes are called *phonons*. Crystals are much easier to deal with analytically than non-crystalline solids, but much of what we do here for crystals applies to non-crystalline solids as well.

To understand the basic mechanical response of crystals we start with the simplest case of a 1-dimensional monatomic lattice. The assumption of a monoatomic lattice (all atoms have identical mass) implies that we are discussing an elemental solid such as pure Si or even pure Al. As such we do not expect polar bonds, and therefore we do not expect dipole active modes (see Chapter 11) and no strong phonon-photon coupling. Nevertheless, the monoatomic lattice model provides valuable insight into vibrations in solids.
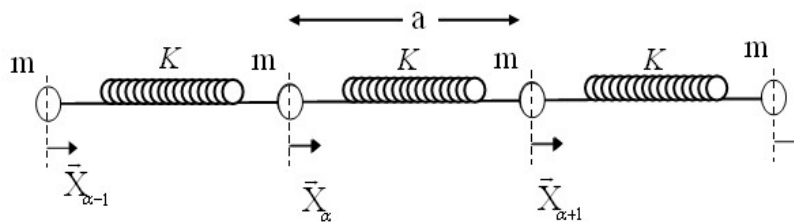
Figure 13.14

In our simple model, a unit cell (length a) contains only one atom with mass m, and there is only one spring constant K that represents the inter-atomic binding potential. For simplicity we consider only nearest-neighbor interactions, meaning that the force on a given atom is affected only by the atoms immediately adjacent to it. The atoms are numbered with a variable α with X_α representing the time dependent position of atom α relative to its equilibrium position. The restoring forces depend on displacement differences. For example if atom 2 has moved more to the right than atom 1, atom 1 will experience a positive force $K(x_2-x_1)$. The total equation of motion thus becomes:

$$-K(X_\alpha - X_{\alpha-1}) + K(X_{\alpha+1} - X_\alpha) = m\ddot{X}_\alpha$$
$$\Rightarrow -K(2X_\alpha - X_{\alpha-1} - X_{\alpha+1}) = m\ddot{X}_\alpha$$

(13.8)

showing that the acceleration of atom α depends only on the distance to its neighbors, *not on its absolute position.*[xxix]

We will again look for solutions where all atoms oscillate at the same frequency, i.e. all X terms have the same time dependence, $e^{-i\omega t}$. In this case the equation of motion becomes

$$m\omega^2 \ddot{X}_\alpha = K(2X_\alpha - X_{\alpha-1} - X_{\alpha+1}) \tag{13.9}$$

We will see that this equation has traveling-wave solutions with the displacement of atom α relative to its center position given by

$$X_\alpha = x_\beta e^{i(k_\beta z_\alpha - \omega_\beta t)} = x_\beta e^{i(\alpha k_\beta a - i\omega_\beta t)} \tag{13.10}$$

where β represents the number of the mode, z_α is the average position of atom α along the chain given by $z_\alpha = \alpha \times a$ and k_β is the wavevector of the βth mode. The center positions of the left and right neighbors are $z_{\alpha-1} = (\alpha a)-a$ and $z_{\alpha+1} = (\alpha a)+a$ respectively, resulting in a displacement

$$X_{\alpha\pm1} = x_\beta e^{i\alpha k_\beta a} e^{\pm i k_\beta a} . \tag{13.11}$$

where the time dependence has been omitted. We substitute this displacement in equation 13.9, resulting in:

$$-m\omega_\beta^2 x_\beta e^{i\alpha k_\beta a} = Kx_\beta \left\{ e^{i(\alpha+1)k_\beta a} + e^{i(\alpha-1)k_\beta a} - 2e^{i\alpha k_\beta a} \right\} \tag{13.12}$$

$$\Rightarrow \omega_\beta^2 = -\frac{K}{m}\left\{ e^{ik_\beta a} + e^{-ik_\beta a} - 2 \right\} = \frac{2K}{m}\left[1 - \cos(k_\beta a)\right] \tag{13.13}$$

Note that the vibration frequency ω_β indeed only depends on the relative phase of the neighbors. We now have a series of allowed modes with wavevector k_β and angular frequency ω_β according to

$$\omega_\beta = \sqrt{\frac{2K}{m}}\sqrt{1 - \cos(k_\beta a)} = \sqrt{\frac{2K}{m}}\sqrt{2}\left|\sin\left(\frac{k_\beta a}{2}\right)\right|$$

$$\Rightarrow \omega_\beta = 2\sqrt{\frac{K}{m}}\left|\sin\left(\frac{k_\beta a}{2}\right)\right| \tag{13.14}$$

This equation represents the *phonon dispersion relation* in a one dimensional mono-atomic lattice. The dispersion relation is shown below. We see that low values of k correspond to low oscillation frequencies. This is – as mentioned before – due to the small *relative* displacement of adjacent atoms for modes with low k values, resulting in a small restoring force.

[xxix] This last observation will become important later, since it implies that oscillations in which neighboring atoms move approximately in-phase will experience little acceleration, resulting in a set of low frequency phonon modes.
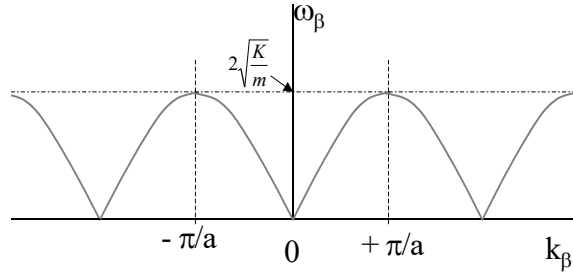
Figure 13.15

Note that the maximum oscillation frequency that a collective mode can have is $2\sqrt{(K/m)}$. This frequency occurs at $k = \pm \pi/a$, in other words when adjacent unit cells (in this case containing 1 atom) are 180 degrees out of phase. A wavenumber π/a corresponds to a vibration wavelength of $2a$. For wavenumbers of magnitude $>\pi/a$, the same physical configuration can also be described by a wavenumber that is less than π/a, so there is no new physical situation outside the range $-\pi/a < k < \pi/a$. This range is known as the first Brillouin Zone, or often simply '*the Brillouin zone*".

Boundary conditions and degrees of freedom

In a 1D lattice of length L, each atom has 1 degree of freedom, so we expect that there are a total of N of these collective modes, i.e. $\beta \in \{1 .. N\}$, where N is the number of atoms in the crystal, given by $N=(L/a)+1$. In a finite crystal, the eigenmodes are described by standing waves with a wavelength that satisfies $\lambda = {}^{2L}/_{\beta}$. with $\beta \in \{0, N\}$ The case $\beta=0$ corresponds to translation, while the longest finite wavelength is described by $k=\pi/L$. The shortest possible physically meaningful wavelength is $2a$. The allowed wavevectors are thus

$$| k |= 0, \frac{\pi}{L}, \frac{2\pi}{L}, \frac{3\pi}{L}, ... , \frac{2\pi}{2a} = \frac{2\pi}{2L/(N-1)} = \frac{\pi}{L}(N-1) \qquad (13.15)$$

representing N allowed modes with evenly spaced k values, and N different wavelengths:

$$\lambda = \infty, \ 2L, \ \frac{2L}{2}, \ \frac{2L}{3}, \ ... , 2a \qquad (13.16)$$

The discrete nature of k is generally not important for the optical properties of large crystals.

In the limit of an *infinite* crystal, the left- and right-propagating modes need to be considered as independent modes, suggesting that a subset of N atoms in this infinite crystal would support 2N modes, which cannot be correct. In fact when calculating the number of allowed modes on this subset of atoms with length L, the set of atoms needs to support the entire wavelength which limits the allowed positive wavevectors to

$$k_+ = \frac{2\pi}{L}, \frac{4\pi}{L}, \frac{6\pi}{L}, ... , \frac{2\pi}{2a} = \frac{2\pi}{2L/(N-1)} = \frac{2\pi}{L}\frac{(N-1)}{2} \qquad (13.17)$$

with an equal number of negative wavevectors and one solution for k=0, bringing the total number of modes for the set of N atoms to

$$N_{total} = 2 \times \frac{(N-1)}{2} + 1 = N \tag{13.18}$$

as expected. Note that the discussion above involved a monatomic lattice, for which the vibrational modes cannot interact with radiation. To look at the interaction of light with lattice modes, we must next examine the lattice modes of a diatomic lattice.

Vibrational modes in a diatomic 1D Lattice
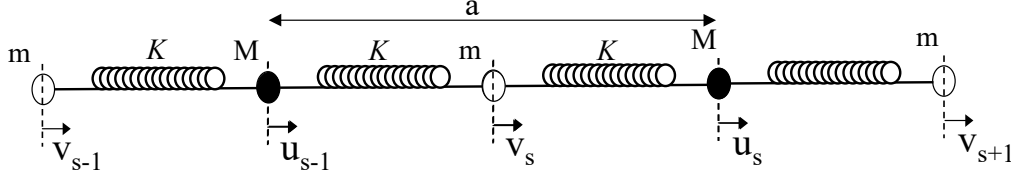
Figure 13.16

In this section we will discuss a linear chain consisting of atoms with masses M and m, characterized by displacement amplitudes u_s and v_s respectively, where s is an index indicating the unit cell. Note that in this case *a* corresponds to the length of the *unit cell*, and that a unit cell contains two atoms, one of each kind. A wavevector of π/a thus implies a phase difference of 180 degrees between the *behavior inside adjacent unit cells*, not between adjacent atoms. We will find that the internal structure of the unit cell adds an internal degree of freedom, giving rise to two phonon modes for each value of the wavevector.

Assuming next-neighbor interactions, the equations of motion are

$$\begin{aligned} M\ddot{u}_s &= K(v_{s+1} + v_s - 2u_s) \\ m\ddot{v}_s &= K(u_s + u_{s-1} - 2v_s) \end{aligned} \tag{13.19}$$

Again, we look for traveling wave solutions, where u_s, v_s have the same frequency and wavenumber, but different amplitudes. We anticipate solutions of the form

$$v_s = v_0 e^{iska} e^{-i\omega t}, \qquad u_s = u_0 e^{iska} e^{-i\omega t}. \tag{13.20}$$

Substituting these trial functions into the equations of motion, we obtain

$$\begin{aligned} -M\omega^2 u_0 &= Kv_0(1 + e^{ika}) - 2Ku_0 \\ -m\omega^2 v_0 &= Ku_0(1 + e^{-ika}) - 2Kv_0 \end{aligned} \tag{13.21}$$

For a solution to exist the determinant needs to be equal to zero:

$$\begin{vmatrix} (2K - M\omega^2) & -K(1 + e^{ika}) \\ -K(1 + e^{-ika}) & (2K - m\omega^2) \end{vmatrix} = 0 \tag{13.22}$$

This leads to an equation of the order ω^4, resulting in two independent solutions for ω^2 :

$$\therefore mM\omega^4 - 2K(m+M)\omega^2 + 2K^2(1-\cos ka) = 0$$

$$\Rightarrow \quad \omega^2 = \frac{K}{mM}\left\{(m+M) \pm \sqrt{(m+M)^2 - 2mM(1-\cos ka)}\right\} \qquad (13.23)$$

This represents the dispersion relation for a diatomic linear lattice, schematically shown below.
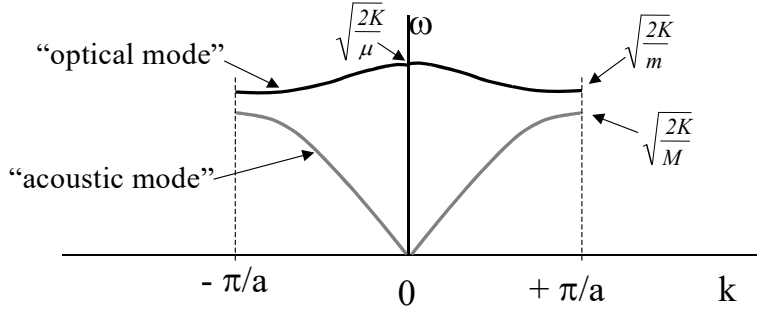
Figure 13.17

Two separate 'phonon branches' are observed, a low frequency or 'acoustic branch', and a high frequency 'optical branch'. To understand the nature of these phonon branches we will investigate the high and low wavevector limits: $k \approx 0$ (or $ka \ll 1$) and $k \cong \pm\pi/a$.

For the latter case, $k \cong \pm\pi/a$, meaning that $1-\cos(ka) \cong 2$, so that the solution simplifies to

$$\omega^2 = \frac{K}{mM}\left\{(m+M) \pm \sqrt{(m+M)^2 - 4mM}\right\}$$

$$= \frac{K}{mM}\left\{(m+M) \pm (m-M)\right\} \qquad (13.24)$$

Hence, at the zone boundary we find two allowed solutions with frequencies corresponding to $\omega^2 = \dfrac{2K}{m}$ and $\omega^2 = \dfrac{2K}{M}$.

For $ka \ll 1$ we can approximate $\cos(x) \approx 1 - \tfrac{1}{2}x^2$ giving $1-\cos(ka) \cong k^2a^2/2$, leading to

$$\omega^2 = \frac{K}{mM}\left\{(m+M) \pm \sqrt{(m+M)^2 - 2mM\frac{(ka)^2}{2})}\right\}$$

$$= K\frac{m+M}{mM}\left\{1 \pm \sqrt{1 - \frac{mM}{(m+M)^2}(ka)^2}\right\} \qquad (13.25)$$

$$\approx K\frac{m+M}{mM}\left\{1 \pm \left[1 - \frac{mM}{(m+M)^2}\frac{(ka)^2}{2}\right]\right\}$$

hence we have two solutions for this range of ka. The solution with the + sign corresponds to high frequency modes:

$$\omega^2 \cong 2K\frac{m+M}{mM} = 2K\left(\frac{1}{m}+\frac{1}{M}\right) = \frac{2K}{\mu}$$

(13.26)

where μ is the reduced mass of the unit cell, $\frac{1}{\mu} = \frac{1}{m}+\frac{1}{M}$.

The '-' case leads to $\omega^2 \cong \frac{(ka)^2}{2}\frac{K}{m+M}$, $\Rightarrow \omega \cong \sqrt{\frac{K}{2(m+M)}}ka$ showing a linear dependence of ω on k at low frequencies.

Three example curves are shown below for identical transverse spring constant K_T and a fixed longitudinal spring constant $K_L = 1.4K_T$. Note that the total mass affects the acoustic branch slope, the reduced mass affects the maximum resonance frequency, and the mass ratio determines the frequency splitting at the zone boundary (k=π/d with d the unit cell length).
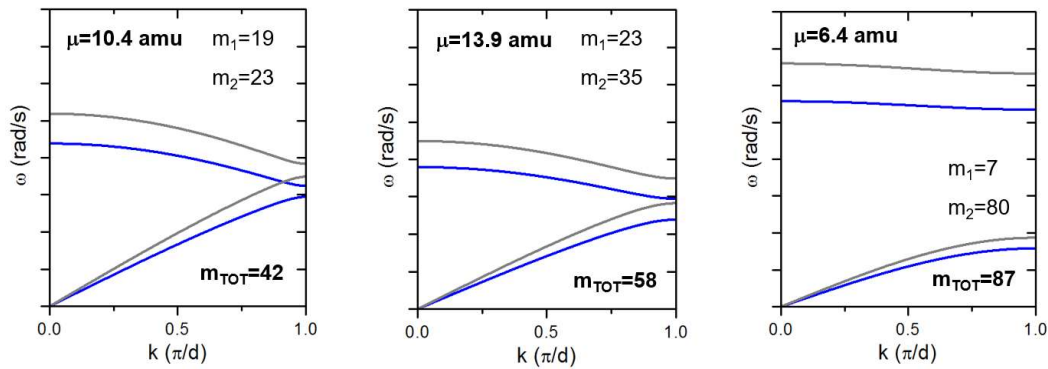
Figure 13.18 Example dispersion curves for phonons assuming a fixed transverse spring constant K_T and a fixed longitudinal spring constant $K_L = 1.4 K_T$.

Interaction of radiation with lattice modes

In solids with more than one type of atom, the different atoms will generally have slightly different charges. This means that the different atoms will experience forces in different directions due to an applied field, and consequently, a macroscopic polarization due to the lattice can be induced by an electric field. The natural frequency of oscillation of such a polarization corresponds to the "optical modes" calculated previously for the diatomic lattice.

Now the wavelength of light is always much greater than the lattice spacing, especially for the infrared region where the frequency of the EM wave is resonant with the optical modes, i.e. $\lambda \gg$ a.
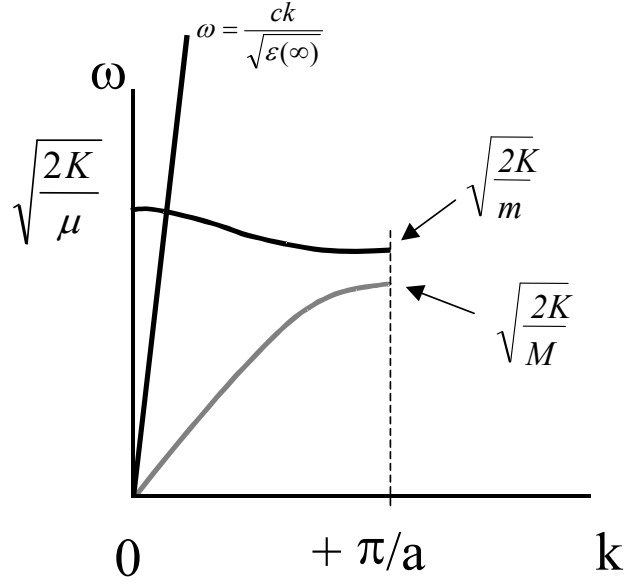
Figure 13.19 Dispersion curves for phonons (lattice modes) and photons, assuming for now that there is no change in index due to the lattice

Hence the optical wave interacts with very long wavelength lattice modes (compared to a). This means that $k \approx 0$ for the optical lattice modes, which is convenient as it simplifies the mathematics. Since $k \approx 0$, we can assume that the applied field is spatially uniform, which is true over many thousands of atomic spacings. Hence,

$$E(t) = E_0 e^{-i\omega t} . \tag{13.27}$$

The coupled equations for displacements u and v are then

$$\begin{aligned} M\ddot{u}_s - K(v_{s+1} + v_s - 2u_s) = +qE_0 e^{-i\omega t} \\ m\ddot{v}_s - K(u_s + u_{s-1} - 2v_s) = -qE_0 e^{-i\omega t} \end{aligned}, \tag{13.28}$$

Since $k \approx 0$ the phase term $e^{ik\alpha} \approx 1$, leading to $u_s(t) = u_0 e^{-i\omega t}$ and $v_s(t) = v_0 e^{-i\omega t}$ independent of s. Substituting u and v gives

$$\begin{aligned} (2K - M\omega^2)u_0 - 2Kv_0 = +qE_0 \\ -2Ku_0 + (2K - m\omega^2)v_0 = -qE_0 \end{aligned} \tag{13.29}$$

For this, the solutions for amplitudes u_0 and v_0 are of the form

$$u_0 = \frac{+qE_0/M}{\omega_T^2 - \omega^2}, \qquad v_0 = \frac{-qE_0/m}{\omega_T^2 - \omega^2} \tag{13.30}$$

where ω_T is the resonant frequency of the optical modes at $k = 0$, $\omega_T = \sqrt{2K/\mu}$. This is sometimes referred to as the "transverse optical phonon" frequency, hence the subscript T. As before, μ is the reduced mass.

Optical properties of polar solids

The lattice contribution to the polarization is

$$P_\ell = Ne(u_0 - v_0),$$ (13.31)

where e is the effective charge on the atoms in the lattice (not usually equal to e.) The total polarization is $P = P_\ell + P_{bound}$, where again, P_{bound} is the electronic polarization. So the total dielectric function is

$$\varepsilon_r(\omega) = 1 + \frac{P}{\epsilon_0 E} = 1 + \frac{P_{bound}}{\epsilon_0 E} + \frac{Ne}{\epsilon_0 E}(u_0 - v_0).$$ (13.32)

But, $u_0 - v_0 = \frac{eE_0}{\mu} \frac{1}{\omega_T^2 - \omega^2}$, so that

$$\begin{aligned}
\varepsilon_r(\omega) &= 1 + \frac{P}{\epsilon_0 E} = 1 + \frac{P_{bound}}{\epsilon_0 E} + \frac{Ne^2}{\epsilon_0 \mu} \frac{1}{\omega_T^2 - \omega^2} \\
&= 1 + \chi_{electronic} + \frac{Ne^2}{\epsilon_0 \mu} \frac{1}{\omega_T^2 - \omega^2} \\
&= \varepsilon_r(\infty) + \frac{Ne^2}{\epsilon_0 \mu} \frac{1}{\omega_T^2 - \omega^2}
\end{aligned}$$ (13.33)

Where $\varepsilon_r(\infty)$ is the high frequency dielectric constant. Note that this is not truly the value at $\omega \to \infty$, which is always 1, but is usually taken to mean the value at frequencies well above ω_T, yet well below any electronic resonances. The overall behavior of $\varepsilon_r(\omega)$ is sketched below. Note we have not included damping, as it is not too important here. We will look at the effect of damping a little later.

We can use this relationship to find a value for the low frequency dielectric constant, $\varepsilon_r(0)$, using

$$\varepsilon_r(0) = \varepsilon_r(\infty) + \frac{Ne^2 / \epsilon_0 \mu}{\omega_T^2}$$ (13.34)
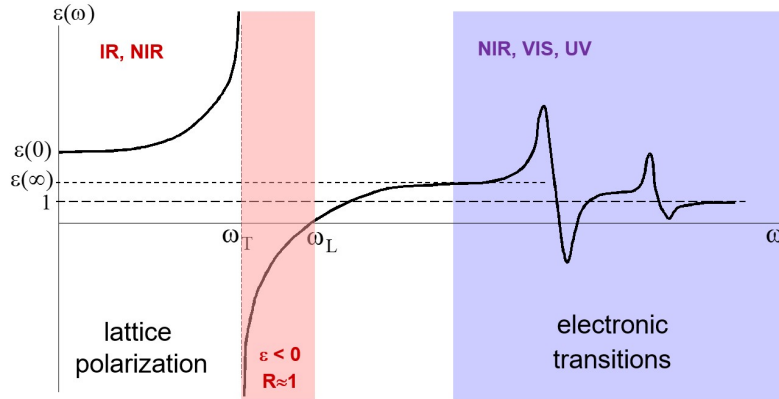
Figure 13.20

The Lyddane-Sachs-Teller relationship

From our expression for $\varepsilon_r(\omega)$, we can write

$$\left[\varepsilon_r(0) - \varepsilon_r(\infty)\right]\omega_T^2 = Ne^2 / \in_0 \mu \qquad (13.35)$$

so that,

$$\begin{aligned}
\varepsilon_r(\omega) &= \varepsilon_r(\infty) + \frac{\left[\varepsilon_r(0) - \varepsilon_r(\infty)\right]\omega_T^2}{\omega_T^2 - \omega^2} \\
&= \varepsilon_r(\infty)\frac{\omega_T^2 - \omega^2}{\omega_T^2 - \omega^2} + \frac{\varepsilon_r(0)\,\omega_T^2}{\omega_T^2 - \omega^2} - \frac{\varepsilon_r(\infty)\,\omega_T^2}{\omega_T^2 - \omega^2} \\
&= \frac{\varepsilon_r(0)\omega_T^2 - \varepsilon_r(\infty)\omega^2}{\omega_T^2 - \omega^2}
\end{aligned} \qquad (13.36)$$

This shows us that $\varepsilon_r(\omega) = 0$ for $\varepsilon_r(0)\omega_T^2 = \varepsilon_r(\infty)\omega^2$. This frequency is labeled ω_L, the "longitudinal optical phonon" frequency, at which $\varepsilon_r = 0$, rather like the plasma frequency for electronic polarizability. Hence,

$$\varepsilon_r(\infty)\omega_L^2 = \varepsilon_r(0)\omega_T^2 \qquad \text{or} \qquad \frac{\varepsilon_r(\infty)}{\varepsilon_r(0)} = \frac{\omega_T^2}{\omega_L^2}, \qquad (13.37)$$

Which is known as the *Lyddane-Sachs-Teller* relationship, which works quite well for polar diatomic materials. Two examples:

GaAs: $\qquad \omega_L/\omega_T = 1.07 \qquad \sqrt{\varepsilon_r(0)/\varepsilon_r(\infty)} = 1.08$

KBr: $\qquad \omega_L/\omega_T = 1.39 \qquad \sqrt{\varepsilon_r(0)/\varepsilon_r(\infty)} = 1.38$

[Ref: C. Kittel, Introduction to Solid State Physics, (Wiley)]

Note that $\omega_L > \omega_T$, always. Hence $\varepsilon(0) > \varepsilon(\infty)$, as might be expected.
Similar to plasma oscillations, ω_L is the frequency for longitudinal long wavelength lattice oscillations.
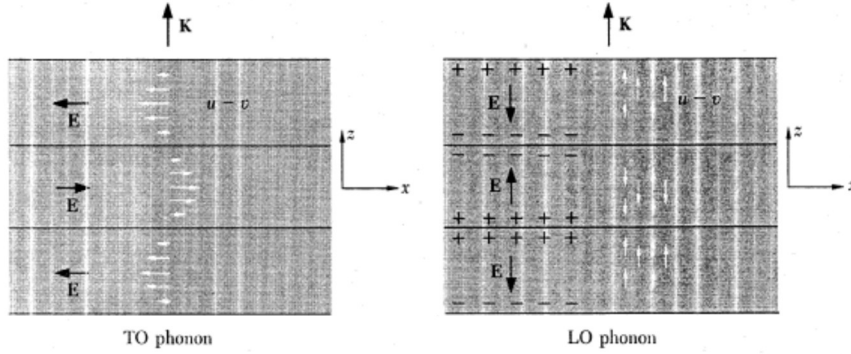
Figure 14 Relative displacements of the positive and negative ions at one instant of time for a wave in an optical mode traveling along the z axis. The planes of nodes (zero displacement) are shown; for long wavelength phonons the nodal planes are separated by many planes of atoms. In the transverse optical phonon mode the particle displacement is perpendicular to the wavevector K; the macroscopic electric field in an infinite medium will lie only in the $\pm x$ direction for the mode shown, and by the symmetry of the problem $\partial E_x/\partial x = 0$. It follows that div $E = 0$ for a TO phonon. In the longitudinal optical phonon mode the particle displacements and hence the dielectric polarization P are parallel to the wavevector. The macroscopic electric field E satisfies $D = E + 4\pi P = 0$ in CGS or $\epsilon_0 E + P = 0$ in SI; by symmetry E and P are parallel to the z axis, and $\partial E_z/\partial z \neq 0$. Thus div $E \neq 0$ for an LO phonon, and $\epsilon(\omega)$ div E is zero only if $\epsilon(\omega) = 0$.

Figure 13.21

Refractive index of polar and ionic solids

The behavior of the refractive index for a transverse optical phonon resonance is similar to that of a Lorentz oscillator. In our model the only difference is that we have ignored damping. In real materials phonon modes also undergo damping or scattering (change of wavevector direction and magnitude), resulting in a finite Γ. In Fig. 13.22 we show the real and imaginary parts of the refractive index for AlSb and the corresponding reflection spectrum.
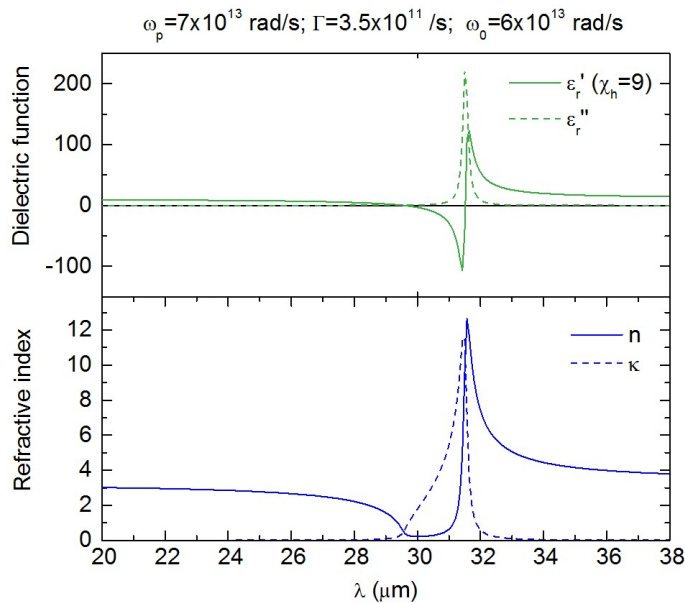
Figure 13.22: Complex dielectric function and refractive index of AlSb based on fit of experimental data by Turner and Reese

Reflectance of polar solids – Reststrahlen band

In the absence of damping, the reflectance must be unity in the region $\omega_T < \omega < \omega_L$, again just like for electronic transitions (see figures below). This region is called the "Reststrahlen" band, where light cannot propagate in the material, so must be absorbed or reflected, see Fig. 13.22. For sufficiently large negative ε_r' we have a large imaginary index, causing R to be very close to 1.
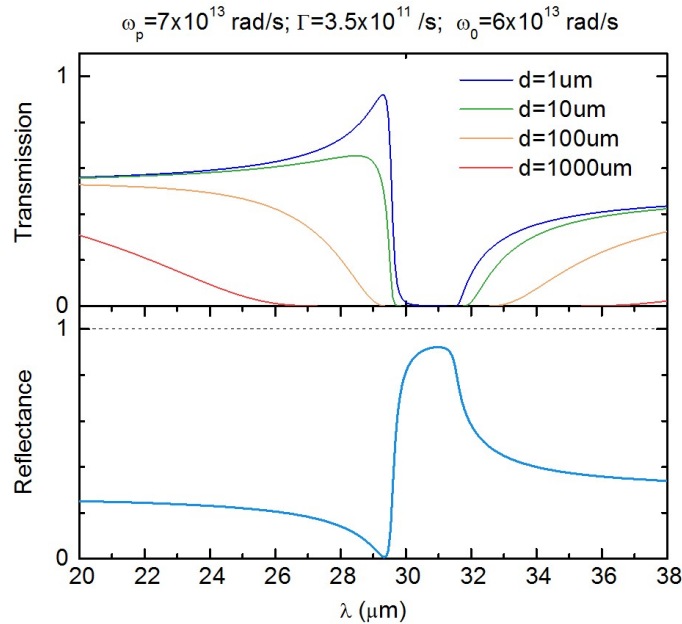
Figure 13.23: Reflection spectrum of AlSb and calculated transmission spectra for four thickness choices, ignoring multiple internal reflections (unphysical for thin films, done here for illustrative purposes)

Effect of phonons on transmission spectra

In the preceding sections we learned that there are dipole active phonons in polar and ionic crystals. In many cases the large number of participating atoms leads to a large modification of the infrared response, resulting in a Reststrahlen band (large reflection) between ω_T and ω_L. Just above ω_L there is a frequency where $n \approx 1$, resulting in a reflection minimum in air.

Based on the reflection spectrum shown in Fig. 13.23 we expect that compound dielectrics are opaque for wavelengths in the Reststrahlen band. Intuitively one might expect a transmission maximum corresponding to this reflection minimum, but in practice for thick materials (e.g. a 1 mm thick slide) this is not observed. The reason for this is that the absorption coefficient at this wavelength is still sufficiently large to produce almost zero transmission, see Fig. 13.23. Note that for a 1mm thick slab of AlSb the no transmission peak is observed when n=1. Also note that the onset of 'zero' transmission does not coincide with ω_L ($\lambda \approx 29.5$ μm) but instead occurs at higher energy ($\lambda \approx 27$ μm) due to absorption.

Coupled Photon-Phonon modes: Phonon-polaritons

Recall that we started out by drawing the dispersion of light (ω versus k) as a straight line. $\omega = ck/\sqrt{\varepsilon_r(\infty)}$. However, clearly close to the vibrational resonance frequencies ($\omega \sim 10^{14}$ rad/sec), ε_r is clearly strongly varying and ω versus k will not be a straight line.

For $\omega \sim 0$, the refractive index is given by $\sqrt{\varepsilon(0)}$, while at high frequencies it is given by $\sqrt{\varepsilon(\infty)}$. In these limits, the wave is described as "photon-like". However, as ω approaches ω_T, the index increases, and the group and phase velocities of the wave slow down to be close to that of the lattice modes. Here, the wave propagates as a strongly coupled polarization - electric field wave, with velocity characteristic of the lattice mode. Here the wave is described as "phonon-like".
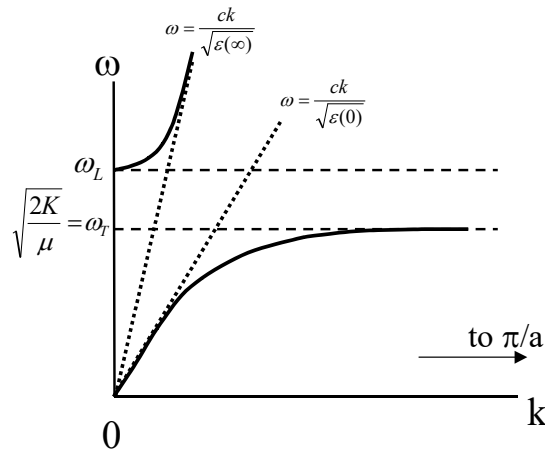
Figure 13.24

Solids with more than one atom per unit cell

This can get complicated, but generally, we see several phonon resonances, as illustrated below for GeO$_2$. In this case,

$$\varepsilon_r(\omega) = \varepsilon_r(\infty) + \sum_j f_j \frac{Ne^2/\epsilon_0 \, \mu_j}{\omega_{Tj}^2 - \omega^2} \tag{13.38}$$
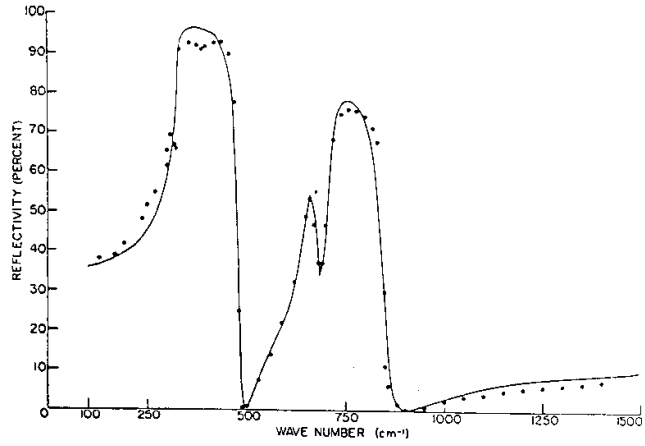
Fig. 5. Reststrahlen spectrum of tetragonal GeO_2 with $E \perp c$. Solid line is classical oscillator fit to experimental data (open circle). (From Kahan *et al.* [6].)

Figure 13.25

Examples of n, κ spectra

These are taken from *Optical Properties of Solids*, by Palik. The next few pages will show some representative materials types and we will make some comments on these.

Lithium Fluoride (LiF)
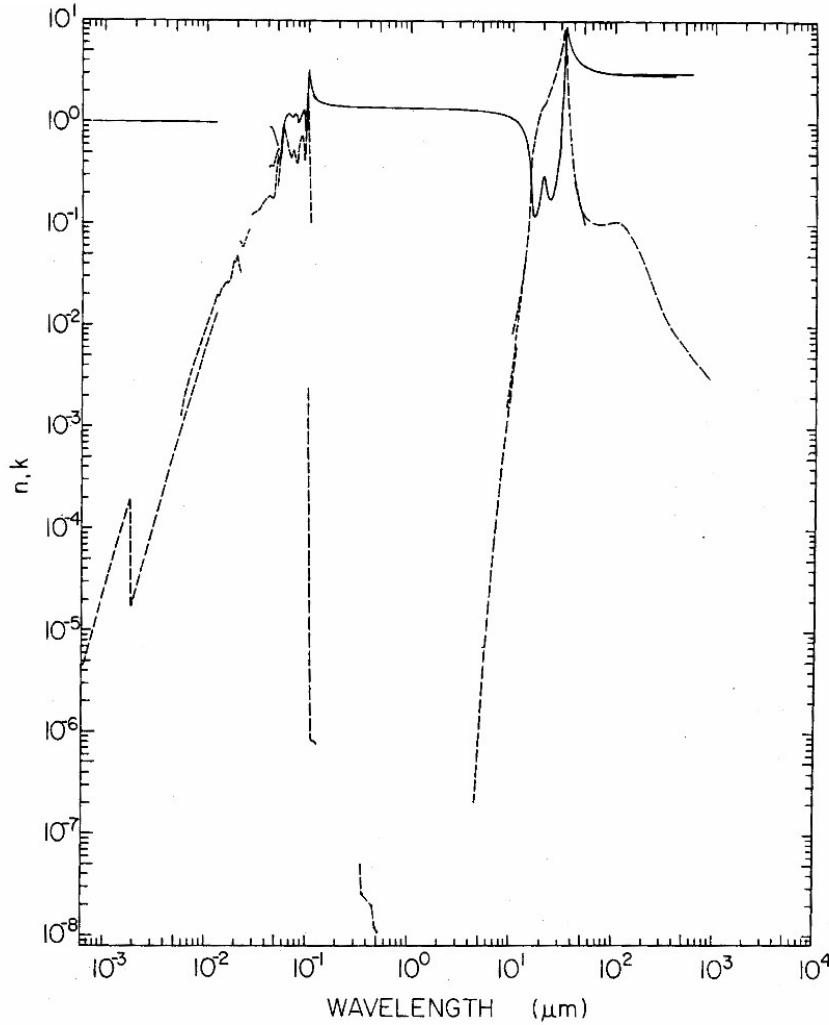
Fig. 6. Log–log plot of n (——) and k (– – – –) versus wavelength in micrometers for lithium fluoride. Note the incredibly small values of k in the transparent region centered near 1 μm.

Figure 13.26

Gallium Arsenide (GaAs)
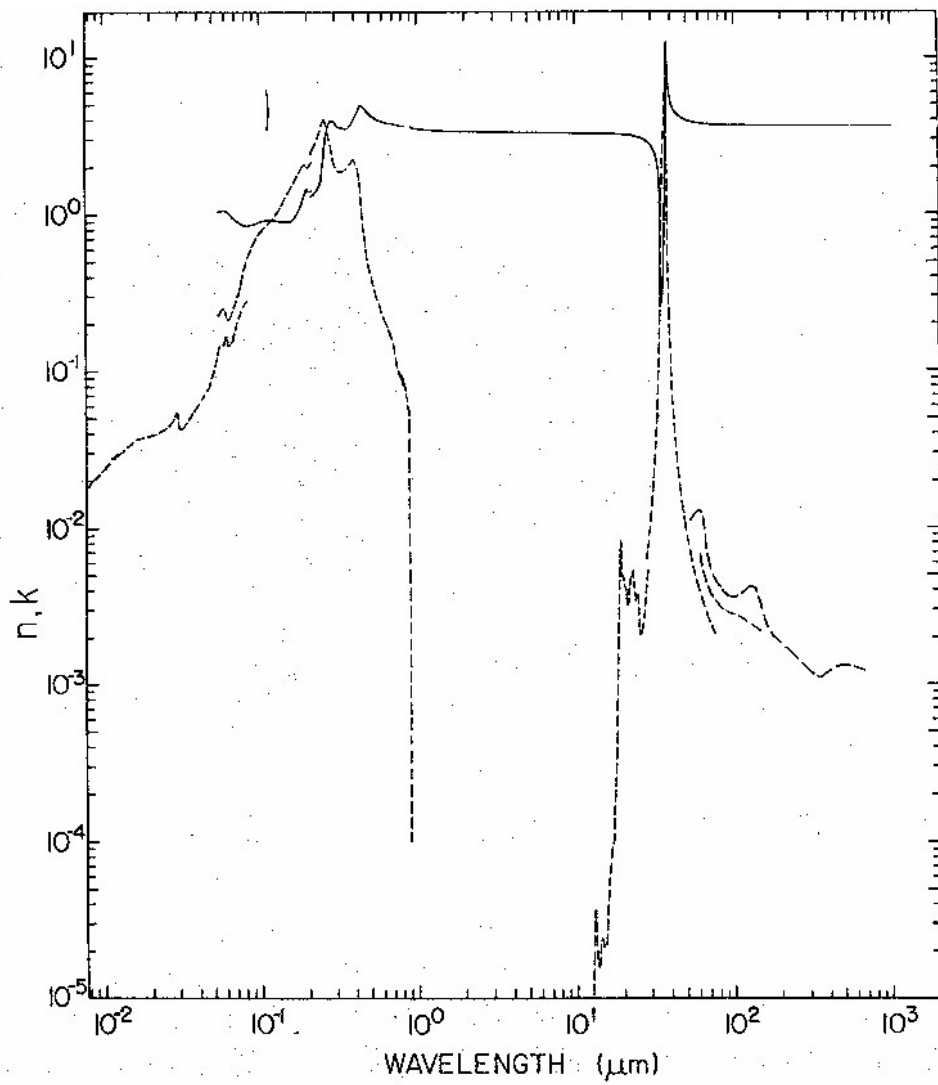
Figure 13.27
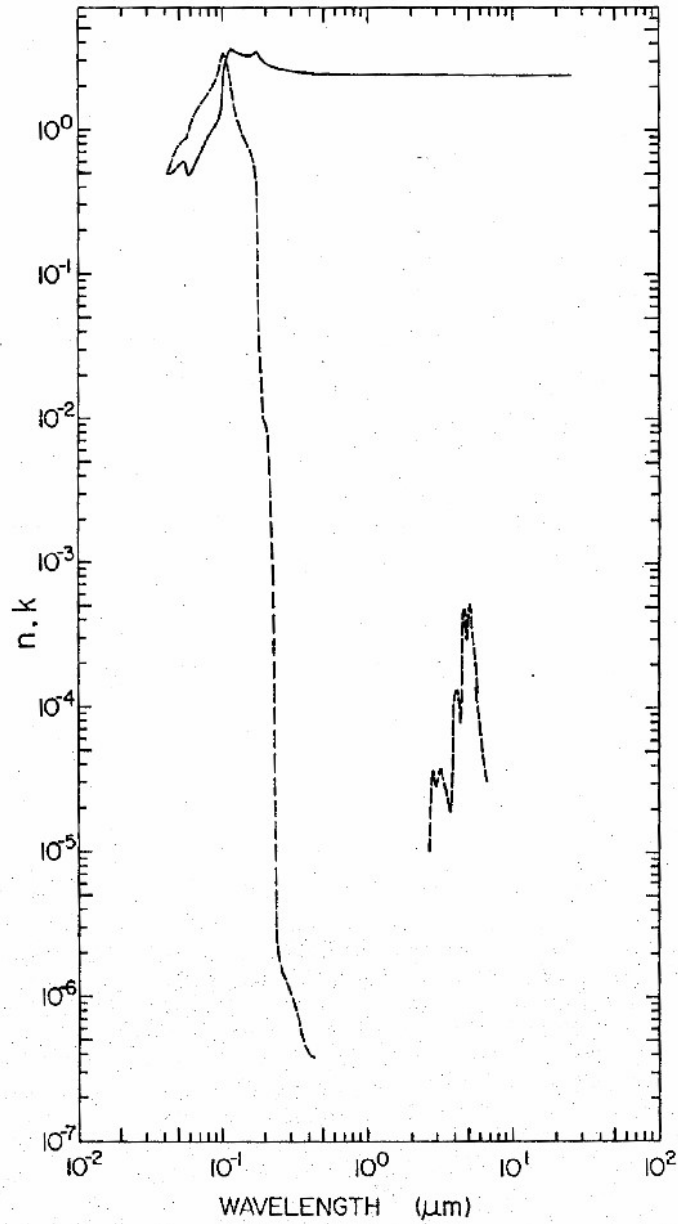
Fig. 5. Log–log plot of n(———) and k(———) versus wavelength in micrometers for cubic arbon.

Figure 13.28

Lithium Niobate (LiNbO₃)
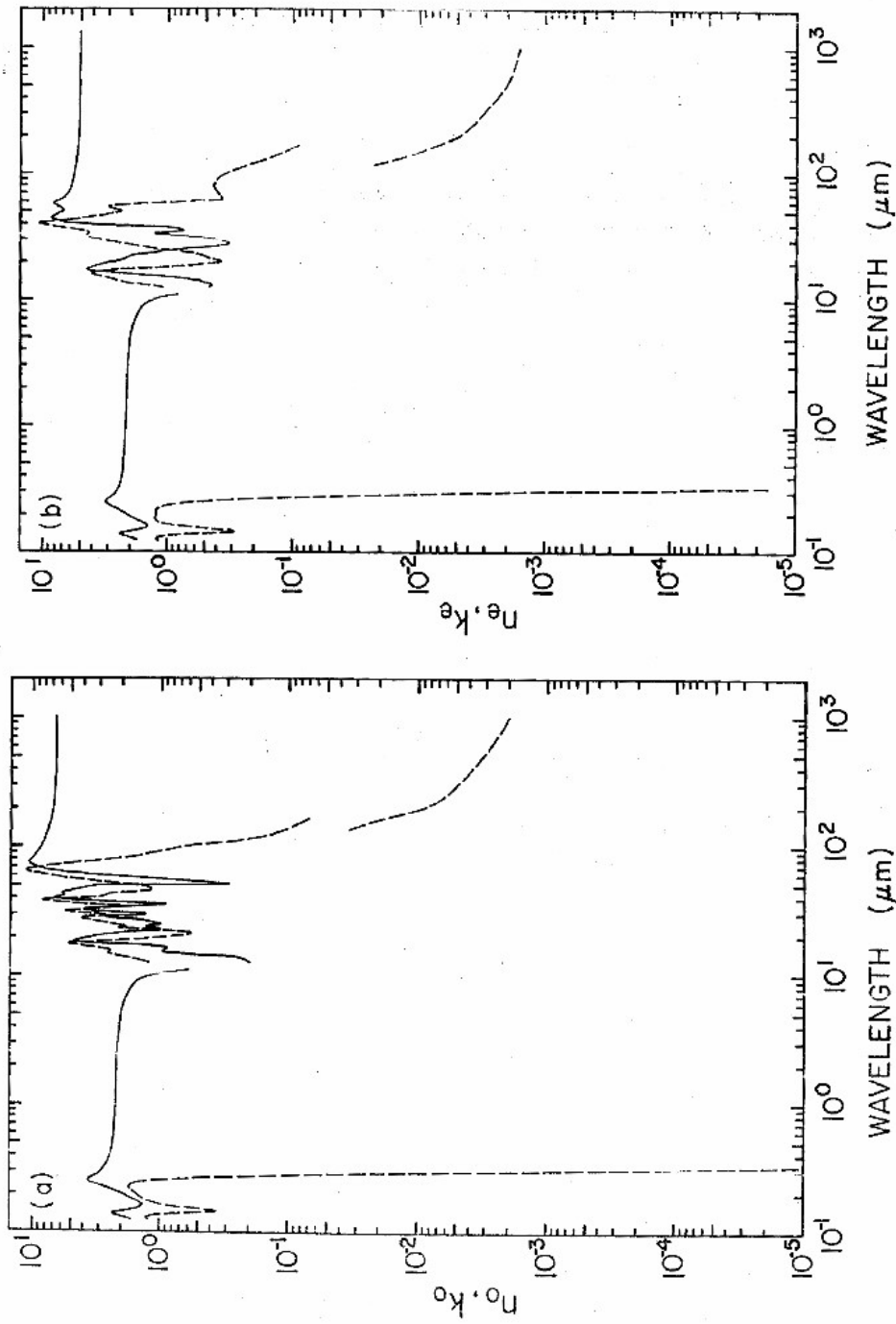
Fig. 7. (a) Log–log plot of n_o (———) and k_o (– – –) versus wavelength in micrometers for lithium niobate. (b) Log–log plot of n_e (———) and k_e (– – –) versus wavelength in micrometers for lithium niobate.

Figure 13.29

Chapter 14 – Optical properties of semiconductors

➢ Corresponding handouts are available on http://kik.creol.ucf.edu/courses.html

In chapter 3 we described the optical properties of insulators. We discussed that the valence electrons in insulators are relatively strongly bound to the individual atoms in the material, resulting in high resistivity and low absorption throughout the visible spectrum. In chapter 6 we discussed metals, in which the valence electrons can be considered free, leading to a high conductivity, negative ε at low frequencies and high absorption and reflection. In this chapter we will discuss an intermediate case: semiconductors. In semiconductors, the valence electrons are generally 'somewhat' bound to the atoms in the material, with binding energies of up to several eV. As a result, at room temperature these materials contain a small concentration of electrons that have broken free from the atoms, resulting in a small conductivity. This is the origin of the word 'semiconductor'.

The optical response of semiconductors is largely due to electronic transitions. In order to understand the possible electronic transitions, it is important to understand the electron dispersion relation or *electronic band structure* in semiconductors.

Electronic Band Structure

As was already mentioned in Chapter 5, the Lorentz model is not an accurate description of solids. While isolated atoms have well defined electronic states representative of the atom, as individual atoms are brought together the atoms start to interact, leading to shifts in the electronic energy levels. At the densities common in solids ($\sim 10^{22}$ atoms/cm^3) significant interaction occurs, causing levels to broaden out into bands, as schematically indicated in Fig. 14.1. The energy bands still retain some of the characteristics of their atomic origins. For example, in GaAs, the valence bands are mainly p-like in nature, while the conduction band is s-like.
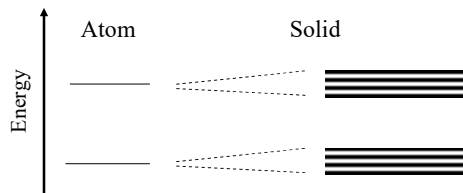
Figure 14.1

In covalent bonded solids, (e.g. GaAs, Si, Ge) outer electrons are quite evenly shared between different atoms, so the electron orbitals are extended throughout the crystal, and the energy bands corresponding to these orbitals are very broad. However in ionic bonded solids, (e.g. NaCl, MgF$_2$, KCl) electrons are much more localized and the bands are narrower. The absorption spectra of these materials retain more of the characteristics of atoms. (See figures 3.6 and 3.7 in Wooten.)

In order to understand the resulting energy band structure, we will use a quantum mechanical description. In quantum mechanics, the behavior of an electron in an electric potential V(x) is described by the Schrödinger equation

$$\left[-\frac{\hbar^2}{2m}\frac{\partial^2}{\partial x^2}+V(x)\right]\Psi(x,t)=i\hbar\frac{\partial}{\partial t}\Psi(x,t) \tag{14.1}$$

Here $\Psi(x,t)$ is called the wavefunction of the electron. The wavefunction Ψ has some similarities to the electric field in the scalar wave equation. For example, the probability of detecting photons is proportional to EE^* or $|E|^2$ (where $*$ indicates taking the complex conjugate) while the probability of detecting an electron is proportional to $\Psi\Psi^*$ or $|\Psi|^2$. As such $\Psi\Psi^*$ represents a probability density function. The operator between the square brackets is called the *Hamiltonian*, also written as H. Similar to the decomposition of vibrations into normal modes, the allowed electronic states can also be described in terms of 'normal modes' or Eigenfunctions of the Schrödinger equation. These eigenmodes satisfy the time independent Schrödinger equation:

$$\left[-\frac{\hbar^2}{2m}\frac{\partial^2}{\partial x^2}+V(x)\right]\Psi(x,t)=E\Psi(x,t) \tag{14.2}$$

where the time dependence of the eigenmodes is harmonic, as given by

$$i\hbar\frac{\partial}{\partial t}\Psi(x,t)=E\Psi(x,t) \tag{14.3}$$

The Schrödinger equation in free space (V(x)=constant) leads to plane wave solutions of the form. $\psi_k(x)=Ae^{j(k_e x-\omega t)}$. Here A is a normalization factor to ensure that the total probability adds up to 1, and $E=\hbar\omega$ (see Eq. 14.3). Note that the time dependence is only related to the *total* energy of the wavefunction (kinetic plus potential). Substituting the plane wave into the Schrödinger equation we find that the total energy of a free electron is given by

$$E=V+\frac{\hbar^2 k_e^2}{2m}, \tag{14.4}$$

where in free space V is some constant potential energy (which we can arbitrarily set to zero) and the other term constitutes the kinetic energy, with k_e being the electron wavevector and m the electron mass.

When an electron travels into a region with a lower potential energy (e.g. closer to a positively charged atom), the kinetic energy goes up, and the wavefunction acquires a shorter wavelength. In a sense, the behavior of electron waves entering a low potential region resembles that of light entering a high refractive index region. Just as for light, changes in wavelength give rise to reflections, in this case electron wave reflection. Inside a crystal, electrons experience a periodic potential due to the regularly spaced atomic cores in the crystal lattice, leading to multiple electron wave reflections, and electron wave interference. The multiple reflections result in eigenmodes that are affected by the exact shape of the periodic potential V(x). For an infinite crystal, the Eigenfunctions describe a state with a well-defined energy and a corresponding spatial distribution of the electron throughout the *entire* crystal. In a simple linear lattice with lattice spacing a, we have V(r) = V(r+a), as shown below.
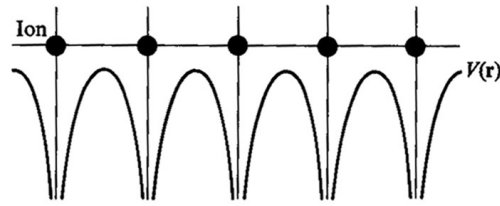
Fig. 5.3 The crystal potential seen by the electron.

Figure 14.2

Since the electrons are bound in a periodic potential, the Eigenfunctions will also have a periodic character. The periodicity of V(x) implies that a wavefunction which satisfies

$$\left[-\frac{\hbar^2}{2m}\frac{\partial^2}{\partial x^2}+V(x)\right]\Psi(x)=E\Psi(x) \tag{14.5}$$

should also satisfy

$$\left[-\frac{\hbar^2}{2m}\frac{\partial^2}{\partial x^2}+V(x)\right]\Psi(x+a)=E\Psi(x+a). \tag{14.6}$$

Wavefunctions that satisfy condition can be described by functions of the form[xxx] $\psi_k(x)=u_k(x)e^{ik_e x}$. Here $u_k(x)=u_k(x+a)$ is a periodic wavefunction called a *Bloch function*, which can be interpreted as (approximately) describing the electron distribution within a single unit cell. The phase term $e^{ik_e x}$ represents a phase difference of the wavefunction in adjacent unit cells.[xxxi] For core electrons (those tightly bound to the nucleus) $u_k(x)$ represents a strongly localized wavefunction similar to the electron orbitals around a hydrogen atom. The less strongly bound valence electrons are described by more extended wavefunctions that have significant amplitude in between neighboring atoms. Free electrons are described by wavefunctions with a high energy E, such that the wavevector remains real in between atoms (where V(x) is high).
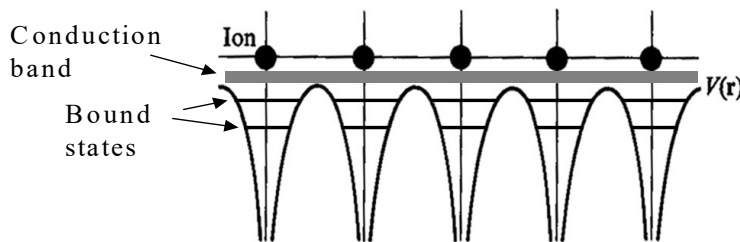
Figure 14.3

To understand the main features in the electronic band structure, it is instructive to start from an electron traveling in a periodic atom lattice with spacing *a* and zero binding

---

[xxx] See for example *Solid State Physics*, N.W. Ashcroft and N. D. Mermin, Chapter 8
[xxxi] Note that in this case the phase function is *continuous* in space, in contrast with the description of phonons, where the phase term represented the phase of a vibration at *discrete* points in space

potential. The dispersion relation will thus be exactly that of a free electron, as shown below.
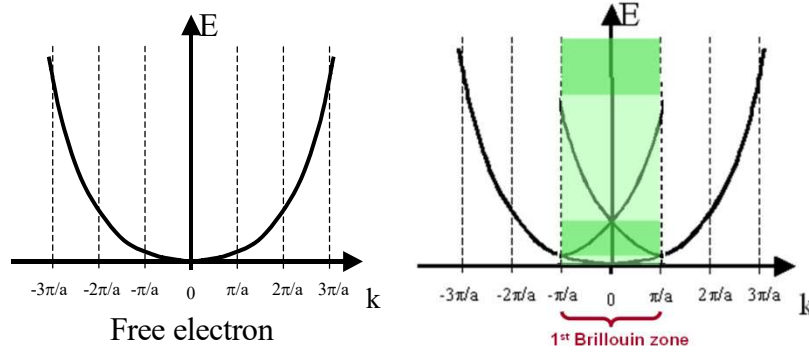
Figure 14.4

For fast electrons, we find that k will exceed π/a. Such rapidly varying wavefunctions can be split up into a part that describes the overall phase difference $\Delta\varphi$ between adjacent atoms $(-\pi<\Delta\varphi<\pi)$ and a part that describes the behavior of the wavefunction within a unit cell, for example

$$\psi_k(x) = e^{i\frac{1.5\pi}{a}x} = e^{i\frac{2\pi}{a}x}e^{i\frac{-0.5\pi}{a}x} = u_k(x)e^{-i\frac{0.5\pi}{a}x} \tag{14.7}$$

Where $u(x) = e^{i2\pi x/a}$ can be seen to satisfy $u(x)=u(x+a)$, and the phase difference between neighboring unit cells $|\Delta\varphi| = 0.5\pi$ is indeed between $-\pi$ and π. This illustrates how high-energy solutions can be described by an overall low k-vector and a Bloch function. This enables us to represent all electron states in this 1D lattice inside the first Brillouin zone, also shown below.

The use of only the first Brillouin zone for the display of the electron dispersion relation is called the 'reduced zone scheme':
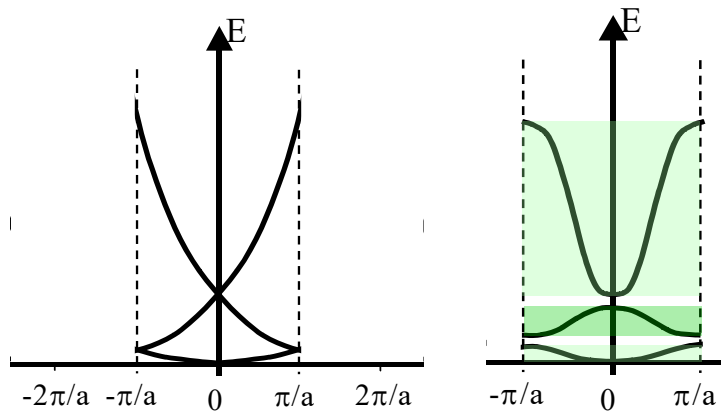
Figure 14.5 The dispersion relation for an electron in a periodic crystal represented in the reduced zone scheme for zero binding potential (left), and finite binding potential (right).

As in the case of phonon dispersion, the zone boundary represents a situation where there is neighboring unit cells are 180° out of phase. This again leads to a splitting of the energies

at the zone boundary. The splitting gives rise to characteristic energy bands that are separated by energy gaps in which no electron states exist, as illustrated in the right side of the figure.

Electrons are *Fermions*, meaning that no two electrons can occupy the same quantum state. Since there is only a finite number of electrons available in a crystal, the available low-energy states are occupied by electrons up to a certain maximum energy. An important feature of semiconductors and insulators is that the highest filled energy state lies just beneath an energy gap (called 'the band gap'), while the states just above the gap are unoccupied. The filled band below the band gap is the *valence band*, and the empty band above the band gap is the *conduction band*.

Charge carriers – free electrons and holes

The existence of a completely filled band has important consequences for the conductivity: an electrical current requires the existence of a net electron momentum, for example more electrons traveling to the right (positive k) than to the left (negative k). In insulators and in semiconductors (at zero Kelvin) all available positive and negative k vector states in the valence band are filled, resulting in zero conductivity. In semiconductors, the energy gap is sufficiently small that at room temperature some valence electrons are thermally excited into the conduction band ('broken free from an atom'), generating a *free electron* and leaving behind a positively charged atom. The resulting unoccupied electron state in the valence band is called a *hole*. Both these states are free to move through the crystal, giving rise to a finite conductivity at room temperature. Hence the term semiconductor. Free electrons and holes also affect the optical properties of semiconductors via free carrier absorption, as described later in this chapter.

Effective mass

In the description of the optical properties of semiconductors it is important to know the 'effective electron mass'. For free electrons the electron mass follows from the relation between E and k:

$$E = V + \frac{\hbar^2 k_e^2}{2m_e},$$ (14.8)

As is clear from the band structure shown above, the dispersion relation in a periodic lattice is no longer a simple parabola for all k vectors. However for energy levels close to a band gap (e.g. near the 'zone center'), the dependence of E vs. k is approximately parabolic. This allows us to ascribe an effective mass, *m**, that fits the band curvature according to

$$E(k) \approx E_g + \frac{\hbar^2 k^2}{2m*}.$$ (14.9)

The effective mass will be dependent on the exact band structure, and as a result will vary from semiconductor to semiconductor. For most semiconductors, m_e* lies in the range 0.1-1.0 m_e. The figure below shows a sketch of a band structure near the zone center, and around the band gap. Note that there are two valence bands that have the same energy at k=0, but that have a different effective mass. This is a situation that occurs in many semiconductors. As a result, holes can have different effective masses, respectively the heavy hole mass $m*_{HH}$ and the light hole mass $m*_{LH}$.

Direct-gap semiconductor:

CB

Energy

$E = E_{C0} + \dfrac{\hbar^2 k^2}{2m_e^*}$

FCA

Interband absorption

Excitons / Donor states

Midgap states

Acceptor states

k

HH

FHA

$E = -\dfrac{\hbar^2 k^2}{2m_{HH}^*}$

$E = -\dfrac{\hbar^2 k^2}{2m_{LH}^*}$

LH

SO
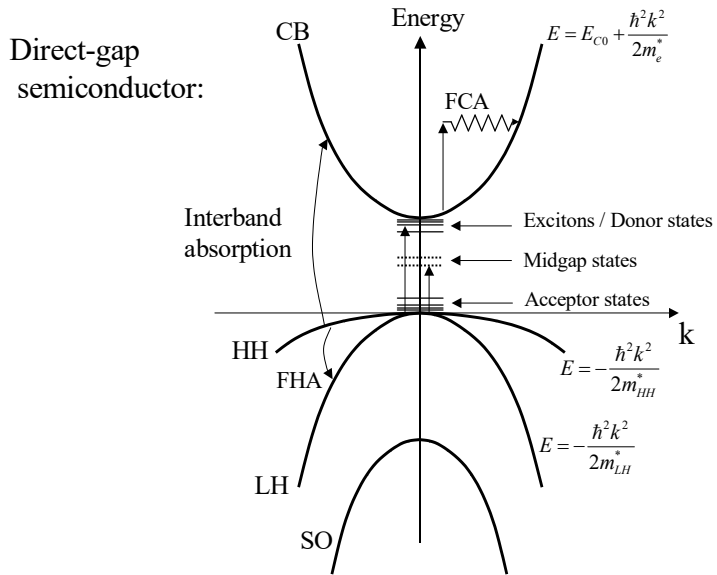
Figure 14.6 Fundamental Absorption Processes

Absorption processes in direct-gap and indirect-gap semiconductors

The figure above includes the main absorption processes that can occur in a *direct-gap* semiconductor. A direct bandgap semiconductor is a material in which the minimum of the conduction band (CB) occurs at the same k-value as the maximum energy in the valence band (VB). A *direct transition* is a transition that does not require a change in the wavevector. Common direct absorption processes are

- interband absorption (VB-CB or VB-VB)
- VB-to-exciton state absorption,
- VB to (unoccupied) donor, acceptor, or mid gap state absorption
- (occupied) donor, acceptor, or mid gap state to CB absorption

Free-carrier absorption is an *indirect* (phonon-assisted) process, which means that the initial and final states have different k-values. All these processes will be summarized below.

Some semiconductors have an *indirect gap*, which means that the longest wavelength (lowest energy) absorptions must occur with the assistance of a phonon, making the absorption edge less sharp than in direct-gap semiconductors.

Indirect-gap semiconductor:
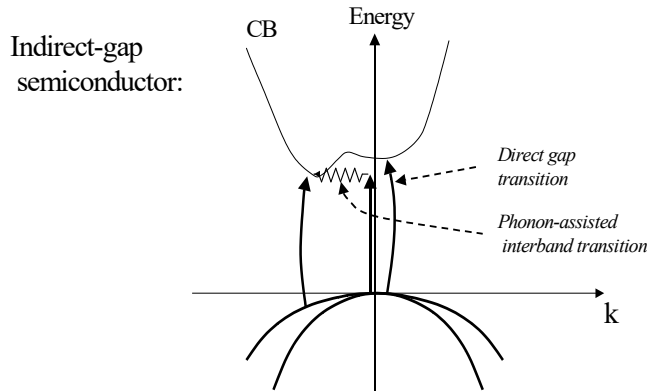
Figure 14.7

A sketch of a plot of absorption coefficient versus photon energy and wavelength for a "typical" semiconductor is shown below. The various absorption processes in each wavelength region are labeled on this graph.
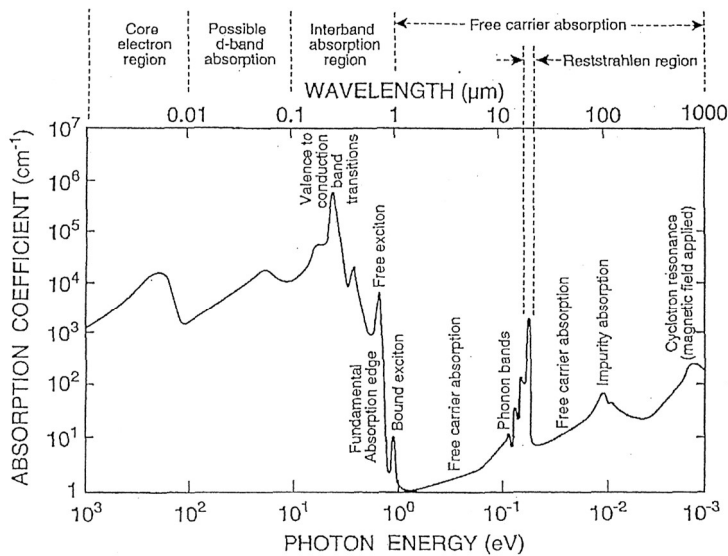
FIGURE 2 Absorption spectrum of a typical semiconductor showing a wide variety of optical processes.

Figure 14.8

In the following paragraphs, we describe these processes in some more detail.

Interband absorption

The dominant feature of the absorption spectrum of a semiconductor is the interband absorption. We will deal with direct-gap semiconductors here, and we will look briefly at indirect gap semiconductors at the end.

Density of States and Fermi Golden Rule

Optical absorption in semiconductors is due to light-induced transitions from occupied electron states to available unoccupied states. For that reason the number of available states is an important quantity. For continuous energy bands this is described in terms of the *Density of States*, g(E). For isolated atoms the density of states (DOS) corresponds to the number of available states per atom per unit energy. This means g(E)dE is the number of states (per atom) in the energy range (E, E+dE). This quantity is used in the quantum mechanical calculation of the transition rate W from initial state k to final state n of the atom upon illumination with photons of energy $\hbar\omega$:

$$W_{k\to n} = \frac{2\pi}{\hbar} E_0^2 |\mu_{kn}|^2 g(E_k + \hbar\omega) \tag{14.10}$$

This relation is called the *Fermi Golden Rule*. Here E_0 is the applied electric field strength, and μ_{kn} is the *transition matrix element* (units C·m in this form) for states k and n. This tells us how strong the transition is. For some states, μ_{kn}=0 (forbidden transition).

We can relate the transition rate for each atom $W_{k\to n}$ to the absorption coefficient, since the absorption rate W of photons with E=$\hbar\omega$ for N atoms per unit volume corresponds to an absorbed power per volume:

$$N\hbar\omega W_{k\to n} = \text{rate of energy absorbed per unit vol.}$$
$$(N = \text{atomic density})$$
$$= \frac{P_{abs}}{\text{unit volume}} = \frac{P_{abs}}{\text{unit area} \times \text{unit length}} \tag{14.11}$$
$$= \frac{I_{abs}}{\text{unit length}} = -\frac{dI}{dz}$$
$$\therefore \quad \frac{dI}{dz} = -N\hbar\omega W_{k\to n}$$

We can express W in terms of the irradiance *I*, since both *W* and *I* depend on E_0^2. We will assume that E_k=0 and we will write the photon energy as E=$\hbar\omega$ so that g(E_k+$\hbar\omega$)=g(E).

$$E_0^2 = \frac{2I}{nc\,\epsilon_0}$$
$$\therefore \quad \frac{dI}{dz} = -\frac{2\pi N}{\hbar} |\mu_{kn}|^2 \hbar\omega g(E) \cdot \frac{2}{nc\,\epsilon_0} I \tag{14.12}$$
$$\therefore \quad \alpha(\omega) = \frac{4\pi N}{nc\,\epsilon_0} |\mu_{kn}|^2 \omega g(E)$$

This shows that the absorption coefficient depends on the dipole transition matrix element, how many atoms are present per unit volume, and on the density of states g(E), given by the number of states per atom in the range (E, E+dE).

For a semiconductor, which has continuous energy bands that describe collective electronic states of the crystal, we need to find an analogous 'number of states per atom'. Instead of

'states per atom' we will use the function $\rho(E)dE$ to describe the number of states *per unit volume* in the range (E, E+dE), so that effectively $g(E)N \equiv \rho(E)$. ('states per atom times atoms per volume equals states per volume'). Therefore we expect to arrive at an expression that looks of the form

$$\alpha(\omega) = \frac{4\pi}{nc\in_0} |\mu_{nk}|^2 \omega\rho(E).$$ (14.13)

We will see in the following that in this expression the function ρ actually needs to be replaced by a quantity $\rho_J(E)$ known as the *joint* density of states.

To calculate the interband absorption, we need to calculate the density of states $\rho(E)$ based on our known E(k) as given by the effective electron mass m*. First, we need to look at how many k values are available in a given band. Since the allowed free electron states described Bloch waves, then

$$\psi_k \propto e^{i\vec{k}\cdot\vec{r}} = \exp\{i(k_x x + k_y y + k_z z)\}.$$ (14.14)

To calculate the number of allowed states per unit volume, we demand that a given volume contains only 'complete waves'. This is equivalent to applying periodic boundary conditions, i.e. demanding

$$\psi_k(x, y, z) = \psi_k(x+L_x, y, z) = \psi_k(x, y+L_y, z) = \psi_k(x, y, z+L_z)$$ (14.15)

where L_x, L_y and L_z are the dimensions of the volume of interest. This requires that $\exp[ik_x(x+L_x)] = \exp[ik_x x]$, and similarly for L_y and L_z, which leads to the following allowed values of k:

$$k_x = \frac{2\pi}{L_x}n_x; \quad k_y = \frac{2\pi}{L_y}n_y; \quad k_z = \frac{2\pi}{L_z}n_z, \quad \left(n_i = 0, \pm 1, \pm 2 ... \pm \frac{N_i - 1}{2}\right)$$ (14.16)

Where N_i is the number of unit cells along L_i, ensuring that the maximum k vector is π/a. The allowed k-values are thus evenly spaced in k-space (or *reciprocal space*). Each of these k-vectors represents an allowed electron state. Hence we can say there is one allowed state per unit volume of k-space, where the "unit volume" in k-space is:

$$\Delta k = \Delta k_x \cdot \Delta k_y \cdot \Delta k_z = \frac{2\pi}{L_x} \cdot \frac{2\pi}{L_y} \cdot \frac{2\pi}{L_z} = \frac{8\pi^3}{V},$$ (14.17)

with V the considered volume of the semiconductor crystal.

To calculate the density of states around some energy E_{max} above the bottom of the conduction band, we first calculate the number of allowed k-values that correspond to an energy E(k) below E_{max}, and then we take the derivative of this number with respect to E to find the number of states within an energy range dE. For a parabolic band, this implies

$$E(k) = \frac{\hbar^2 k^2}{2m*} < E_{max} \implies k_{max} = \sqrt{\frac{2m_e E_{max}}{\hbar^2}}$$ (14.18)

157

Now the number of k vectors that have satisfy $|k|<|k_{max}|$ is given by the volume of a sphere in reciprocal space with radius k_{max}, divided by the unit volume Δk:
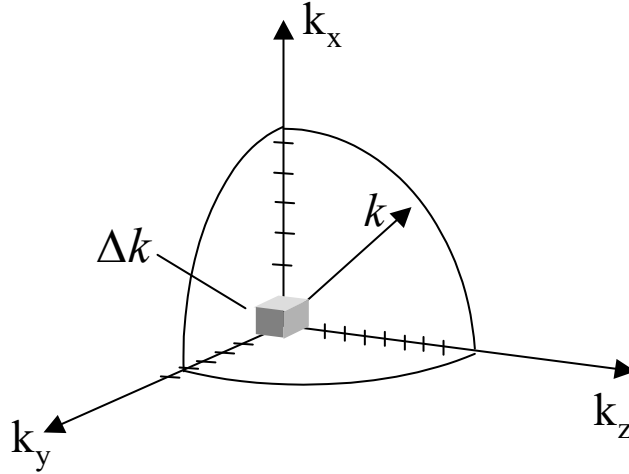
Figure 14.9

Hence the number of k-values/unit volume in (k, k+dk) = $\rho(k)dk$ is given by the surface area of the sphere * dk /V, divided by Δk, *i.e.*

$$\rho(k)dk = \frac{4\pi k^2 dk / V}{\Delta k} = \frac{4\pi k^2 dk / V}{8\pi^3 / V} = \frac{k^2 dk}{2\pi^2}$$

(14.19)

The number of electron states in that same interval is actually $2\rho(k)dk$ since each k-value can contain two electrons with opposite spin. If can now rewrite this density of states in into a quantity that represents the number of states in an *energy* interval dE, we will have found $\rho(E)$. This can be done by multiplying $2\rho(k)$ by the derivative of k to E:

$$2\rho(k)dk = \left[2\rho(k)\frac{dk}{dE}\right]dE = \rho(E)dE$$

(14.20)

Now, for a parabolic band,

$$E(k) = \frac{\hbar^2 k^2}{2m*},$$

(14.21)

so that

$$k = \sqrt{\frac{2m*E}{\hbar^2}},$$

(14.22)

giving

$$\rho(E) = 2\rho(k)\frac{dk}{dE} = 2 \cdot \frac{k^2}{2\pi^2}\frac{d}{dE}\left(\sqrt{\frac{2m^*E}{\hbar^2}}\right)$$

$$= 2 \cdot \frac{1}{2\pi^2}\frac{2m^*E}{\hbar^2}\sqrt{\frac{2m^*}{\hbar^2}}\frac{d}{dE}\left(E^{\frac{1}{2}}\right) \qquad . \tag{14.23}$$

$$\Rightarrow \rho(E) = \frac{1}{2\pi^2}\left(\frac{2m^*}{\hbar^2}\right)^{\frac{3}{2}}E^{\frac{1}{2}}$$

If we define the top of the valence band as E=0, then the lowest energy in the conduction band becomes $E=E_g$. The density of states for electrons in the conduction band then becomes

$$\rho_e(E) = \frac{1}{2\pi^2}\left(\frac{2m_e^*}{\hbar^2}\right)^{\frac{3}{2}}\left(E - E_g\right)^{\frac{1}{2}}. \tag{14.24}$$

The figure below shows a sketch of the resulting electron density of states function.
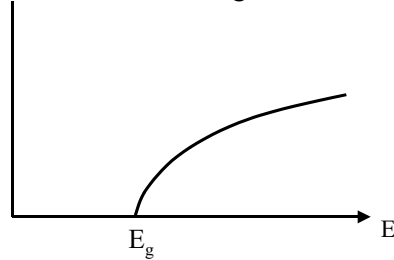
Figure 14.10

For the light and heavy holes, the densities of states defined at an energy E with respect to E=0 at the top of the valence band are

$$\rho_{LH}(E) = \frac{1}{2\pi^2}\left(\frac{2m_{LH}^*}{\hbar^2}\right)^{\frac{3}{2}}\left(-E\right)^{\frac{1}{2}}, \tag{14.25}$$

$$\rho_{HH}(E) = \frac{1}{2\pi^2}\left(\frac{2m_{HH}^*}{\hbar^2}\right)^{\frac{3}{2}}\left(-E\right)^{\frac{1}{2}} \tag{14.26}$$

Absorption due to interband transitions

For optical absorption to occur, we must have energy conservation: $E_f=E_i+\hbar\omega$ as well as momentum conservation: $\hbar k_f=\hbar k_i+\hbar k$, where k is the optical wave vector and k_i, k_f are the initial and final electron wavevectors. Since the photon momentum is very small, it is a very good approximation to demand that $\hbar k_f=\hbar k_i$, so that transitions are essentially "vertical" or "direct". For HH-CB transitions, the initial and final energies are

$$E_i = E_V = -\frac{\hbar^2k^2}{2m_{HH}}, \qquad E_f = E_c = \frac{\hbar^2k^2}{2m_e^*} + E_g. \tag{14.27}$$

159
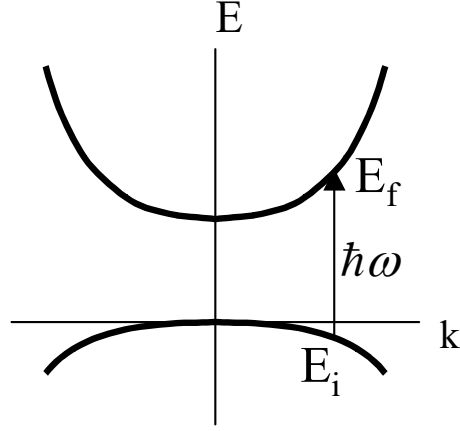
Figure 14.11

Hence the requirement for a direct transition with energy E_{direct} is

$$E_{direct} = E_C(k) - E_V(k) = \left(\frac{\hbar^2 k^2}{2m_e^*} + E_g \right) - \left(-\frac{\hbar^2 k^2}{2m_{HH}} \right) = E_g + \frac{\hbar^2 k^2}{2\mu_{HH}} , \qquad (14.28)$$

where we have introduced the heavy-hole reduced mass μ_{HH} as:

$$\frac{1}{\mu_{HH}} = \frac{1}{m_e^*} + \frac{1}{m_{HH}} \qquad (14.29)$$

For LH→CB transitions, we simply use the light-hole mass in place of the heavy-hole mass to find the appropriate reduced mass, μ_{LH}. Be careful not to confuse this effective mass with the transition matrix element μ_{kn}. The expression we found for the energy difference in a direct transition links the energy to the wavevector.

Optical absorption doesn't just require a high density of initial states; there also must be allowed final states at higher energy. If we are to count the number of states that can contribute to an absorption event with energy difference $\hbar\omega$, when need to count the number of allowed k values in the valence band that are separated from the conduction band by an energy $\hbar\omega$. Since we have an expression for $E_{direct}(k) = E_c(k)-E_v(k)$, we can find the joint density of states ρ_J using $E_{direct}(k)$ using the approach that we used previously for finding ρ_e based on $E_c(k)$. In other words, we can calculate the '*density of momentum conserving transitions per unit volume*', known as the *joint density of states*:

$$\rho_J(E) = 2\rho(k) \frac{dk}{dE_{direct}} \qquad (14.30)$$

Note that $\rho(k)$ is the same quantity as in the previous analysis: it still represents the number of states available in an interval dk. Hence, the joint density of states is

$$\rho_J(E) = \frac{1}{2\pi^2} \left(\frac{2\mu}{\hbar^2} \right)^{\frac{3}{2}} (E - E_g)^{\frac{1}{2}}. \qquad (14.31)$$

This result, which followed from the requirement of energy conservation, momentum conservation, and the conduction and valence band structure near the band edges (described by electron and hole effective masses), allows us to calculate the absorption coefficient according to the Fermi golden rule (Eq. (14.10)):

$$\alpha(\omega) = \frac{4\pi}{nc\epsilon_0}|\mu_{nk}|^2\omega\rho_J(E) = \frac{2\omega}{nc\epsilon_0}\frac{1}{\pi}|\mu_{nk}|^2\left(\frac{2\mu}{\hbar^2}\right)^{\frac{3}{2}}(\hbar\omega - E_g)^{\frac{1}{2}}. \tag{14.32}$$

This expression is only valid for $\hbar\omega \geq E_g$. The details of the transition matrix elements are tricky to calculate and as a result we cannot easily use the above formulation for a quantitative prediction of the absorption spectrum. However, sufficiently close to the band edge, ω and $|\mu_{nk}|^2$ can be considered approximately constant, and in practice the product $\omega|\mu_{nk}|^2$ remains approximately constant over a significant frequency range, so that we can write:

$$\alpha(\omega) \propto (\mu)^{\frac{3}{2}}(\hbar\omega - E_g)^{\frac{1}{2}}. \tag{14.33}$$

The graph below shows the example of interband absorption in InAs, where the above analysis works well (from "*Optical Properties of Solids*", M. Fox). Here, $\alpha^2(\omega) \propto (\hbar\omega - 0.35$ eV), as predicted above, where $E_g = 0.35$ eV. For comparison the effect of a fixed transition matrix element is plotted as a dashed line.
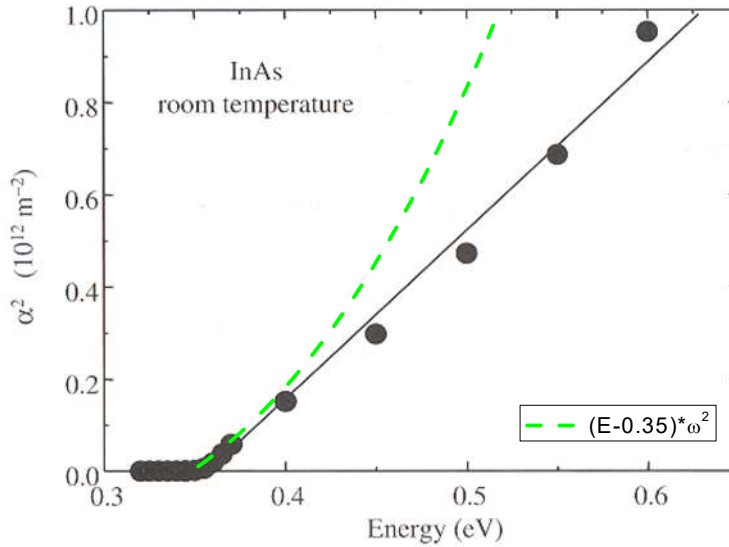
Figure 14.12

In most cases, the effect of excitons (a bound electron-hole state due to Coulomb interactions, see next section) causes the density of states to be enhanced for $\hbar\omega \approx E_g$, so that the absorption coefficient has a rather different shape than the $(\hbar\omega - E_g)^{1/2}$ dependence. (See e.g. the figure for GaAs in the next section.)

Exciton absorption

In a semiconductor, an *exciton* refers to a bound state of an electron (e) and a hole (h). The electron is excited out of the valence band, leaving behind a hole. The electron can become bound to the hole due to Coulomb interaction, resulting in hydrogen-like bound states (n=1, 2, …). The *e-h* pair is free to move about the material as a single, uncharged particle. In this bound state the electron still has characteristics similar to that of free electrons, but its energy is a little lower than that of conduction band electrons as a result of the Coulomb interaction, and similarly the bound hole state lies a little above the valence band. The exciton binding energy, E_b, is the energy required to separate the pair, producing a "free" electron in the conduction band and a free hole in the valence band. The existence of exciton states allows the absorption of light by valence electrons at energies slightly lower than the bandgap energy. In these VB→exciton absorption a bound e-h pair is created in any of its allowed states (n=1,2, …), giving rise to multiple absorption lines just below the band-to-band, or interband absorption energy.
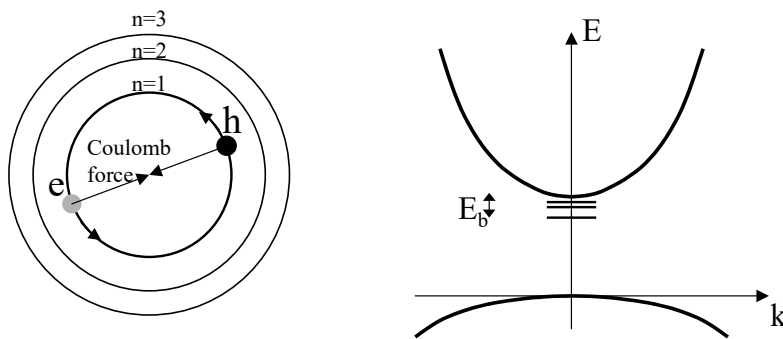
Figure 14.13 Schematic representation of an exciton in real space (left) and in k space (right). The sketch on the left assumes an equal electron and hole mass, while in general the hole has a larger mass.
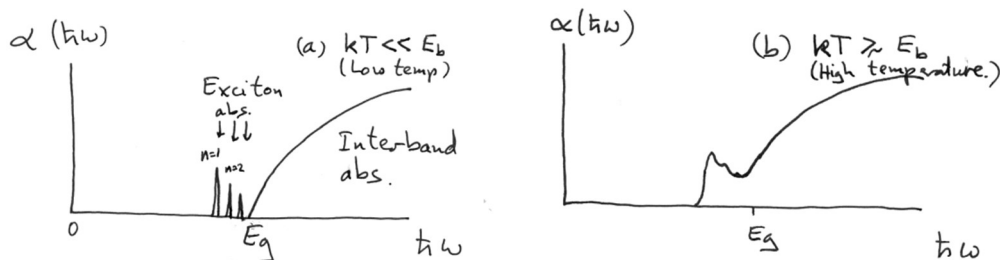
Figure 14.14 Sketch of VB→exciton absorption (left) at low temperature, resulting in absorption lines just below the interband absorption, and (right) at elevated temperatures, resulting in reduced exciton lifetime, and therefore an ill-defined exciton energy and broadened absorption lines

For most semiconductors E_b is 5-20 meV, which is on the order of kT at room temperature. As a result, that exciton lines are generally not sharp and not clearly separated from band-edge absorption unless the sample is cooled, as illustrated in the above sketch, and in the figure below for GaAs at 4 K and 300K.
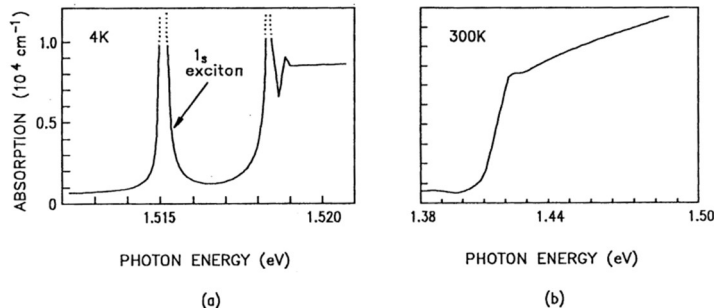
Figure 7.5. Absorption spectrum of GaAs at (a) low temperatures (after Ref. 7.4) and (b) room temperature (after Ref. 7.5).

Figure 14.15

Impurity absorption
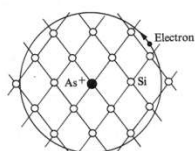
Fig. 6.8 Orbit of an electron around a donor. Fig. 6.9 The donor level in a semiconductor.
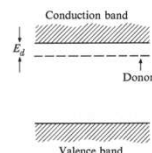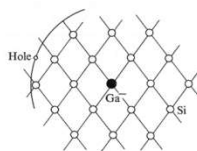
Fig. 6.10 A Ga impurity in a Si crystal. The extra hole migrates through the crystal. Fig. 6.11 The acceptor level in a semiconductor
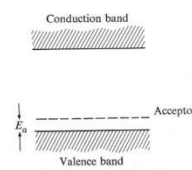
Figure 14.16

Impurities added to a semiconductor can usually be categorized as "donors" or "acceptors". *Donors* are atoms that have one extra valence electron compared to the atoms in the surrounding lattice. For example, in silicon or germanium, which are group IV elements, As or Sb atoms which are group V elements have an extra valence electron. The extra electron does not participate in bonding orbitals and hence is only weakly bound to the impurity by the Coulomb force. At low temperature, the electron orbits around the impurity in a way that can be modeled by the Bohr model of the atom. The binding energy, E_d, is typically of the order of kT at room temperature so at room temperature the electron is ionized into the conduction band and is free to move around as a conduction electron. *Acceptors* have one valence electron less than the host material, e.g. a group III element in Si or Ge. In this case, the acceptor provides an empty state or a "hole" where a valence electron could sit. If this hole moves away from the acceptor (i.e. if a neighboring valence electron occupies this available state), the acceptor becomes negatively charged and the

positive hole may end up being bound by Coulomb interactions, just like the donor electrons. Again, though, the binding energy is small and at room temperature, the holes may move freely around as positive charge-carriers. Because these are so weakly bound, the VB-acceptor and donor-CB transitions are not seen at room temperature. They can, however, be observed at low temperatures, such as the example of VB-to-acceptor absorption in Boron-doped Si at low temperature, shown below. These absorption resonances occur in the far infrared (here at least ~30 meV).
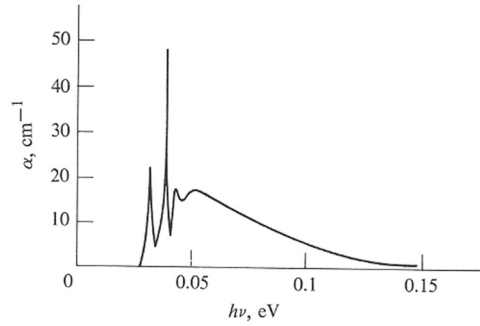
ig. **6.35** Absorption coefficient of a boron-doped Si sample versus photon energy *hv*. ifter Burstein, *et al., Proc. Photoconductivity Conference*, New York: Wiley, 1956]

Figure 14.17

All the various possible donor and acceptor related absorption processes at low temperature are shown below. However, at room temperature, the main optical consequence of donors or acceptors is free-carrier absorption.
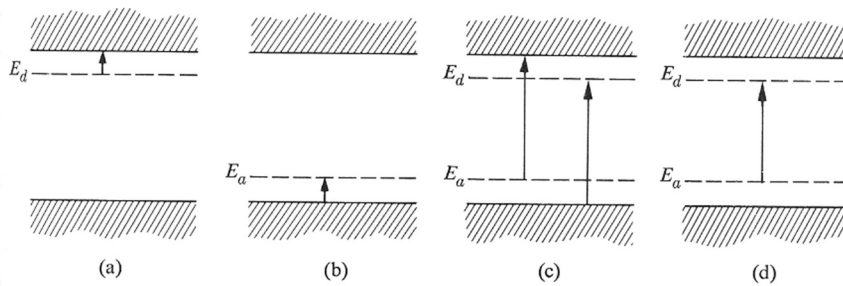
Fig. 6.34 Various absorption processes involving impurities (see text).

Figure 14.18

Free carrier absorption

Free carrier absorption results from the excitation of a free carrier into an available state higher in its respective band (e.g. electrons higher into the CB). As a result, free carrier absorption is quite different for electrons and for holes, mainly due to the presence of multiple valence bands. Free electrons located at k=0 in a single parabolic conduction band can reach higher energy states if their momentum is increased. This means that in n-type semiconductors, conduction band electrons may only be excited by the simultaneous absorption of a photon and absorption or emission of a phonon, in order to conserve momentum. By contrast, p-type semiconductors can have direct (i.e. no phonon needed)

164

transitions between the heavy and light hole bands (see the FHA process sketched earlier in this chapter). This causes the holes to produce much stronger free carrier absorption than conduction electrons. The conduction electron absorption process may be described by the Drude model. For semiconductors, the free electron density is often small ($\sim 10^{14}/cm^3$ or about 10^8 smaller than in a metal) so that the plasma frequency is small. (about 10^4 lower than a metal). Recall that, for frequencies well above the plasma frequency, the Drude model gives

$$\varepsilon_r{}'(\omega) \approx 1 - \frac{\omega_p^2}{\omega^2}, \qquad \varepsilon_r{}''(\omega) \approx \frac{\omega_p^2}{\omega^3 \tau} = \frac{\omega_p^2 \Gamma}{\omega^3}, \tag{14.34}$$

so that the absorption coefficient is hence given by,

$$\alpha(\omega) \cong \frac{\omega}{c} \varepsilon''(\omega) \cong \frac{\omega_p^2 \Gamma}{c\omega^2} = \frac{\Gamma}{c} \frac{\lambda^2}{\lambda_p^2}. \tag{14.35}$$

Hence we see a λ^{-2} dependence for free carrier absorption due to electrons. This can be seen in the broad-spectrum plot of absorption for a typical semiconductor shown earlier. Note that the formulas above do not take into account the susceptibility of the host material, which is not negligible. Assuming that the host semiconductor at frequencies well below the band gap has a dielectric constant ε_∞, the real part of the dielectric function of the doped semiconductor becomes (see "Weak absorption approximation" in Appendix H)

$$\varepsilon_r{}'(\omega) \approx \varepsilon_\infty - \frac{\omega_p^2}{\omega^2}, \tag{14.36}$$

while the imaginary part remains the same. This leads to a similar expression for α but scaled by the refractive index of the host $n_h = \sqrt{\varepsilon_\infty}$, giving

$$\alpha(\omega) \cong \frac{\omega}{n_h c} \varepsilon''(\omega) \cong \frac{\omega_p^2 \Gamma}{n_h c \omega^2} = \frac{\Gamma}{n_h c} \frac{\lambda^2}{\lambda_p^2}. \tag{14.37}$$

The form of the free-hole absorption in p-type semiconductors is less well defined, as it depends in the band structure as well as the hole density. In semiconductors with equal numbers of electrons and holes, the free hole absorption dominates.

Semiconductors of reduced dimension
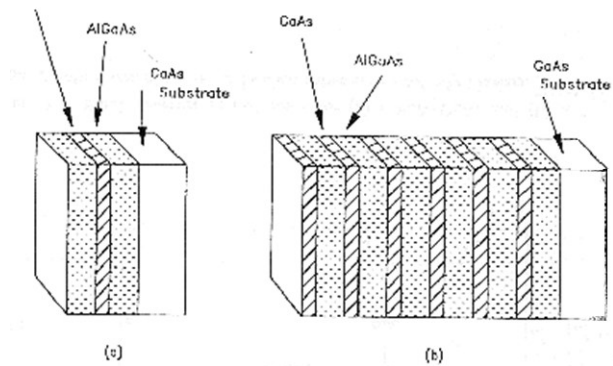
Figure 8.1. Schematics of (a) a single quantum well and (b) a multiple quantum well.

Figure 14.19

Semiconductors can now be artificially structured on nanometer scales. Quantum wells are layered semiconductor structures with alternate layers of materials with different energy gaps. The layers can be so thin as to confine the motion of the electrons perpendicular to the layers so that only certain quantized energy states are allowed. Motion in the other 2 dimensions is still like for a bulk semiconductor. However, the density of states is changed. It is left as an exercise to calculate this, but the result is that the density of states becomes step-like.
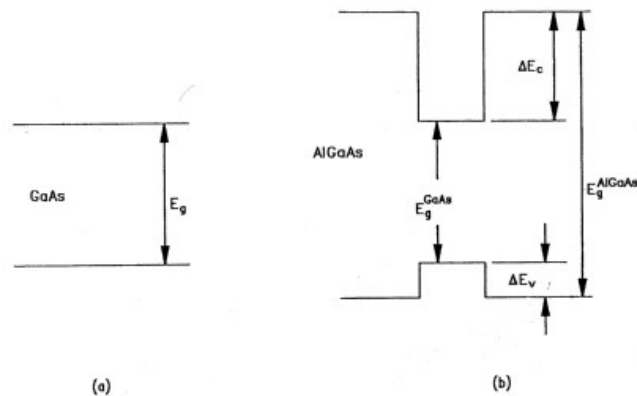
Figure 8.2. Band structure in real space for (a) a bulk GaAs and (b) a single quantum well of GaAs sandwiched between two AlGaAs barriers.

Figure 14.20

Because the energies associated with motion perpendicular to the wells are quantized, for each of these quantized energy states, there is a whole band of energies associated with motion in the other two dimensions. These are referred to as "sub-bands"
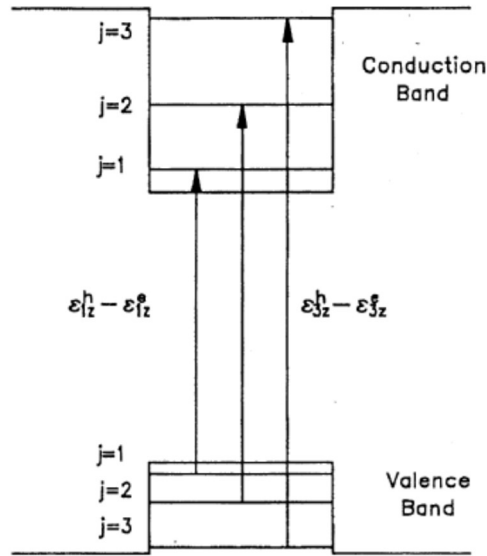
Figure 14.21

As a result, the density of states, and hence the absorption spectrum, takes on the shape of a staircase, with n steps of energy $\propto n^2$, as shown below.
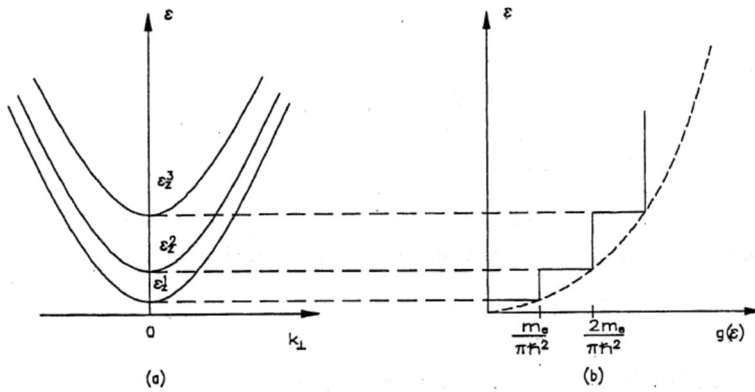
Figure 14.22

A density of states of this type gives very strong enhancement of the absorption and emission of light at the very lowest photon energies. This can lead to very low-threshold semiconductor laser operation. Reducing the dimensionality further can further enhance these effects. For example, "quantum wires", which allow only 1-D motion of electrons gives a density of states proportional to $E^{-1/2}$. Meanwhile, "quantum dots" confine motion in all dimensions, so that the semiconductor nanoparticles are rather like large atoms, with a density of states that looks like a series of narrow lines (i.e. Dirac delta functions).

Chapter 15 – From dipole radiation to refractive index

In several of the model descriptions of refractive index that were discussed in previous chapters, we treated matter as an array of atoms that are polarized by an EM wave. These induced dipoles in turn radiate a field that interferes with the incident field so as to produce refraction (phase shifting of the incident wave) and perhaps absorption (attenuation of the incident wave.) In Chapter 1 this was discussed qualitatively. In the present chapter we will examine the radiated field from an oscillating dipole in more detail, and look how the addition of dipole radiation from multiple dipoles gives rise to a macroscopic refractive index. A more extensive description of these arguments is given in Wooten, Chapter 2.

Mathematical description of dipole radiation

To analytically describe how a large collection of driven oscillating dipoles adds up to a refractive index, we first need to mathematically describe dipole radiation of an isolated oscillating dipole. We will describe our point dipole as an oscillating current localized at a point in space (i.e. a current density described by a delta function in space), and then apply Maxwell's equations to derive the magnetic and electric field components around the dipole. To facilitate our analysis, we will make use of the *vector potential*, A.

The vector potential

There is a general vector theorem that states for a vector field **V**, we always have $\nabla \cdot \left(\nabla \times \vec{V} \right) = 0$. From Maxwell's equations we know that $\nabla \cdot \vec{B} = 0$ which implies that if we construct a vector potential, **A**, such that

$$\vec{B} = \nabla \times \vec{A}, \tag{15.1}$$

then we automatically satisfy $\nabla \cdot \vec{B} = 0$. Since in this approach **B** is derived from the rotation of **A**, one can actually define **A** in different ways, as long as the rotation of **A** is not affected. We use the form of **A** known as the "Coulomb gauge" or "transverse gauge" where $\nabla \cdot \vec{A} = 0$. In the following we will derive a wave equation for **A** which will we expressed in terms of current density. From Maxwell's equations we have

$$\nabla \times \vec{E} = -\frac{\partial \vec{B}}{\partial t} \quad \Rightarrow \quad \nabla \times \vec{E} = -\frac{\partial \left(\nabla \times \vec{A} \right)}{\partial t} \tag{15.2}$$

Taking the time derivative on each side, we obtain an expression for d**E**/dt:

$$\nabla \times \frac{\partial \vec{E}}{\partial t} = \nabla \times -\frac{\partial^2 \vec{A}}{\partial t^2} \quad \Rightarrow \quad \frac{\partial \vec{E}}{\partial t} = -\frac{\partial^2 \vec{A}}{\partial t^2} \tag{15.3}$$

where we have used that **E** and **A** are divergence-free ('if the rotations are equal, the terms could still have different divergence, however $\nabla \cdot E = 0$ in the absence of free charge and $\nabla \cdot A = 0$ in the Lorentz Gauge'). Substituting the expression for d**E**/dt into

$$\nabla \times \vec{B} = \mu_0 \vec{J} + \mu_0 \varepsilon_0 \frac{\partial \vec{E}}{\partial t} \tag{15.4}$$

and applying

$$\nabla \times \vec{B} = \nabla \times \nabla \times \vec{A} = \nabla(\nabla \cdot \vec{A}) - \nabla^2 \vec{A} = -\nabla^2 \vec{A} \qquad (15.5)$$

we find the following wave equation for **A** in the Coulomb gauge is

$$\nabla^2 \vec{A} - \mu_0 \in \frac{\partial^2 \vec{A}}{\partial t^2} = -\mu_0 \vec{J}_\perp . \qquad (15.6)$$

Here we have assumed that we will be looking at transverse wave, implying that only the component of J normal to the direction of propagation ($\vec{J}_\perp$) is relevant. This equation has a general solution:

$$\vec{A}(\vec{r},t) = \frac{1}{4\pi \in_0 c^2} \int \frac{\vec{J}_\perp(\vec{r}',t - \frac{|\vec{r}-\vec{r}'|}{c}) d^3\vec{r}'}{|\vec{r} - \vec{r}'|}, \qquad (15.7)$$

showing that the appearance of a finite vector potential at point r is due to the current at a point r' at an earlier time, which satisfies causality. This expression can be used to find the dipole radiation field.

We assume a "point dipole", placed at the origin:
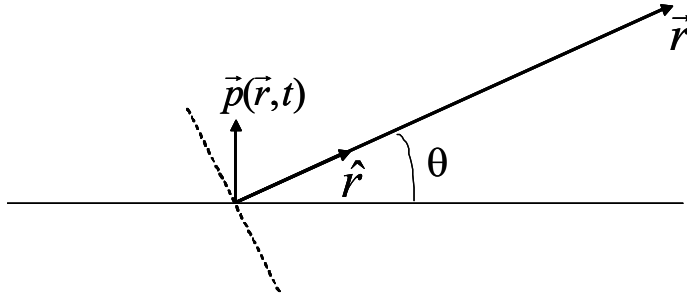
Figure 15.6

The time dependence is chosen to be harmonic, and since this is a "point dipole" placed at the origin, the description of the dipole includes a delta function around r=0:

$$\vec{p}(\vec{r},t) = p_0 \cos(\omega t)\delta(\vec{r})\hat{p}_0 \qquad (15.8)$$

Associated with this dipole is a current density at r=0:

$$\vec{J} = \frac{\partial \vec{P}}{\partial t} = -\omega p_0 \sin(\omega t)\delta(\vec{r})\hat{p}_{0\perp} \qquad (15.9)$$

The component of the current that generates transverse components of A is given by

$$\vec{J}_\perp = -\omega p_0 \sin(\omega t)\delta(\vec{r})\{\hat{p}_0\}_\perp \qquad (15.10)$$

Where $(\hat{p}_0)_\perp$ is the component of the unit vector that is perpendicular to r:
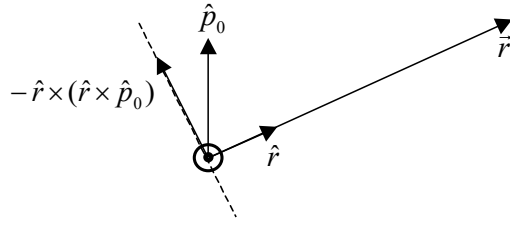
Figure 15.7

It follows that

$$\left(\hat{p}_0\right)_\perp = -\hat{r} \times \left(\hat{r} \times \hat{p}_0\right),$$

(15.11)

which has the magnitude of $\cos(\theta)$ (note: θ is defined relative to the horizontal in the sketch). A polar plot of this angular dependence of the magnitude of A is sketched below:
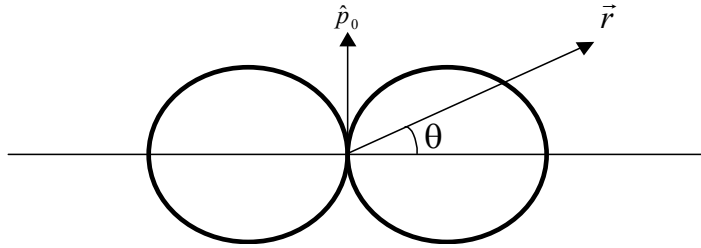
Figure 15.8

Now we can substitute for $\vec{J}_\perp$ in our solution for A to get

$$\vec{A}(\vec{r},t) = \frac{-\hat{r} \times \left(\hat{r} \times \hat{p}_0\right)}{4\pi \in_0 c^2} \omega \, p_0 \, \frac{\sin\left[\omega\left(t - \frac{|\vec{r}|}{c}\right)\right]}{|\vec{r}|}$$

(15.12)

Based on this solution we can now extract E according to

$$\nabla \times \vec{E} = -\frac{\partial\left(\nabla \times \vec{A}\right)}{\partial t} \quad \Rightarrow \quad \vec{E} = \frac{\partial \vec{A}}{\partial t}$$

(15.13)

where again we used the Lorentz Gauge. This results in the following description of the radiated electric field from the induced dipole:

$$\vec{E} = -\frac{\partial \vec{A}}{\partial t} = \frac{-\hat{r} \times \left(\hat{r} \times \hat{p}_0\right)}{4\pi \in_0 c^2} \omega^2 \, p_0 \, \frac{\cos\left[\omega\left(t - \frac{|\vec{r}|}{c}\right)\right]}{|\vec{r}|}$$

(15.14)

$$\therefore \quad \vec{E} = \frac{-k^2 p_0}{4\pi \in_0} \frac{\cos\left[\omega\left(t - \frac{r}{c}\right)\right]}{r} \left[\hat{r} \times \left(\hat{r} \times \hat{p}_0\right)\right]$$

$$\underbrace{\qquad\qquad}_{\text{Spherical wave}} \underbrace{\qquad\qquad}_{\text{Dipole pattern}}$$
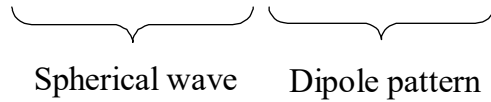
We will be calculating the radiated power, which means finding the Poynting vector, which in turn requires us to find the magnetic field. In isotropic media we have the following relation between $\nabla \times E$ and B:

$$\nabla \times \vec{E} = -\dot{\vec{B}} \quad \Rightarrow \quad i\vec{k} \times \vec{E} = i\omega\vec{B}$$

(15.15)

$$\Rightarrow \quad \vec{B} = \frac{\vec{k} \times \vec{E}}{\omega} = \frac{1}{c}\hat{r} \times \vec{E}$$

where in the last step we used the fact that $\hat{r} = \hat{k}$ for a point dipole placed at the origin. The direction of B is now related to the previously obtained direction of E according to

$$\hat{r} \times \left[-\hat{r} \times (\hat{r} \times \hat{p}_0)\right] = \hat{r} \times \hat{p}_0 .$$

(15.16)

This gives us the following description of the magnetic flux resulting from a harmonic point dipole placed at the origin:

$$\vec{B} = \frac{k^2 p_0}{4\pi \in_0 c} \frac{\cos\left[\omega\left(t - \frac{r}{c}\right)\right]}{r} (\hat{r} \times \hat{p}_0) .$$

(15.17)

The expressions for E and B now allow us to calculate the Poynting vector and the radiated power emitted by the dipole.

Effect of re-radiated field from induced dipoles

We are interested in the case where a plane wave is incident on a polarizable atom or molecule. This induces an oscillating dipole which radiates a field that interferes with the incident field, as shown below.

Figure 15.9
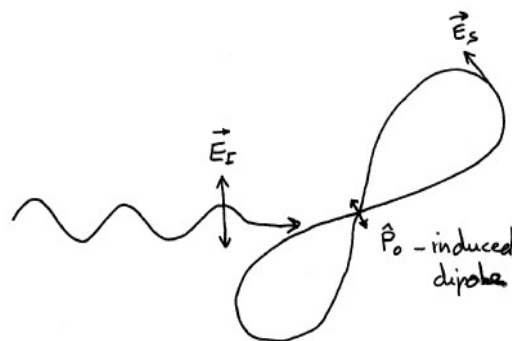
From the Lorentz model we have determined the magnitude of the induced dipole to be

172

$$\mu = p_0 = \frac{e^2}{m} \frac{\left(\hat{p}_0 \cdot \vec{E}_I\right)}{\omega_0^2 - \omega^2 - i\Gamma\omega} \tag{15.18}$$

Note that this description leaves open the possibility of an anisotropic polarizability, which is relevant in the description of molecules. The complete radiation pattern that develops due to the induced dipole is caused by the sum of the incident field, E_I, and the field re-radiated by the dipole (the *scattered* field), E_S. Hence the *total* Poynting vector is

$$\vec{S} = \left(\vec{E}_I + \vec{E}_S\right) \times \frac{1}{\mu_0} \left(\vec{B}_I + \vec{B}_S\right)$$

$$= \frac{1}{\mu_0} \left[\left(\vec{E}_I \times \vec{B}_I\right) + \left(\vec{E}_I \times \vec{B}_S + \vec{E}_S \times \vec{B}_I\right) + \left(\vec{E}_S \times \vec{B}_S\right)\right] \tag{15.19}$$

$$= \quad \vec{S}_{incident} \quad + \quad \vec{S}_{absorbed} \quad + \quad \vec{S}_{scattered}$$

The last step can be understood by requiring energy conservation. Energy conservation requires that the integral of the Poynting vector across a spherical surface around the dipole should produce a total emitted power of zero. The first term $E_I \times B_I$ clearly represents the power in the incident plane wave, which integrates to zero. The final term clearly represents the total power radiated by the dipole. For energy conservation to be satisfied, the cross terms must add up to a negative quantity if there is finite scattered power. This suggests that finite scattering is accompanied by a finite loss term representing absorption.

Scattered Power

$$\vec{S}_{scatt} = \frac{1}{\mu_0} \vec{E}_S \times \vec{B}_S, \text{ where,} \tag{15.20}$$

$$\vec{E}_S = -\frac{k^2}{4\pi \epsilon_0 r} \left\{\tfrac{1}{2} p_0 \exp[i(kr - \omega t)] + c.c.\right\} \left[\hat{r} \times \left(\hat{r} \times \hat{p}_0\right)\right] \tag{15.21}$$

and

$$\vec{B}_S = \frac{k^2 p_0}{4\pi \epsilon_0 cr} \left\{\tfrac{1}{2} p_0 \exp[i(kr - \omega t)] + c.c.\right\} \left(\hat{r} \times \hat{p}_0\right). \tag{15.22}$$

Since $\left[\hat{r} \times \left(\hat{r} \times \hat{p}_0\right)\right] \times \left(\hat{r} \times \hat{p}_0\right) = \hat{r} \cos^2 \theta$, then the time average of the Poynting vector for the scattered light is

$$\left\langle \vec{S}_{scatt} \right\rangle_t = \frac{k^4 c |p_0|^2}{2(4\pi)^2 \epsilon_0 r^2} \cos^2 \theta \, \hat{r}$$

$$= \frac{\omega^4}{2(4\pi)^2 c^3 \epsilon_0} \frac{|p_0|^2}{r^2} \cos^2 \theta \, \hat{r}. \tag{15.23}$$

The scattered time-averaged power is then given by integrating over all directions of propagation:

$$P_{scatt} = \int_0^{2\pi} d\phi \int_0^{\pi} r^2 \sin\theta d\theta \left[\hat{r} \cdot \left\langle \vec{S}_{scatt} \right\rangle_t\right]$$

$$= \frac{\omega^4}{12\pi \in_0 c^3} |p_0|^2 \tag{15.24}$$

and since,

$$|p_0|^2 = \frac{e^4}{m^2} \frac{\left(\hat{p}_0 \cdot \vec{E}_I\right)^2}{\left(\omega_0^2 - \omega^2\right)^2 + \Gamma^2\omega^2} \tag{15.25}$$

then,

$$P_{scatt} = \frac{\omega^4}{12\pi \in_0 c^3} \frac{e^4}{m^2} \frac{\left(\hat{p}_0 \cdot \vec{E}_I\right)^2}{\left(\omega_0^2 - \omega^2\right)^2 + \Gamma^2\omega^2} \tag{15.26}$$

Hence, in the limit of $\omega \ll \omega_0$, the scattered power is proportional to ω^4 or λ^{-4} – this is known as *Rayleigh scattering*.

We can also define a *molecular scattering cross section*, $\sigma_{scatt}(\omega)$:

$$P_{scatt} = \sigma_{scatt}(\omega)\langle S_I \rangle_t \tag{15.27}$$

and since $\left\langle S_I \right\rangle_t = \frac{1}{2}\varepsilon_0 c |E_I|^2$, then

$$\Rightarrow \quad \sigma_{scatt}(\omega) = \frac{\omega^4 e^4}{6\pi \in_0^2 c^4 m^2} \frac{\left(\hat{p}_0 \cdot \hat{E}_I\right)^2}{|D(\omega)|^2} \tag{15.28}$$

where $D(\omega) = \omega_0^2 - \omega^2 - i\Gamma\omega$. Here, we have not done an average over molecular orientations.

Absorbed Power

Since the scattered field is weak compared to the incident field, we can treat the scattered intensity as being negligible compared to the incident. Hence the transmitted irradiance is primarily affected by S_{abs}, which is the term that describes interference between the incident and scattered fields. We will not take the time to go through the math here, only look at the result, as sketched in the figure below. This shows that the time average of S_{abs}, i.e. $<S_{abs}>_t$, oscillates rapidly with angle θ around the dipole for most angles, but behind the dipole $<S_{abs}>_t$ varies slowly and is negative, as shown in the polar plot below. (From Hopf & Stegeman, chapter 4)
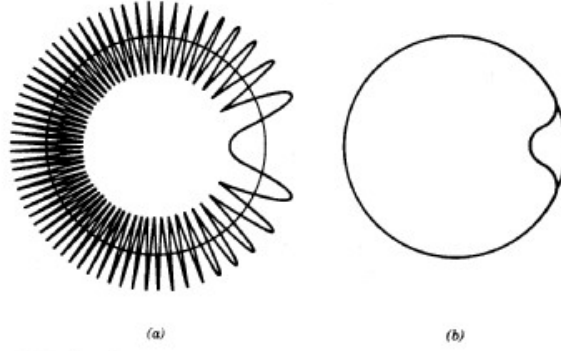
Figure 4.2. Interference pattern observed around a sphere surrounding the dipole. The circle intersects the graph of the flux at points where the flux is zero. Fluxes inside the circle are negative, outside the circle are positive. (a) Detailed structure of the interference. (b) Result of average over a small area.

Figure 15.10

Hence, the effect of the dipole is to impress a small "shadow" on the transmitted field behind it. If we integrate the outward-flowing component of $<S_{abs}>_t$ over all angles, the result is the total absorbed power, P_{abs}, i.e.

$$P_{abs} = -\int \left\langle \vec{S}_{abs} \cdot \hat{r} \right\rangle_t d\Omega, \tag{15.29}$$

where the integral is over all solid angle Ω. This yields,

$$P_{abs} = -\frac{\omega}{2} \left(\hat{p}_0 \cdot \hat{E}_I \right) \text{Im}\left\{ \mu^*(\omega) E_I \right\} \tag{15.30}$$

Where,

$$\mu(\omega) = \frac{e^2}{m} \frac{(\hat{p}_0 \cdot \hat{E}_I) E_I(\omega)}{\left(\omega_o^2 - \omega^2 - i\Gamma\omega \right)} = \frac{e^2}{m} \frac{(\hat{p}_0 \cdot \hat{E}_I) E_I(\omega)}{D(\omega)}. \tag{15.31}$$

Hence,

$$\begin{aligned} \text{Im}\left\{ \mu^*(\omega) E_I \right\} &= \frac{e^2 \left(\hat{p}_0 \cdot \hat{E} \right)}{m} \left| E_I \right|^2 \text{Im}\left\{ \frac{1}{D^*(\omega)} \right\} \\ &= \frac{e^2 \left(\hat{p}_0 \cdot \hat{E} \right)}{m} \left| E_I \right|^2 \frac{-\Gamma\omega}{\left| D(\omega) \right|^2} \end{aligned} \tag{15.32}$$

Now we may define a molecular *absorption cross-section* $\sigma_{abs}(\omega)$, that relates the absorbed power to the incident irradiance, by

$$P_{abs} = \sigma_{abs} \left\langle S_I \right\rangle_t. \tag{15.33}$$

Hence

$$\sigma_{abs} \left\langle S_I \right\rangle = -\frac{\omega}{2} \left(\hat{p}_0 \cdot \hat{E}_I \right) \text{Im}\left\{ \mu^*(\omega) E_I \right\}. \tag{15.34}$$

175

Since

$$S_I = \tfrac{1}{2} c \in_0 |E_I|^2 ,$$ (15.35)

we obtain

$$\sigma_{abs}(\omega) = \frac{\omega}{c} \left\langle \left(\hat{p}_0 \cdot \hat{E}_I\right)^2 \right\rangle_\theta \frac{e^2}{\in_0 m} \frac{\Gamma \omega}{|D(\omega)|^2}$$ (15.36)

where the averaging is now over all angles between the dipole coordinates and the applied field. For a medium containing randomly oriented molecules, (i.e. isotropic), we have already seen that $\left\langle \left(\hat{p}_0 \cdot \hat{E}_I\right)^2 \right\rangle_\theta = \frac{1}{3}$.

Since P_{abs} is an absorbed power per molecule, we can find the net absorbed power per unit volume as $N\,P_{abs} = N\sigma_{abs}S_I$. But the power absorbed per unit volume for a plane wave is just $-dS_I/dz$. Hence

$$\frac{dS_I}{dz} = -N\sigma_{abs}S_I = -\alpha S_I$$ (15.37)
$$\Rightarrow \quad S_I(z) = S_I(0)e^{-\alpha z} = S_I(0)e^{-\sigma N z}$$

Hence, the absorption coefficient is given by

$$\alpha(\omega) = \sigma_{abs}(\omega)N.$$ (15.38)

This result makes sense in terms of our result for $\sigma_{abs}(\omega)$ above, as in the weak susceptibility approximation, $\alpha(\omega)=(c/\omega)\chi''(\omega)$.

Complex refractive index for a sheet of induced dipoles

Unlike absorption, we cannot calculate the refractive index from the field of a single dipole. We must look at the field due to an ensemble of induced dipoles. To calculate the refractive index (real and imaginary), we look at the field produced by a sheet of dipoles all induced by the same incident plane wave.
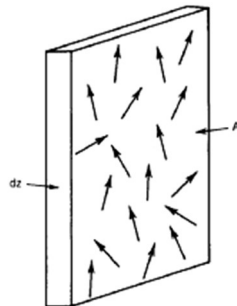
Figure 4.3. Illustration of sheet of dipoles of density N, thickness dz and area A, where we are ultimately interested in the limit A → ∞.

Figure 15.11

176

Summing over the N·A·dz dipoles in the sheet, we find (see *Hopf & Stegeman*) that the net radiated field is *also a plane wave*, described some distance behind the sheet by:

$$E_R(t) = \frac{-i\omega}{2\,\epsilon_0\,c} Ndz \cdot \tfrac{1}{2}\left\langle \hat{z} \times \left(\hat{z} \times \vec{p}_0\right)\right\rangle_\theta e^{i(\vec{k}\cdot\vec{r}-\omega t)} + c.c. \tag{15.39}$$

and since $\vec{B} = \tfrac{1}{c}\hat{z}\times\vec{E}$,

$$\vec{B}_R(t) = \frac{i\omega}{2\,\epsilon_0\,c^2} Ndz \cdot \tfrac{1}{2}\left\langle \hat{z} \times \vec{p}_0\right\rangle_\theta e^{i(\vec{k}\cdot\vec{r}-\omega t)} - c.c \tag{15.40}$$

where the averaging is over molecular orientations.

Note that the factor *i* in both field terms means that the radiated field, E_R is 90° out of phase with the oscillation phase of the dipole. This implies that for a real p_0 and a cosinusoidal incident field, the reradiated field is sinusoidal. Hence in the absence of loss, the reradiated field is 90° out of phase with the applied field. For a very weak reradiated field (always the case), this translates to a phase shift on the incident field, rather than an amplitude change.
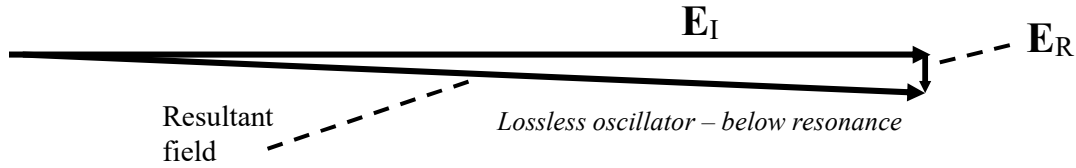
Figure 15.12

For the Lorentz oscillator model given above, we find

$$E_R = E_I \cdot i \cdot \frac{k}{2}\frac{Ne^2}{\epsilon_0\,m} dz \left\langle \frac{\left(\hat{p}_0 \cdot \hat{E}\right)^2}{D(\omega)}\right\rangle_\theta = E_I \cdot i \cdot \frac{k\omega_p^2}{2} dz \left\langle \frac{\left(\hat{p}_0 \cdot \hat{E}\right)^2}{D(\omega)}\right\rangle, \tag{15.41}$$

where the averaging is over the molecular orientations.
Now the total *change ΔE in field amplitude* E(z) after a propagation distance of Δz is,

$$\Delta E = E(\Delta z) - E(0) = E_I(\Delta z) + E_R(\Delta z) - E_I(0)$$

$$= E_I e^{ik_0\Delta z} + E_I i \frac{k_0\omega_p^2}{2}\left\langle \frac{\left(\hat{p}_0 \cdot \vec{E}_I\right)^2}{D(\omega)}\right\rangle_\theta \Delta z - E_I$$

$$\approx E_I\left((1 + ik_0\Delta z) + i\frac{k_0\omega_p^2}{2}\left\langle \frac{\left(\hat{p}_0 \cdot \vec{E}_I\right)^2}{D(\omega)}\right\rangle_\theta \Delta z - 1\right) \tag{15.42}$$

$$\Rightarrow \quad \frac{dE}{dz} = ik_0\left(1 + \frac{\omega_p^2}{2}\left\langle \frac{\left(\hat{p}_0 \cdot \vec{E}_I\right)^2}{D(\omega)}\right\rangle_\theta\right)\vec{E}_I$$

The second step makes use of exp(x) ≈1+x for small real x.

We also know

$$\Rightarrow \quad \frac{dE_I}{dz} = ik\,\eta E_I.$$
(15.43)

Comparing this with equation 15.42 gives the following expression for refractive index:

$$\eta = (n + i\kappa) = 1 + \frac{1}{2}\omega_p^2 \left\langle \frac{(\hat{p}_0 \cdot \hat{E})^2}{D(\omega)} \right\rangle_\theta.$$
(15.44)

And therefore

$$\in_r = \eta^2 \cong 1 + \omega_p^2 \left\langle \frac{(\hat{p}_0 \cdot \hat{E})^2}{D(\omega)} \right\rangle_\theta,$$
(15.45)

which is the Lorentz oscillator model result, including orientational averaging.

Clearly, then, the phase of the induced dipoles, and hence the phase of the re-radiated field, dictates the optical properties of the material. On resonance, the oscillators are $\pi/2$ out of phase with the driving field. The re-radiated field is shifted by yet another $\pi/2$ upon propagation, so that E_R is π out of phase with E_I.

E_I

Resultant field

E_R

Lossy oscillator – at resonance
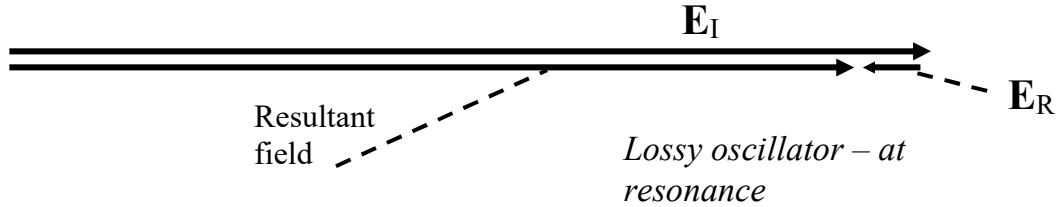
Figure 15.13

Clearly, we may extend these arguments to gain. If the phase of the oscillator is $-\pi/2$, then the radiated field will *add* to E_I.

Appendix A – Vector relations and theorems

Unit vectors (Cartesian)

$$\hat{x} = (1,0,0), \qquad \hat{y} = (0,1,0), \qquad \hat{z} = (0,0,1)$$

Vector

$$\vec{F} = \left(F_x, F_y, F_z\right) = F_x\hat{x} + F_y\hat{y} + F_z\hat{z}$$

Vector field: if a field E has a direction at every point in space, is called a vector field, which is written as $\vec{E}(x,y,z)$ or $\vec{E}(\vec{r})$ where $\vec{r} = (x,y,z)$. A time depent vector field is written as $\vec{E}(\vec{r},t)$.

Dot product

$$\vec{A} \cdot \vec{B} = A_x B_x + A_y B_y + A_z B_z$$

Cross product

$$\vec{A} \times \vec{B} = \left(A_y B_z - A_z B_y, A_z B_x - A_x B_z, A_x B_y - A_y B_x\right) = \begin{vmatrix} \hat{x} & \hat{y} & \hat{z} \\ A_x & A_y & A_z \\ B_x & B_y & B_z \end{vmatrix}$$

'Del' operator

$$\vec{\nabla} = \left(\frac{\partial}{\partial x}, \frac{\partial}{\partial y}, \frac{\partial}{\partial z}\right)$$

Divergence

$$\vec{\nabla} \cdot \vec{F} = \frac{\partial}{\partial x}F_x + \frac{\partial}{\partial y}F_y + \frac{\partial}{\partial z}F_z = \lim_{\Delta V \to 0} \frac{1}{\Delta V} \oint \vec{F} \cdot d\vec{S}$$

Curl

$$\vec{\nabla} \times \vec{F} = \begin{vmatrix} \hat{x} & \hat{y} & \hat{z} \\ \frac{\partial}{\partial x} & \frac{\partial}{\partial y} & \frac{\partial}{\partial z} \\ F_x & F_y & F_z \end{vmatrix} = \hat{n} \lim_{\Delta S \to o} \frac{1}{\Delta s} \oint \vec{F} \cdot d\vec{\ell}$$

with $\hat{n}$ the unit vector normal to surface S

For a scalar field V(x,y,z), the *gradient* is a vector field defined as

$$\vec{\nabla}V = \left(\frac{\partial V}{\partial x}, \frac{\partial V}{\partial y}, \frac{\partial V}{\partial z}\right)$$

The operator 'del squared' is called the *Laplacian*. When acting on a scalar field V(x,y,z) the result is given by

$$\bar{\nabla}^2 V = \bar{\nabla} \cdot (\bar{\nabla} V) = \frac{\partial^2 V}{\partial x^2} + \frac{\partial^2 V}{\partial y^2} + \frac{\partial^2 V}{\partial z^2}$$

When operating on a vector field $\bar{E}(x,y,z)$, del squared is called the *vector Laplacian*, given by

$$\bar{\nabla}^2 \vec{E} = \left(\frac{\partial^2 E_x}{\partial x^2}, \frac{\partial^2 E_y}{\partial y^2}, \frac{\partial^2 E_z}{\partial z^2} \right)$$

For any vector field $\bar{E}(x,y,z)$:

$$\bar{\nabla} \times \left(\bar{\nabla} \times \bar{E} \right) = -\nabla^2 \bar{E} + \bar{\nabla} \left(\bar{\nabla} \cdot \bar{E} \right)$$

$$\bar{\nabla} \cdot \left(\bar{\nabla} \times \bar{E} \right) = 0$$

For conservative fields only:

$$\int \bar{\nabla} \cdot \bar{F} dv = \oint \bar{F} \cdot d\bar{s} \quad \text{(Divergence Theorem or Gauss' theorem)}$$

$$\int \bar{\nabla} \times \bar{F} \cdot d\bar{S} = \oint \bar{F} \cdot d\bar{l} \quad \text{(Stokes' Theorem)}$$

Vector fields

The electric field E has a direction at every point in space. This is written as $\vec{E}(x,y,z)$ or $\vec{E}(\vec{r})$ where $\vec{r} = (x,y,z)$.

Divergence

The divergence of a vector field $\vec{F}(x,y,z)$ is given by the following relation:

$$\vec{\nabla} \cdot \vec{F} = \frac{\partial F_x}{dx} + \frac{\partial F_y}{\partial y} + \frac{\partial F_z}{\partial z} = \lim_{\Delta V \to 0} \frac{1}{\Delta V} \oiint \vec{F} \cdot d\vec{S} \qquad (2.32)$$

where the double integral represents an integration across a closed surface, with enclosed volume ΔV. The term $d\vec{S}$ represents an infinitesimally small vector locally normal to the surface with a magnitude corresponding to a differential area (infinitesimally small area) on the surface. We have also used the 'differential vector' *nabla* $\vec{\nabla} = \left(\frac{\partial}{dx}, \frac{\partial}{\partial y}, \frac{\partial}{\partial z} \right)$.
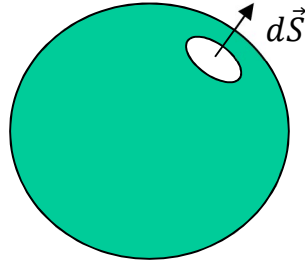
Figure 2.1. Schematic of a spherical volume with surface S and a differential surface element vector $d\vec{S}$ locally normal to the surface.

As you can see the divergence of a vector field is a *number* (i.e. a *scalar*) that represents the degree to which there is a net change in the vector length as we move along its direction. In a way it describes the '*outwardness*' of the vector field.

Gauss' Theorem (or Divergence Theorem)

Electric fields and magnetic fields inside homogenous media represent a special class of vector fields known as conservative fields.[xxxii] Broadly speaking this means that electric fields cannot suddenly appear out of nowhere or discontinuously change direction inside a continuous medium. For such fields, any net divergence within a volume V must result in fields pointing out of the surface. This is captured by Gauss' theorem:

$$\oiiint \vec{\nabla} \cdot \vec{F} \, dV = \oiint \vec{F} \cdot d\vec{S} \tag{2.33}$$

where dV represents an infinitesimal volume dV=dx×dy×dz.

Curl

$$\vec{\nabla} \times \vec{F} = \hat{n} \lim_{\Delta S \to o} \frac{1}{\Delta s} \oint \vec{F} \cdot d\vec{\ell} \tag{2.34}$$

$\hat{n}$ unit normal to surface

Stoke's Theorem

$$\int \vec{\nabla} \times \vec{F} \cdot d\vec{S} = \oint \vec{F} \cdot d\vec{l} \tag{2.35}$$

These and other vector relations are summarized in appendix C.

[xxxii] see e.g. http://mathworld.wolfram.com/ConservativeField.html
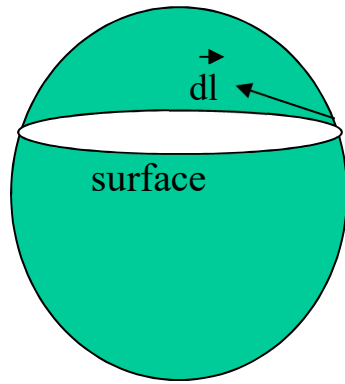
Figure 2.2

Appendix B – Maxwell's Equations

James Clerk Maxwell deduced a set of equations that describe the relation between charges, electric fields, and magnetic fields. Charge is described as smoothly distributed with charge density ρ (C/m^3), which can contain contributions from free charge and polarization charge.

The complete Maxwell Equations are as follows:

$$\nabla \cdot \vec{E} = \frac{\rho}{\epsilon_0}$$

$$\nabla \cdot \vec{B} = 0$$

$$\nabla \times \vec{E} = -\frac{\partial \vec{B}}{\partial t}$$

$$\nabla \times \vec{B} = \epsilon_0 \mu_0 \frac{\partial \vec{E}}{\partial t} + \mu_0 \left[J_f + \nabla \times \vec{M} + \frac{\partial \vec{P}}{\partial t} \right]$$

The latter two relations are often expressed in terms of magnetic field intensity H and displacement D, taking into account magnetization M, using the following relations.

$$\vec{D} = \epsilon_0 \vec{E} + \vec{P}$$

$$\vec{B} = \mu_0 (\vec{H} + \vec{M})$$

Gauss' law for B

No magnetic monopoles: following Gauss' Law

$$\vec{\nabla} \cdot \vec{B} = 0 \tag{2.36}$$

i.e.

$$\oint_s \vec{B}(\vec{r}) \cdot d\vec{s} = \frac{\text{magnetic charge}}{\mu_0} = 0 = \int_v \vec{\nabla} \cdot \vec{B} dv \tag{2.37}$$

Ampere's Law

For magnetic fields, the flux density, B, is related to the magnetic field intensity, H and the induced magnetization, M, by

$$\vec{B} = \mu_0 (\vec{H} + \vec{M}) \tag{2.38}$$

$$\vec{\nabla} \times \vec{H} = \vec{J}_{free} + \frac{\partial D}{dt} \tag{2.39}$$

4 Maxwell equations $+$
$$\vec{D} = \varepsilon_0 \vec{E} + \vec{P}$$
$$\vec{B} = \mu_0 \left(\vec{H} + \vec{M} \right)$$

(Henceforth we will use J in place of J_{free}.)

Current Sources

$$\vec{\nabla} \times \vec{H} = \vec{J} + \frac{\partial \vec{D}}{dt} \qquad\qquad (2.40)$$

$$\nabla \times \left\{ \frac{\vec{B}}{\mu_0} - \vec{M} \right\} = \vec{J} + \frac{\partial}{dt} \left(\varepsilon_0 \vec{E} + \vec{P} \right) \qquad\qquad (2.41)$$

$$\vec{\nabla} \times \vec{B} = \mu_0 \vec{J} + \mu_0 \vec{\nabla} \times \vec{M} + \varepsilon_0 \mu_0 \frac{\partial \vec{E}}{dt} + \mu_0 \frac{\partial \vec{P}}{dt}$$

free charge   magnetism   bound or polarization
current density   current density   current density

vacuum displacement
current density

$$= \mu_0 \vec{J}_{tot} + \mu_0 \varepsilon_0 \frac{\partial \vec{E}}{dt} \qquad\qquad (2.42)$$

or

$$\vec{\nabla} \times \vec{B} = \mu_0 J_{tot} + \frac{1}{c^2} \frac{\partial \vec{E}}{dt} \qquad\qquad (2.43)$$

where

$$\vec{J}_{tot} = \vec{J} + \vec{\nabla} \times \vec{M} + \frac{\partial \vec{P}}{dt} \qquad\qquad (2.44)$$

184

Appendix C – Empirical descriptions of refractive index

Sellmeier equations

Sellmeier equations are essentially empirical fits to the actual refractive index of a material, using the result for χ' for Lorentz oscillators as basic functions. Hence, Sellmeier equations are of the form

$$n^2(\omega) = 1 + \sum_j \frac{\omega_{pj}^2}{\omega_{0j}^2 - \omega^2}$$

These equations are very useful ways of providing data on the refractive index of materials vs. wavelength, without the need for extensive tables. They are usually valid only in high transparency spectral regions, far from resonances, where χ is real. Often, but not always, Sellmeier equation for a material may contain a pole (i.e. a resonance) at low frequency ($\omega_0 \ll \omega$) and one at very high frequency ($\omega_0 \gg \omega$). Hence one could write

$$n^2(\omega) = 1 + \frac{\omega_{p\infty}^2}{\omega_{0\infty}^2} + \sum_j \frac{\omega_{pj}^2}{\omega_{0j}^2 - \omega^2} - \frac{\omega_{p0}^2}{\omega^2},$$

where, $1 + \omega_{p\infty}^2 / \omega_{0\infty}^2$ is more commonly written as ε_∞.

In practice, these equations are usually expressed in terms of wavelength:

$$n^2(\omega) = 1 + A + \sum_j \frac{\lambda_{pj}^{-2}}{\lambda_{0j}^{-2} - \lambda^{-2}} - d\lambda^2 = a + \sum_j \frac{b_j \lambda^2}{\lambda^2 - c_j} - d\lambda^2,$$

so that coefficients a, b_j, c_j, and d may completely describe the refractive index vs. wavelength for a material. There are usually only one or two values of j (i.e. only one or two resonances) in the Sellmeier equation for a given material. This may depend on the material and on the level of accuracy required. To get an idea of the wide variety of Sellmeier equations, some Sellmeier equations are given in the following table from the OSA handbook of Optics:

Material	Dispersion formula (wavelength, λ, in μm)	Range (μm)	Ref.
Ag_3AsS_3	$n_o^2 = 7.483 + \dfrac{0.474}{\lambda^2 - 0.09} - 0.0019\lambda^2$	0.63–4.6(o) 0.59–4.6(e)	168
	$n_e^2 = 6.346 + \dfrac{0.342}{\lambda^2 - 0.09} - 0.0011\lambda^2$		
AgBr	$\dfrac{n^2 - 1}{n^2 + 2} = 0.452505 + \dfrac{0.09939\lambda^2}{\lambda^2 - 0.070537} - 0.00150\lambda^2$	0.49–0.67	169
AgCl	$n^2 - 1 = \dfrac{2.062508\lambda^2}{\lambda^2 - (0.1039054)^2} + \dfrac{0.9461465\lambda^2}{\lambda^2 - (0.2438691)^2} + \dfrac{4.300785\lambda^2}{\lambda^2 - (70.85723)^2}$	0.54–21.0	110
$AgGaS_2$	$n_o^2 = 3.6280 + \dfrac{2.1686\lambda^2}{\lambda^2 - 0.1003} + \dfrac{2.1753\lambda^2}{\lambda^2 - 950}$	0.49–12	170
	$n_e^2 = 4.0172 + \dfrac{1.5274\lambda^2}{\lambda^2 - 0.1310} + \dfrac{2.1699\lambda^2}{\lambda^2 - 950}$		
$AgGaSe_2$	$n_o^2 = 4.6453 + \dfrac{2.2057\lambda^2}{\lambda^2 - 0.1879} + \dfrac{1.8377\lambda^2}{\lambda^2 - 1600}$	0.73–13.5	170
	$n_e^2 = 5.2912 + \dfrac{1.3970\lambda^2}{\lambda^2 - 0.2845} + \dfrac{1.9282\lambda^2}{\lambda^2 - 1600}$		
β-AgI	$n_o = 2.184; \quad n_e = 2.200@0.659\ \mu m$	—	171
	$n_o = 2.104; \quad n_e = 2.115@1.318\ \mu m$		
AlAs	$n^2 = 2.0792 + \dfrac{6.0840\lambda^2}{\lambda^2 - (0.2822)^2} + \dfrac{1.900\lambda^2}{\lambda^2 - (27.62)^2}$	0.56–2.2	172
AlN	$n_o^2 = 3.1399 + \dfrac{1.3786\lambda^2}{\lambda^2 - (0.1715)^2} + \dfrac{3.861\lambda^2}{\lambda^2 - (15.03)^2}$	0.22–5.0	173
	$n^2 = 3.0729 + \dfrac{1.6173\lambda^2}{} + \dfrac{4.139\lambda^2}{}$		
Al_2O_3	$n_o^2 - 1 = \dfrac{1.4313493\lambda^2}{\lambda^2 - (0.0726631)^2} + \dfrac{0.65054713\lambda^2}{\lambda^2 - (0.1193242)^2} + \dfrac{5.3414021\lambda^2}{\lambda^2 - (18.028251)^2}$	0.2–5.5	174
	$n_e^2 - 1 = \dfrac{1.5039759\lambda^2}{\lambda^2 - (0.0740288)^2} + \dfrac{0.55069141\lambda^2}{\lambda^2 - (0.1216529)^2} + \dfrac{6.5927379\lambda^2}{\lambda^2 - (20.072248)^2}$		
ALON	$n^2 - 1 = \dfrac{2.1375\lambda^2}{\lambda^2 - 0.10256^2} + \dfrac{4.582\lambda^2}{\lambda^2 - 18.868^2}$	0.4–2.3	175
BBO	$n_o^2 = 2.7405 + \dfrac{0.0184}{\lambda^2 - 0.0179} - 0.0155\lambda^2$	0.22–1.06	104
	$n_e^2 = 2.3730 + \dfrac{0.0128}{\lambda^2 - 0.0156} - 0.0044\lambda^2$		
BaF_2	$n^2 - 1 = \dfrac{0.643356\lambda^2}{\lambda^2 - (0.057789)^2} + \dfrac{0.506762\lambda^2}{\lambda^2 - (0.10968)^2} + \dfrac{3.8261\lambda^2}{\lambda^2 - (46.3864)^2}$	0.27–10.3	176
$BaTiO_3$	$n_o^2 - 1 = \dfrac{4.187\lambda^2}{\lambda^2 - (0.223)^2}$	0.4–0.7	177
	$n_e^2 - 1 = \dfrac{4.064\lambda^2}{\lambda^2 - (0.211)^2}$		
BeO	$n_o^2 - 1 = \dfrac{1.92274\lambda^2}{\lambda^2 - (0.07908)^2} + \dfrac{1.24209\lambda^2}{\lambda^2 - (9.7131)^2}$	0.44–7.0	178
	$n_e^2 - 1 = \dfrac{1.96939\lambda^2}{\lambda^2 - (0.08590)^2} + \dfrac{1.67389\lambda^2}{\lambda^2 - (10.4797)^2}$		

For fused silica, a good fit can be obtained by using a 3-pole Sellmeier equation, with poles at approximately 9.9 μm, 116 nm and 68 nm. The contributions of the individual poles can be seen below:

$$f1(\lambda) := \frac{0.6961663 \cdot \lambda^2}{\lambda^2 - 0.0684043^2} \qquad f2(\lambda) := \frac{0.4079426 \cdot \lambda^2}{\lambda^2 - 0.1162414^2} \qquad f3(\lambda) := \frac{0.8774794 \cdot \lambda^2}{\lambda^2 - 9.896161^2}$$

$$n(\lambda) := \sqrt{1 + f1(\lambda) + f2(\lambda) + f3(\lambda)}$$

Reference: Handbook of Optics (OSA)
(valid 0.21 - 3.71 μm)
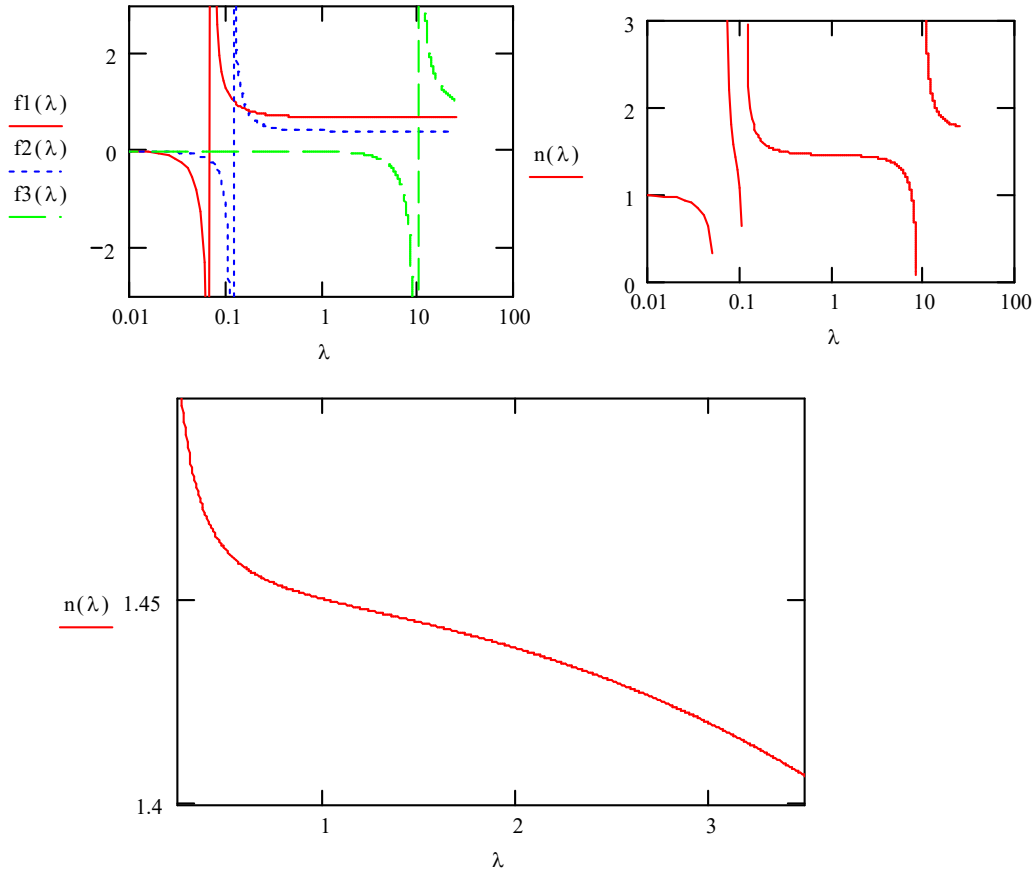
Schott glass description (power series)

$$n^2 = a_0 + a_1\lambda^2 + a_2\lambda^{-2} + a_3\lambda^{-4} + a_4\lambda^{-6} + a_5\lambda^{-8}$$

Hertzberger description (mixed power series and Sellmeier)

$$n^2 = A + \frac{B}{\lambda^2 - \lambda_0^2} + \frac{C}{\left(\lambda^2 - \lambda_0^2\right)^2} + D\lambda^2 + E\lambda^4$$

Abbe number

The Abbe number, ν_d, is a very commonly used single-number measure of the dispersion of glasses. It is defined by

$$\nu_d = \frac{n_d - 1}{n_f - n_c},$$

where n_d is the refractive index at $\lambda = 587.6$ nm (the sodium "d"-line), and n_f and n_c are the refractive indices at $\lambda = 486.1$ nm and 656.3 nm, respectively. Typical values are in the range $20 \sim 60$. A low Abbe number indicates high chromatic dispersion. Some examples are given in the following table.

Material	Refractive index	Abbe number
Crown Glass	1.52	58
Polycarbonate	1.59	31
BK-7	1.52	62
CaF_2	1.433	94

Appendix D – Fourier transforms

Time dependent fields can be represented as a sum of many oscillatory components, each with their individual angular frequency ω. In this text, we use the following convention

$$E(t) = \int_{-\infty}^{\infty} E(\omega)e^{-i\omega t} d\omega$$

If the time dependent signal E(t) is known, the Fourier amplitudes E(ω) can be determined using

$$E(\omega) = \frac{1}{2\pi} \int_{-\infty}^{\infty} E(t)e^{i\omega t} dt$$

Here E(ω) is the Fourier transform of E(t), which is also written as E(ω) = $\mathcal{F}$[E(t)]. In this text, the only exception to the notation shown above is the susceptibility, which we define as

$$\chi(\omega) = \int_{-\infty}^{\infty} \chi(t)e^{i\omega t} dt$$

and conversely

$$\chi(t) = \frac{1}{2\pi} \int_{-\infty}^{\infty} \chi(\omega)e^{i\omega t} dt$$

It can be shown that

$$\mathcal{F}[P(t)Q(t)] = C \;\; \mathcal{F}[P(t)] \otimes \mathcal{F}[Q(t)]$$

Where the symbol ⊗ stands for the convolution operation. The prefactor C depends on the choice of the form of the Fourier transform. Under our definition of the Fourier transform, we have C=2π. The convolution operation is defined as

$$(A\otimes B)(\omega) = \int_{-\infty}^{\infty} A(\omega)B(\omega - \omega') d\omega'$$

Important convolution relations are A⊗B = B⊗A, and A(ω)⊗δ(ω)= A(ω). Here δ(ω) represents the Dirac delta function, which is zero everywhere except when its argument is zero, and which is normalized according to

$$\int_{-\infty}^{\infty} \delta(\omega) d\omega = 1$$

Appendix E – Optical response: formulas and definitions

Permittivity (linear)

$$\epsilon(\omega) = \epsilon_0 \epsilon_r(\omega) = \epsilon_0(1 + \chi_e(\omega))$$

with ϵ_r the complex dielectric function, and χ_e the complex electric susceptibility.

Permeability (linear)

$$\mu(\omega) = \mu_0 \mu_r(\omega) = \mu_0(1 + \chi_m(\omega))$$

with μ_r the relative permeability, and χ_m the magnetic susceptibility.

Wave vector (scalar notation)

$$k = \frac{2\pi}{\lambda}$$

Light dispersion relation in isotropic materials

$$k^2 = \mu\epsilon\omega^2 = n\left(\frac{\omega}{c}\right)^2$$

Complex dielectric function, link to complex index in absence of magnetic effects

$$\epsilon_r(\omega) = \epsilon_r'(\omega) + i\epsilon_r''(\omega) = \eta(\omega)^2$$

Complex refractive index, link to dielectric function in absence of magnetic effects

$$\eta(\omega) = n(\omega) + i\kappa(\omega) = \sqrt{\varepsilon_r(\omega)}$$

Manual conversion between complex dielectric function and refractive index:

$$\eta^2 = (n + i\kappa)^2 = n^2 - \kappa^2 - 2n\kappa i = \varepsilon_r = \varepsilon_r' + i\varepsilon_r''$$

$$\epsilon_r'' = \chi'' = 2n\kappa$$

$$\epsilon_r' = 1 + \chi' = n^2 - \kappa^2$$

$$n = \sqrt{\frac{1}{2}(|\epsilon_r| + \epsilon_r')}$$

$$\kappa = \sqrt{\frac{1}{2}(|\epsilon_r| - \epsilon_r')}$$

$$\kappa = \frac{\epsilon_r''}{2n} = \frac{\chi''}{2n}$$

Phase velocity of an electromagnetic wave in isotropic medium:

$$v_p = \frac{\omega}{k} = \sqrt{\frac{1}{\mu\epsilon}}$$

Phase velocity of an electromagnetic wave in vacuum:

$$c = \sqrt{\frac{1}{\mu_0 \epsilon_0}}$$

Refractive index in isotropic materials

$$n = \frac{c}{v_p} = \sqrt{\frac{1}{\mu_r \epsilon_r}}$$

Absorption coefficient

$$\alpha = 2\kappa \frac{\omega}{c}$$

Group velocity in isotropic materials:

$$v_g = \left(\frac{dk}{d\omega}\right)^{-1}$$

Plasma frequency for free electron gas:

$$\omega_p^2 = \frac{Ne^2}{m_e \epsilon_0}$$

Poynting vector: instantaneous flow of optical energy per unit area.

$$\vec{S} = \frac{1}{\mu_0} \vec{E} \times \vec{B}$$

Irradiance: magnitude of the time averaged flow of optical energy per unit area

$$I(W/m^2) = \left|\langle \vec{S}(t) \rangle\right| = \frac{1}{2} nc\epsilon_0 E_0^2$$

where the last step assumes a plane wave with field amplitude E_0 in an isotropic medium.

Electromagnetic energy density in vacuum:

$$u = \frac{1}{2} \epsilon_0 E^2 + \frac{1}{2\mu_0} B^2$$

Reflection coefficient under normal incidence from air on planar surface

$$R = \frac{(n-1)^2 + \kappa^2}{(n+1)^2 + \kappa^2}$$

Reflection coefficient from medium 1 to medium 2 under normal incidence

$$R(\omega) = \left|\frac{\eta_2 - \eta_1}{\eta_2 + \eta_1}\right|^2 = \frac{(n_2 - n_1)^2 + (\kappa_2 - \kappa_1)^2}{(n_2 + n_1)^2 + (\kappa_2 + \kappa_1)^2}$$
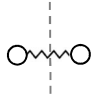
Appendix F – Springs, Masses, and Resonances
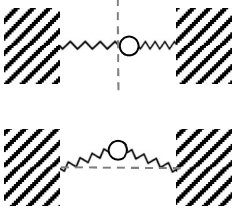
When discussing movement of bound masses (bound electrons, atoms in molecules, atoms in solids) we encounter mechanical resonances. To help understand and memorize the corresponding frequencies, this appendix shows all of them on one page.

One mass on fixed spring:

$$\omega = \sqrt{\frac{K}{m}}$$

Two equal masses on shared spring

$$\omega = \sqrt{\frac{2K}{m}}$$

Two unequal masses on shared spring

$$\omega = \sqrt{\frac{K}{\mu}}$$

One mass on two springs

$$\omega = \sqrt{\frac{2K}{m}}$$

Unequal masses with shared springs on each side

$$\omega = \sqrt{\frac{2K}{\mu}}$$
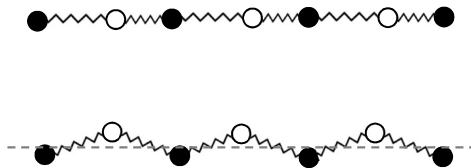
Appendix G – Rules of thumb and orders of magnitude

Photon energy vs. wavelength

$$E(eV) \approx \frac{1.24}{\lambda(\mu m)}$$

Wavelength vs. photon energy

$$\lambda(\mu m) \approx \frac{1.24}{E(eV)}$$

Energy vs. wavenumber

$$E(meV) \approx wavenumbers/8$$

Field strength vs. irradiance in medium with refractive index n

$$E_{max}(V/m) = \sqrt{\frac{2I}{nc\epsilon_0}} \approx 27\sqrt{\frac{I}{n}}$$

Order of magnitude irradiance needed in vacuum for 1 V/nm (expect NLO response)

$$I \approx 10^{15} \frac{W}{m^2} = 1 \frac{PW}{m^2}$$

Irradiance order of magnitude for 1 V/nm, expressed in energy per area for a 1ns pulse

$$I \approx \frac{1\,MJ}{m^2}\,ns^{-1} = \frac{1\,J}{mm^2}\,ns^{-1} = \frac{1\,\mu J}{\mu m^2}\,ns^{-1}$$

Irradiance order of magnitude for 1 V/nm, expressed in energy per area for a 1ps pulse

$$I \approx \frac{1\,kJ}{m^2}\,ps^{-1} = \frac{1\,mJ}{mm^2}\,ps^{-1} = \frac{1\,nJ}{\mu m^2}\,ps^{-1}$$

Appendix H – Approximations

When calculating the optical properties of dilute materials (gases) or doped host materials, we need to consider changes to the real and imaginary susceptibility caused by the dopants. To find the refractive index of the doped material, calculate the complete dielectric function and use the relation $\eta = \sqrt{\varepsilon_r}$. In some specific cases, we can use approximations that will simplify the work.

Dilute medium approximation

In dilute media $|\eta| \approx 1$ and therefore $|\chi| \ll 1$. This allows us to use $\sqrt{1+x} \approx 1 + \frac{1}{2}x$:

$$\eta = \sqrt{1 + \chi' + i\chi''} \approx 1 + \frac{1}{2}\chi' + \frac{1}{2}i\chi''$$

This gives

$$n \approx 1 + \frac{1}{2}\chi' \quad \text{and} \quad \kappa \approx \frac{\chi''}{2}$$

For dilute media we thus have a quick way of finding α, given by

$$\alpha = 2\kappa k_0 = 2\kappa\frac{\omega}{c} \approx \frac{\chi''\omega}{c}$$

Weak absorption approximation

In a medium with a complex index with a magnitude $|\eta| \gg 1$, the dilute limit no longer applies. In this case we cannot use $\kappa \approx \chi''/2$. Instead, we would have to use the exact relation $2n\kappa = \chi''$. However, for weak absorption, we can derive an approximate relation for κ and α.

To approximate α in this case, we split the term into a real prefactor and complex contribution with length ~1. In the case of a host with real dielectric function ε_h and a small dopant susceptibility contribution χ_d this can be done as follows:

$$\eta = \sqrt{\varepsilon_h + \chi_d' + i\chi_d''} = \sqrt{\varepsilon_h}\sqrt{1 + \frac{\chi_d'}{\varepsilon_h} + \frac{i\chi_d''}{\varepsilon_h}}$$

For low absorption (small imaginary contribution to η and ε_r), we can approximate η as

$$\eta \approx \sqrt{\varepsilon_h}\left(1 + \frac{\chi_d'}{2\varepsilon_h} + \frac{i\chi_d''}{2\varepsilon_h}\right)$$

For small dopant susceptibility we thus have

$$n \approx \sqrt{\varepsilon_h}\left(1 + \frac{\chi_d'}{2\varepsilon_h}\right) \approx \sqrt{\varepsilon_h} = n_h$$

$$\kappa \approx \sqrt{\varepsilon_h}\frac{\chi_d''}{2\varepsilon_h} \approx \frac{\chi_d''}{2n_h}$$

The latter expression looks like the exact relation: $2n\kappa = \chi''$, but note that in the approximated form the denominator contains the index of the *undoped* material. This highlights the fact that our approximation assumes that the host index is not significantly affected by the dopants. This is NOT allowed if the dopant introduces strong absorption, or if the host already has a significantly complex index.

Effect of dopants on reflection for weak absorption

In many real world applications, we consider transmission through 1mm or even 1cm thick windows. In these cases, transmission < 1 can be due to either reflection losses or absorption losses (or scattering, diffraction, not covered in this class). When we add dopants to a non-absorbing, approximately non-dispersive material, we expect that the transmission will change due to dopant induced absorption, as well as due to any changes in the reflection coefficient. In many cases the reflection changes associated with dopants will be minimal.

Example: if we consider a host with index n=2 (similar to the index of Si_3N_4), we find that a 1mm thick undoped Si_3N_4 slab would transmit a fixed fraction of $(1-R)^2 \approx 0.78$ of the light. Now let's assume that we include dopants that add a susceptibility of 0.008 + 0.008i. This would lead to a dielectric function

$$\varepsilon_{doped} = \varepsilon_{host} + \chi_{dopant} = 4 + 0.008 + 0.008i = 4 * (1 + 0.002 + 0.002i)$$

This gives a complex index that is approximately

$$n_{doped} \approx 2 + 0.001 + 0.001i$$

This change in complex index will have only a small effect on the total reflection:

$$R_{undoped} = \left| \frac{\eta_{slab} - \eta_{air}}{\eta_{slab} + \eta_{air}} \right|^2 = \frac{(n_{slab} - 1)^2 + \kappa_{slab}^2}{(n_{slab} + 1)^2 + \kappa_{slab}^2} = 0.11111$$

vs.

$$R_{doped} = \frac{1.001^2 + 0.001^2}{3.001^2 + 0.001^2} = 0.11126$$

We see that the single interface reflection coefficient changes by only 0.14%. Compare this to the introduced absorption loss by this same dopant. After the 1mm slab we would have a total transmission of $(1-R)^2 \, e^{-\alpha z}$. Here $\alpha = 2\kappa \, k_0$ which for $\lambda = 1$ μm gives us $\alpha = 4\pi \times 0.001/1\text{um} = 12.6$ /mm, giving $T=(1-R)^2 \, e^{-12.6} = 2.7 \times 10^{-6}$. We find that the dopant barely changes the reflection, but reduces the transmission almost to zero. We therefore conclude that <u>if a dopant allows appreciable (> ~1%) transmission through a thick (mm, cm) sample, we can safely assume that the dopant does not have a significant effect on the magnitude of the refractive index and therefore the reflection coefficient</u>.

Appendix I – Thermal distribution functions

In many physical systems, the probability of certain states being populated (or 'the chance of certain configurations being present') depends on the temperature. Temperature is a measure of the kinetic energy in a system, which can take the form of movement of entire molecules, vibrations of molecules and solids, and rotations of molecules.

Typically, states and configurations with high energy are unlikely to occur, unless the temperature is very high. This effect can be expressed in terms of thermal distribution functions $f(E)$ that describe occupation (probability) of a state with energy E as a function of temperature. Depending on the type of system, these distribution functions have a different form. Below are commonly encountered distribution functions.

Boltzmann probability distribution

The probability distribution in systems of many classical particles (no quantum mechanical effects) that are in thermal equilibrium follow Boltzmann statistics. The probability of a particular particle having an energy E is proportional to a factor

$$f(E) \propto e^{-E/k_B T}$$

with k_B the Boltzmann constant $k_B \approx 1.38 \times 10^{-23}$ J/K. This shows that it is most likely to find a particle occupying a low energy state. We use this distribution in describing dipole orientation in polar liquids (Debye model) and indirectly in describing inhomogeneous broadening due to Doppler shift in gases with velocity distributions described by the related Maxwell-Boltzmann velocity distribution.

Maxwell-Boltzmann velocity distribution

According to statistical mechanics of ideal gases, atoms (or molecules) in the gas phase have an isotropic temperature-dependent velocity distribution. The probability of having a velocity in the range {v, v+dv} depends on the kinetic energy ½ mv^2 according to the Boltzmann distribution, multiplied by a factor that considers the number of possible directions for this velocity which adds a factor $4\pi v^2$, times a normalization constant. The resulting formula is the Maxwell-Boltzmann distribution:

$$f_{MB}(v) = \left(\frac{m}{2\pi kT}\right)^{3/2} 4\pi v^2 e^{-\frac{1}{2}mv^2/kT}.$$

Here $f_{MB}(v)dv$ represents the fraction of atoms in a gas with a thermal velocity magnitude between v and v+dv, with m the mass of the atom (or ion, or molecule), and k the Boltzmann constant.

Bose-Einstein probability distribution

In systems where a quantum mechanical description is used, two distinct thermal distributions are encountered. Quantum particles that are derived from forces are typically Bosons, which in this book are encountered as photons ('electromagnetic force particles') and phonons ('mechanical forces particles', related to molecular binding forces in solids). While not discussed in detail in this text, more generally, Bosons are particles with integer

spin[xxxiii]. Bosons are special in the sense that a given Boson quantum state can in principle contain an unlimited number of Bosons. For example, for photons in a cavity this means that the fundamental optical mode can have an 'unlimited' number of photons and unlimited field strength. This means the occupation function f(E) for Bosons can exceed 1, and consequently the magnitude of the quantum mechanical expansion coefficient 'a' can exceed 1 (see e.g. Miller, *QM for scientists and engineers*). The corresponding thermal distribution function is of the form

$$f_{BE}(E) = \frac{1}{e^{E/kT} - 1}$$

known as the Bose-Einstein distribution, where we have assumed that all energy is from the particles themselves. If there are other sources of energy involved, the energy term is replaced by E-μ with μ the chemical potential. Note that the exponential term can reach any positive value from one to infinity, and consequently f_{BE} can in principle range from infinity to zero (when the exponential term goes to infinity). Note that at energies well above kT this distribution function approaches the Boltzmann energy distribution.

Fermi-Dirac probability distribution

Particles that represent matter (electrons, protons, etc.) are usually Fermions.[xxxiv] Unlike Bosons they have half-integer spin. These particles follow the Pauli exclusion principle, which states that a (Fermionic) quantum state can only contain a single Fermion. Consequently, the thermal distribution functions that describe Fermions cannot exceed a value of 1. The corresponding distribution function is the Fermi-Dirac distribution:

$$f_{FD}(E) = \frac{1}{e^{(E-E_F)/kT} + 1}$$

where E_F is known as the Fermi level, corresponding to the energy where the probability of a state being occupied is f(E_F)=½. Note that at energies many times kT above the Fermi level this distribution function approaches the Boltzmann energy distribution.
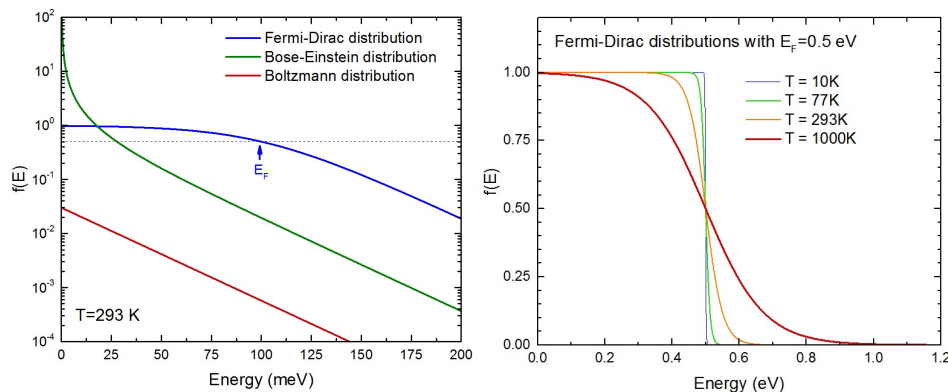
Scaled examples of Fermi-Dirac, Bose-Einstein, and Boltzmann energy distribution (left), and examples of the Fermi-Dirac distribution at four different temperatures.

---

xxxiii See https://en.wikipedia.org/wiki/Spin_(physics)
xxxiv See https://en.wikipedia.org/wiki/Fermion

Appendix J – Wavefunctions of the Hydrogen atom

The energy Eigensolutions of an electron in a Coulomb like binding potential are written as

$$\psi_{n,l,m}(r,\theta,\phi) = R_{n,l}(r)\, Y_l^m(\theta,\phi)$$

The spherical Harmonics are given by the following relations:

$$Y_l^m(\theta,\phi) = C_{l,m}\, P_l^m(\cos(\theta))e^{im\phi}$$

With normalization constant

$$C_{l,m} = \sqrt{\frac{2l+1}{4\pi}\frac{(l-m)!}{(l+m)!}}$$

And

$$P_l^m(z) = (-1)^m(1-z^2)^{m/2}\frac{d^m}{dz^m}P_l(z)$$

Where

$$P_l(z) = \frac{1}{2^l l!}\frac{d^l}{dz^l}\,[(z^2-1)^l]^2$$

Are Legendre polynomials.

The radial wavefunction depends only on n and l, and is given by

$$R_{n,l}(\rho) = \rho^l \sum_{k=0}^{n-l-1} a_k \rho^k e^{-\rho/2}$$

With

$$\rho = \frac{2}{na_0}r$$

And

$$a_{k+1} = \frac{k+l+1-n}{(k+1)(k+2l+2)}a_k$$

where a_0 is the Bohr radius, given by

$$a_0 = \frac{4\pi\varepsilon_0\hbar^2}{m_e e^2}$$

With a numerical value of $a_0 \approx 0.529$ Å.

Appendix K – OSE5312 Quantum Mechanics topics

The full table of contents of Miller's quantum book (1st edition) is shown below, showing topics that are covered in CREOL course OSE5312. Topics that are skipped or only briefly discussed in are shown in light gray.

Chapter 1 Introduction
1.1 Quantum mechanics and real life
1.2 Quantum mechanics as an intellectual achievement
1.3 Using quantum mechanics

Chapter 2 Waves and quantum mechanics – Schrödinger's equation
2.1 Rationalization of Schrödinger's equation
2.2 Probability densities
2.3 Diffraction by two slits
2.4 Linearity of quantum mechanics: multiplying by a constant
2.5 Normalization of the wavefunction
2.6 Particle in an infinitely deep potential well ("particle in a box")
2.7 Properties of sets of Eigenfunctions
2.8 Particles and barriers of finite heights
2.9 Particle in a finite potential well
2.10 Harmonic oscillator
2.11 Particle in a linearly varying potential

Chapter 3 The time-dependent Schrödinger equation
3.1 Rationalization of the time-dependent Schrödinger equation
3.2 Relation to the time-independent Schrödinger equation
3.3 Solutions of the time-dependent Schrödinger equation
3.4 Linearity of quantum mechanics: linear superposition
3.5 Time dependence and expansion in the energy eigenstates
3.6 Time evolution of infinite potential well and harmonic oscillator
3.7 Time evolution of wavepackets
3.8 Quantum mechanical measurement and expectation values
3.9 The Hamiltonian
3.10 Operators and expectation values
3.11 Time evolution and the Hamiltonian operator
3.12 Momentum and position operators
3.13 Uncertainty principle
3.14 Particle current
3.15 Quantum mechanics and Schrödinger's equation

Chapter 4 Functions and operators
4.1 Functions as vectors
4.2 Vector space
4.3 Operators
4.4 Linear operators
4.5 Evaluating the elements of the matrix associated with an operator
4.6 Bilinear expansion of linear operators
4.7 Specific important types of linear operators
4.8 Identity operator

Background mathematics
A.1 Geometrical vectors
A.2 Exponential and logarithm notation
A.3 Trigonometric notation
A.4 Complex numbers
A.5 Differential calculus
A.6 Differential equations
A.7 Summation notation
A.8 Integral calculus
A.9 Matrices
A.10 Product notation
A.11 Factorial

Background physics
B.1 Elementary classical mechanics
B.2 Electrostatics
B.3 Frequency units
B.4 Waves and diffraction

Vector calculus
C.1 Vector calculus operators
C.2 Spherical polar coordinates
C.3 Cylindrical coordinates
C.4 Vector calculus identities

Maxwell's equations and electromagnetism
D.1 Polarization of a material
D.2 Maxwell's equations
D.3 Maxwell's equations in free space
D.4 Electromagnetic wave equation in free space
D.5 Electromagnetic plane waves
D.6 Polarization of a wave

Appendix L – Recognizing material types

The topics covered in this text as well as in additional study materials for CREOL course OSE5312 enable you to recognize materials based on their optical response, and conversely, allow you to predict trends in optical properties given material type or composition. Briefly: refractive index is due to light-induced charge motion $\Rightarrow$ <u>optical properties can be understood by knowing how many charges are involved, and how easily they can be moved by an electric field.</u>

Dilute gases

- Index near one
- χ near zero
- Mostly transparent
- Narrow absorption lines
- If gas molecules are polar or have dipole active vibrations $\rightarrow$ groups of sharp absorption lines associated with combined rotation-vibration transitions. In addition: polar molecules $\rightarrow$ far infrared 'rotation-only' absorption lines

Polar liquids

- Large static ε_r, broad absorption and drop in static ε_r at GHz frequencies (Debye model)

Insulators

- low absorption throughout visible, $\kappa < \sim 0.001$.
- Significant absorption onset above 4 eV ('significant' $\approx \kappa > 0.001$)
- Normal dispersion throughout VIS
- Typical refractive index 1.2 - 2 (few valence electrons per atom, strongly bound $\Rightarrow$ little charge motion $\Rightarrow$ small dipole moment $\Rightarrow$ low χ $\Rightarrow$ small index of refraction)
- Low index $\Rightarrow$ low single interface reflection: $R \approx$ 1-10%
- <u>Compound</u> insulators: strong phonon-related resonances in infrared: Reststrahlen band, strong asymmetric absorption peak(s), large dispersion near ω_T; large $\varepsilon_r(0)$

Semiconductors

- Electronic absorption starts below 4eV ($\kappa > \sim 0.001$)
- Broad absorption bands
- Normal dispersion below first strong absorption (e.g. in the infrared)
- Typical refractive index 2.5 – 4 at low frequency (weak spring and multiple valence electrons per atom $\Rightarrow$ large motion of many charges $\Rightarrow$ large index)
- Typically: entirely real index at low frequency
- Possibly free carrier absorption at low frequency, giving $\alpha \propto \lambda^2$ (due to dopants or thermally/optically excited charges)
- High single-interface reflection coefficient , $R \approx$ 20-40%

- <u>Compound</u> semiconductors: strong phonon-related resonances in infrared: Reststrahlen band, strong asymmetric absorption peak(s), large dispersion near ω_T; large static $\varepsilon_r(0)$
- Direct gap: sudden onset of interband absorption
- Indirect gap: gradual rise of absorption, peaks/steps related to phonon-assisted transitions at low temperature
- Low temperature: exciton-related peaks near band-edge
- Low temperature, doped semiconductors: IR absorption due to dopant ionization

Metals

- Large κ at low frequency
- Real part of index less than one at low frequency
- Real part of ε_r negative at low frequency
- Plasma frequency ($\varepsilon_r' = 0$ or $\kappa = n$) typically in the VIS or near-UV
- Large reflection coefficient (typically $R > {\sim}0.8$)
- Sometimes evidence of d-band transition (bump in ε')
- Typical low-frequency (VIS–NIR) skin depth: tens of nm ($\alpha \approx 10^7$–10^8 /m)
- No clear phonon resonances in optical response (metals cannot sustain polar bonds)

Appendix M – Fundamental physical constants

Quantity	Symbol	Value	Unit	Relative std. uncert. u_r
speed of light in vacuum	c, c_0	299 792 458	m s^{-1}	(exact)
magnetic constant	μ_0	$4\pi \times 10^{-7}$	N A^{-2}	
		$= 12.566\,370\,614... \times 10^{-7}$	N A^{-2}	(exact)
electric constant $1/\mu_0 c^2$	ϵ_0	$8.854\,187\,817... \times 10^{-12}$	F m^{-1}	(exact)
Newtonian constant of gravitation	G	$6.6742(10) \times 10^{-11}$	m^3 kg^{-1} s^{-2}	1.5×10^{-4}
Planck constant	h	$6.626\,0693(11) \times 10^{-34}$	J s	1.7×10^{-7}
$h/2\pi$	$\hbar$	$1.054\,571\,68(18) \times 10^{-34}$	J s	1.7×10^{-7}
elementary charge	e	$1.602\,176\,53(14) \times 10^{-19}$	C	8.5×10^{-8}
magnetic flux quantum $h/2e$	Φ_0	$2.067\,833\,72(18) \times 10^{-15}$	Wb	8.5×10^{-8}
conductance quantum $2e^2/h$	G_0	$7.748\,091\,733(26) \times 10^{-5}$	S	3.3×10^{-9}
electron mass	m_e	$9.109\,3826(16) \times 10^{-31}$	kg	1.7×10^{-7}
proton mass	m_p	$1.672\,621\,71(29) \times 10^{-27}$	kg	1.7×10^{-7}
proton-electron mass ratio	m_p/m_e	$1836.152\,672\,61(85)$		4.6×10^{-10}
fine-structure constant $e^2/4\pi\epsilon_0 \hbar c$	α	$7.297\,352\,568(24) \times 10^{-3}$		3.3×10^{-9}
inverse fine-structure constant	α^{-1}	$137.035\,999\,11(46)$		3.3×10^{-9}
Rydberg constant $\alpha^2 m_e c/2h$	R_∞	$10\,973\,731.568\,525(73)$	m^{-1}	6.6×10^{-12}
Avogadro constant	N_A, L	$6.022\,1415(10) \times 10^{23}$	mol^{-1}	1.7×10^{-7}
Faraday constant $N_A e$	F	$96\,485.3383(83)$	C mol^{-1}	8.6×10^{-8}
molar gas constant	R	$8.314\,472(15)$	J mol^{-1} K^{-1}	1.7×10^{-6}
Boltzmann constant R/N_A	k	$1.380\,6505(24) \times 10^{-23}$	J K^{-1}	1.8×10^{-6}
Stefan-Boltzmann constant $(\pi^2/60)k^4/\hbar^3 c^2$	σ	$5.670\,400(40) \times 10^{-8}$	W m^{-2} K^{-4}	7.0×10^{-6}

Non-SI units accepted for use with the SI

Quantity	Symbol	Value	Unit	Relative std. uncert. u_r
electron volt: (e/C) J	eV	$1.602\,176\,53(14) \times 10^{-19}$	J	8.5×10^{-8}
(unified) atomic mass unit $1\ \mathrm{u} = m_u = \frac{1}{12}m(^{12}\mathrm{C})$ $= 10^{-3}$ kg mol$^{-1}/N_A$	u	$1.660\,538\,86(28) \times 10^{-27}$	kg	1.7×10^{-7}

Index